



Fundamental relationships for traffic flows at signalised intersections

Rahmi Akçelik

with contributions by:

Mark Besley

Ron Roper



Research Report ARR 340

Fundamental relationships for traffic flows at signalised intersections

Rahmi Akçelik

with contributions by:

Mark Besley

Ron Roper



Research sponsored by
Roads and Traffic Authority New South Wales

Information Retrieval

AKÇELİK, R., BESLEY, M. and ROPER, R. (1999). **FUNDAMENTAL RELATIONSHIPS FOR TRAFFIC FLOWS AT SIGNALISED INTERSECTIONS.** ARRB Transport Research Ltd. Research Report No. 340. 268 pages including 33 tables, 197 figures and 225 equations.

This report presents findings of a study of fundamental traffic characteristics at signalised intersections based on surveys of queue discharge headways and speeds for individual vehicles and jam spacings at eighteen intersections in Sydney and Melbourne. Exponential queue discharge flow, headway and speed models are given. Other traffic parameters considered are spacing, gap length, density, gap time, occupancy time, space time, occupancy ratios, queue clearance wave speed, departure response time, saturation flow rate, start loss and end gain times. The report presents basic material on fundamental traffic flow relationships, describes the survey methodology, survey site characteristics, data processing, analysis method, calibration method, and presents calibration results. Results on uninterrupted flow models and downstream queue interference at paired intersections are presented. Implications of findings on capacity and performance modelling and adaptive signal control practice are discussed. Relationships for use in practice are given.

About the authors

Rahmi Akçelik

Dr Akçelik is a leading scientist in the area of traffic management with over 180 technical publications. He is the author of the SIDRA software package. Dr Akçelik represents ARRB TR at the AUSTRROADS Traffic Management Reference Group. He is a member of the Signalised Intersections Subcommittee of the US Transportation Research Board (TRB) Committee on Highway Capacity and Quality of Service, and the TRB Committee on Traffic Signal Systems. Dr Akçelik graduated as a Civil Engineer from Istanbul Technical University (1968), and received a Ph.D. in Transportation Engineering from Leeds University, England. After working as a traffic engineer-planner with the National Capital Development Commission, Canberra, he joined ARRB TR (1979). Dr Akçelik was awarded the 1999 Clunies Ross National Science and Technology award.

Mark Besley

Mark Besley joined ARRB TR in 1980 after studying applied mathematics at Monash University. Mark has been involved in many aspects of research on traffic operations including incident detection, traffic network models, fuel consumption estimation, traffic data collection and analysis, as well as software development, user support and training. He has made a significant contribution to the development and support of the SIDRA computer package for intersection analysis.

Ron Roper

Ron Roper joined ARRB Transport Research in 1988. He has been involved in development of software and electronic hardware, field data collection methods and operation of productivity tools for asset management. Ron has wide experience in data analysis and processing using dedicated analysis packages, spreadsheets and purpose written applications. Prior to joining ARRB TR, Ron worked for the Federal Airports Corporation and its predecessors for twenty years in the field of electrical and electronic systems.

Acknowledgement

The authors thank Peter Lowrie and other RTA NSW staff for support given towards organising and for help in conducting the surveys in Sydney, as well as providing SCATS data for Sydney sites. Thanks to Peter Lowrie for his help in explaining various aspects of SCATS operation and his valuable comments on this report. Also thanks to Ngoc Nguyen (RTA NSW) for his useful comments on various aspects of this report, and to David Nash and other Vic Roads staff for providing SCATS data for Melbourne sites. John Dods contributed to the early stages of the project to establish a survey method for paired intersections. Edward Chung contributed to conducting field surveys.

ARR 340
SEPTEMBER 1999

ISBN 0 86910 796 8
ISSN 0158-0728

Any material may be reproduced without permission provided the source is acknowledged.

Although the Report is believed to be correct at the time of publication, ARRB Transport Research Limited, to the extent lawful, excludes all liability for loss (whether arising under contract, tort, statute or otherwise) arising from the contents of the Report or from its use. Where such liability cannot be excluded, it is reduced to the full extent lawful. Without limiting the foregoing, people should apply their own skill and judgement when using the information contained in the Report.

Wholly prepared and printed by
ARRB Transport Research Ltd
500 Burwood Highway
Vermont South VIC 3133
AUSTRALIA

ARR 340

Fundamental relationships for traffic flows at signalised intersections

Contents

Executive Summary	v
Notations and Basic Relationships	xiii
1 Introduction	1
2 Survey Method	5
3 Survey Sites	19
4 Data Processing	39
5 Fundamental Traffic Flow Relationships	55
6 Data Analysis Method	73
7 Queue Discharge Models	79
8 Model Calibration Method	89
9 Model Calibration Results	95
10 Uninterrupted Flow Models for Signalised Intersections	111
11 Downstream Queue Interference at Paired Intersections	119
12 Saturation Flow, Start Loss and End Gain	123
13 SCATS Control Parameters	139
14 Detection Zone Length and Gap Setting	147
14.1 Optimum detection zone length	147
14.2 Gap setting	162
15 Fundamental Relationships at the Signal Stop Line - An Example	165
16 Useful Relationships for Practice	177
17 Conclusion	185
REFERENCES	191
APPENDIX A – SCATS Intersection Geometry and Phasing Diagrams for Sydney and Melbourne 1998 Survey Sites	
APPENDIX B – Figures Showing Measured and Predicted Queue Discharge Speeds, Headways, Flow Rates and Spacings for Sydney and Melbourne 1998 Survey Sites	
APPENDIX C – Diagrams Showing Space Time - Speed - Detection Zone Length Relationships for Sydney and Melbourne 1998 Survey Sites	

ARRB Transport Research Ltd

ACN 004620651

HEAD OFFICE:

500 Burwood Highway
Vermont South
VIC 3133
AUSTRALIA

Tel: (03) 9881 1555
Fax: (03) 9887 8104

Email: info@arrb.org.au
Internet: www.arrb.org.au

PERTH OFFICE:

Street address:
Unit 5, 4 Brodie Hall Drive
Technology Park
Bentley, WA 6102
AUSTRALIA

Postal address:
PO Box 1068
Bentley, WA 6983
AUSTRALIA

Tel: (08) 9472 5544
Fax: (08) 9472 5533

Email: maryl@arrb.org.au

ARR 340

Fundamental relationships for traffic flows at signalised intersections

Executive Summary

Background

This research report presents findings of a comprehensive study of fundamental traffic characteristics at signalised intersections. The emphasis of the study is on queue discharge characteristics of traffic at the signal stop line.

The research was carried out in two stages during the period 1991-1999. The first stage of the study was carried out under several ARRB TR research projects on *Paired Intersections*. The second stage of the study was funded by the Roads and Traffic Authority of New South Wales (ARRB TR research project RC 7057 *Fundamental Relationships for Adaptive Control*; RTA NSW project 63521/8). The survey methodology established during the first stage of the study was employed and further refined during this stage to establish queue discharge characteristics at five intersection sites in Sydney and six intersection sites in Melbourne. The revised method was also applied to data collected at seven intersections in Melbourne during the first stage of the study, including paired (closely-spaced) intersection sites.

The results given in earlier reports are brought together in this research report. All previous reports produced during this study are superseded by this report.

Information given in this report is useful in modelling of actuated signal timing and performance.

Related work carried out under the *Paired Intersections* projects included modelling of platooned arrivals generated by coordinated signals, modelling of queue interaction at paired intersections, and explanation of the relationship between interrupted and uninterrupted traffic flow characteristics. The results of this work are also included in this report.

During 1998-1999, an associated study of the fundamental characteristics of freeway traffic flows was also undertaken. The study was funded by AUSTRROADS (ARRB TR research project RC 7082 *Reassessment of Fundamental Speed-Flow Relationships for Freeway Traffic Control*; AUSTRROADS project NRUM 9712). The results of the project are presented in Research Report ARR 341.

Research Context

The traditional queue discharge model for traffic signals uses a constant saturation flow rate and associated start loss and end gain times. The displayed green time is converted to an effective green time using these parameters. Capacity and performance (delay, queue length) models are based on the use of effective green time and saturation flow rate. This report presents an exponential queue discharge flow rate (or headway) model that represents queue discharge behaviour of traffic directly, i.e. without resorting to various simplifying assumptions needed to derive saturation flows and effective green times. However, the exponential model can be used to derive the traditional saturation flow rate, start loss and end gain parameters.

Executive Summary *continued*

Fundamental relationships for traffic flows at signalised intersections

An exponential queue discharge speed model associated with the queue discharge headway model is also presented. The queue discharge headway and speed models can be used together to derive traffic parameters such as vehicle spacing, gap (space) length, density, time and space occupancy ratios, gap time, occupancy time and space time. Thus, a complete set of fundamental relationships for queue discharge behaviour at traffic signals can be obtained. These relationships are useful for adaptive control purposes.

Calibration results are presented for exponential queue discharge flow rate and speed models based on data from all survey sites. The queue discharge model parameters given for individual sites include maximum queue discharge flow rate and speed, minimum queue discharge headway, vehicle spacing and space time at maximum queue discharge flow, jam spacing, queue clearance wave speed, and departure response time for the next vehicle in the queue to start moving.

Average values of queue discharge model parameters determined for through (isolated), through (paired intersection) and fully-controlled right turn (isolated) sites are also given. The term *isolated* used in this context means a single intersection site with a reasonably long distance to the downstream intersection as opposed to a *paired* (or closely-spaced) intersection site, and does not relate to the signal control method used at the site.

The data collection method involved the measurement of queue discharge headways and speeds for individual vehicles crossing the signal stop line using the VDAS traffic detection equipment developed by ARRB TR. The survey method also involved measurement of average spacings of vehicles in the queue (jam spacings). Exponential queue discharge speed and flow models were calibrated to determine model parameters using data with light vehicles (cars) only. The method is applied on a lane-by-lane basis.

This report

The report describes the survey methodology, survey site characteristics and data processing, and presents basic material on fundamental traffic flow relationships. Issues involved in data analysis are discussed and queue discharge models are described. The model calibration method is discussed and the calibration results for queue discharge models are given. Results on uninterrupted flow models and paired intersections from the first stage of the study are also given.

Implications of findings on queue discharge characteristics for capacity and performance analysis (saturation flows and lost times) and adaptive signal control practice (SCATS control parameters, optimum detector loop length, and gap setting) are discussed. Graphs showing queue discharge characteristics and the relationships between fundamental traffic variables at the signal stop line are given for an example.

Useful relationships for use in practice based on the findings of this study, including survey methods to measure saturation flow and saturation speed, simple regression equations to estimate queue discharge characteristics and determine optimum loop length and signal gap setting, and recommendations for further research are given.

Appendices present intersection geometry and phasing diagrams, and figures showing measured and predicted queue discharge speeds, headways, flow rates, spacings and space time - speed - detection zone length relationships for Sydney and Melbourne 1998 Survey Sites. *Notations and Basic Relationships* are given at the start of the report.

Executive Summary *continued*

Fundamental relationships for traffic flows at signalised intersections

Summary of Findings

The results of detailed analysis of **queue discharge characteristics** at signalised intersections show that the characteristics of through and right-turn movements differ significantly, and there are also significant differences between through lanes at isolated sites and paired (closely spaced) intersection sites.

Maximum queue discharge flow rates for right-turn sites are found to be similar to those for isolated through sites. Lower jam spacing and lower departure response time (higher queue clearance speed) at right-turn sites help to achieve low queue discharge headways, therefore high maximum flow rates. Parameters for through movements at paired intersection sites are between the through (isolated) and right turn (isolated) site values although lower maximum flow rates are observed at these sites.

The exponential queue discharge flow (headway) and speed models presented in this report are found satisfactory in view of:

- (i) ability to derive a complete set of fundamental relationships for queue discharge behaviour at traffic signals, useful for general traffic analysis as well as adaptive control purposes;
- (ii) reasonableness (compared with current knowledge and overseas data) of predicted queue discharge parameters, namely speed, flow rate, headway, spacing, gap (space) length, density, time and space occupancy ratios, gap time, vehicle passage time, occupancy time and space time, as well as implied optimum loop length;
- (iii) consistency of relative values of model parameters for through (isolated), through (paired intersection) and fully-controlled right turn (isolated) sites;
- (iv) consistency of saturation flow rate, start loss and end gain values derived from the exponential queue discharge flow model with those used in traditional signal analysis; and
- (v) a reasonable match between the SCATS parameters MF (maximum flow), HW (headway at maximum flow), KP (occupancy time at maximum flow) and the space time (HW – KP), and the corresponding analytical estimates, as well as the ability to relate the SCATS DS parameter to the traditional degree of saturation parameter.

It is often stated in the literature that saturation flow rate may decrease with time, especially in the case of long green times. The survey results presented in this report do not support this except in the case of downstream queue interference.

Additional analysis for **uninterrupted flow conditions** at signalised intersections, as relevant to conditions after queue clearance (unsaturated part of the green period), indicates that speed - flow - density models for these conditions are consistent with general models for uninterrupted conditions. Alternative models were assessed, and Akçelik's speed-flow model was recommended for this purpose. This model complements the exponential queue discharge models for saturated conditions, thus allowing for a complete analysis of traffic flow conditions at signalised intersections. This is demonstrated through an example. The findings also support the general explanation of the relationship between speed-flow functions for interrupted and uninterrupted flow conditions presented in the report.

Executive Summary *continued*

Fundamental relationships for traffic flows at signalised intersections

Queue discharge model parameters for **paired (closely-spaced) intersection** sites were derived using data points not affected by queue interference. The model parameters for these sites are found to be significantly different from those for isolated through traffic sites. In summary, maximum queue departure flow rates, speeds at maximum flow and spacings at maximum flow are lower, and queue discharge flow and speed model parameters m_q and m_v are higher indicating quicker acceleration to the maximum speed and achievement of the maximum flow rate sooner.

Although based on a small number of paired intersection sites, analysis of conditions with downstream queue interference indicate that the downstream queue interference occurs only when the distance to the back of queue is very small. For all practical purposes, it is concluded that queue interaction occurs when the downstream queue storage space is fully occupied.

Analyses of **cycle-by-cycle variations** in minimum queue discharge headway, cycle capacities and space time at maximum flow at a given site (carried out for five sites) indicated that distributions of these parameters varied considerably from site to site. For example, the 98th percentile space time at maximum flow can be as high as twice the average value, as observed at site 335 (right turn movement with short green time), and as low as 13 per cent higher than the average value, as observed at the site 511 (through movement with very long green time).

Of particular interest is the **variance to mean ratio of cycle capacity** which is important in modelling the effect of randomness in departure flows for predicting traffic performance (delay, queue length and queue move-up rate) for signalised intersections. Although this parameter is included in basic theoretical treatment of delay modelling, it has not been used explicitly in most delay models used in practice. Some coordinated signal delay models allow for filtering/metering of departure flows for saturated cycles at the upstream intersection, thus reducing the amount of randomness (e.g. see the US Highway Capacity Manual and the SIDRA User Guide). This may lead to the prediction of zero delays at the downstream intersection when the upstream intersection is oversaturated since the effect of variations in cycle capacity is ignored.

Analysis results for the five survey sites show that the variance to mean ratio of cycle capacity was in the range 0.08 to 0.34. It appears that 0.10 is a typical value for isolated sites. Interestingly, a high value of 0.34 was observed at the CBD site 413, suggesting that further attention needs to be paid to this parameter for coordinated signal modelling.

During this research, extensive effort has gone into fine-tuning the data analysis and calibration methods to improve the **headway and speed predictions at low speeds**. This is due to the lack of data at very low speeds and low flow rates related to the measurement of speed and headway for the first few vehicles in the queue at the start of the green period. Although the queue discharge models were generally satisfactory, there were several cases where the predicted headway and flow rate values for low speeds were not entirely satisfactory. This was particularly observed for the sites with low values of maximum queue discharge speed, which applied to most right-turn sites.

The data collection method and queue discharge models were investigated in detail, developing **alternative calibration methods** to derive queue discharge model parameters using different values of headway and speed variables obtained from raw detector data. The use of measured jam spacing vs the jam spacing estimated using model parameters from headway regression was considered. The start response time

Executive Summary *continued*

Fundamental relationships for traffic flows at signalised intersections

was introduced into the exponential queue discharge headway and speed models as a result of this effort. Alternative calibration methods were applied to data from three sites, namely Site 335 (Melbourne), Site 610 (Sydney) and Site 511 (Sydney). The following conclusions are drawn from the analysis:

- (i) The headway regression method results in estimated jam spacing values that are significantly greater than the measured values. Correct prediction of this parameter is very important for the space time - speed relationships and the optimum loop length as discussed in *Section 14*. Therefore this method is not preferred, thus confirming the calibration procedure that employs the measured jam spacing.
- (ii) Determining the start response time parameter freely from speed model regression gave acceptable results for the right-turn lane sites (335 and 610), but gave a negative value for the through lane site (511). The use of a specified value of 1.0 s appeared to be reasonable.
- (iii) Alternative methods using different speed and headway variables derived from raw detector data using the standard calibration method (with the measured jam spacing) gave close results although some improvements were obtained in queue discharge speed, headway and flow rate predictions. For a given site, the ratio m/m_q , which is the parameter in the speed-flow model, does not vary significantly for alternative calibration methods that use the measured jam spacing. This is a satisfactory result, in that the speed - flow and space time - speed relationships and the optimum loop length values indicate low sensitivity to the method used (assuming the calibration procedure using the measured jam spacing).
- (iv) Although alternative calibration methods using measured jam spacings give similar results in terms of the resulting speed - flow and space time - speed relationships and the optimum loop length values, it is recommended that calibration method 13 is used in future data analyses. This method uses the standard calibration procedure with a specified start response time of 1.0 s, and employs the speed based on the leading end of the vehicle and headways measured at the downstream detector. This method improves the queue discharge headway prediction at low speeds, particularly for right-turn sites where the queue discharge speeds are low.

Diagrams showing **space time - speed - detection zone length** relationships for individual sites, and for average through (isolated and paired intersection) and average right turn (isolated) sites are given in the report. These relationships are used for determining **optimum loop (detection zone) length** for adaptive control purposes.

For the dual purpose of counting vehicles and measuring space time, the optimum length for a loop is one that is as short as possible but not so short as to result in a double valued space-time relationship. Vehicle counts and space times are both used by the SCATS control system, and the space time measurement is relevant to traditional actuated control. To determine the optimum loop length, a limiting (low) speed value that gives zero space time can be chosen. Three limiting speeds are considered for this purpose, namely 0, 5 and 10 km/h. It is shown that the optimum loop length equals the gap length at the limiting speed. Choosing a speed above zero provides an increased loop length so to allow for increased jam gap length under adverse driving conditions (e.g. wet weather). Tables summarising queue discharge model parameters and presenting the optimum loop length results for individual sites and for "average" right-turn and through traffic sites are given in the report.

Executive Summary *continued*

Fundamental relationships for traffic flows at signalised intersections

The following conclusions are drawn regarding optimum loop length for adaptive control:

- (i) The optimum detection zone length appears to be independent of the maximum queue discharge speed, the maximum flow rate and the spacing at maximum flow. There seems to be a linear decreasing relationship between the optimum loop length and the speed-flow model parameter m_v / m_q . The maximum queue discharge speed and the spacing at maximum flow may have some effect on the optimum loop length for right-turn lanes, but it is not possible to establish this due to the small number of right-turn sites surveyed.
- (ii) The optimum detection zone length is clearly related to *jam gap length*. *Heavy vehicles* increase vehicle spacings due to longer vehicle length but the gap lengths are not increased as dramatically. Although it is possible that heavy vehicles have some impact on the jam gap length and gap length values at low speeds, the overall impact on these parameters, therefore on the optimum loop length, would be minimal with low heavy vehicle percentages. If the overall jam gap length increases significantly due to a large percentage of heavy vehicles in the traffic stream, then the optimum loop length could be increased proportionately. However, further research is recommended on the effect of heavy vehicles on jam gap length.
- (iii) It appears that it is possible to reduce the current loop length of 4.5 m used with the SCATS system to about 3.5 m for **through traffic lanes** and 3.0 m **right-turn lanes** under green arrow control. This is based on a chosen limiting speed of 5 km/h. On this basis, the range of optimum loop length for through traffic lanes is 3.0 to 3.8 m, with an average value of 3.4 m, considering all through traffic sites. There was no obvious difference between through sites in Sydney and Melbourne although the number of sites in Sydney is too small to arrive at a firm conclusion regarding this.

Considering all right-turn traffic sites, the range of optimum loop length is 2.2 to 3.1 m, with an average value of 2.6 m. The optimum loop length is shorter for the two right-turn sites in Sydney (2.2 and 2.3 m) and larger for the two right-turn sites in Melbourne (2.9 and 3.1 m). This is in line with the corresponding jam spacing values observed at the two Sydney sites (5.9 and 6.0 m) and at the two Melbourne sites (6.6 and 6.9 m).

Further data from a larger number of sites would be useful to arrive at a more conclusive result about the appropriate level of safety margin in determining the optimum loop length.

- (iv) Optimum loop length values obtained using queue discharge speed and flow models based on **alternative calibration methods** are essentially the same. This is valid for the methods that use the standard calibration procedure that employs the measured jam spacing value. The methods that estimate the jam spacing using parameters from headway model regression are not appropriate since they overestimate the jam spacing significantly.

The results given in the report are based on the definition of headway and spacing parameters from the *front* of the leading vehicle to the *front* of the following vehicle. Alternatively, headway and spacing parameters may be measured from the *back* of the leading vehicle to the *back* of the following vehicle. Limited analysis of parameters using the latter method indicated that the difference between the two methods would not affect the conclusions of the report.

Executive Summary *continued*

Fundamental relationships for traffic flows at signalised intersections

Recommendations for future research

Based on the findings of this study, the following are the recommendations for further research.

- (i) The database for queue discharge models and optimum loop length results has relatively few points, particularly for right-turn and paired intersection sites. Therefore, further surveys are recommended at paired (closely-spaced) intersection and CBD type intersection sites.

Right-turn traffic lanes surveyed in this study included single right-turn lanes only. Surveys at dual right-turn lane sites are recommended with a view to establishing differences in queue discharge parameters of the inside and outside lanes. This should include the consideration of separation distance from the right-turn movement from opposite direction under "diamond" turn arrangements. The effect of signal phasing (leading vs lagging turn arrow), turn radius, and angle of turn on queue discharge model parameters could also be investigated.

An investigation of the effect of the distance to the downstream intersection on queue discharge model parameters (without the effect of downstream queue interference) is recommended for paired intersection and CBD type intersection sites.

Surveys described in this report were carried out mostly during morning and afternoon peak periods. It would be useful to conduct surveys during day off-peak (business) periods at selected sites where morning and afternoon peak period surveys were carried out. The purpose of these additional surveys would be to investigate differences between peak and off-peak traffic characteristics.

Similarly, conducting surveys at the same site under adverse light and weather conditions (dark, rainy) would be useful in order to determine impact of such adverse conditions on queue discharge parameters. These surveys could be limited to the assessment of effects on jam spacing (or jam gap length) since this parameter is the main factor in optimum loop length determination.

- (ii) The survey method used during this study is very comprehensive and costly. Simple survey methods to measure saturation flow and saturation speed described in the report could be used to extend the data base.
- (iii) Regression equations given for use in practice can be improved by extending the data base through further surveys.
- (iv) Heavy vehicle effects should be analysed, particularly with a view to the effect on jam spacing and jam gap length.
- (v) A simple procedure for use in practice can be developed to enable traffic engineers to determine optimum loop length for through and right-turn lanes. The procedure should require collection of minimal amount of data. For this purpose regression equations could be developed for use when a parameter is not known. The simplest method would be the use of reliable regression equations (based on a large database and structured to cover different site characteristics) to determine the optimum loop length from jam gap length (or jam spacing).

Cycle-by-cycle variations of the minimum queue discharge headway, the cycle capacity, and the space time at maximum queue discharge flow should be investigated further. In particular, investigation of the *variance to mean ratio* of

Executive Summary *continued*

cycle capacity is recommended since this is important in modelling traffic performance (delay, queue length and queue move-up rate) for signalised intersections, especially for coordinated signals.

- (vi) The exponential queue discharge speed model implies a non-linear decreasing acceleration model with the maximum acceleration rate at the start of the acceleration manoeuvre. The acceleration time (time to accelerate to the maximum queue discharge headway) implied by the model is large because of the exponential nature of the model. Adjusting the model parameter m_v to obtain decreased acceleration times results in too sharp an increase compared with measured speed - time data. Further research on acceleration characteristics at the signal stop line would be useful considering an S-shaped speed - time model. However, the exponential queue discharge speed model is simpler to use and appears to be adequate for the purpose of this study.

NOTATIONS AND BASIC RELATIONSHIPS

a	Acceleration rate (m/s ²)
a _m	Maximum acceleration rate (m/s ²)
a _s	Acceleration rate during queue discharge (m/s ²)
c	Average cycle time (seconds) $c = r + g$
C	Average displayed cycle time (seconds) $C = R + G + t_y$
DS	SCATS DS parameter (original definition analogous to degree of saturation)
e _h	Actuated signal gap setting as a <i>headway time</i> value (seconds) $e_h = e_s + t_{ou}$
e _s	Gap setting as a <i>space time</i> value for actuated signals (headway time less occupancy time) as used with presence detection (seconds) $e_s = e_h - t_{ou}$
f _c	A traffic composition factor for saturation flow estimation (pcu/veh) $f_c = 1 + p_{HV} (f_{HV} - 1)$
f _e	A factor used for determining an appropriate gap time setting
f _{HV}	Saturation flow factor for heavy vehicles (pcu/veh), typically 1.5 to 2.0
f _{vHV}	Speed factor for heavy vehicles
f _q	A factor in the formula for estimating the queue clearance time
g	Average effective green time (seconds) $g = G - t_s + t_e - t_b$
g _{DS}	Effective green time for SCATS DS purposes (seconds) $g_{DS} = G + I_t$
g _s	Average queue clearance time, or duration of the saturated part of the effective green period (seconds) $g_s \leq g$
g _u	Duration of the unsaturated part of the effective green period (seconds) (during this uninterrupted flow period after the queue clearance, the vehicles depart as they arrive at the arrival flow rate, $q_u = q_{ag}$) $g_u = g - g_s$

G	Average displayed green time (seconds)
G_{\max}	Maximum green time setting for actuated signals (seconds)
G_s	Duration of the saturated part of the displayed green period (average queue clearance time) (seconds) $G_s = g_s + t_s + t_b \leq G$
G_u	Duration of the unsaturated part of the displayed green period (average queue clearance time) (seconds) $G_u = G - G_s = g_u - t_e$
h	Headway, or headway time: the time between passage of the <i>front</i> ends of two successive vehicles at an observation point (seconds/veh) (alternatively, this can be defined as the time measured between passage of the <i>rear</i> ends of two successive vehicles; with both definitions, headway is associated with the following vehicle) $h = 1 / q = L_h / v = t_o + t_s = t_g + t_v$ (q in veh/s, v in m/s) $h = 3600 / q$ (q in veh/h)
h_a	Average arrival headway (seconds/veh) measured at a point upstream of the back of queue at the arrival flow rate q_a (veh/h) $h_a = 3600 / q_a$
h_{ag}	Average arrival headway (seconds/veh) measured at a point upstream of the back of queue at the arrival flow rate q_{ag} (veh/h) during the green period $h_{ag} = 3600 / q_{ag}$
h_{ar}	Average arrival headway (seconds/veh) measured at a point upstream of the back of queue at the arrival flow rate q_{ar} (veh/h) during the red period $h_{ar} = 3600 / q_{ar}$
h_{dg}	Average headway of all vehicles departing during the green period including both saturated and unsaturated intervals (seconds/veh) $h_{dg} = 1 / q_{dg} = g / n_{vg}$ (q_{dg} in veh/s)
h_m	Minimum headway (seconds/pcu) corresponding to the maximum queue discharge flow rate with passenger car units only, q_m (pcu/h)
h_n	Minimum headway (seconds/veh) corresponding to the maximum queue discharge flow rate, q_n (veh/h)
h_s	Departure headway during queue discharge (seconds/veh) $h_s = 3600 / q_s = t_{os} + t_{ss}$ (q_s in veh/h)

h_{sa}	<p>Average queue discharge headway during the saturated part of the green period, or the saturation headway (seconds/veh)</p> $h_{sa} = 3600 / s \quad (s \text{ in veh/h})$
h_u	<p>Average departure headway during unsaturated portion of the green period (seconds/veh): this occurs during g_u, and corresponds to the departure flow rate for the actual traffic mix, which is equal to the arrival flow rate during the unsaturated portion of the green period, $q_u = q_a$ (veh/h)</p>
HW	<p>SCATS headway time (seconds/pcu) corresponding to the Maximum Flow (MF) parameter</p> $HW = 3600 / MF \quad (MF \text{ in pcu/h})$
I	<p>Intergreen time (clearance time consisting of yellow and all-red times) (seconds)</p> $I = t_y + t_{ar}$
I_s	<p>Starting intergreen time (intergreen time that precedes the current green period) (seconds)</p>
I_t	<p>Terminating intergreen time (intergreen time that follows the current green period) (seconds)</p>
k	<p>Density (concentration): number of vehicles per unit distance</p> $k = q / v = 1 / L_h \text{ in veh/m, or } k = 1000 / L_h \text{ in veh/km}$
k_j	<p>Jam density: number of vehicles per unit distance at zero speed, i.e. for a stationary queue</p> $k_j = 1 / L_{hj} \text{ in veh/m, or } k_j = 1000 / L_{hj} \text{ in veh/km}$
k_n	<p>Density (veh/km) corresponding to the maximum queue discharge flow rate</p> $k_n = q_n / v_n \quad (q_n \text{ in veh/h and } v_n \text{ in km/h})$
KP	<p>SCATS occupancy time (seconds/pcu) corresponding to the Maximum Flow (MF) parameter</p>
l	<p>Lost time for a traffic movement (the sum of starting intergreen time plus start loss plus blocked green time less end gain) (seconds)</p> $l = I_s + t_s - t_e + t_b$
L_{dq}	<p>Distance from the upstream stop line to the back of downstream queue (m)</p>

L_h	Spacing (m/veh): the headway <i>distance</i> as measured between the <i>front</i> ends of two successive vehicles (sum of space length and vehicle length) (alternatively, this can be defined as the distance measured between the <i>rear</i> ends of two successive vehicles; with both definitions, spacing is associated with the following vehicle) $L_h = v h = v / q = L_s + L_v$ (q in veh/s, v in m/s)
L_{hj}	Average jam spacing (m/veh), which is the sum of vehicle length and average space (gap) length for vehicles in a stationary queue $L_{hj} = L_{sj} + L_v$
L_{hjHV}	Average jam spacing for <i>heavy vehicles</i> (m/veh)
L_{hjLV}	Average jam spacing for <i>light vehicles</i> , or passenger car units (m/LV or m/pcu)
L_{hm}	Average spacing (m/pcu) the maximum queue discharge flow rate with passenger car units only, q_m
L_{hn}	Average spacing (m/veh) at the maximum queue discharge flow rate of the actual traffic mix, q_n $L_{hn} = v_n h_n = v_n / q_n = L_{sn} + L_v$ (q_n in veh/s, v_n in m/s)
L_{hs}	Spacing (m/veh) during queue discharge (i.e. for vehicles during the saturated part of the green period)
L_{hu}	Average spacing (m/veh) for the actual traffic mix under uninterrupted flow conditions (as observed at the signal stop line during the unsaturated part of the green period)
L_p	Effective detection zone length (m) (typically within ± 0.5 m of the detector loop length)
L_{p0}	Optimum loop length based on zero speed ($t_s = 0$ at $v_o = 0$) (m) $L_{p0} = L_{sj}$
L_{p5}	Optimum loop length based on 5 km/h ($t_s = 0$ at $v_o = 5$) (m)
L_{p10}	Optimum loop length based on 10 km/h ($t_s = 0$ at $v_o = 10$) (m)
L_s	Space (gap) length (m/veh): the following distance between two successive vehicles as measured between the <i>back</i> end of the leading vehicle and the <i>front</i> end of the following vehicle $L_s = L_h - L_v = v t_g$
L_{sj}	Average jam space (gap) length for vehicles (average distance between vehicles in a stationary queue) (m)

L_{sm}	Space (gap) length (m/veh) at the maximum queue discharge flow rate with passenger car units only, q_m
L_{sn}	Space (gap) length (m/veh) corresponding to the maximum queue discharge flow rate of the actual traffic mix, q_n
L_{ss}	Space (gap) length (m/veh) during queue discharge (i.e. for vehicles during the saturated part of the green period)
L_{su}	Average space (gap) length (m/veh) for uninterrupted flow conditions (as observed at the signal stop line during the unsaturated part of the green period)
L_v	Average vehicle length (m/veh) for the actual traffic mix $L_v = (1 - p_{HV}) L_{vm} + p_{HV} L_{vHV}$
L_{vHV}	Average vehicle length for <i>heavy vehicles</i> (m/HV)
L_{vLV}	Average vehicle length for <i>light vehicles</i> , or passenger car units (m/LV or m/pcu)
L_y	Distance between two detectors (m)
m_q	A parameter in the queue discharge flow rate (or headway) model representing the rate of increase of the flow rate as a function of the time since the start of the green period
m_v	A parameter in the queue discharge speed model representing the rate of increase of the speed as a function of the time since the start of the green period
MF	SCATS Maximum Flow (MF) parameter (pcu/h) $MF = 3600 / HW \text{ (HW in seconds/pcu)}$
n_c	Number of signal cycles during an observation period
n_{cs}	Number of fully-saturated signal cycles during an observation period
n_e	Number of vehicles that depart after the end of the green period, i.e. during the terminating intergreen time (yellow and all-red intervals)
n_r	Residual queue: the number of vehicles in the queue at the start of the effective red period (vehicles)
n_s	Cumulative queue discharge flow rate since the start of the green period (vehicles)
n_{vg}	Number of vehicles that depart during the green period: (n_{vgs} or n_{vgu}): $n_{vg} = n_{vs} + n_{vu} \text{ when the green period is not fully saturated } (G_s < G)$ $n_{vg} = n_{vs} + n_e \text{ during a fully saturated green period } (G_s = G)$

n_{vi}	Number of vehicles that depart from the queue during the initial part of the green period (0 to t_i) for saturation flow calculation purposes
n_{vs}	Number of vehicles that depart during queue clearance, i.e during the saturated part of the green period (G_s); this is the number of queued vehicles
n_{vT}	Number of vehicles that depart from the queue during the interval t_1 to t_2 after the start of the green period and before the end of the saturated part of the green period ($t_r \leq t_1 \leq t_2 \leq G_s$)
n_{vu}	Number of vehicles that depart after queue clearance (during the unsaturated part of the green period); this is the number of unqueued vehicles $n_{vu} = q_u g_u / 3600$ (q_u in veh/h)
O_s	Space occupancy ratio: the <i>proportion of road space</i> (length) covered by vehicles $O_s = L_v / L_h = k L_v$
O_t	Time occupancy ratio: the <i>proportion of time</i> in an analysis period when the detector at a given point along the road is occupied by vehicles $O_t = t_o / h = (L_v + L_p) / L_h$ (with presence detection)
pcu	Passenger car units (used to allow for the effect of heavy vehicles)
p_{HV}	Proportion of heavy vehicles (HVs) in the stream, e.g. $p_{HV} = 0.05$ means 5 % HVs and 95 % LVs (light vehicles, or pcus)
p_{LV}	Proportion of light vehicles in the traffic stream
P_A	Platoon arrival ratio for coordinated signals: the ratio of the average arrival flow rate during the green period to the average arrival flow rate during the signal cycle (R_p in HCM notation) $P_A = q_{ag} / q_{ac} = P_G / u$
P_G	Proportion of traffic arriving during the green period (P in HCM notation) $P_G = q_{ag} g / q_{ac} c = P_A u$
P_R	Proportion of traffic arriving during the red period $P_R = q_{ar} r / q_{ac} c = 1 - P_G = 1 - P_A u$
q	Flow rate (veh/s or veh/h): number of vehicles per unit time passing (<i>arriving</i> or <i>departing</i>) a given reference point
q_a	Arrival (demand) flow rate (veh/s or veh/h): the average number of vehicles per unit time as measured at a point upstream of the back of queue ($q_a = q_{ac} = (q_{ar} r + q_{ag} g) / c$ for platooned arrivals)

q_{ac}	Average arrival (demand) flow rate during the cycle (veh/s or veh/h) (for platooned arrivals: $q_{ac} = q_a$) $q_{ac} = (q_{ar} r + q_{ag} g) / c$
$q_a c$	Number of arrivals (veh) per cycle as measured at the back of the queue (for platooned arrivals: $q_a c = q_{ac} c = q_{ar} r + q_{ag} g$)
q_{ag}	Arrival flow rate (veh/s or veh/h) during the green period (for non-platooned arrivals: $q_{ag} = q_a$) $q_{ag} = P_A q_a$
q_{ar}	Arrival flow rate (veh/s or veh/h) during the red period (for non-platooned arrivals: $q_{ar} = q_a$) $q_{ar} = q_a (c - P_A g) / r = q_a (1 - P_A u) / (1 - u)$
q_d	Departure flow rate (veh/s or veh/h): the number of vehicles per unit time measured at the signal stop line: $q_d = q_s$ during the saturated part of the green period $= q_u$ during the unsaturated part of the green period
q_{dc}	Average departure flow rate during the signal cycle (veh/s) $q_{dc} = (s g_s + q_u g_u) / (3600 c) = n_{vg} / c$ (s and q_u in veh/h)
q_{dg}	Average departure flow rate during the green period (veh/s) $q_{dg} = (s g_s + q_u g_u) / (3600 g) = n_{vg} / g$ (s and q_u in veh/h)
q_m	Maximum queue discharge flow rate (pcu/h) for light vehicles, or passenger car units (maximum departure flow rate observed at the signal stop line without any downstream queue interference)
q_n	Maximum queue discharge flow rate for the actual traffic mix (veh/h) (for uninterrupted traffic, this is the maximum flow rate, or capacity) $q_n = q_m / f_c$
q_s	Queue discharge flow rate (veh/h or veh/s): departure flow rate during the saturated part of the green period
q_{sa}	Average queue discharge flow rate during the saturated part of the green period (veh/h); $q_{sa} = s$ approximately $q_{sa} = 3600 n_{vs} / G_s$
q_u	Flow rate (veh/h) during the unsaturated part of the green period ($q_u = q_a$: departure flow rate = arrival flow rate)
Q_e	Capacity of a lane (veh/h): maximum arrival flow rate that can be serviced <i>under prevailing flow conditions</i> $Q_e = s g / c$ for interrupted traffic (where s is in veh/h) $Q_e = q_n$ for uninterrupted traffic

r	Average effective red time (seconds) $r = c - g = R + t_s - t_e + t_y + t_b$
R	Average displayed red time (seconds) $R = C - G - t_y$
s	Average saturation flow rate during the effective green period (veh/h) for the actual traffic mix without any downstream queue interference $s = s_m / f_c$
s _m	Average saturation flow rate for a traffic stream consisting of passenger car units only (or light vehicles) without any downstream queue interference (pcu/h)
s _{MF}	Saturation flow calculated using the principle of the SCATS Maximum Flow (MF) parameter (pcu/h)
s _o	Saturation flow based on zero start loss and zero end gain definition ($t_s = t_e = 0$, therefore $g = G$) (veh/h)
s g	Cycle capacity (veh) (s in veh/s, g in seconds)
t	Time (seconds) (in queue discharge models, this is the time since the start of the displayed green period)
t _a	Acceleration time (seconds)
t _{ar}	All-red time (seconds)
t _b	Blocked green time: duration of blockage due to downstream queue interference, opposing vehicles or pedestrians (seconds)
t _e	End gain for a traffic movement, which is associated with the effective use of terminating intergreen time (yellow and all-red intervals) (duration of the interval between the end of displayed green period and the end of effective green period) (seconds) $t_e = 3600 n_e / s$ (s in veh/h)
t _{em}	End gain based on the maximum queue discharge flow rate (seconds) $t_{em} = 3600 n_e / q_m$ (q _m in veh/h)
t _g	Gap time (seconds/veh): the time between the passage of the <i>back</i> end of leading vehicle and the <i>front</i> end of the following vehicle as measured at a given point along the road, e.g. at a passage detector, or at the leading edge of a presence detector loop; this is the time taken to travel the space (gap) length, L _s $t_g = L_s / v = h - t_v$ (v in m/s)

t_i	Duration of the initial part of the green period for saturation flow calculation purposes (seconds) ($t_i = 10$ seconds in ARR 123 (Akçelik 1981))
t_o	Detector occupancy time (seconds/veh): duration of the period when the detection zone is <i>occupied</i> by a vehicle (sum of the vehicle passage time and the time to travel the detection zone length) at speed v (m/s) $t_o = h - t_s = t_v + L_p / v = (L_v + L_p) / v$
t_{og}	Average occupancy time of all vehicles departing during the green period including both saturated and unsaturated intervals (seconds/pcu) $t_{og} = n_{vs} t_{osa} + n_{vu} t_{ou}$
t_{om}	Occupancy time (seconds/pcu) at the maximum queue discharge flow rate, q_m , and the maximum queue discharge speed, v_m
t_{on}	Occupancy time (seconds/veh) corresponding to the maximum queue discharge flow rate, q_n , and the maximum queue discharge speed, v_n
t_{os}	Occupancy time (seconds/veh) during queue discharge (i.e. for vehicles departing during the saturated part of the green period) at speed v_s
t_{osa}	Average occupancy time (seconds/veh) during queue discharge
t_{ou}	Occupancy time (seconds/veh) for uninterrupted flow conditions (as observed at the signal stop line during the unsaturated part of the green period, i.e. after queue clearance, for vehicles arriving and departing at speed, $v_u = v_{ac}$) $t_{ou} = 3.6 (L_v + L_p) / v_{ac}$
t_r	Start response time in the queue discharge model representing average driver response time for the first vehicle to start moving at the start of the displayed green period (seconds)
t_s	Start loss time for a traffic movement, which is associated with driver reaction time and acceleration delays until the steady saturation flow rate is reached (duration of the interval between the start of displayed green period and the start of effective green period) (seconds)
t_s	Space time (seconds/veh): the duration of the time between the detection of two consecutive vehicles when the presence detector loop is not occupied (this is equivalent to the gap time less the time taken to travel the effective detection zone length, L_p) at speed v (m/s) $t_s = h - t_o = t_g - L_p / v = (L_s - L_p) / v$
t_{sg}	Average space time of all vehicles departing during the green period including both saturated and unsaturated intervals (seconds/pcu) $t_{sg} = n_{vs} t_{ssa} + n_{vu} t_{su}$

t_{sm}	Space time (seconds/pcu) corresponding to the maximum queue discharge flow rate, q_m
t_{sn}	Space time (seconds/veh) corresponding to the maximum queue discharge flow rate, q_n $t_{sn} = h_n - t_{on}$
t_{ss}	Space time (seconds/veh) during queue discharge (i.e. for vehicles departing during the saturated part of the green period) $t_{ss} = h_s - t_{os}$
t_{ssa}	Average space time (seconds/veh) during queue discharge
t_{su}	Space time (seconds/veh) for uninterrupted flow conditions (as observed at the signal stop line during the unsaturated part of the green period)
t_v	Vehicle passage time (seconds/veh): time it takes for the vehicle length (from front end to back end) to pass a given point at speed v (m/s) (this can be considered to be the occupancy time, $t_o \approx t_v$, when the detection zone length is negligible, $L_p \approx 0$). $t_v = L_v / v$
t_x	Average departure response time: average driver response time for the next vehicle in the queue to start moving (seconds)
t_y	Yellow time (duration of yellow interval) (seconds)
T_h	Total headway time for vehicles departing during the green and intergreen periods (seconds) $T_h = n_{vs} h_{sa} + n_{vu} h_u = g$
T_L	Travel time between two VDAS passage detectors for the leading end of a vehicle (seconds)
T_o	Total occupancy time for vehicles departing during the green and intergreen periods (seconds) $T_o = n_{vs} t_{osa} + n_{vu} t_{ou} + t_b$
T_s	Total space time for vehicles departing during the green and intergreen periods (seconds) $T_s = n_{vs} t_{ssa} + n_{vu} t_{su}$
T_T	Travel time between two VDAS passage detectors for the trailing end of a vehicle (seconds)
u	Green time ratio $u = g / c$

v	Speed (m/s or km/h): distance travelled per unit time $v = L_h / h = q L_h = q / k$
v _a	Average speed (m/s or km/h)
v _{ac}	Average approach cruise speed (km/h) for the actual traffic mix as measured at a point upstream of the back of queue under uninterrupted conditions: this is the average cruise speed of the arrival stream at arrival flow rate q _a
v _d	Average speed for interrupted traffic including the effect of delays at traffic interruptions (km/h)
v _f	Free-flow (zero-flow) speed in the uninterrupted speed-flow model for the actual traffic mix (average speed under near-zero flow conditions) (km/h)
v _{fm}	Free-flow (zero-flow) speed in the uninterrupted speed-flow model for passenger car units, or light vehicles (average speed under near-zero flow conditions) (km/h)
v _L	Speed based on time measurements for the leading end of the vehicle (km/h) $v_L = 3.6 L_y / t_L$
v _m	Maximum queue discharge speed for passenger car units, or light vehicles (km/h)
v _n	Maximum queue discharge speed for the actual traffic mix (km/h) corresponding to the maximum queue discharge flow rate, q _n (for uninterrupted traffic, this is the average uninterrupted travel speed at maximum flow)
v _o	Limiting speed value that gives a zero space time value (t _s = 0) used for the purpose of determining optimum loop length (km/h)
v _{of}	Free-flow (zero-flow) speed for interrupted traffic (average speed under near-zero flow conditions) (km/h)
v _Q	Average travel speed when the demand flow rate equals the capacity for interrupted traffic (km/h)
v _r	Queue discharge speed reduced due to downstream queue interference at paired intersections (veh/h)
v _s	Queue discharge speed for the actual traffic mix (km/h): departure speed across the signal stop line during the saturated part of the green period (in terms of uninterrupted flows, this is the speed under congested conditions observed at a reference point along the road)
v _{sa}	Average departure speed during queue discharge (corresponding to the average queue discharge flow rate, q _{sa})

v_{sm}	Queue discharge speed for light vehicles, or passenger car units (km/h)
v_T	Speed based on time measurements for the trailing end of the vehicle (km/h) $v_T = 3.6 L_y / t_T$
v_u	Average <i>uninterrupted</i> travel speed (km/h or m/s) (at the signal stop line, this is the average speed during the unsaturated part of the green period) ($v_u = v_{ac}$)
v_{um}	Uninterrupted flow speed for light vehicles, or passenger car units (km/h or m/s)
v_x	Average departure wave speed (km/h or m/s)
v_y	Average arrival wave speed (km/h or m/s)
x	Degree of saturation: the ratio of arrival (<i>demand</i>) flow rate to capacity, equivalent to the ratio of arrivals per cycle ($q_{ac} c$ vehicles) to the maximum number of vehicles that can depart per cycle (sg vehicles) $x = q_{ac} / Q_e = (q_{ac} c) / (sg)$ (for non-platooned arrivals, $x = q_a / Q_e$)
x_a	Acceleration distance (m)
y	Flow ratio: the ratio of arrival (demand) flow rate to the saturation flow rate $y = q_{ac} / s$ (for non-platooned arrivals, $y = q_a / s$)

1 INTRODUCTION

Background

This research report presents findings of a comprehensive study of fundamental traffic characteristics at signalised intersections. The emphasis of the study is on queue discharge characteristics of traffic at the signal stop line.

The research was carried out in two stages during the period 1991-1999. The first stage of the study was carried out under several ARRB TR research projects on "*Paired Intersections*". The findings of the first stage on fundamental traffic characteristics at signals were described in the working document WD R 96/043 (Akçelik and Besley 1996), and a related paper (Akçelik 1997). The working document presented results of surveys of traffic streams crossing the signal stop-line at seven intersections in Melbourne, including paired intersection sites.

The second stage of the study was funded by the Roads and Traffic Authority of New South Wales (ARRB TR research project RC 7057 *Fundamental Relationships for Adaptive Control*; RTA NSW project 63521/8). The survey methodology established during the first stage of the study was employed and further refined during this stage to establish queue discharge characteristics at five intersection sites in Sydney and six intersection sites in Melbourne. The findings of the second stage were described in working documents WD R 98/015 (Akçelik and Roper 1998), WD R 98/041 (Akçelik, Roper and Besley 1998) and contract report RC 7057 (Akçelik, Roper and Besley 1999a).

The results given in earlier reports are brought together in this research report. All previous reports produced during this study are superseded by this report.

Information given in this report is useful in modelling of actuated signal timing and performance (Akçelik 1995a).

Related work carried out under the *Paired Intersections* projects included modelling of platooned arrivals generated by coordinated signals (Akçelik 1995b), modelling of queue interaction at paired intersections (Roughail and Akçelik 1991, 1992; Johnson and Akçelik 1992; Akçelik 1998), and explanation of the relationship between interrupted and uninterrupted traffic flow characteristics (Akçelik 1996). The results of this work are also included in this report.

During 1998-1999, an associated study of the fundamental characteristics of freeway traffic flows was also undertaken. The study was funded by AUSTROADS (ARRB TR research project RC 7082 *Reassessment of Fundamental Speed-Flow Relationships for Freeway Traffic Control*; AUSTROADS project NRUM 9712). The results of the project are presented in Research Report ARR 341 (Akçelik, Roper and Besley 1999b).

Research Context

The traditional queue discharge model for traffic signals (Webster and Cobbe 1966, Akçelik 1981, TRB 1998) uses a constant saturation flow rate and associated start loss and end gain times. The displayed green time is converted to an effective green time using these parameters. Capacity and performance (delay, queue length) models are

based on the use of effective green time and saturation flow rate. This report presents an exponential queue discharge flow rate (or headway) model that represents queue discharge behaviour of traffic directly, i.e. without resorting to various simplifying assumptions needed to derive saturation flows and effective green times. However, the exponential model can be used to derive the traditional saturation flow rate, start loss and end gain parameters.

An exponential queue discharge speed model associated with the queue discharge headway model is also presented. The queue discharge headway and speed models can be used together to derive traffic parameters such as vehicle spacing, gap (space) length, density, time and space occupancy ratios, gap time, occupancy time and space time. Thus, a complete set of fundamental relationships for queue discharge behaviour at traffic signals can be obtained. These relationships are useful for adaptive control purposes.

Calibration results are presented for exponential queue discharge flow rate and speed models based on data from all survey sites. The queue discharge model parameters given for individual sites include:

- maximum queue discharge flow rate,
- minimum queue discharge headway,
- maximum queue discharge speed,
- vehicle spacing at maximum queue discharge flow,
- space time at maximum queue discharge flow,
- jam spacing,
- queue clearance wave speed, and
- response time for the next vehicle in the queue to start moving.

Average values of queue discharge model parameters determined for through (isolated), through (paired intersection) and fully-controlled right turn (isolated) sites are also given. The term *isolated* used in this context means a single intersection site with a reasonably long distance to the downstream intersection, and does not relate to the signal control method used at the site.

The data collection method involved the measurement of queue discharge headways and speeds for individual vehicles crossing the signal stop line using the VDAS traffic detection equipment developed by ARRB TR (Leschinski and Roper 1993). The survey method also involved measurement of average spacings of vehicles in the queue (jam spacings). Exponential queue discharge speed and flow models were calibrated to determine model parameters using data with light vehicles (cars) only. The method is applied on a lane by lane basis.

This report

The report describes the survey methodology, survey site characteristics and data processing (*Sections 2, 3 and 4*), and presents basic material on fundamental traffic flow relationships (*Section 5*). More complicated issues involved in data analysis are discussed in *Section 6*, and queue discharge models are described in *Section 7*. The model calibration method is discussed in *Section 8*, and the calibration results are given in *Section 9*. Results on uninterrupted flow models and paired intersections from the first stage of the study are given in *Sections 10 and 11*. The effect of the downstream

queue length on upstream departure speeds and flow rates at paired intersection sites is discussed in *Section 11*.

Implications of findings on queue discharge characteristics for capacity and performance analysis (saturation flows and lost times) and adaptive signal control practice (SCATS control parameters, optimum detector loop length, and gap setting) are discussed in *Sections 12 to 14*.

Graphs showing queue discharge characteristics and the relationships between fundamental traffic variables at the signal stop line are given for an example in *Section 15*.

Useful relationships for use in practice based on the findings of this study, including survey methods to measure saturation flow and saturation speed, simple regression equations to estimate queue discharge characteristics, and determine optimum loop length and signal gap setting are summarised in *Section 16*.

Section 17 presents conclusions and recommendations for further research.

Appendices A to C present SCATS intersection geometry and phasing diagrams, and figures showing measured and predicted queue discharge speeds, headways, flow rates, spacings and space time - speed - detection zone length relationships for Sydney and Melbourne 1998 Survey Sites.

Notations and Basic Relationships are given at the start of the report.

2 SURVEY METHOD

The survey method involves the collection of the following data for each lane measured:

- (i) Queue discharge headway and speed data for individual vehicles crossing the signal stop line collected using the VDAS detector equipment. The VDAS treadle switch (passage) detectors are placed over the signal detector loop as shown in *Figure 2.1*. In earlier paired intersection surveys, VDAS detector strips were placed immediately downstream of the signal stop line as seen in *Figure 2.2*. VDAS equipment and detector placement is further discussed in this section.
- (ii) The times when the third through seventh queued vehicles cross the VDAS detectors recorded by an observer manually by pressing a hand held button connected to a laptop computer.
- (iii) The time when the *last vehicle from the back of queue* crosses the VDAS detector in an undersaturated signal cycle recorded by an observer who presses a second button connected to the laptop computer via a long cable (*Figures 2.1, 2.2 and 2.3*). In the case of an oversaturated signal cycle, this is not recorded since the *last departing queued vehicle* is determined automatically (*Figure 2.4*).

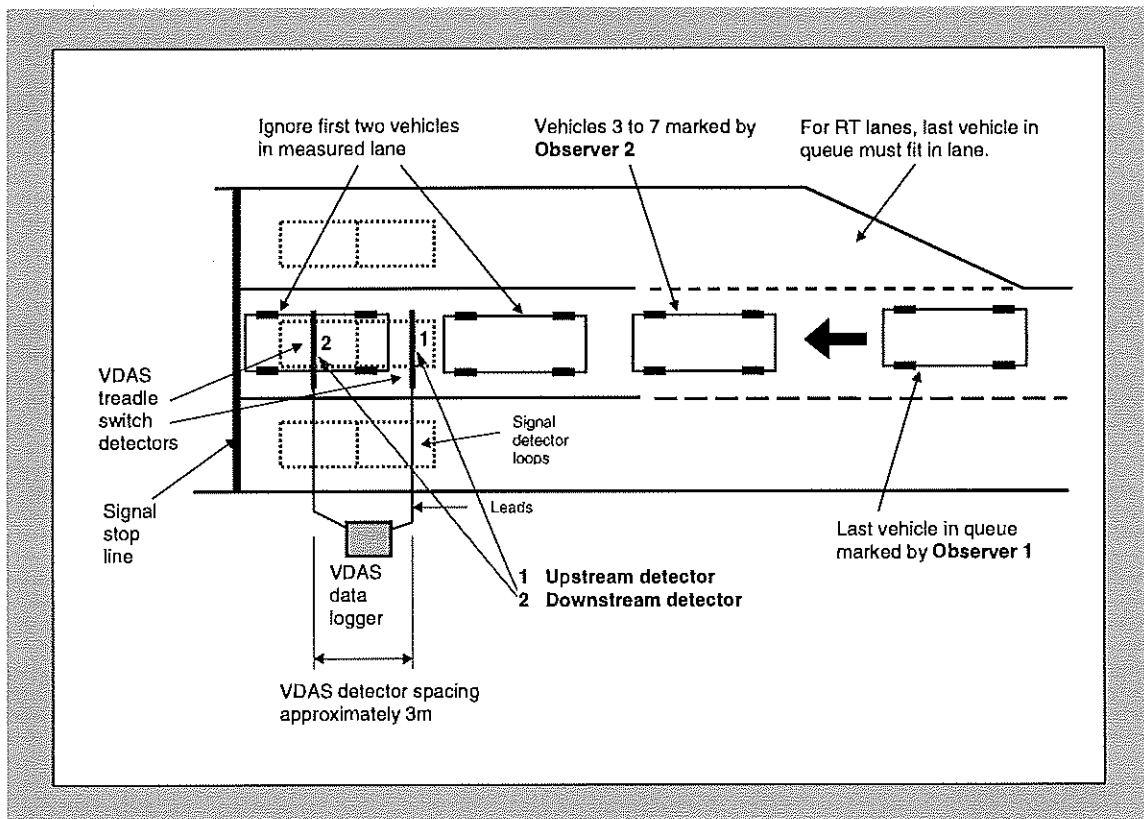


Figure 2.1 – Passage detection system using two VDAS detectors located centred over the traffic signal loop detector

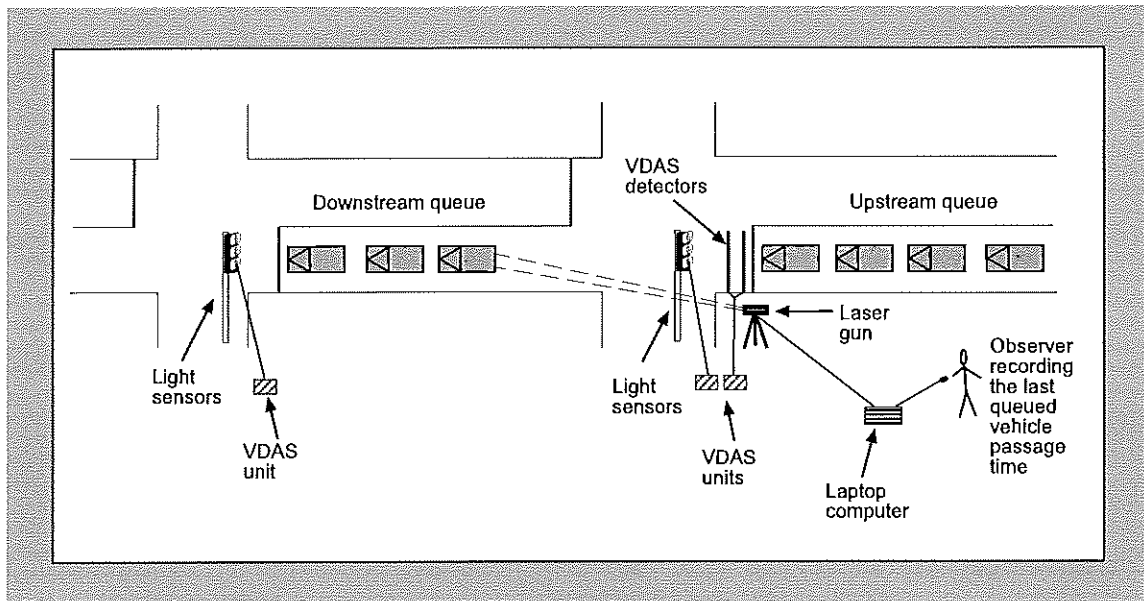


Figure 2.2 – Paired intersection survey method (in these early surveys, detectors were located immediately downstream of the signal loop detector)

- (iv) The number of vehicles in a given distance from the signal stop-line, e.g. 90 m, for the purpose of determining the *jam spacing* (see *Figures 2.3 and 2.4*).
- (v) Signal change times recorded automatically using two temporary light sensors placed on the green and yellow signal lanterns and linked to a second VDAS unit (see *Figure 2.5*).
- (vi) For paired intersections, distance to the back of downstream queue recorded using a *laser gun* activated at the start of the green period at the upstream signal, and at various intervals during the green period. The laser gun was connected to the laptop computer as seen in *Figure 2.2*. Paired intersection surveys are discussed in more detail later in this section.

The timings of the laptop computer and the VDAS units are synchronised.

At the first few sites during earlier paired intersection surveys, the start and end times of the green periods were recorded by one of the observers who pressed the keys on the laptop computer. The accuracy of this method was found to be not satisfactory in relation to the first few vehicles departing from the queue. Subsequently, the light sensors were devised and used in the surveys.

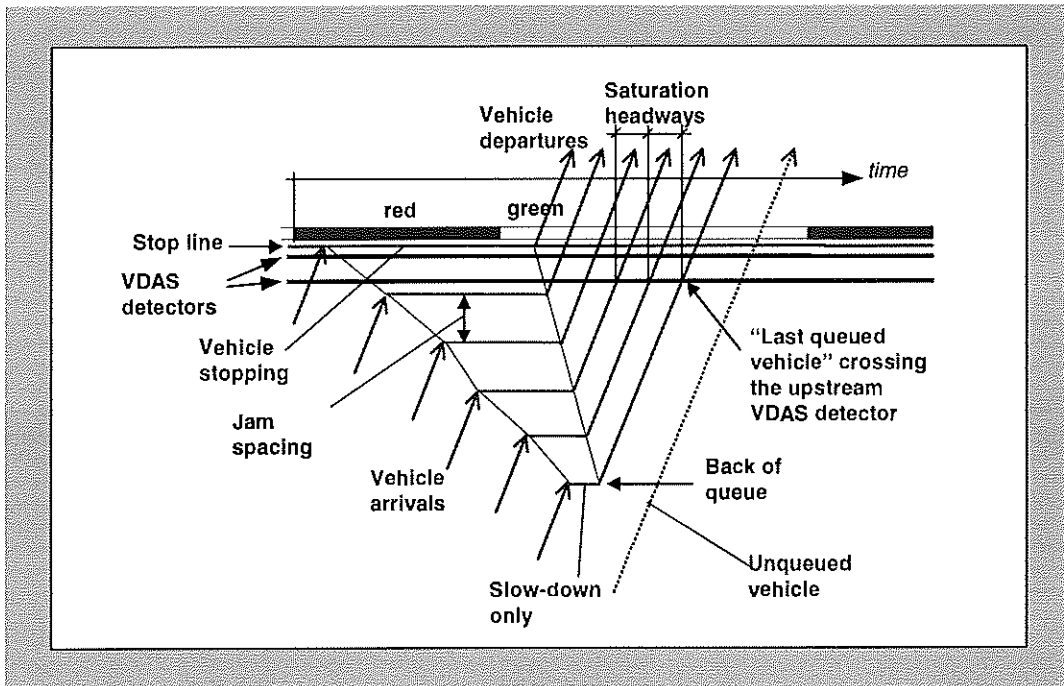


Figure 2.3 – Back of queue and last queued vehicle definition (using idealised speed-time trajectories): Undersaturated cycle

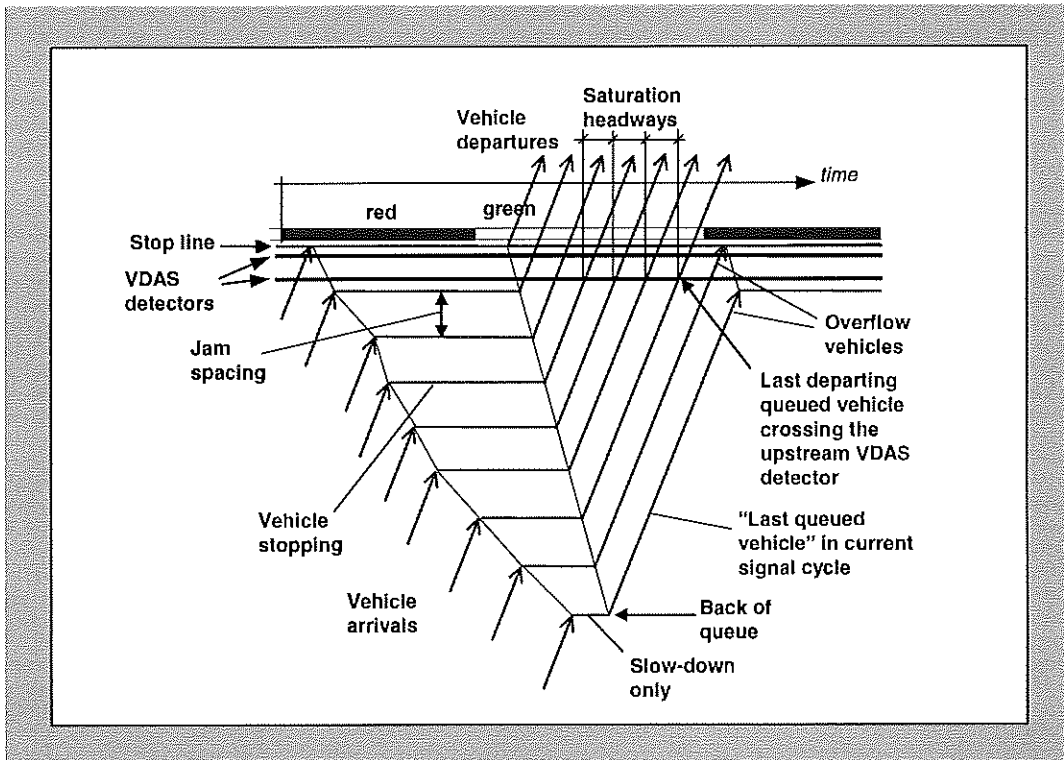


Figure 2.4 – Back of queue and last queued vehicle definition (using idealised speed-time trajectories): Oversaturated cycle

VDAS Equipment

VDAS is a traffic classifier developed by ARRB TR (Leschinski and Roper 1993). It offers options to produce a variety of vehicle classification and speed data formats. The VDAS 3000 model was used in these surveys. The VDAS system is easy to use, comprising a single printed cpu card housed in a weatherproof enclosure (see *Figure 2.6*). VDAS records data from treadle (switch) detectors or road tubes. Two treadle detectors were used in the surveys.

The two VDAS detector strips installed centred over the signal detector loop forms a *passage detection* system for data collection at signal stop line (*Figure 2.1*). With the 4.5 m signal detector loop, one of the detectors is located 0.75 m from the downstream edge of the loop and the other detector is located further upstream at a spacing of approximately 3.0 m. The latter will be referred to as the *first (upstream) detector*. Treadle switch positions and loop positions relative to the stop line are noted in the survey forms. *Figure 2.7* shows the VDAS setup used at the signal stop-line location.

In earlier surveys (sites Mel1 to Mel6 in 1996 surveys as described in *Section 3*), VDAS detector strips were placed immediately downstream of the signal stop line (*Figure 2.2*). The first VDAS detector was placed about 0.5 to 1.0 m downstream of the stop line and the second VDAS detector was placed further downstream at a spacing of about 3 m. After the analysis of data from these six sites, a different detector position was used. The detectors were centred over the signal detector loop so that data collected corresponds to loop data more closely. This method was used at site Mel7 in the 1996 surveys. In this case, the two VDAS detectors were placed over the signal loop, the first detector placed 1.5 m upstream of the stop line and the second detector placed further upstream at a spacing of 4.5 m.

Communication with VDAS is via an IBM compatible laptop computer. Normally, a software package called VCOM is used providing a menu-driven set of options for data collection and analysis. In the surveys described in this report, a special program written by Ron Roper (SIGCLASS) was used to analyse the raw survey data and produce data including time, class, number of axles, speed, headway and wheel base for individual vehicles crossing the stop line.

VDAS measures the headway and speed with reference to the times when the front (leading) and rear (trailing) axles of two consecutive vehicles cross the first (upstream) and second (downstream) detectors. This information is used to determine leading and trailing headways at the first and second detectors, and to calculate speeds based on time measurements for the leading and trailing ends of the vehicle, as well as an acceleration rate based on the assumption of constant acceleration over a short distance. The method used to determine these variables is described in detail in *Section 6*.



Figure 2.5 – Light sensors to record signal change times

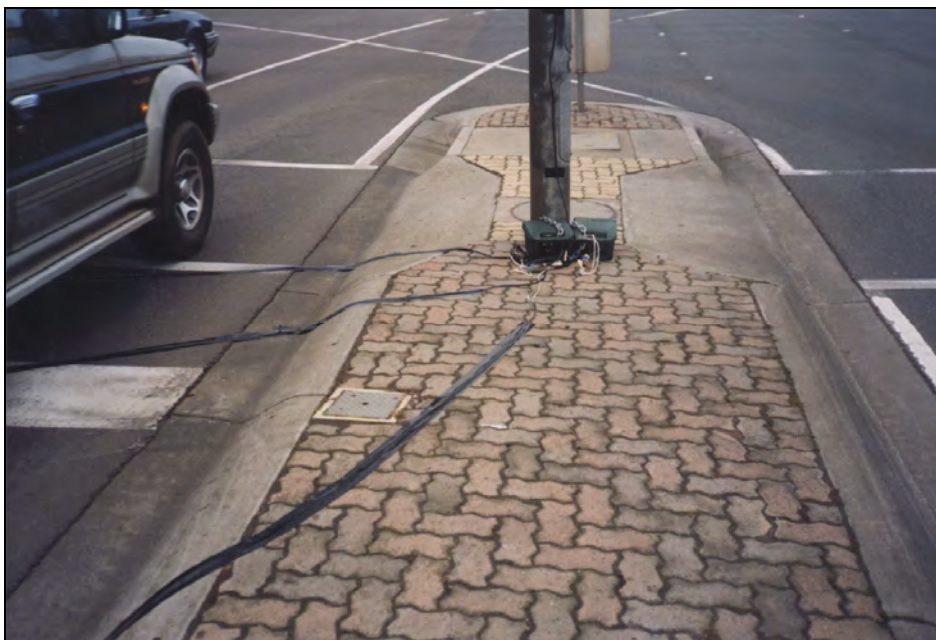


Figure 2.6 – The use of VDAS unit at the signal stop-line location



Figure 2.7 – The use of VADAS treadle switch detectors at the signal stop-line location

Observer Tasks

There are three tasks that are performed by three individual observers during each survey. Observers 1 and 2 must be physically located in the same area since the hand held buttons used to record movements are connected to the same laptop computer. The position chosen is selected to give as clear a view as possible of the traffic building at the back of queue of the measured lane and a clear view of the position of the treadle detectors. The opposite side of the road is often better than the near side.

Tasks 1 and 2 are performed for every cycle during the survey period. It is not necessary to perform Task 3 for every cycle.

General conditions of the survey site are recorded in the form shown in *Figure 2.8*.

Task 1 (Observer 1)

Observer 1 is required to identify and monitor the movement of the *last queued vehicle* in the measured lane. Once identified, the observer must then track, and press a hand held button attached to the laptop computer as the front of the vehicle crosses the *first (upstream) treadle detector*. The button used by Observer 1 has a long lead which allows free movement to assist in observing long queues.

Identifying the last queued vehicle is not an easy task in practice. As shown in *Figure 2.3* for the case of an undersaturated cycle, the queue building from the beginning of each red phase is observed and the last vehicle which either stops or is slowed noticeably by the queue in front is defined as the last queued vehicle. This is the same as the last vehicle at the *back of queue*. If the observer is uncertain whether a vehicle has slowed or not, the previous vehicle should be selected as the last queued vehicle.

In oversaturated signal cycles where the last queued vehicle cannot pass through the intersection during the current green phase (becomes an overflow vehicle as shown in *Figure 2.4*), the button should NOT be pressed. In analysing data, this will indicate an oversaturated cycle.

Special considerations apply to *short lanes* as in the case of dedicated right turn lanes. If the short lane is not full, i.e. the back of queue is contained within the short lane space, the normal method for identifying the last queued vehicle applies. If the short lane is full, the last queued vehicle is recorded as the last vehicle in the short lane space which is not queuing into the adjacent lane (provided it crosses the upstream VDAS detector in the current cycle).

Task 2 (Observer 2)

Observer 2 monitors the movements of the first few vehicles departing from the queue at the start of each green period. The first two vehicles in the queue are ignored as it is most likely that one or both of these vehicles has already crossed the treadle detectors or is stationary over the top of them. For the next five vehicles in the queue, the observer presses a hand held button as the front of the vehicle crosses the *first (upstream) treadle detector*. This task is necessary, as these early vehicles are difficult to identify automatically due to their low speed and acceleration.

Task 3 (Observer 3)

Observer 3 records manually on a clipboard information about the number of vehicles and the type of vehicles in the queue using forms shown in *Figures 2.9 and 2.10*.

For full-length lanes, the number of vehicles from the stop line out to 90 metres is recorded. For short lanes as in the case of dedicated right-turn lanes, the number of vehicles to the end of the short lane space or 90 metres, whichever is shorter, is counted.

In each of the above cases the type of vehicle is also noted, e.g. car, car towing, bus, rigid truck, articulated truck, and so on.

Where the lane is a shared lane, the proportion of turning vehicles and those going straight ahead is recorded.

Signalised Intersection Queue Discharge Flow and Speed Survey Form

Site No.: _____	Date: _____	Time: _____
Measured road: _____	Cross street: _____	
Suburb: _____	State: _____	
Intersection leg: _____	Lane No.: _____	Movement (T / L / R): _____
Weather: _____	Short Lane Length (m): _____	
Daylight conditions: _____	Map reference: _____	
Yellow time (s): _____	All-red time (s): _____	Speed limit (km/h): _____

Treadle Detectors		Upst.	Downst.
Distances (m) Stop Line to Downstream Detector: _____ Downstream to Upstream Detector: _____ To Upstream Intersection: _____ To Downstream Intersection: _____	Channel No.: <input type="checkbox"/> <input type="checkbox"/> <input type="checkbox"/> <input type="checkbox"/> VDAS No: _____ File name: _____ Clock correction: _____		

Signal Sensors	Clocks synchronised: <input type="checkbox"/>								
	Left Turn			Through			Right Turn		
Phases monitored:	R	Y	G	R	Y	G	R	Y	G
Channel No.:	<input type="checkbox"/>	<input type="checkbox"/>	<input type="checkbox"/>	<input type="checkbox"/>	<input type="checkbox"/>	<input type="checkbox"/>	<input type="checkbox"/>	<input type="checkbox"/>	<input type="checkbox"/>
VDAS No:	_____			_____			_____		
File name:	_____			_____			_____		
Clock corrections:	_____			_____			_____		

Observations	
Back of queue: <input type="checkbox"/>	Front of queue: <input type="checkbox"/>
Queue count & mix: <input type="checkbox"/>	PC log file name: _____

Traffic Conditions	
SCATS report requested:	Yes <input type="checkbox"/> No <input type="checkbox"/>
Description of intersection:	_____
Downstream restrictions:	_____
Adjacent lane restrictions:	_____
Unusual events:	_____

Comments / Photos / Diagrams

Figure 2.8 – Queue discharge flow and speed survey form

Vehicle Queue Spacing Survey Form

Site No: _____	Date: _____	Sheet _____	of _____					
Measured road: _____								
Intersection leg: _____		Lane No.: _____ Movement (T / L / R): _____						
Vehicle	Start of RED time (h:m:s)							
-2								
-1								
1								
2								
3								
4								
5								
6								
7								
8								
9								
10								
11								
12								
13								
14								
15								
16								
17								
18								
19								
20								
Space filled <input type="checkbox"/>								
Tick boxes if short lane space, or if 90 m space is filled.								
Instructions								
For car category, mark with a tick, dash or C. For other vehicle types use codes below or define new codes as needed Record motorcycles only if they are occupying lane space. Stop recording vehicles when short lane space or 90 m space is filled.								
Vehicle Codes								
✓ - C Car, 4WD, light van				ST Small rigid truck				
CT Car towing				LT Large rigid truck				
M Motor Cycle				AT Articulated truck				
				B Bus				

Figure 2.9 – Vehicle queue spacing survey form

**Vehicle Queue Discharge Movement Survey Form
For Shared Lanes Only**

Site No: _____		Date: _____		Sheet _____		of _____								
Measured road: _____		Intersection leg: _____		Lane No.: _____		Movement (T / L / R): _____								
	Start of RED time (h:m:s)													
Vehicle	Veh	Mov	Veh	Mov	Veh	Mov	Veh	Mov	Veh	Mov	Veh	Mov	Veh	Mov
1														
2														
3														
4														
5														
6														
7														
8														
9														
10														
11														
12														
13														
14														
15														
16														
17														
18														
19														
20														
Instructions														
For car category: leave vehicle type blank, just record the movement type, e.g. car turning right (R)														
For other vehicles: record vehicle and movement types, e.g. large truck (LT) going straight through (T)														
Vehicle Codes							Movement Codes							
(blank)	Car, 4WD, light van		ST	Small rigid truck			T	Through						
CT	Car towing		LT	Large rigid truck			L	Left Turn						
M	Motor Cycle		AT	Articulated truck			R	Right Turn						
			B	Bus										

Figure 2.10 – Survey form for shared lanes

Paired Intersection surveys

At the start of the first stage of this study, a significant amount of research effort went into establishing a survey method that produced data relevant to the paired intersection situation. This required covering a large area of traffic operations simultaneously since data about the back of upstream and downstream queues needed to be recorded.

The methods considered included the ARRB TR CAMDAS system for video-picture recording and subsequent laboratory analysis. This system is used with a trailer that can provide 10 m camera height. The use of several cameras with precise synchronisation would have been required. Wireless techniques including infra-red data and UHF radio links were considered for data transmission. Some of these techniques required some developmental work before they could be employed for the surveys. Considering the costs involved, these possibilities were discarded.

Single-camera techniques considered and trialed included video recording of the traffic operations at selected paired intersection using a helicopter (with a person filming manually) and a remote controlled model plane with a camera attached. These methods were not found feasible for technical, practical and cost reasons, and abandoned. The use of satellite, light aircraft, model helicopter and balloon were also considered but found not feasible from technical and cost viewpoints.

Finally, a relatively simple and practical survey method was designed which involved the use of laser gun to measure the distance to the back of downstream queue as well as the speed at the back of downstream queue, used in conjunction with the VDAS equipment (*Figure 2.2*). At the upstream stop line, the two VDAS detectors and two light sensors installed on the green and yellow signal lanterns were linked to VDAS units.

The laser gun was linked to the laptop computer and the readings were recorded automatically when an observer pressed the trigger. A second observer pressed a button connected to the laptop via a long cable to record the time at which the last queued vehicle crossed the stop line. Various comments were also entered directly into the laptop computer by a third observer who also had a supervisory role. Two additional light sensors installed on the green and yellow signal lanterns at the downstream stop line were linked to a third VDAS unit. The timings of the laptop computer and the VDAS units were synchronised.



Figure 2.11 – Photo showing the upstream queue and the laser gun aimed in the downstream direction at a paired intersection site (Site Mel5 in Melbourne)

3 SURVEY SITES

The survey sites consist of two main groups:

- (i) 1998 Sydney and Melbourne Sites (five sites in Sydney and six sites in Melbourne), and
- (ii) 1996 Melbourne sites (seven sites).

All sites in group (i) are isolated intersection sites although one site has CBD intersection characteristics (Site 413 in Sydney). These include through and right-turn traffic lanes (one site in Melbourne is a shared through and left-turn traffic lane). The term *isolated* used in this context means a single intersection site with a reasonably long distance to the downstream intersection as opposed to a *paired* (or closely-spaced) intersection site, and does not relate to the signal control method used at the site.

Group (ii) includes isolated and paired intersection sites, located in the eastern suburbs of Melbourne. They are all through traffic lanes except one site which is a shared through and left-turn traffic lane. These surveys were actually carried out during late 1993 to mid-1994, but are referred to by the year of the original report (Akçelik and Besley 1996). The calibration results given for these sites (*Section 9*) differ from those given in the original report due to the revised calibration method.

For all sites, queue discharge data relates to a single lane of traffic with negligible effect of slip lane or short lane traffic on through traffic lanes. All sites are controlled by vehicle-actuated signals.

Survey site characteristics for Sydney and Melbourne 1998 sites are summarised in *Tables 3.1 and 3.2*. These survey sites are labelled using their SCATS intersection numbers. Data collected during AM and PM peak periods at Site 163 in Sydney were combined together in calibrating the queue discharge models for this site. Heavy vehicle percentages for Sydney and Melbourne 1998 sites are given in *Tables 9.1 and 9.2* in *Section 9* which summarises queue discharge model calibration results.

Site characteristics for Melbourne 1996 sites are summarised in *Tables 3.3*. Site Mell in *Table 3.3* is the same as Site 456 in *Table 3.1*. This provides an opportunity to compare results from surveys carried out at two different dates (although the survey method used in 1998 was more refined).

In *Tables 3.1 to 3.3*, lane numbers indicated are based on lane counting from kerb side towards the middle of the road looking towards the downstream direction.

For all Sydney and Melbourne 1998 sites:

- (i) the photos from each site are shown in *Figures 3.1 to 3.11* given at the end of this section, and
- (ii) SCATS intersection geometry and phasing diagrams are shown in *Appendix A*.

An effort was made to select survey sites in Sydney and Melbourne with similar characteristics although analysis in terms of comparing traffic in different cities may not be meaningful due to many factors affecting traffic behaviour.

Table 3.1

Sydney 1998 Survey Site Characteristics

Site no.	Intersection	Lane	Speed limit (km/h)	Period
TCS163 AM	Pacific Hwy and Mowbray Rd. in Chatswood. 3 through lanes, 1 right turn lane. Major divided urban arterial with intersecting collector road.	Lane 4: Right turn lane on Pacific Hwy. Short lane. South approach (against heavy through traffic on North approach). Lane width: 2.8 m Lane length: 69 m Downstream dist: 350 m	60	6.30 - 9.00 am Sunrise 6.34 am
TCS163 PM	As for TCS163 AM	As for 163 AM except right turn lane now carrying heavier traffic and through traffic on North approach is lighter.	60	4.00 - 6.00 pm Sunset 5.09 pm
TCS610	Military Rd. and Murdoch St. in Cremorne. 2 through lanes, 1 right turn lane. Narrow divided urban arterial with intersecting collector road.	Lane 3: Right turn lane on Military Rd. Short lane. West approach carrying evening peak. Lane width: 2.9 m Lane length: 52 m Downstream dist: 400 m	60	4.00 - 6.00 pm Sunset 5.09 pm
TCS1081	Lilyfield Rd. and James St. in Lilyfield. 2 through lanes. Collector with 9% grade on approach, flat after intersection. Intersecting collector.	Lane 2 on Lilyfield Rd (Through traffic). Northwest approach carrying morning peak traffic to Southeast. Lane width: 3.2 m Downstream dist: 1000 m	60	6.40 - 8.40 am Sunrise 7.01 am
TCS413	Broadway and City Rd. in Broadway. 3 through lanes, 1 left turn lane. Inner urban divided arterial with intersecting arterial on left.	Lane 3 on Broadway (Through traffic). East approach carrying evening peak. Lane width: 3.0 m Downstream dist: 140 m	60	4.00 - 6.00 pm Sunset 4.55 pm
TCS511	General Holmes Dve and Bestic St. in Kyeemagh 3 through lanes. Urban divided arterial with intersecting collector on left.	Lane 2 on General Holmes Dve (Through traffic). South approach carrying morning peak. Lane width: 3.4 m Downstream dist: 2700 m	70	6.30 - 9.00 am Sunrise 7.01 am

Table 3.2

Melbourne 1998 Survey Site Characteristics

Site no.	Intersection	Lane	Speed limit (km/h)	Period
TCS121	Maroondah Hwy and Mitcham Rd in Mitcham. 3 through lanes, 1 right turn lane. Major divided urban arterial with intersecting undivided arterial.	Lane 4: Right turn lane on Maroondah Hwy. East approach. Lane width: 2.85 m Lane length: 110 m Downstream dist: 160 m	70	4.00 - 6.00 pm Sunset 6.30 pm
TCS335	Doncaster Rd and Blackburn Rd in East Doncaster. 3 through lanes, 1 right turn lane. Divided urban arterial with intersecting divided collector	Lane 4: Right turn lane on Doncaster Rd. East approach. Lane width: 3.0 m Lane length: 110 m Downstream dist: 780 m	70	4.00 - 6.00 pm Sunset 6.35 pm
TCS3196	Middleborough Rd and Highbury Rd in East Burwood. 1 through & left, 1 through & right lane. Undivided arterial with intersecting collector road.	Lane 1: Through and left turn lane on Middleborough Rd. North approach. No slip lane. Lane width: 3.15 m Downstream dist: 1400 m	60	4.00 - 6.00 pm Sunset 6.35 pm
TCS4273	Toorak Rd and Tooronga Rd in Hawthorn East. 2 through lanes, right turn lane. Narrow undivided arterial with uphill grade on approach (approx. 6 %), reduced grade after intersection. Intersecting collector road.	Lane 2 on Toorak Rd (Through traffic). West approach. Lane width: 2.8 m Downstream dist: 900 m	60	4.30 - 6.30 pm Sunset 6.24 pm
TCS849	Canterbury Rd and Mitcham Rd in Vermont. 1 through & left, 2 through, 2 right turn lanes. Narrow divided arterial with intersecting collector.	Lane 2 on Canterbury Rd (Through traffic). West approach. Lane width: 3.05 m Downstream dist: 1600 m	70	4.00 - 6.00 pm Sunset 6.37 pm
TCS456	Ferntree Gully Rd and Stud Rd in Scoresby. 1 through & left, 3 through, 2 right turn lanes. Wide major divided arterial with intersecting divided arterial.	Lane 4 on Ferntree Gully Rd (Through traffic). West approach. Lane width: 3.5 m Downstream dist: 1000 m	80	4.00 - 6.00 pm Sunset 6.30 pm

Table 3.3

Melbourne 1996 Survey Site Characteristics

Site no.	Intersection	Lane	Speed limit (km/h)	Period
Mel1	Ferntree Gully Road and Stud Road in Scoresby. Isolated intersection site.	Lane 4 of 4 through lanes on Ferntree Gully Road West approach.	80	4.00 - 6.00 pm
Mel2	Kooyong Road and Dandenong Road in Armadale. Paired intersection site (a wide-median intersection with the median storage area downstream of the lane surveyed).	Lane 1 of 2 through lanes on Kooyong Road North approach (shared through and left-turn lane).	60	4.00 - 6.00 pm
Mel3	South Eastern Arterial and Burke Road in Glen Iris. Isolated intersection site. Grade-separated since the surveys.	Lane 3 of 3 through lanes on South Eastern Arterial West approach.	80	4.00 - 6.00 pm
Mel4	Canterbury Road and Middleborough Road in Box Hill. Isolated intersection site.	Lane 1 of 2 through lanes on Canterbury Road West approach (shared through and left-turn slip lane).	60	4.00 - 6.00 pm
Mel5	Pedestrian Crossing on Canterbury Road in East Camberwell. Paired intersection site (upstream of two closely-spaced pedestrian crossings).	Lane 1 of 2 through lanes on Canterbury Road East approach.	60	8.00 - 9.00 am
Mel6	Boronia Road and Wantirna Road in Wantirna. Paired intersection site (upstream of the intersection of Boronia Road and Mountain Highway).	Lane 2 of 3 through lanes on Boronia Road West approach.	80	4.20 - 6.20 pm
Mel7	Ferntree Gully Road and Scoresby Road in Knoxfield. Isolated intersection site.	Lane 3 of 3 through lanes on Ferntree Gully Road West approach.	80	4.00 - 6.00 pm

Surveys were carried out mostly during morning and afternoon peak periods. Morning peak surveys were conducted typically from 7.00 am to 9.00 am. Afternoon peak surveys were conducted for a maximum of about two and half hours each, typically from 4.00 pm to 6.30 pm. At the Melbourne 1996 survey site Mel5, queue interaction effects were observed during the period 8.00 am to 9.00 am.

Isolated intersection sites were selected to ensure that there were no downstream queue interference to the departures of vehicles from the subject approach lane. For this purpose, the distance to the nearest upstream and downstream intersections were recorded and any downstream and upstream interference (interruption to the flow of traffic) were recorded in the survey form (*Figure 2.8*).

Paired intersection sites included in group (ii) are closely spaced relative to a downstream signalised intersection which affects the queue discharge characteristics at the survey site. However, signal cycles with any downstream queue interference (speed reduction or blockage due to the downstream queue at the survey lane) were not included in the calibration of the basic queue discharge speed and flow rate models for the paired intersection sites (Mel2, Mel5 and Mel6). Thus, the queue discharge model parameters represent the geometric and environmental conditions only rather than direct queue interference which is a function of demand levels and signal timing parameters. Downstream queue interference at paired intersection sites is considered separately. The results are discussed in *Section 11*.

In selecting the survey sites, the aim was to cover different lane types at intersections of different size, including the following:

- (i) through traffic lane at a high design intersection (large intersection on a major arterial road, open-feel environment, wide lanes clearway, minimal or no friction),
- (ii) through traffic lane at a low design intersection (small intersection on an arterial road with a restricted-feel environment, narrow lanes, but with clearway conditions and minimal or no friction),
- (iii) through traffic lane on an approach road with significant uphill grade prior to stop line,
- (iv) shared through and left-turn lane (both movements subject to signal control, i.e. not slip lane sites),
- (v) fully-controlled right-turn lane (short lane or full-length lane), with short and long green times.

Right-turn traffic lanes surveyed included single right-turn lane sites only. All right-turn movements were fully controlled (i.e. subject to green and red arrow signals).

For all 1998 survey sites, SCATS control parameters MF (maximum flow) and KP (occupancy time at maximum flow) were obtained from road traffic authorities in Sydney and Melbourne (see *Sections 4 and 13*).

Various comments on observed site conditions are given below.

Observed Site Conditions at SYDNEY 1998 Sites

The following notes on observed site conditions provide a qualitative assessment of the conditions that prevailed at the time the surveys were conducted. Weather conditions during all the surveys were fine with dry roads and good visibility. The surveys were conducted during May and June hence part of each survey was conducted either before sunrise or after sunset.

Site 163

During the morning survey when traffic in the right turn lane was opposing peak city-bound traffic, green times were very short with only a handful of vehicles getting through each cycle. Close following behaviour and red arrow running were quite noticeable during this survey. Many vehicles were in the queue for several cycles before getting through. The afternoon survey at this site showed less frantic behaviour with the longer green times. Drivers also seemed less inclined to run the red arrow at the end of the phase.

Site 610

This site appeared to be operating in a similar fashion to the afternoon survey at Site 163. The only abnormal behaviour noticed was occasional drivers who ignored the red arrow well after the end of the turn phase and continued into the intersection to complete a filtered right turn. This behaviour was probably due to the absence of the permitted filtered right-turn which normally operates at this site during afternoon peak periods. This phase was disabled for the duration of the survey to ensure that a fully controlled right-turn phase was operating.

Site 413

This site appeared to have a greater number of vehicles changing lanes prior to passing through the intersection than was observed at other sites. This had the effect of leaving occasional larger headways between vehicles than would otherwise have been the case. Observation of the end of the queue was difficult at this site due to obscured vision from adjacent lane traffic.

Site 1081

This site operated at saturated conditions for most of the survey period. It was noted that the majority of heavy vehicles chose to travel in the left lane rather than the right lane under observation in this study. The signal controller developed a technical fault before the end of the planned survey period, no SCATS data was available from this site due to this technical problem.

Site 511

This very busy site was running at saturation for the entire survey period with very long green times. Traffic appeared to be very consistent during each cycle and very little lane changing was observed. This survey ended earlier than planned due to the VDAS detectors being ripped up by a street sweeper.

Observed Site Conditions at MELBOURNE 1998 Sites

Site 121

The right turn lane at this site operated at saturation for much of the survey period. The lane is over 100m in length and quite narrow at 2.85 m. Several instances of downstream blockage were observed which caused a delay in the departure of the right turn traffic. Signal cycles with this effect were not included in the data analysed.

Site 335

The length of the right turn lane at this site is similar to Site 121 however the width is slightly wider at 3 m. Traffic here is generally less congested than Site 121 both in the measured lane and the through lanes. Cross traffic was also much lighter with no downstream obstructions observed. At this site and Site 121, vehicles performing U-turns were observed on several occasions, reducing the speed of the following vehicle. Signal cycles with this effect were not included in the data analysed.

Site 3196

Traffic on Middleborough Road became very heavy during the survey period. Queues extended from Burwood Hwy to Highbury Rd in both directions for much of the survey period. The flow of through traffic was affected by the left turning traffic (15 per cent) in the measured lane.

Site 4273

Toorak Road carries evening peak traffic exiting the Southeastern Freeway from the city towards the Eastern suburbs. The approach to the intersection has an uphill grade of around 6% flattening out significantly on the downstream side. A relatively high proportion of large vehicle spacings in the stationary queue (jam spacings) were observed at this site, presumably influenced by the steep grade.

Site 849

The lanes at this site are quite narrow on the approach to the intersection due to the addition of two right turn lanes. Geometrically, this site appears similar to Site 413 in Sydney as it has a slight uphill grade on the approach with narrow lanes.

Site 456

This large intersection carries high traffic volumes in all directions during evening peak. The end of queue was marked prematurely in many instances due to traffic leaving the measured lane and entering the two right-turn lanes. A brief rain and wind squall during the survey did not appear to interfere with traffic flow although the sensors attached to the signals failed to record some cycles during this period. Signal cycles with this effect were not included in the data analysed (except in the analysis of jam spacing).

Melbourne 1996 Survey Sites

At the early stages of this study, the emphasis was on paired intersections with downstream queue interference. Difficulty was experienced finding paired intersection sites that gave adequate data for this purpose, and the effort for finding sites that gave useful data was not entirely successful. The reason was that most paired intersection sites had good signal phasing design that solved the queue interaction problem, or queue interaction occurred only in a limited number of ways providing few data points per site. The latter was the main reason for discarding full surveys at the intersection of Ferntree Gully Road with Springvale Road and Brandon Park Drive, and the intersection of Warrigal Road with Highbury Road and Burwood Highway.

Sites Mel1 to Mel4 and Mel7 provide data without downstream queue effects. Sites Mel5 and Mel6 are paired intersection sites selected to analyse queue interaction effects. The distances between the upstream and downstream stop lines at Sites Mel5 and Mel6 were about 190 m and 170 m, respectively.

Site Mel2 is a wide-median intersection, where the median storage area was downstream of the through lane surveyed. The signal phasing arrangement at Site Mel2 resulted in no queue interaction effects. The queue discharge characteristics of this lane are also affected by the left-turn traffic in the lane.

**Photographs showing
Sydney and Melbourne 1998 Survey Sites**



Figure 3.1 – Intersection 163: Pacific Highway - Mowbray Road (Chatswood, Sydney). Lane 4 on Pacific Highway, South approach, right-turn traffic



***Figure 3.2 – Intersection 610: Military Road - Murdoch Street (Cremorne, Sydney).
Lane 3 on Military Road, West approach, right-turn traffic***



Figure 3.3 – Intersection 1081: Lilyfield Road - James Street (Lilyfield, Sydney). Lane 2 on Lilyfield Road, Northwest approach, through traffic, 9% uphill grade



*Figure 3.4 – Intersection 413: Broadway - City Road (Ultimo, Sydney).
Lane 3 on Broadway, East approach, through traffic*



Figure 3.5 – Intersection 511: General Holmes Drive and Bestic Street (Kyeemagh, Sydney). Lane 2 on General Holmes Drive, South approach, through lane



Figure 3.6 – Intersection 121: Maroondah Highway and Mitcham Road (Mitcham, Melbourne). Lane 4 on Maroondah Highway, East approach, right turn lane



Figure 3.7 – Intersection 335: Doncaster Road and Blackburn Road (East Doncaster, Melbourne). Lane 4 on Doncaster Road, East approach, right turn lane



Figure 3.8 – Intersection 3196: Middleborough Road and Highbury Road (East Burwood, Melbourne). Lane 1 on Middleborough Road, North approach, shared through and left-turn lane



Figure 3.9 – Intersection 4273: Toorak Road and Tooronga Road (Hawthorn East, Melbourne). Lane 2 on Toorak Road, West approach, through lane, 6% uphill grade



Figure 3.10 – Intersection 849: Canterbury Road and Mitcham Road (Vermont, Melbourne). Lane 2 on Canterbury Road, West approach, through lane



Figure 3.11 – Intersection 456: Ferntree Gully Road and Stud Road (Scoresby, Melbourne). Lane 4 on Ferntree Gully Road, West approach, through lane

4 DATA PROCESSING

Initial Data Processing

Careful processing of raw data collected by VDAS equipment was carried out to maximise the useful vehicle data, especially for those vehicles departing during the initial part of each green period. For this purpose, the data files were processed to identify vehicles which had not been correctly classified by VDAS automatically. This involved merging the unclassified axle detections with the classified vehicles, signal detections and observer comments into one chronological file for each site. Each file was then closely examined for either incorrectly classified vehicles or unclassified detections, and where errors existed, manual classification and adjustment of headways enabled virtually all vehicles to be accounted for.

Preparation of the data files for the regression analyses required the exclusion of some vehicles from the traffic stream during each cycle. The following criteria were used to exclude these vehicles:

- All vehicles recorded after the yellow signal in each cycle.
- All vehicles recorded after the manually recorded end of queue signal.
- All AUSTROADS (1988) class 2 vehicles and larger (“heavy vehicles”).
- The first vehicle following an AUSTROADS (1988) class 2 vehicle or larger.
- Vehicles that had clearly been unduly delayed by a vehicle ahead which was either significantly slower than the vehicle in front of it or very slow to begin moving.
- Vehicles at the front of the queue where a valid headway or speed could not be determined.

The first vehicle in the queue was usually stationary over the detectors prior to the green signal and therefore neither a valid speed nor headway could be determined. The second vehicle was usually stationary behind the detectors, therefore a valid speed could be determined, but a headway could not be calculated due to the first axle of the vehicle ahead having crossed the detectors prior to the green signal.

In some instances, it was evident from the data that a slow moving vehicle had fully crossed the detectors during the red phase and had stopped at some point beyond the detectors. Taking into account the relative position of the next vehicle in the queue in relation to the detectors and the measured distance from the stop line to the detectors, it was possible to make a judgment about whether the first vehicle was actually in the queue or not. In cases where it was apparent that the first vehicle had stopped downstream of the stop line, that vehicle was not considered to be part of the queue.

The initial processing of VDAS data produced a file with time, vehicle class, number of axles, wheelbase, speed, headway, queue position and time since start of green for each vehicle, and markers for signal change times, vehicles 3-7 and the last vehicle from the back of queue. These files were imported into Excel spreadsheets for further analysis. *Figure 4.1* shows an example of the processed survey data file. In the case of earlier paired intersection surveys for downstream queue effects, additional data were entered into the processed file including the distance to the back of downstream queue and the corresponding speed. An example is given in *Figure 4.2*.

Time	Time in Seconds	Comment	Vehicle class	No. of axles	Speed	Headway	Wheelbase	Queue position	Time since green	Cycle No.
15:56:34.895	57394.895	GREEN								
15:56:37.588	57397.588		1	2				1		1
15:56:38.662	57398.662		1	2	15.74		2478	2	3.767	1
15:56:40.394	57400.394	VEHICLES 3-7	1	2	22.41	1.73	2668	3	5.499	1
15:56:42.367	57402.367	VEHICLES 3-7	1	2	24.86	1.97	2506	4	7.472	1
15:56:44.195	57404.195	VEHICLES 3-7	1	2	28.57	1.83	2395	5	9.300	1
15:56:45.202	57405.202	VEHICLES 3-7	1	2	30.13	1.01	2354	6	10.307	1
15:56:47.058	57407.058	VEHICLES 3-7	1	2	34.23	1.86	2528	7	12.163	1
15:56:49.212	57409.212		1	2	37.71	2.15	2589	8	14.317	1
15:56:50.354	57410.354		1	2	41.07	1.14	2438	9	15.459	1
15:56:51.591	57411.591		1	2	34.73	1.24	2800	10	16.696	1
15:56:52.840	57412.840		1	2	36.99	1.25	2505	11	17.945	1
15:56:54.533	57414.533		1	2	41.07	1.69	2524	12	19.638	1
15:56:57.194	57417.194	EOQ	1	2	55.82	2.66	2646	13	22.299	1
15:56:59.660	57419.660		3	2	34.84	2.47	3239	14	24.765	1
15:57:01.579	57421.579		1	2	37.76	1.92	2770	15	26.684	1
15:57:04.194	57424.194		1	2	37.57	2.62	2730	16	29.299	1
15:57:06.544	57426.544		1	2	40.53	2.35	2429	17	31.649	1
15:57:07.790	57427.790		1	2	41.15	1.25	2886	18	32.895	1
15:57:09.028	57429.028		1	2	41.54	1.24	2806	19	34.133	1
15:57:10.476	57430.476		1	2	43.99	1.45	2319	20	35.581	1
15:57:12.586	57432.586		1	2	45.57	2.11	2672	21	37.691	1
15:57:14.459	57434.459		2	3	52.09	1.87	5682	22	39.564	1
15:57:15.773	57435.773	YELLOW								
15:58:41.955	57521.955	GREEN								
15:58:43.816	57523.816		1	2				1		2
15:58:45.116	57525.116		1	2	16.75		2483	2	3.161	2
15:58:48.610	57528.610	VEHICLES 3-7	1	2	20.04	3.49	2284	3	6.655	2
15:58:50.237	57530.237	VEHICLES 3-7	1	2	19.91	1.63	2569	4	8.282	2
15:58:52.140	57532.140	VEHICLES 3-7	1	2	25.16	1.90	2952	5	10.185	2
15:58:53.843	57533.843	VEHICLES 3-7	1	2	28.16	1.70	2539	6	11.888	2
15:58:55.835	57535.835	VEHICLES 3-7	1	2	32.64	1.99	2332	7	13.880	2
15:58:57.214	57537.214		1	2	32.10	1.38	2614	8	15.259	2
15:58:58.801	57538.801		1	2	35.24	1.59	2436	9	16.846	2
15:59:00.090	57540.090		1	2	39.42	1.29	2393	10	18.135	2
15:59:03.236	57543.236		1	2	39.06	3.15	2516	11	21.281	2
15:59:04.444	57544.444		1	2	36.86	1.21	2858	12	22.489	2
15:59:06.117	57546.117		1	2	38.78	1.67	2935	13	24.162	2
15:59:08.544	57548.544		1	2	39.85	2.43	2934	14	26.589	2
15:59:11.013	57551.013		1	2	37.18	2.47	2713	15	29.058	2
15:59:12.514	57552.514		1	2	40.83	1.50	2728	16	30.559	2
15:59:14.174	57554.174		1	2	42.35	1.66	2578	17	32.219	2
15:59:16.035	57556.035		1	2	45.38	1.86	2673	18	34.080	2
15:59:18.844	57558.844		1	2	47.68	2.81	2815	19	36.889	2
15:59:20.195	57560.195	EOQ	1	2	51.31	1.35	2585	20	38.240	2
15:59:24.968	57564.968		1	2	53.47	4.77	2584	21	43.013	2
15:59:25.746	57565.746	YELLOW								
15:59:27.210	57567.210		1	2	53.07	2.24	2617	22	45.255	2
15:59:29.026	57569.026		1	2	53.20	1.82	2231	23	47.071	2
16:00:42.942	57642.942	GREEN								

Figure 4.1 – An example of processed survey data file

Hour	Min	Sec	Vehicle class	Number of axles	Speed	Headway	Wheelbase
8	22	41.9	UPSTREAM GREEN				
8	22	42.5	-15	98.9			
8	22	44.6	1	2	18.24	2.7	2665
8	22	47.0	1	2	22.18	2.4	2753
8	22	50.4	DOWNSTREAM GREEN			←	Signal marker
8	22	51.6	1	2	20.85	4.66	2397
8	22	53.8	1	2	23.68	2.16	2749
8	22	55.7	1	2	27.98	1.88	2440
8	22	57.4	1	2	25.65	1.77	2529
8	22	59.5	1	2	24.6	2.09	2521
8	23	1.4	1	2	27.84	1.87	2690
8	23	3.2	-27	← 24.4			Speed of vehicle at back of downstream queue
8	23	3.6	1	2	28.88	2.22	2743
8	23	5.7	1	2	26.6	2.06	2519
8	23	6.9	-25	21.7	←		Distance to back of downstream queue
8	23	8.4	1	2	25.17	2.68	2811
8	23	11.0	1	2	25.23	2.66	2411
8	23	11.3	-2	18			
8	23	13.8	1	2	20.34	2.75	2960
8	23	15.9	1	2	17.91	2.16	2298
8	23	17.7	1	2	10.47	1.74	2375
8	23	19.7	-1	15.3			
8	23	24.2	1	2	14.4	6.5	2663
8	23	27.5	1	2	15.93	3.29	2752
8	23	29.5	1	2	17.14	2.08	2704
8	23	32.0	1	2	22	2.48	2450
8	23	34.3	1	2	24.05	2.25	2759
8	23	36.2	1	2	26.8	1.95	2947
8	23	40.5	1	2	34.29	4.26	2619
8	23	41.7	1	2	35.76	1.21	2602
8	23	43.6	1	2	36.86	1.93	2447
8	23	45.3	1	2	33.13	1.67	2530
8	23	47.3	1	2	34.39	2.01	2942
8	23	49.2	-20	28			
8	23	49.5	1	2	33.64	2.17	2943
8	23	51.6	1	2	25.59	2.12	2744
8	23	53.6	1	2	22.04	1.99	2687
8	23	54.4	-2	23.9			
8	23	55.2	1	2	20.26	1.64	2780
8	24	12.7	1	2	6	17.49	1812
8	24	17.2	1	2	6.52	4.51	2840
8	24	22.2	1	2	14.15	4.99	2504
8	24	23.4	1	2	14.15	1.25	2495
8	24	24.4	UPSTREAM YELLOW			←	Signal marker
8	24	28.4	1	2	20.45	4.93	2670
8	24	28.6	-17	13.7			
8	24	29.9	DOWNSTREAM YELLOW				
8	24	51.8	UPSTREAM GREEN				

Figure 4.2 – An example of processed data file for paired intersection surveys

Jam Spacing

During the red phase of each cycle, an observer recorded the number and type of stationary vehicles in the first 90 m of the queue for through lanes or in the case of the right turn lane sites, the vehicles in the short lane space. This data enabled average *jam spacing* to be calculated for the actual mix of traffic in the queues, for light vehicles only and for heavy vehicles only as follows.

The average jam spacing considering all vehicles is given by:

$$L_{hj} = (1 - p_{HV}) L_{hjLV} + p_{HV} L_{hjHV} \quad (4.1)$$

where

L_{hj} = average jam spacing for all traffic in queue,

L_{hjLV} = average jam spacing for light vehicles,

L_{hjHV} = average jam spacing for heavy vehicles, and

p_{HV} = proportion of heavy vehicles in queue.

The method is applied as follows:

- (i) L_{hj} is calculated using data from all the observed queues,
- (ii) L_{hjLV} is calculated using data from queues where no heavy vehicles were present, and
- (iii) L_{hjHV} is then calculated from:

$$L_{hjHV} = [L_{hj} - (1 - p_{HV}) L_{hjLV}] / p_{HV} \quad (4.2)$$

The resulting average jam spacing values for each site are listed in *Section 9*.

Non-linear regression analyses were carried out to calibrate the queue discharge speed model using the SPSS package (Norusis and SPSS 1993). The measured light vehicle jam spacing values (L_{hjLV}) were used in calibrating the queue discharge flow rate model. The model calibration procedure is described in *Section 8*, and calibration results are given in *Section 9*.

SCATS Control Parameters

The SCATS control parameters MF (maximum flow), HW (headway time at maximum flow) and KP (occupancy time at maximum flow) for each site as reported by road traffic authorities are presented in *Tables 4.1 and 4.2* for the Sydney and Melbourne 1998 sites. These values were reported by the SCATS system on the day prior to the survey for Sydney sites, and on the day following the survey for Melbourne sites.

These parameters are further discussed in *Section 13*.

Table 4.1**SCATS Parameters for Measured Lanes at SYDNEY Sites**

Parameter	Right-turn lane sites		Through lane sites		
	TCS163	TCS610	TCS1081	TCS413	TCS511
MF (pcu/h)	1895	1579	1818	1714	2156
HW (seconds/pcu)	1.90	2.28	1.98	2.10	1.67
KP (seconds/pcu)	1.27	1.54	0.96	1.19	0.75

Table 4.2**SCATS Parameters for Measured Lanes at MELBOURNE Sites**

Parameter	Right-turn lane sites		Through lane sites			
	TCS121	TCS335	TCS3196	TCS4273	TCS849	TCS456
MF (pcu/h)	1925	1915	1905	1827	2034	2236
HW (seconds/pcu)	1.87	1.88	1.89	1.97	1.77	1.61
KP (seconds/pcu)	1.26	1.24	0.91	na	0.76	0.76

na: not available

Measured Green and Cycle Times

Tables 4.3 and 4.4 summarise measured green times and cycle times for the Sydney and Melbourne 1998 sites. Measured green and cycle times for the Melbourne 1996 sites are given in Table 4.5.

From Table 4.3 it can be seen that the average length of the right turn green phase at Site 163 was considerably longer during the evening peak than during the morning peak. Table 4.3 also highlights the consistently long green phase observed at Site 511 in comparison with the other through lane sites.

Measured Intergreen Times

At most sites, the intergreen time was 6.0 s, consisting of 4.0 s yellow time and 2.0 s all-red time. Exceptions were:

Site 413: Intergreen time = 6.5 s (yellow time = 4.0 s, all-red time = 2.5 s)

Site 511: Intergreen time = 6.5 s (yellow time = 4.5 s, all-red time = 2.0 s)

Sites 121 and 335: Intergreen time = 5.0 s (yellow time = 3.0 s, all-red time = 2.0 s)

Site 456: Intergreen time = 7.0 s (yellow time = 4.5 s, all-red time = 2.5 s)

Table 4.3**Measured Green Times and Cycle Times (seconds) from Signal Detectors at SYDNEY 1998 Sites**

	Right-turn lane sites			Through lane sites		
	TCS163 PM	TCS163 AM	TCS610	TCS1081	TCS 413	TCS 511
Green Times						
Minimum	8	6	11	51	35	111
Average	19	7	13	64	60	120
Maximum	30	20	20	81	82	125
Cycle Times						
Minimum	114	74	130	110	118	148
Average	148	139	149	131	140	160
Maximum	177	154	162	163	165	172

Table 4.4**Measured Green Times and Cycle Times (seconds) from Signal Detectors at MELBOURNE 1998 Sites**

	Right-turn lane sites		Through lane sites			
	TCS121	TCS335	TCS3196	TCS4273	TCS849	TCS456
Green Times						
Minimum	12	12	18	31	41	25
Average	20	23	32	43	52	36
Maximum	40	29	43	66	59	55
Cycle Times						
Minimum	114	98	109	80	121	118
Average	139	112	120	109	130	140
Maximum	159	125	142	129	138	168

Table 4.5

Measured Green Times and Cycle Times (seconds) from Signal Detectors at MELBOURNE 1996 Sites

	Isolated intersection sites				Paired intersection sites		
	Mel 1	Mel 3	Mel 4	Mel 7	Mel 2	Mel 5	Mel 6
Green Times							
Minimum	31	31	58	11	21	39	31
Average	43	59	67	35	33	102	42
Maximum	58	82	80	59	45	148	54
Cycle Times							
Minimum	129	94	118	40	115	61	103
Average	158	131	130	75	138	129	121
Maximum	195	186	142	101	159	175	136

Cumulative Queue Discharge Flow Rates

To visualise the relative mean queue discharge rates of each intersection, the mean time since start of green (t) was calculated using queue position as the aggregation variable. The results are presented graphically in *Figure 4.3* for the right-turn lane sites and *Figure 4.4* for the through lane sites in Sydney. It can be seen from *Figure 4.3* that the morning survey at Site 163 showed a noticeably higher flow rate than either of the other two right-turn lane surveys (due to very short green time). This is consistent with the observed behaviour during the survey where short headways were evident. Site 163 during the afternoon survey and Site 610 produced very similar traces.

From *Figure 4.4*, the consistent heavy flow at Site 511 can be seen to extend right through until the end of the very long green phase at this site. The traces for Site 413 and Site 1081 show a slight flattening near the end of the green phase indicating under-saturated conditions.

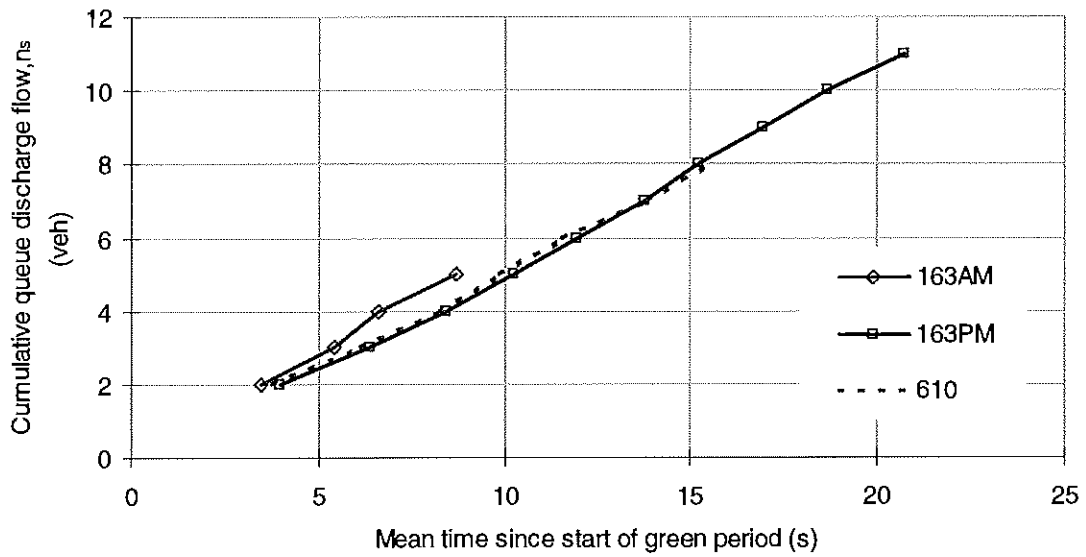


Figure 4.3 – Mean cumulative queue discharge flows - Right turn lane sites

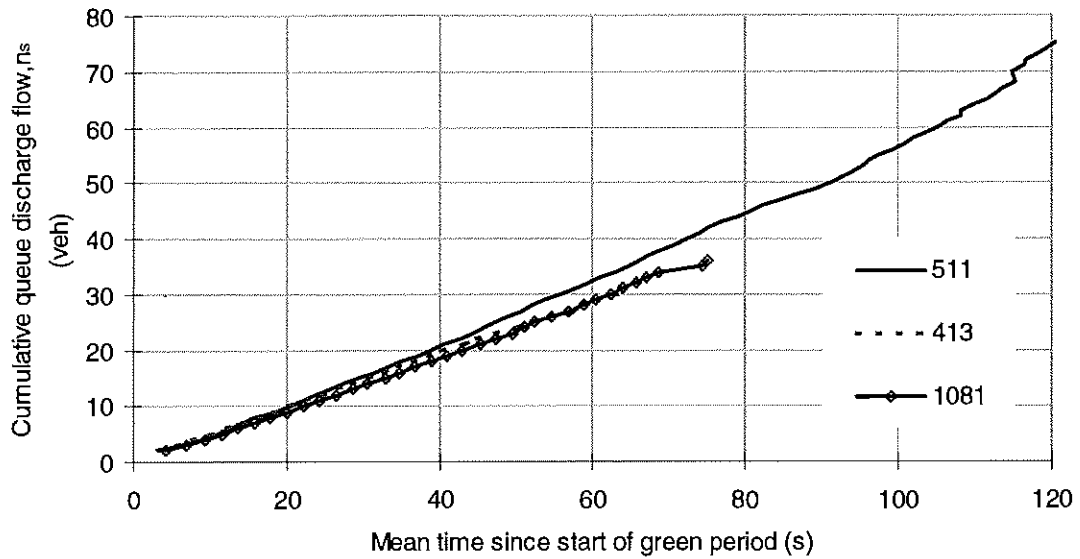


Figure 4.4 – Mean cumulative queue discharge flows - Through lane sites

Comparison of SCATS and VDAS Vehicle Counts

At Sites 511 and 610, SCATS vehicle counts for the survey period were obtained to permit a comparison with vehicle counts obtained from the VDAS system on a cycle by cycle basis. The number of vehicle departures per cycle as measured during the phase time (green plus terminating intergreen time, $G + I_t$) is used for this purpose. For undersaturated cycles, this represents the number of vehicles arriving during the signal cycle, i.e. the total demand (“ $q_a c$ ” in signal analysis as discussed in *Section 7*). For oversaturated cycles, this represents the capacity per cycle (“ $s g$ ” in signal analysis as discussed in *Section 7*).

The two sites are very different in that site 610 is a right turn lane with a short green time, and Site 511 is a through lane with a very long green time. Only two heavy vehicles were observed at the right turn lane site (less than 1%) while at the through lane site approximately 7 % were heavy vehicles.

SCATS reports two volume count parameters, VO and VK. The VO parameter is the direct volume count based on detector actuations. The VK parameter is the volume count derived from the measured DS and phase time ($G + I_t$) values for the cycle and the current value of the MF (maximum flow in pcu/h) parameter, thus representing an estimate of demand in passenger car units:

$$VK = (DS / 100) (G + I_t) MF / 3600 \quad (4.3)$$

The DS value reported by SCATS includes an adjustment for short greens (for timing purposes), and the effect of this is included in the reported VK value. The adjustment factor is $(G + I_t + 2) / (G + I_t)$. Therefore, for comparison with the VDAS count, the VK value reported by SCATS needs to be adjusted down by the factor $(G + I_t) / (G + I_t + 2)$.

Furthermore, for DS values above 100 %, the VK count needs to be adjusted by a factor $100 / DS$ so that a departure volume count (capacity per cycle) is used for comparison with VDAS counts rather than using the demand volume estimate. In some cycles, SCATS reported $VK < VO$ which may be associated with the MF value being less than the saturation flow rate in the cycle. In such cases, $VK = VO$ needs to be used.

Thus, to allow for the factors mentioned above, an adjusted value of the VK parameter (VK') was calculated as follows:

$$DS' = \min [100, DS (G + I_t) / (G + I_t + 2)] \quad (4.4)$$

$$VK' = \max [VO, VK (DS' / DS)] \quad (4.5)$$

Furthermore, VDAS counts need to be adjusted for heavy vehicles for the purpose of comparison with the adjusted VK' values. A passenger car equivalent of 1.65 was used for both through (Site 511) and right-turning traffic (Site 610). The selected factor is the default value used in the SIDRA package (Akçelik and Besley 1999). No additional adjustment was applied for right-turning traffic since SCATS counts include the effect of the turning manoeuvre.

Tables 4.6 and 4.7 list the DS, VO and VK parameters reported by the SCATS system, the adjusted DS' and VK' values, and the unadjusted and adjusted VDAS counts for the two sites.

Only two heavy vehicles were observed at Site 610 (right-turn lane), representing less than 1 % of total traffic. Therefore the unadjusted and adjusted VDAS counts are the same for all but two cycles at Site 610. On the other hand, heavy vehicles represent approximately 7 % of total traffic at Site 511 (through lane), and adjusted and unadjusted VDAS counts are different for most cycles.

The *Time* column in Tables 4.6 and 4.7 is the SCATS report time of each cycle. This time is generally several minutes after the actual time of the cycle being reported. Therefore, to ensure that comparisons were made between the same cycles from each system, the pattern of green times over the duration of the survey from both the SCATS system and the VDAS system were compared by plotting the two sets of green times against time of day. An example plot is shown for Site 511 in Figure 4.5. It is seen that the VDAS and SCATS phase times (green plus intergreen times) are almost identical.

For the purposes of counting the vehicles recorded by the VDAS system on a cycle by cycle basis, each cycle is considered to start at the end of the intergreen period after the green phase. Hence any vehicles crossing the detectors during the latter part of the red phase are counted with the vehicles in the next green phase.

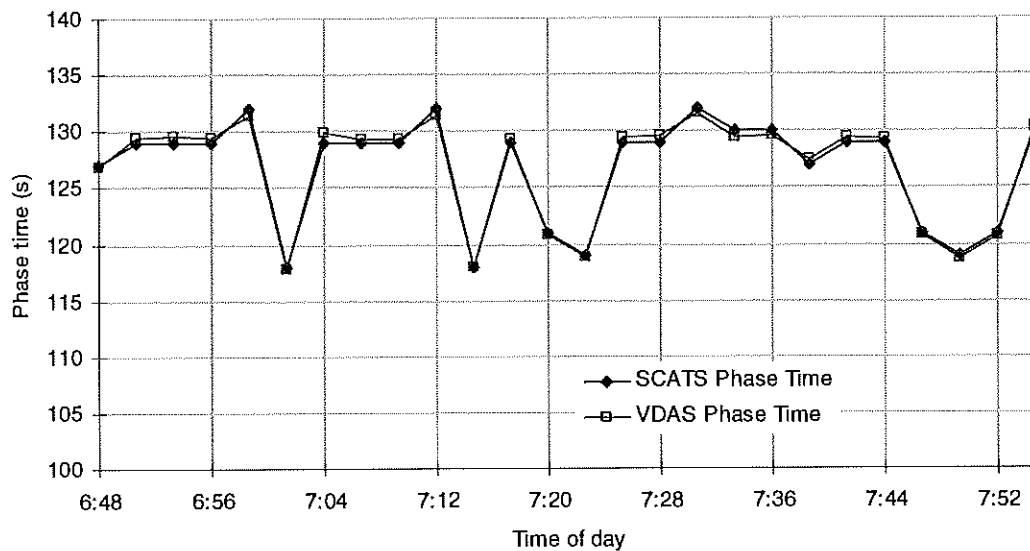


Figure 4.5 – SCATS and VDAS phase times measured at Site 511

Figures 4.6 and 4.7 show the comparison between the SCATS VO values and the unadjusted VDAS counts for Site 610 and Site 511, respectively. *Figures 4.8 and 4.9* show the comparison between the adjusted VK' parameter and the adjusted VDAS count for Site 610 and Site 511, respectively. The trendlines, i.e. linear regression lines for the SCATS counts vs VDAS counts (forced through the origin) are also given as an indication of how well the volume counts compare.

As seen in *Figure 4.7*, the counts are very close (SCATS VO count is 2 % less than the VDAS count) at site 511 (through traffic with long green time). The difference is larger (SCATS VO count is 14 % less than the VDAS count) at site 610 (right-turn traffic with short green time) as seen in *Figure 4.6*. This is as expected since the direct SCATS count from the detector loop is likely to undercount the first few vehicle departures at low speed (due to overlapping of detector occupancy times), and the effect of this undercounting is larger for a short green time. There were also difficulties with the VDAS counts during the early part of the green period although accuracy levels are higher with VDAS. Furthermore, VDAS counts were checked manually using data from the manual records of the passage times of 2nd to 7th vehicles from the queue.

From *Figure 4.8*, it can be seen that at the right turn lane Site 610, the adjusted VK' counts are very close to the adjusted VDAS counts (about 2 per cent difference).

At the through lane Site 511 (*Figure 4.9*), the adjusted VK' counts are about 5 per cent lower than the adjusted VDAS counts.

Table 4.6

Comparison of cycle by cycle vehicle counts from SCATS and VDAS for Site 610

Time	SCATS parameters				Adjusted SCATS parameters		VDAS counts	
	G + I _t	DS	VO	VK	DS'	VK'	Unadjusted	Adjusted for HVs
16:21	18	68	4	6	61	5	5	5
16:24	19	74	4	6	67	5	6	6
16:26	18	98	6	8	88	7	7	7
16:29	18	109	4	9	98	8	7	7
16:31	18	81	5	7	73	6	5	5
16:34	19	73	6	6	66	6	6	6
16:36	18	111	6	9	100	8	9	9
16:39	18	97	7	8	87	7	7	7
16:41	18	71	5	6	64	5	5	5
16:44	18	123	7	10	100	8	8	8
16:46	18	123	9	10	100	9	9	9
16:49	18	63	4	5	57	4	5	5
16:51	18	90	6	7	81	6	7	7
16:54	18	104	6	9	94	8	8	8
16:56	18	140	4	12	100	9	7	7
16:59	22	124	8	12	100	10	10	10
17:01	22	78	5	8	72	7	5	5
17:04	22	84	7	8	77	7	7	7
17:06	18	130	8	11	100	8	9	9
17:09	18	140	8	12	100	9	8	8
17:11	22	78	6	8	72	7	8	8
17:14	18	73	6	6	66	6	5	5
17:16	19	57	2	5	52	5	5	5
17:19	20	57	3	5	52	5	5	5
17:21	22	98	7	10	90	9	8	9
17:24	18	59	4	5	53	4	4	4
17:26	22	140	9	14	100	10	10	10
17:29	22	128	7	13	100	10	8	8
17:31	26	77	8	9	71	8	8	8
17:34	22	57	6	5	52	6	8	8
17:36	17	35	4	3	31	4	3	3
17:39	17	38	3	3	34	3	5	5
17:41	18	91	4	8	82	7	8	8
17:44	18	91	7	8	82	7	7	7
17:46	18	109	8	9	98	8	7	8
17:49	18	144	7	13	100	9	8	8
17:51	26	91	10	11	84	10	10	10
17:54	19	46	4	4	42	4	5	5
17:56	24	68	7	7	63	7	7	7
17:59	22	62	7	6	57	7	6	6
Total			238	321		282	275	277

Table 4.7

Comparison of cycle by cycle vehicle counts from SCATS and VDAS for Site 511

Time	SCATS parameters				Adjusted SCATS parameters		VDAS counts	
	G + I ₁	DS	VO	VK	DS'	VK'	Unadjusted	Adjusted for HVs
6:48	126	94	73	72	93	73	72	74
6:51	129	82	61	64	81	63	61	66
6:54	129	92	65	72	91	71	71	76
6:56	129	92	69	72	91	71	71	73
6:59	131	92	73	73	91	73	73	76
7:02	117	93	63	66	91	65	64	67
7:04	129	85	61	66	84	65	62	67
7:07	129	85	65	66	84	65	65	72
7:10	129	103	79	80	100	79	83	86
7:12	131	89	69	71	88	70	71	77
7:15	117	100	65	71	98	70	66	69
7:18	129	90	69	70	89	69	71	75
7:20	120	90	63	66	89	65	65	68
7:23	118	102	73	70	100	73	75	77
7:26	129	101	77	79	99	78	79	80
7:28	129	85	69	66	84	69	70	71
7:31	131	96	75	76	95	75	76	80
7:34	129	86	61	67	85	66	62	67
7:36	129	96	75	75	95	75	76	77
7:39	127	87	59	67	86	66	61	68
7:42	129	86	65	67	85	66	65	68
7:44	129	89	67	69	88	68	68	71
7:47	120	86	61	63	85	62	61	66
7:50	118	98	67	70	96	69	72	73
7:52	120	88	63	64	87	63	63	66
7:55	130	94	71	74	93	73	75	76
Total			1758	1816		1801	1798	1886

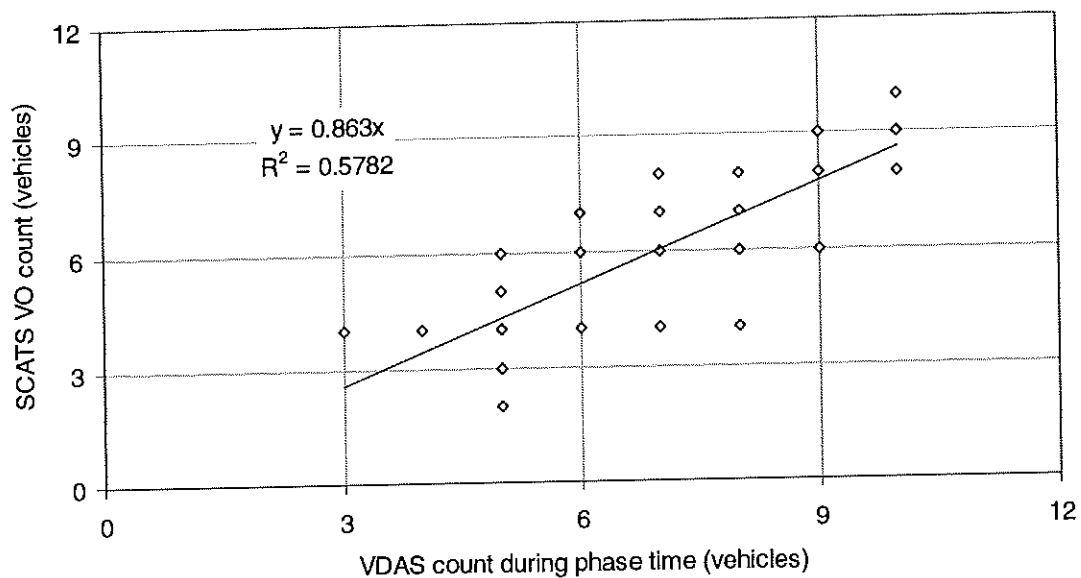


Figure 4.6 – Comparison of vehicle counts during green plus intergreen time: SCATS (VO) vs VDAS (vehicles) for Site 610

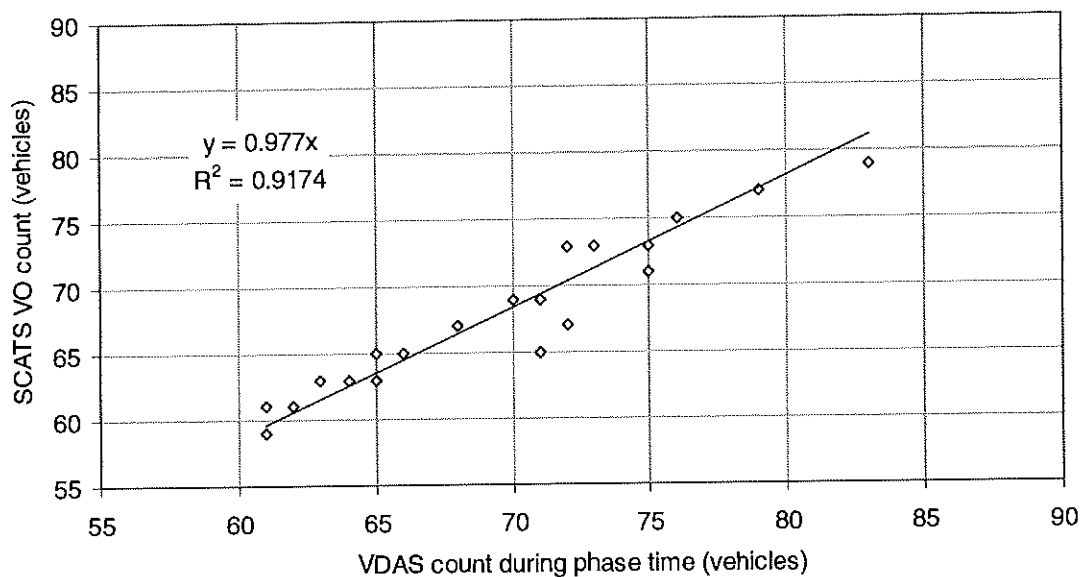


Figure 4.7 – Comparison of vehicle counts during green plus intergreen time: SCATS (VO) vs VDAS (vehicles) for Site 511

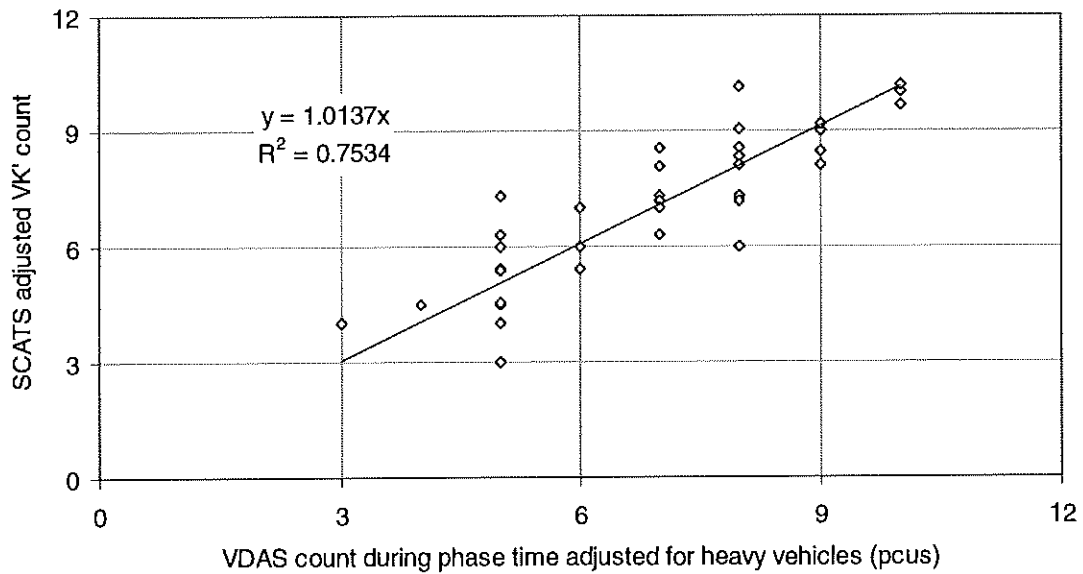


Figure 4.8 – Comparison of vehicle counts during green plus intergreen: SCATS (VK') vs VDAS (equivalent cars) for Site 610

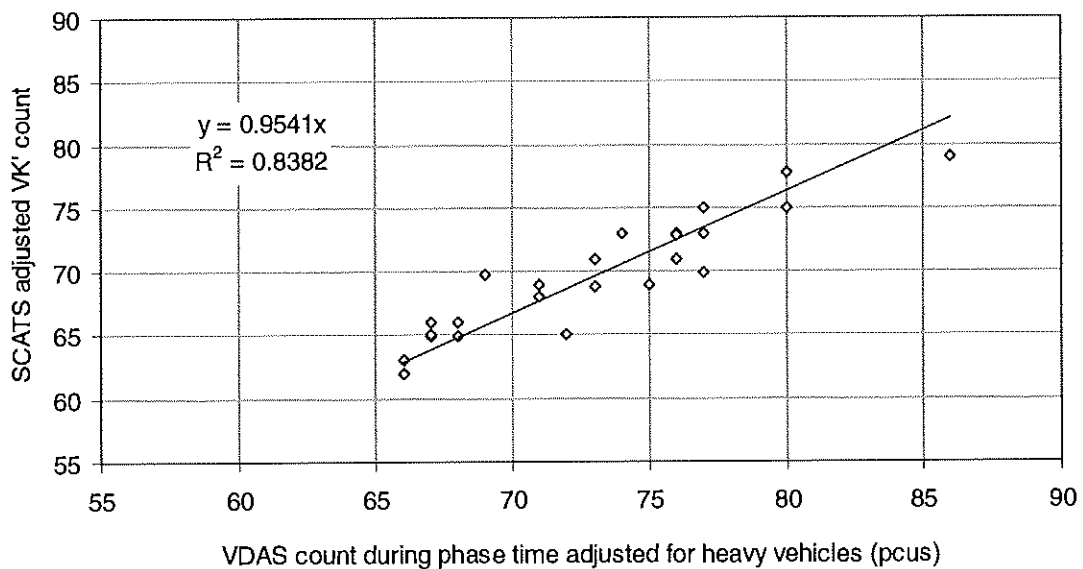


Figure 4.9 – Comparison of vehicle counts during green plus intergreen: SCATS (VK') vs VDAS (equivalent cars) for Site 511

5 FUNDAMENTAL TRAFFIC FLOW RELATIONSHIPS

Fundamental traffic flow parameters are discussed in this section before more complicated cases involved in measurement of these parameters are discussed in *Section 6*.

Fundamental traffic flow parameters include flow rate, speed, density, headway, detector occupancy and space times, vehicle gap and passage times, spacing, space (gap) length, vehicle length, and time and space occupancy ratios (Akçelik 1998). These can be grouped as follows:

- (i) time-based traffic flow parameters: headway (h), occupancy time (t_o), space time (t_s), gap time (t_g), vehicle passage time (t_v);
- (ii) distance-based traffic flow parameters spacing (L_h), space (gap) length (L_s), vehicle length (L_v); and
- (iii) other traffic flow parameters that relate the time-based and distance-based parameters or are derived from them: speed (v), flow rate (q), density (k), time occupancy ratio (O_t), and space occupancy ratio (O_s).

The reader should be aware of differences between the terminology used here and that used in the literature, and should note the lack of uniformity in the use of terminology in the literature. In particular, note that:

- *headway* in this report is the "headway time", but the term *headway* is sometimes used to mean "headway distance" (the term *spacing* in this report means headway distance),
- *space headway* is sometimes used to mean "spacing" (e.g. Drew 1968),
- *gap* is sometimes used to mean "headway time" (e.g. "gaps in a traffic stream" as referred to in the gap-acceptance theory),
- *gap and headway settings* used in actuated signal control terminology have very different meanings (see Akçelik 1995a),
- *spacing* is sometimes used to mean "gap length" (e.g. AUSTRROADS 1993),
- *concentration* is often used to mean "density",
- *occupancy* is often used to mean *time occupancy ratio* (e.g. Lowrie 1996), and sometimes to mean *space occupancy ratio*,
- the terms used in the US Highway Capacity Manual (TRB 1998, Chapter 2) for *time occupancy ratio* and *space occupancy ratio* are *occupancy in time* and *occupancy in space*, respectively.

The relationships among fundamental traffic flow parameters described in this report apply to a *single lane* of traffic. The time-based, distance-based and related traffic flow parameters can be depicted by means of time-distance diagrams as seen in *Figures 5.1 to 5.4*. Constant and equal vehicle speeds are shown in these figures for the purpose of simplicity. More complicated cases that involve vehicle accelerations and different speeds for the leading and following vehicles are discussed in *Section 6*.

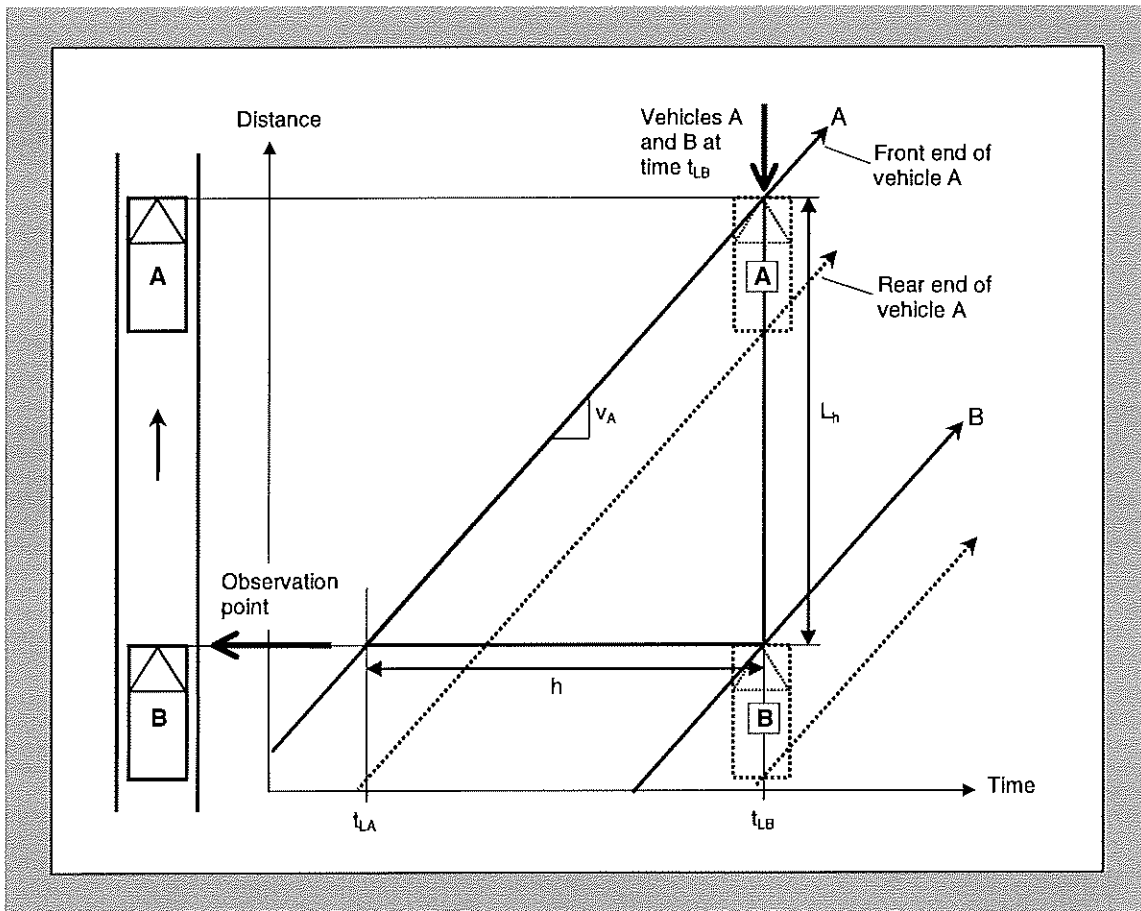


Figure 5.1 – Time-distance diagram showing the relationships between basic traffic flow parameters

Figure 5.1 shows the time-distance traces of front and rear ends of two vehicles, and explains how traffic flow parameters headway, spacing and speed can be defined in relation to observations:

- (a) at a *point* along the road length (e.g. by means of a passage detector such as a VDAS strip), and
- (b) at an *instant* in time (e.g. by means of aerial photography).

Headway (h) is the time between passage of the front (leading) ends of two successive vehicles, and **spacing** (L_h) is the distance corresponding to the headway time, i.e. the distance between the front ends of two successive vehicles. While these definitions are used in this report, it is also possible to define and measure the headway and spacing parameters with reference to the rear (trailing) ends of two successive vehicles.

Space (gap) length (L_s) is the following distance between two successive vehicles as measured between the rear end of one vehicle and the front end of the next vehicle (spacing less **vehicle length**, L_v).

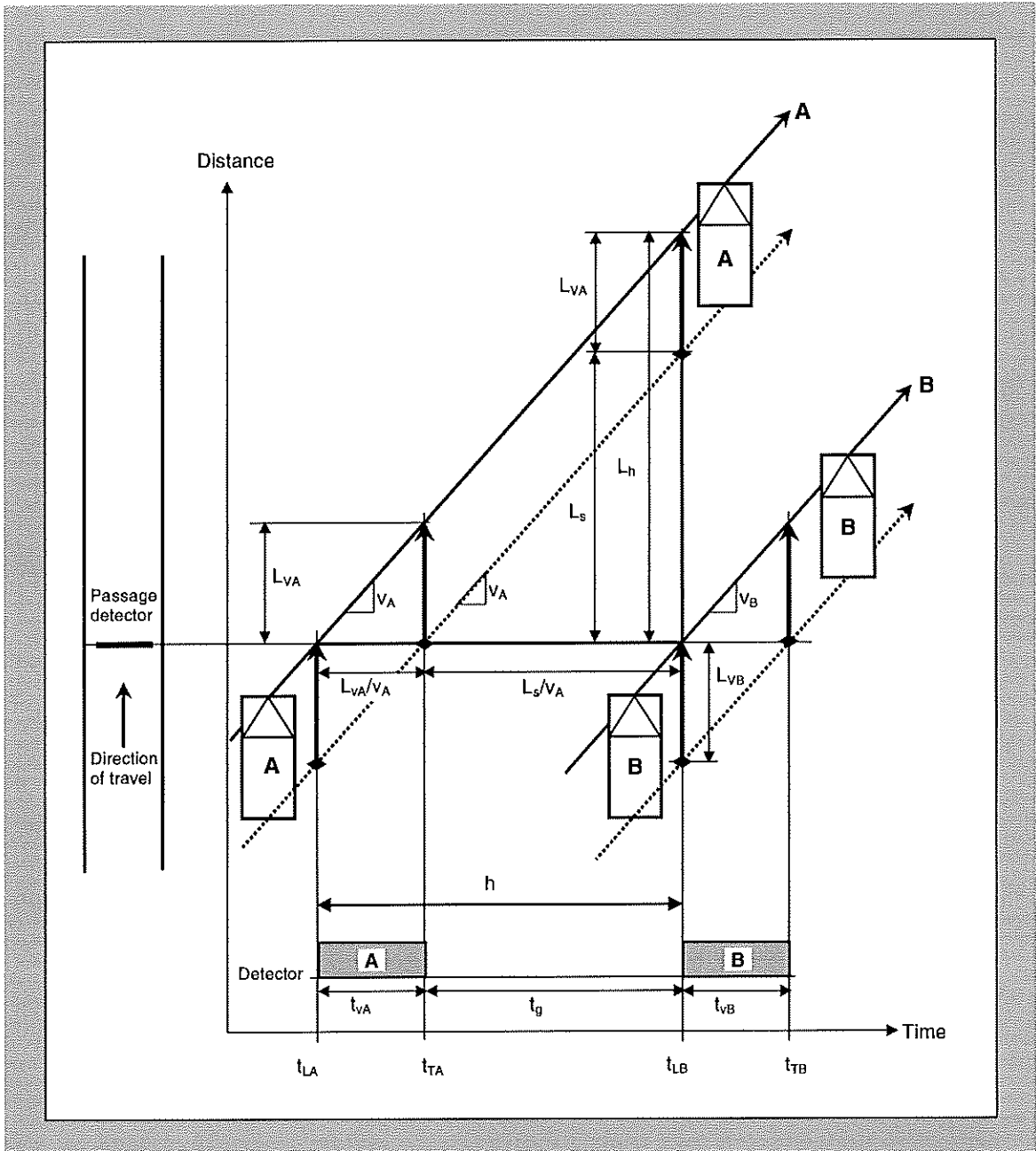


Figure 5.2 – Time-distance diagram explaining the observation of traffic flow parameters with passage detection (constant speeds)

In *Figure 5.1*, the headway time at an observation point along the road is measured as:

$$h = t_{LB} - t_{LA} \quad (5.1)$$

where t_{LA} and t_{LB} are the passage times of the front (leading) ends of vehicles A and B at the observation point.

The positions of vehicles A and B at time t_{LB} are shown on the left-side of *Figure 5.1*. Spacing (L_h) is observed as the distance between the front ends of vehicles A and B at time t_{LB} .

Speed is the distance travelled per unit time. In a time-distance diagram, the slope of the time-distance trace of a vehicle is its speed. In *Figure 5.1*, the speed (km/h) is seen to be given by (constant speed shown):

$$v_A = 3.6 L_h / h \quad (5.2)$$

In practice, speed is measured using an instrumented car, or externally by measuring the time to travel a fixed distance. Measuring speed using two VDAS passage detectors (treadle switches) placed at 3 m distance used for surveys to determine queue discharge characteristics at traffic signals is discussed in *Section 6*. For freeway surveys, two presence loops of size 2 x 2 m placed at 5 m distance between the trailing edges of the two loops were used (Akçelik, Roper and Besley 1999b).

Figure 5.2 depicts observation of headway, vehicle passage time and gap time with *passage detection* at a point along the road. The term passage detection used here should be understood as a form of presence detector with a very short detection zone length, $L_p \approx 0$ (a detector strip such as the VDAS detector).

Vehicle passage time (t_v) is the time between the passage of the front and back ends of a vehicle from a given point along the road (at the passage detector in *Figure 5.2*).

Gap time (t_g) is the time between the passage of the rear end of one vehicle and the front end of the next vehicle, measured at a given point along the road, and is equivalent to headway time less vehicle passage time.

In *Figure 5.2*, the vehicle passage times for vehicles A and B, and the gap time between vehicles A and B are measured as:

$$t_{vA} = t_{TA} - t_{LA} \quad (5.3)$$

$$t_{vB} = t_{TB} - t_{LB} \quad (5.4)$$

$$t_g = t_{LB} - t_{TA} = h - t_{vA} \quad (5.5)$$

where t_{LA} and t_{TA} are the passage times of the front (leading) and rear (trailing) ends of vehicle A, and t_{LB} and t_{TB} are the passage times of the front (leading) and rear (trailing) ends of vehicle B.

The *headway* between vehicles A (leading) and B (following) is associated with the following vehicle, i.e. considered to be in front of vehicle B ($h = h_B$). From *Figure 5.2*, it is seen that this consists of the gap time in front of vehicle B ($t_g = t_{gB}$) and the passage time of vehicle A ($t_v = t_{vA}$). From *Equation (5.5)*:

$$h = t_{vA} + t_{gB} \quad (5.6)$$

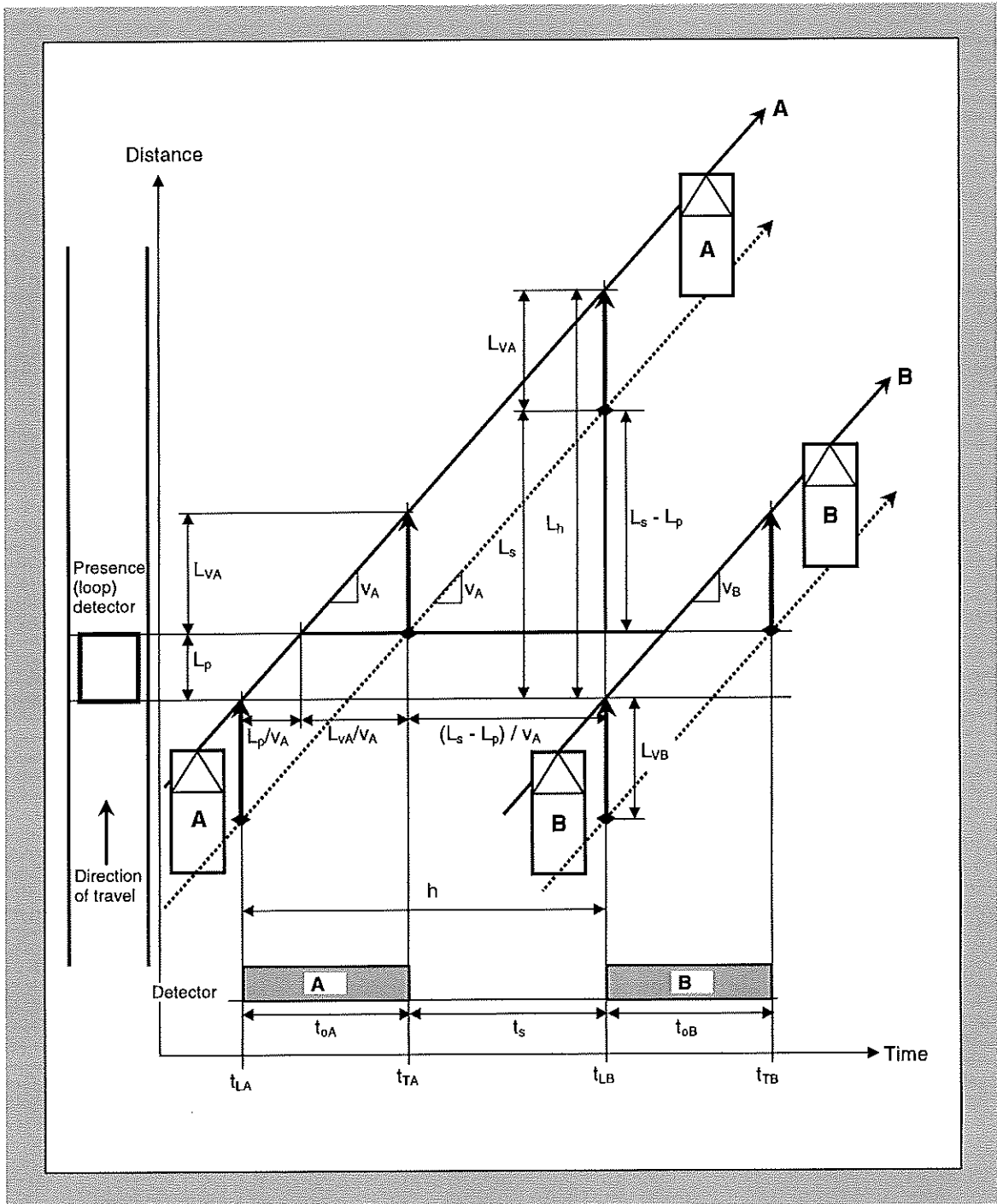


Figure 5.3 – Time-distance diagram explaining the observation of traffic flow parameters with presence detection (constant speeds)

Similarly, *spacing* is associated with vehicle B (i.e. in front of vehicle B). From *Figure 5.2*, it is seen that the spacing measured at time t_{LB} consists of the space (gap) length in front of vehicle B ($L_s = L_{sB}$) and the length of vehicle A ($L_v = L_{vA}$):

$$L_h = L_{vA} + L_{sB} \quad (5.7)$$

These relationships are consistent in terms of the use of speed associated with vehicle A (v_A in km/h from *Equation 5.2*) to calculate the passage time of vehicle A (t_{vA}) and the gap time in front of vehicle B (t_{gB}):

$$t_{vA} = 3.6 L_{vA} / v_A \quad (5.8)$$

$$t_{gB} = 3.6 L_{sB} / v_A \quad (5.9)$$

From *Equations (5.2), (5.7) and (5.8)*:

$$\begin{aligned} h &= 3.6 (L_h / v_A) = 3.6 (L_{vA} + L_{sB}) / v_A \\ &= t_{vA} + t_{gB} \end{aligned} \quad (5.10)$$

which is consistent with *Equation (5.6)*.

While vehicle passage time (t_v) and gap time (t_g) are measured with passage detection, the corresponding parameters measured with presence detection are occupancy time (t_o) and space time (t_s). *Figure 5.3* depicts observation of headway, occupancy time and space time with *presence detection* using a detector loop at a point along the roadway.

Occupancy time (t_o) starts when the front of a vehicle enters the detection zone and finishes when the back of the vehicle exits the detection zone. Thus, it is the duration of the period when the detection zone is occupied by a vehicle, and is equivalent to the sum of the vehicle passage time and the time to travel the effective detection zone length.

Space time (t_s) is the duration of the time between the detection of two consecutive vehicles when the presence detection zone is not occupied. It is equivalent to gap time less the time taken to travel the *effective detection zone length*, L_p .

In *Figure 5.3*, the vehicle occupancy times for vehicles A and B (t_{oA} , t_{oB}), and the space time between vehicles A and B, considered to be in front of vehicle B (t_s) are:

$$t_{oA} = t_{TA} - t_{LA} \quad (5.11)$$

$$t_{oB} = t_{TB} - t_{LB} \quad (5.12)$$

$$t_s = t_{LB} - t_{TA} = h - t_{oA} \quad (5.13)$$

where t_{LA} is the time when the front (leading) edge of vehicle A enters the detection zone, t_{TA} is the time when the rear (trailing) end of vehicle A exits the detection zone, t_{LB} is the time when the front (leading) edge of vehicle B enters the detection zone, and t_{TB} is the time when the rear (trailing) end of vehicle B exits the detection zone.

As in the case of passage detection, it is considered that *headway* between vehicles A (leading) and B (following) is in front of vehicle B ($h = h_B$). From *Figure 5.3*, it is seen that this consists of the space time in front of vehicle B ($t_s = t_{sB}$) and the occupancy time of vehicle A ($t_o = t_{oA}$).

From Equation (5.13):

$$h = t_{oA} + t_{sB} \quad (5.14)$$

Equation (5.7) for spacing applies in this case as well ($L_s = L_{sB}$, $L_v = L_{vA}$ and $L_h = L_{vA} + L_{sB}$).

The occupancy time of vehicle A (t_{oA}) and the space time in front of vehicle B (t_{sB}) are calculated using the speed of vehicle A (v_A in km/h from Equation 5.2):

$$t_{oA} = 3.6 (L_p + L_{vA}) / v_A \quad (5.15)$$

$$t_{sB} = 3.6 (L_{sB} - L_p) / v_A \quad (5.16)$$

From Equations (5.2), (5.7) and (5.15):

$$\begin{aligned} h &= 3.6 (L_h / v_A) = 3.6 (L_{vA} + L_{sB}) / v_A \quad (5.17) \\ &= (L_p + L_{vA}) / v_A + (L_{sB} - L_p) / v_A \\ &= t_{oA} + t_{sB} \end{aligned}$$

which is consistent with Equation (5.14).

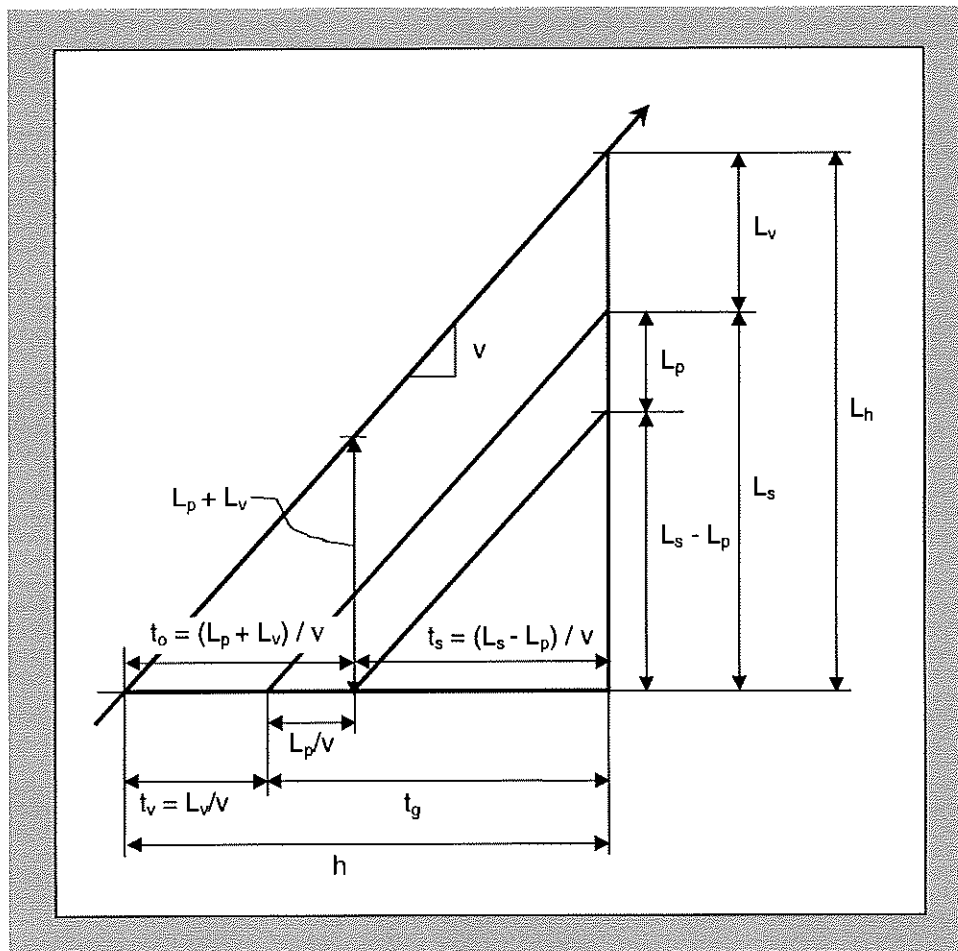


Figure 5.4 – Simple diagram showing the relationships among basic traffic flow parameters

Figure 5.4 is given as a simple diagram that summarises the relationships among basic traffic flow parameters with passage and presence detection without reference to individual vehicles. In Figure 5.4, all time-based parameters are in seconds, distance based parameters are in metres, and speed is in m/s. Using speed in km/h, the basic relationships can be summarised as follows:

$$v = 3.6 L_h / h = 3.6 L_s / t_g \quad (5.18)$$

$$h = 3.6 L_h / v = 3.6 (L_v + L_s) / v = t_v + t_g = t_o + t_s \quad (5.19)$$

$$t_v = 3.6 L_v / v \quad (5.20)$$

$$t_g = h - t_v = h - 3.6 L_v / v = 3.6 L_s / v \quad (5.21)$$

$$t_s = h - t_o = t_g - 3.6 L_p / v = 3.6 (L_s - L_p) / v \quad (5.22)$$

$$t_o = h - t_s = t_v + 3.6 L_p / v = 3.6 (L_p + L_v) / v \quad (5.23)$$

$$L_h = L_v + L_s = h v / 3.6 \quad (5.24)$$

$$L_s = L_h - L_v = t_g v / 3.6 = L_p + t_s v / 3.6 \quad (5.25)$$

where

- v = vehicle speed (km/h)
- h = headway (seconds),
- t_v = vehicle passage time (seconds),
- t_g = gap time (seconds),
- t_o = occupancy time (seconds),
- t_s = space time (seconds),
- L_v = vehicle length (m),
- L_h = spacing (m),
- L_s = space (gap) length (m), and
- L_p = detection zone length (m).

Figure 5.5 presents another summary of the basic concepts and parameters in presence and passage detection. It was developed from Figure 7.1 of AUSTRROADS (1993).

Figure 5.5 is based on the definition of headway and spacing from the *front* of the leading vehicle to the *front* of the following vehicle. For completeness, Figure 5.6 is given to show the relationships when headway and spacing are defined and measured from the *back* of the leading vehicle to the *back* of the following vehicle.

In this report headway and spacing parameters are defined and measured in accordance with the method summarised in Figure 5.5. Limited analysis of parameters based on the method shown in Figure 5.6 indicated that the difference between the two methods would not affect the conclusions of this report.

A discussion of the aggregation of individual vehicle headway, occupancy time, space time, gap time, vehicle passage time, spacing, space (gap) length, and speed parameters to represent average values for a continuous traffic stream is given in Akçelik, Roper and Besley (1999b).

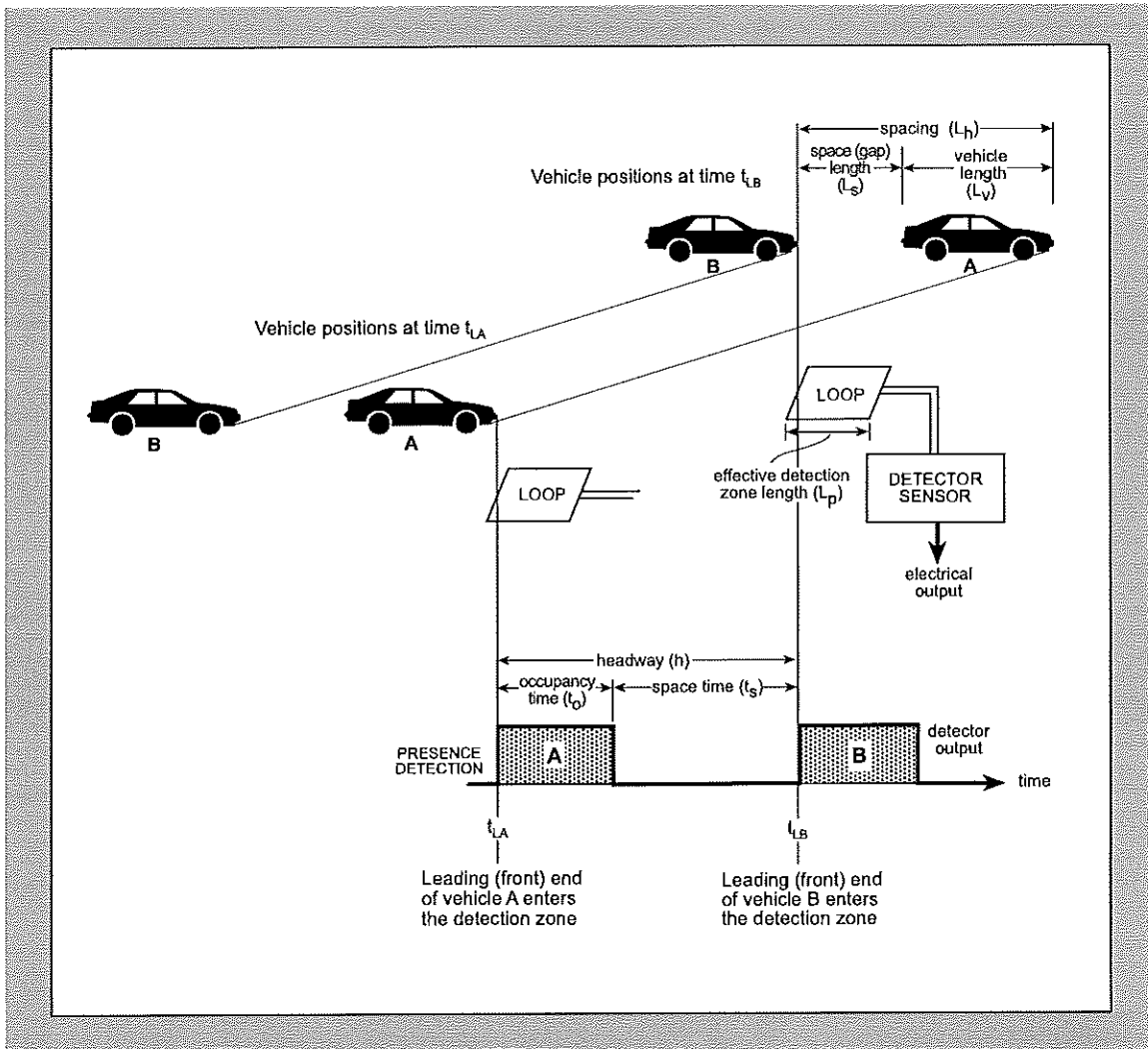


Figure 5.5 – Traffic flow parameters and basic relationships in presence and passage detection: headway and spacing defined from the front of the leading vehicle to the front of the following vehicle

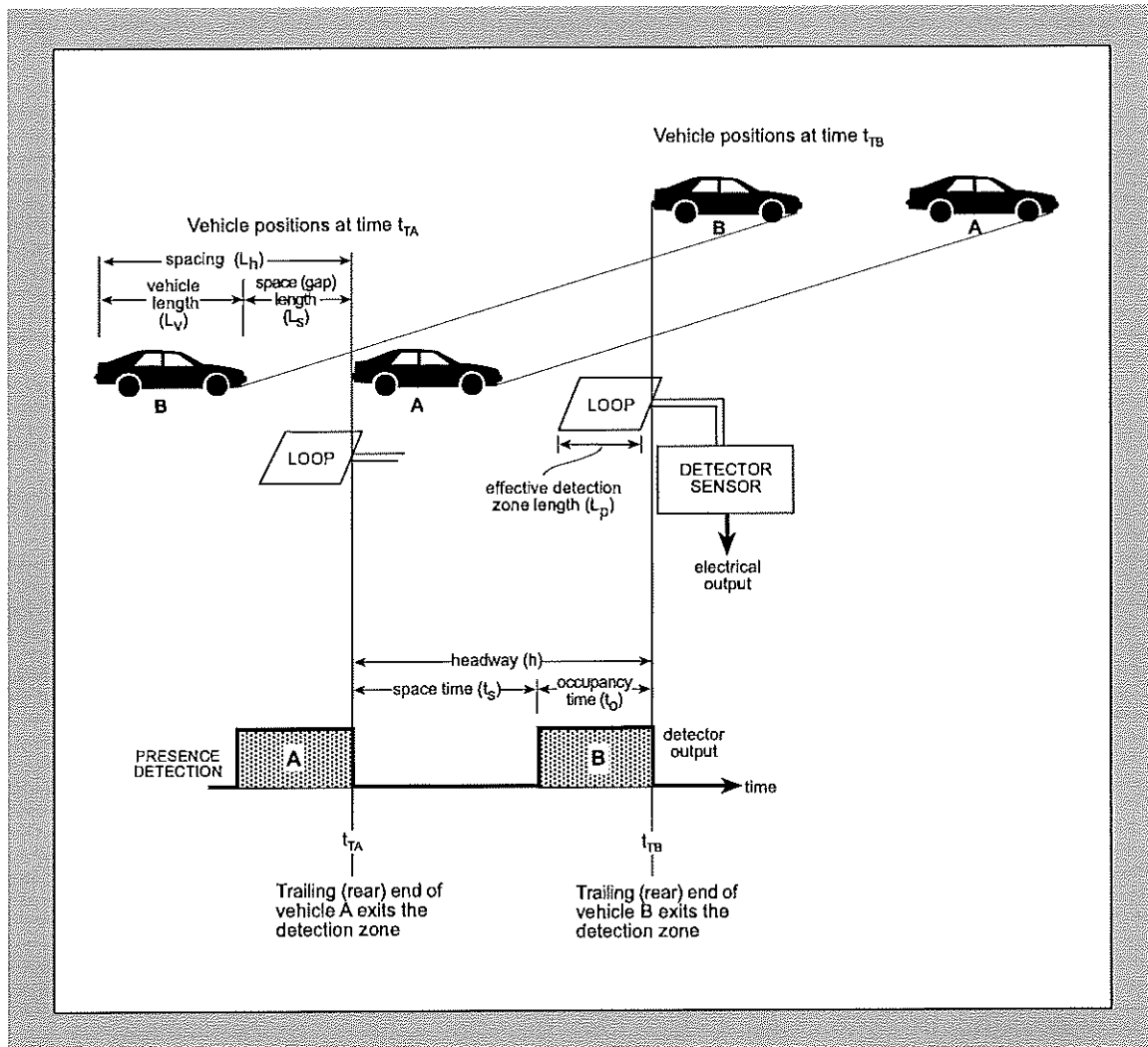


Figure 5.6 – Traffic flow parameters and basic relationships in presence and passage detection: headway and spacing defined from the back of the leading vehicle to the back of the following vehicle

Vehicle Length

In the calculations relating to average traffic conditions, the vehicle length should represent the actual traffic composition. Where the traffic stream is represented as a mixture of light vehicles (LVs) and heavy vehicles (HVs), the average vehicle length can be calculated as:

$$L_v = (1 - p_{HV}) L_{vLV} + p_{HV} L_{vHV} \quad (5.26)$$

where

p_{HV} = proportion of heavy vehicles in the traffic stream,

L_{vLV} = average vehicle length for light vehicles (passenger car units) (m/LV or m/pcu),
and

L_{vHV} = average vehicle length for heavy vehicles (m/HV).

Typical average vehicle lengths of $L_{vm} = 4.4$ m and $L_{vHV} = 9.0$ m can be used where information is not available. For example, with 10 % heavy vehicles ($p_{HV} = 0.05$), the average vehicle length is found as $L_v = 0.90 \times 4.4 + 0.10 \times 9.0 = 4.9$ m.

Detection Zone Length

For traffic signals, the typical stop-line presence loop length used in Australia is 4.5 m. This is a single loop that does not measure the speed.

The *effective detection zone length* for presence detection is not necessarily the same as the detector loop length. Morris, Dean and Hulscher (1984) suggest that due to the *spill-over sensitivity* at the ends of the loop, the effective length of a loop is usually greater than its physical length. Figure 3 of Morris, et al. (1984) shows that excess of effective over physical length is about 0.5 m for the commonly-used symmetripole loops with high sensitivity (Leschinski 1994). Thus, for a loop length of 4.5 m, the effective detection zone length is $L_p = 5.0$ m. On the other hand, RTA NSW (1991) suggests that for a loop length of 4.5 m, the effective detection zone length is $L_p = 4.0$ m. On the basis of this information, the effective detection zone length may be considered to be in the range from (loop length – 0.5 m) to (loop length + 0.5 m).

For general analysis purposes where specific loop sensitivity information is not available, the effective detection zone length may be considered to be equal to the physical loop length as used in this report.

Average flow rate, density and occupancy ratios

Flow rate (q) is the number of vehicles per unit time passing (arriving or departing) a given reference point along the road. With queuing at interrupted traffic facilities, demand flow rate can be measured as the arrival flow rate at the back of the queue.

Flow rate (veh/h) can be calculated from the headway, h (seconds):

$$q = 3600 / h \quad (5.27)$$

Thus, using the flow rate, q (veh/h) from Equation (5.27) and speed, v (km/h) from Equation (5.18), the average spacing, L_h (m) is given by:

$$L_h = 1000 v / q \quad (5.28)$$

Density (k) is the number of vehicles per unit distance along the road as measured at an instant in time. It is recommended that density (veh/km) is calculated using the average spacing, L_h (m) from *Equation (2.2.7)*:

$$k = 1000 / L_h \quad (5.29)$$

From *Equations (5.28) and (5.29)*, flow rate (veh/h), density (veh/km) and speed (km/h) for a traffic stream are related through:

$$q = v k \quad (5.30)$$

Time occupancy ratio (O_t) is the proportion of time in an analysis period when the passage or occupancy detector at a point along the road is occupied by vehicles. Time occupancy ratio as a percentage value can be estimated as follows.

For presence detection:

$$O_t = 100 t_o / h = 100 (L_v + L_p) / L_h \quad (5.31)$$

subject to $O_t \leq 100\%$

For passage detection:

$$O_t = 100 t_v / h = 100 L_v / L_h \quad (5.32)$$

where t_o , t_v and h are the occupancy time, vehicle passage time and headway parameters (in seconds), and L_h , L_v are the average spacing and average vehicle length (m), and L_p is the detection zone length (m).

If the average time occupancy ratio and headway are known, the average occupancy time and vehicle passage time can be estimated from:

$$t_o = O_t h / 100 \quad \text{with presence detection} \quad (5.33)$$

$$t_v = O_t h / 100 \quad \text{with passage detection} \quad (5.34)$$

If the time occupancy ratio, spacing and effective detection zone length (loop length) are known, the average vehicle length can be estimated from:

$$L_v = O_t L_h / 100 - L_p \quad \text{with presence detection} \quad (5.35)$$

$$= O_t L_h / 100 \quad \text{with passage detection} \quad (5.36)$$

Space occupancy ratio (O_s) is the proportion of a road section (distance) occupied by vehicles at an instant in time. The space occupancy ratio as percentage value can be estimated from:

$$O_s = 100 L_v / L_h \quad (5.37)$$

where L_h and L_v are the average spacing and average vehicle length (m).

From *Equations (5.32) and (5.37)*, it is seen that space occupancy and time occupancy ratios are equivalent with passage detection, $O_s = O_t$.

From *Equations (5.28), (5.30) and (5.37)*, space occupancy ratio (percentage), flow rate (veh/h), density (veh/km) and speed (km/h) for a traffic stream are related through:

$$O_s = L_v q / (10 v) = L_v k / 10 \quad (5.38)$$

where L_v is the average vehicle length (m).

Other relationships which may be useful when the time occupancy ratio is known rather than the occupancy time are given below:

$$t_s = (1 - O_t/100) h \quad (5.39)$$

$$L_v = (v/3.6) (O_t/100) h - L_p \quad (5.40)$$

Jam Spacing, Jam Gap Length and Jam Density

The jam spacing, L_{hj} (or spacing in queue) equals the vehicle length, L_v plus the average gap length in queue (or jam gap length), L_{sj} measured from the back of the leading vehicle to the front of the following vehicle. Thus, the jam spacing and gap length can be calculated from:

$$L_{hj} = L_{sj} + L_v \quad (5.41a)$$

$$L_{sj} = L_{hj} - L_v \quad (5.41b)$$

The density that corresponds to the jam spacing is called the jam density (i.e. the number of vehicles per unit distance in a stationary queue) in veh/km:

$$k_j = 1000 / L_{hj} = 1000 / (L_v + L_{sj}) \quad (5.42)$$

For a jam space length of $L_{sj} = 2.6$ m, and typical average vehicle lengths of $L_{vm} = 4.4$ m and $L_{vHV} = 9.0$ m, the jam spacing is $L_{hj} = 7.0$ m per pcu (car or light vehicle) and 11.6 m per heavy vehicle. With 5 % heavy vehicles, the average vehicle length is $L_v = 0.95 \times 4.4 + 0.05 \times 9.0 = 4.6$ m, and the average jam spacing is $L_{hj} = 4.6 + 2.6 = 7.2$ m per vehicle. The corresponding jam densities are $k_j = 1000 / 7.0 = 143$ pcu/km and $k_j = 1000 / 7.2 = 139$ veh/km.

The time occupancy and space occupancy ratios at jam density are:

$$O_{ij} = 100 (L_v + L_p) / L_{hj} \quad \text{with presence detection} \quad (5.43a)$$

subject to $O_{ij} \leq 100$ %

$$O_{ij} = 100 L_v / L_{hj} \quad \text{with passage detection} \quad (5.43b)$$

$$O_{sj} = 100 L_v / L_{hj} \quad (5.44)$$

In the above example ($L_v = 4.6$ m, $L_{hj} = 7.2$ m) for presence detection with a loop length of $L_p = 4.5$ m, $O_{ij} = 100$ % and $O_{sj} = 64$ % are found.

It is seen that the space occupancy ratio at jam density is always less than one ($O_{sj} < 100$ %) since $L_v < L_{hj}$ (or $L_{sj} > 0$). On the other hand, the space occupancy ratio at jam density can reach 100 % when the detection zone length is increased: $O_{ij} = 100$ % when $(L_v + L_p) = L_{hj}$ or $L_p = L_{sj}$. In fact, $O_t = 100$ % can result even when $v > 0$. The condition for this is $L_p > L_s$ or $L_h < (L_p + L_v)$. This also corresponds to zero space time condition as seen from *Equation (5.22)*.

Maximum Flow Rate, Capacity and Free-Flow Speed

As vehicles speed up from a stationary queue, the gap length between vehicles increases gradually, and therefore the spacing increases and the density decreases. The corresponding flow rate increases to a **maximum flow rate** (q_n) and then decreases as the speed increases towards the **free flow speed** (v_f).

Capacity is the maximum flow rate that can be sustained during a reasonably long period of time. The US Highway Capacity Manual (TRB 1998) uses a flow period of 15 min for defining the capacity. Traffic flow conditions with demand flow rates below and above capacity are referred to as *undersaturated* and *oversaturated* conditions, respectively. This is further discussed in this section.

The parameter values corresponding to the maximum flow rate (indicated by subscript n) can be calculated from:

$$\begin{aligned} h_n &= 3600 / q_n & (5.45) \\ &= 3.6 L_{hn} / v_n = 3.6 (L_v + L_{sn}) / v_n = t_{vn} + t_{gn} = t_{on} + t_{sn} \end{aligned}$$

$$t_{on} = h_n - t_{sn} = t_{vn} + L_p / v_n = (L_p + L_v) / v_n \quad (5.46)$$

$$t_{vn} = 3.6 L_v / v_n \quad (5.47)$$

$$t_{gn} = h_n - t_{vn} = h - 3.6 L_v / v_n = 3.6 L_{sn} / v_n \quad (5.48)$$

$$t_{sn} = h_n - t_{on} = t_{gn} - 3.6 L_p / v_n = 3.6 (L_{sn} - L_p) / v_n \quad (5.49)$$

$$L_{hn} = 1000 v_n / q_n = v_n h_n / 3.6 \quad (5.50)$$

$$L_{sn} = L_{hn} - L_v \quad (5.51)$$

$$k_n = 1000 / L_{hn} = q_n / v_n \quad (5.52)$$

$$O_{tn} = 100 t_{on} / h_n \quad (5.53)$$

$$O_{sn} = 100 L_v / L_{hn} \quad (5.54)$$

where h_n is the minimum headway (seconds), v_n is the speed (km/h), t_{on} , t_{sn} , t_{vn} , t_{gn} are the occupancy time, space time, vehicle passage time and gap time values (seconds), L_{hn} and L_{sn} are the spacing and gap length values (m), k_n is the density (veh/km), O_{tn} and O_{sn} are the time and space occupancy ratios.

The **free-flow speed** is obtained at near-zero flow rates under very light traffic conditions. The free-flow speeds and the ratio of the speed at maximum flow to the free-flow speed (v_n/v_f) increase as the facility type improves, e.g. freeways have higher values than signalised arterials. As a rough guide where information is not available, the speed ratio can be estimated from $v_n/v_f = 0.008 v_f + 0.05$ where the free-flow speed v_f is in km/h (e.g. $v_f = 100-120$ km/h for freeways, $60-90$ km/h for arterials, $40-50$ km/h for sub-arterials).

Speed-Flow Relationships for Uninterrupted and Interrupted Conditions

The relationship between speed, density and flow (*Equation 5.30*) is known as the fundamental relationship in traffic flow theory. This relationship is often discussed in the context of uninterrupted flows, e.g. as observed on freeways and rural roads, but is also valid for departures across the stop line of a signalised intersection as observed during the saturated and unsaturated parts of the green period.

A vast amount of literature exists on the fundamental speed - density - flow models of traffic theory (e.g. Drew 1968, May 1990, TRB 1975, 1998) and various travel time (cost) - flow models used for transport planning and demand management purposes (e.g. Akçelik 1991). There is often confusion about how these two groups of models are related, especially in terms of *congested* traffic conditions.

The speed-flow relationships observed at a point along the road and the speed-flow relationships determined by travel time surveys through congested areas are different. For undersaturated conditions ($q < q_n$), the two types of speeds coincide. A clear understanding of the difference between the two types of speed-flow relationships is necessary for an improved understanding of speed-flow relationships and the capacity concept for uninterrupted and interrupted traffic facilities, e.g. freeways and traffic signals, respectively (see Akçelik 1996, BTCE 1996).

An explanation of the relationships between speed, density, flow and travel time models for uninterrupted and interrupted traffic flows was discussed by Akçelik (1996). In this context, the difference between *arrival* flows measured upstream of a queuing section, and *departure* flows measured at a reference point along the road is emphasised. The former is related to *demand* while the latter is related to *capacity*. The difference is of particular importance in oversaturated (congested) conditions where demand exceeds capacity.

The speed measured at a reference point along the road under congested conditions can be better understood as a queue discharge, queue formation or moving queue speed. This speed is associated with departure flow which cannot exceed the capacity flow. On the other hand, the average speed based on travel time through a road section including the travel distance upstream of the queuing section is associated with the demand flow rate that can exceed the capacity.

The reader is also referred to an earlier paper by Fehon and Moore (1982) who discussed the relation between the speed - flow - concentration variables and the SCATS DS parameter.

Figures 5.7 and 5.8 show the speed-flow relationships for uninterrupted and interrupted traffic facilities, respectively. These are discussed below.

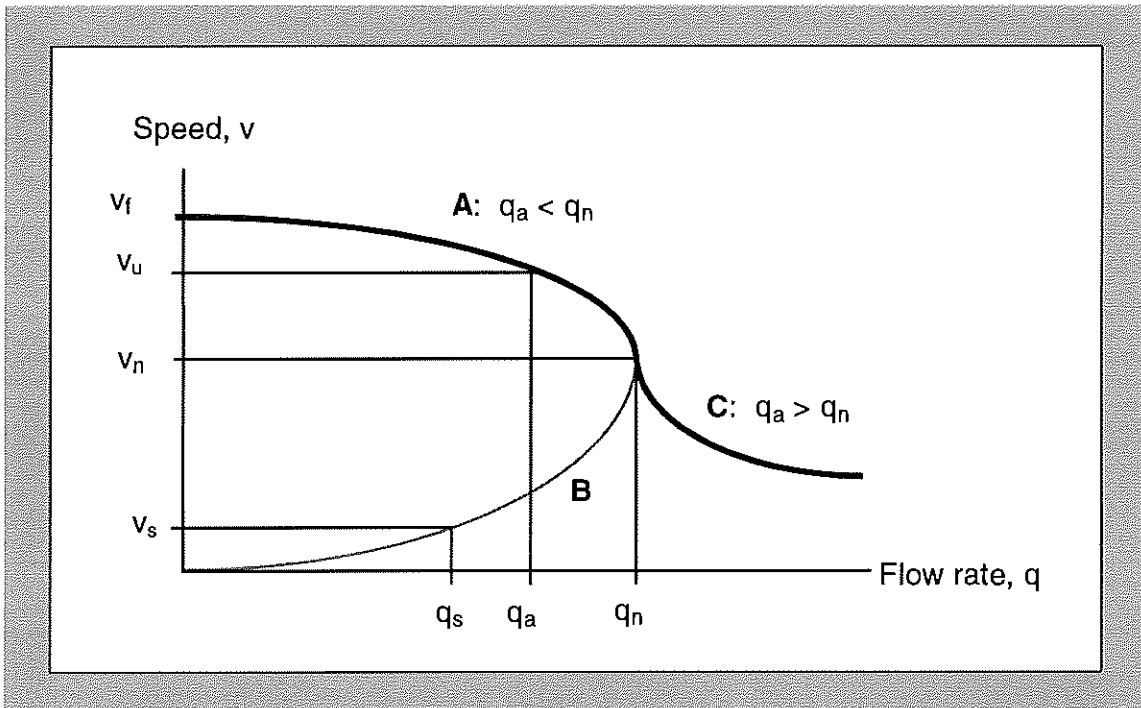


Figure 5.7 – Speed as a function of flow rate: uninterrupted flow conditions

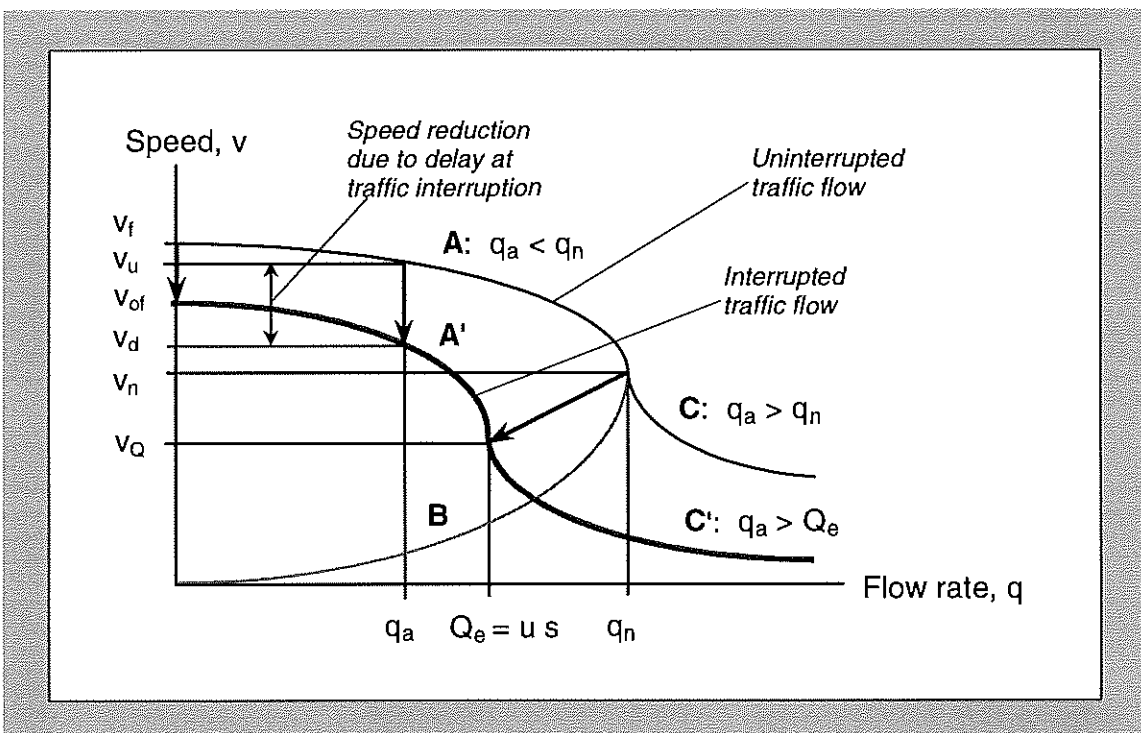


Figure 5.8 – Speed as a function of flow rate: interrupted flow conditions

Uninterrupted traffic facilities

As seen in *Figure 5.7*, capacity for uninterrupted traffic facilities is the maximum flow rate ($Q_c = q_n$). Region A represents *arrival (demand) flow rates* below capacity ($q_a < q_n$) that are associated with uninterrupted flow speeds (v_u) between the speed at maximum flow (v_n) and the free-flow speed (v_f): $v_n < v_u < v_f$. Region B represents the saturated conditions behind a bottleneck point with flow rates below the capacity rate ($q_s < q_n$) and the saturated flow speeds below the speed at capacity flow ($0 < v_s < v_n$). In Region B, the flow rate is not the arrival (demand) flow rate. It is the flow rate based on the number of vehicles passing an observation point along the road (passage or presence detection).

Changes in conditions from Region A to Region B through the maximum flow point represent queue formation, and changes in condition from region B to Region A represent queue discharge conditions. The point on the speed-flow curve would depend on the position of the observation point relative to the bottleneck point.

While Region B represents *spot speeds* and flow rates under saturated conditions as observed at a point along the road, Region C represents *travel speeds* and demand flow rates under oversaturated conditions. For region C, the flow rate is the demand flow rate that exceeds the capacity value ($q_a > q_n$) as measured upstream of the queues that develop at the capacity point, and the speed is based on the travel time through the road section from a point upstream of the queuing area to a point past the bottleneck point. The speeds for Region C can only be measured by means of instrumented car surveys, i.e. by travelling through the congested section of road, starting beyond the point where the queues develop.

Model 4 given in *Section 10* is a time-dependent speed-flow relationship model that applies to both undersaturated and oversaturated conditions (Regions A and C).

The relationship between headway and flow rate (*Equation 5.27*) is not applicable for flow rates above the maximum flow rate. If applied, such flow rates would imply headways below the minimum headway (h_n) that corresponds to the maximum flow rate. Since headway is related to vehicles passing a point, headways cannot be lower than the minimum value. In fact, when the demand flow rate exceeds the capacity, the flow rate passing a point upstream of the bottleneck point drops below the maximum flow rate. This is associated with the density increasing above the density corresponding to the maximum flow rate ($k > k_n$). This corresponds to the average vehicle spacing dropping below the spacing at the maximum flow rate ($L_h < L_{hn}$). For safe driving reasons, this results in lower speeds, and therefore increased headways.

Refer to Akçelik, Roper and Besley (1999b) for a detailed discussion of fundamental flow relationships for uninterrupted flows (also see *Section 10*).

Interrupted traffic facilities

It is seen in *Figure 5.8* for interrupted facilities that the capacity is obtained by reducing the maximum flow rate (or saturation flow rate, $s = q_n$) by the proportion of time available (u). Thus, the capacity is $Q = u s$ (at traffic signals, $u = g/c$ where g is the effective green time and c is the cycle time).

Average travel speeds with interruption (control) delays (v_d) in Regions A' and C are seen to be reduced from the uninterrupted flow speeds (v_u) in Regions A and C due to delays experienced at the interruption point, e.g. traffic signals ($v_d < v_u$). The zero-flow speed for interrupted traffic (v_{of}) includes the free-flow travel time for uninterrupted travel (at v_f) plus the minimum delay time at the traffic interruption. The average interrupted travel speed at capacity is v_Q .

The flow rate for the congested region (B) at a signalised intersection stop line is the queue discharge flow rate (*Section 7*). This flow rate during the green period increases to a maximum flow rate (q_n). This consideration helps to explain the speed-flow models for uninterrupted flows as well: the flow rate measured for saturated conditions represents a reduced capacity (departure) flow rate, not an arrival flow rate. This is a result of vehicles (or moving queues) in the traffic stream interfering in the same way as the downstream queue interferes with the departure rate at the signal stop line, resulting in reduced vehicle spacings, speeds and flow rates. Wardrop's (1965) study of speed-flow relationships based on traffic in a circular track is interesting in this respect.

6 DATA ANALYSIS METHOD

In *Section 5*, traffic flow parameters are explained using time-distance diagrams with the assumption of constant and equal vehicle speeds for the purpose of simplicity (*Figures 5.1 to 5.4*). Queue discharge characteristics at the signal stop line present more complicated cases that involve vehicle accelerations and different speeds for the leading and following vehicles.

The data collection method used in this study is based on two VDAS detector strips. This will be referred to as a *passage detection* system. *Figure 6.1* shows the two VDAS detectors (upstream and downstream) installed centred over the traffic signal detector loops. With the 4.5 m signal detector loop, one of the VDAS detectors is located 0.75 m from the downstream edge of the loop and the other VDAS detector is located further upstream at a spacing of approximately 3.0 m. This system differs from the two-loop *presence detection* system used for recent freeway surveys (Akçelik, Roper and Besley 1999b), although the analysis methods used for these two systems have much in common.

As the vehicles accelerate at the start of the green period and as the time since the start of green period increases, the queue discharge headways measured at the VDAS detectors (h_s) reduce and the queue discharge speeds (v_s) increase. Eventually, vehicle speeds and headways measured at the two VDAS detector locations become steady and equal, approaching v_n and h_n (also see *Figure 7.2* in *Section 7*). As a result of this, the headways and speeds measured at the two VDAS detectors differ until steady departure flow is achieved.

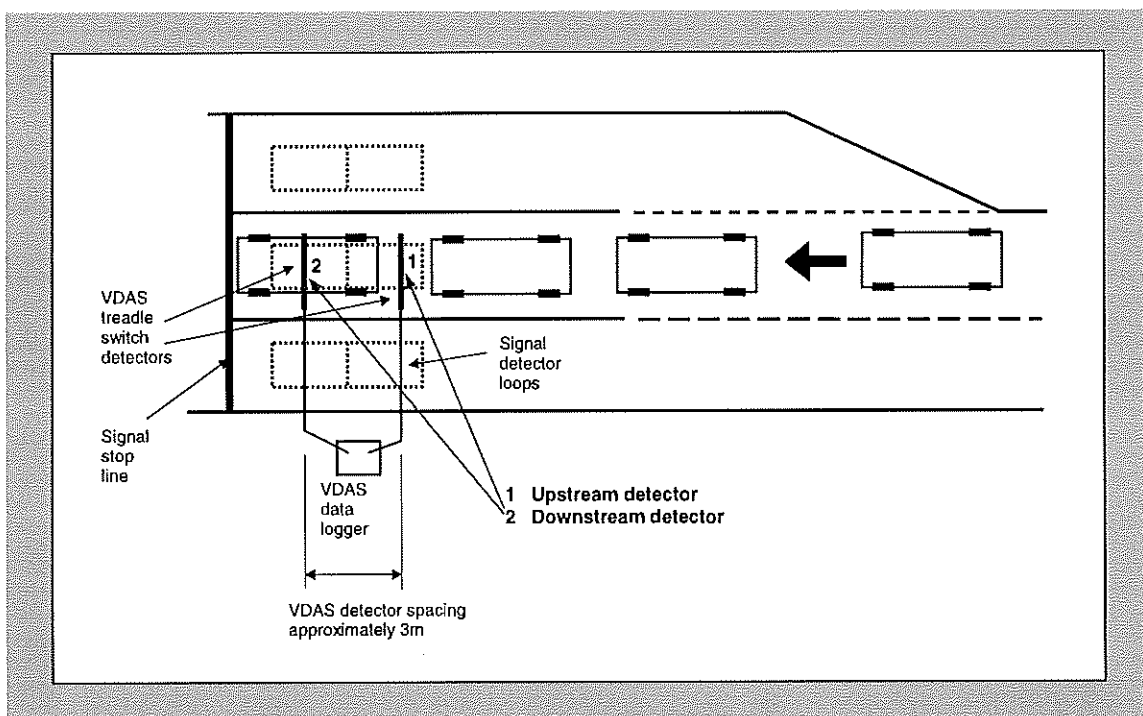


Figure 6.1 – Passage detection system using two VDAS detectors located centred over the traffic signal loop detector

Another difficulty experienced in the calibration of queue discharge models is lack of data at low speeds which is a result of difficulty in collecting headway and speed data for the first three vehicles. For a given vehicle, headway is the difference between the times of passage of the front of the previous vehicle and the front of the subject vehicle at a given detector location. For this reason headway is not defined for the first vehicle. Furthermore, positioning of the first vehicle makes it difficult to determine the headway for the second vehicle as well.

A detailed description of how the raw data collected by the VDAS system are converted to individual vehicle headway and speed information used in calibrating queue discharge models is presented below.

The method used for deriving headway and speed data for individual vehicle parameters can be explained with the help of *Figures 6.2 and 6.3*. These figures give time-distance diagrams explaining the observation of traffic flow parameters with two passage detectors. *Figure 6.2* shows the simple case of vehicles with constant speeds (during the later part of the green period), and *Figure 6.3* shows the more complicated case of vehicles accelerating (during the earlier part of the green period).

The constant speed case shown in *Figure 6.2* does not present any difficulty as the headways between vehicles remain constant, and as a result, the headways measured at the first and second detector tend to be equal ($h_1 = h_2$).

A good understanding of the acceleration case is important in relation to the problem of improved accuracy of headways and speeds measured for vehicles departing from the queue during the earlier part of the green period. As seen in *Figure 6.3*, the headways and speeds measured at the two detectors may vary considerably for vehicles in acceleration.

In *Figures 6.2 and 6.3*, vehicles A and B are the leading and following vehicles, respectively. The parameters related to the passage detection system and vehicles are as follows:

- L_y : distance between the two detectors (m)
- L_{vA} : length of vehicle A (m)
- L_{vB} : length of vehicle B (m)

As indicated in *Figure 6.1*, $L_y = 3.0$ was used in the surveys.

The raw data recorded by the VDAS detection system are the base actuation times (in seconds) shown on the time axis at the bottom of *Figures 6.2 and 6.3*. These are:

- t_{1LA} : the time when the *leading* (front) end of vehicle **A** crosses *Detector 1*
- t_{1TA} : the time when the *trailing* (rear) end of vehicle **A** crosses *Detector 1*
- t_{2LA} : the time when the *leading* end of vehicle **A** crosses *Detector 2*
- t_{2TA} : the time when the *trailing* end of vehicle **A** crosses *Detector 2*
- t_{1LB} : the time when the *leading* end of vehicle **B** crosses *Detector 1*
- t_{1TB} : the time when the *trailing* end of vehicle **B** crosses *Detector 1*
- t_{2LB} : the time when the *leading* end of vehicle **B** crosses *Detector 2*
- t_{2TB} : the time when the *trailing* end of vehicle **B** crosses *Detector 2*

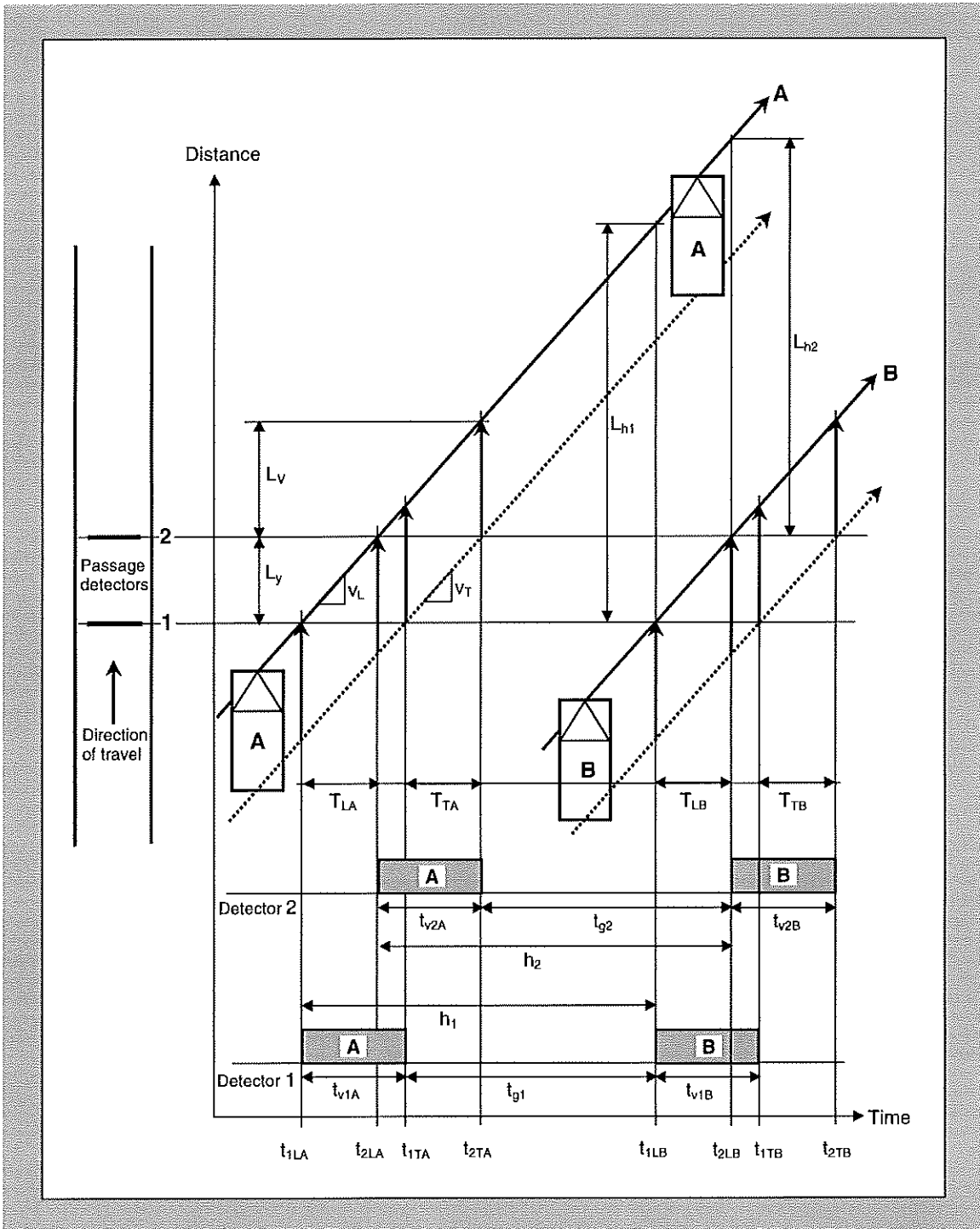


Figure 6.2 – Time-distance diagram explaining the observation of traffic flow parameters with two passage detectors: vehicles with constant speeds

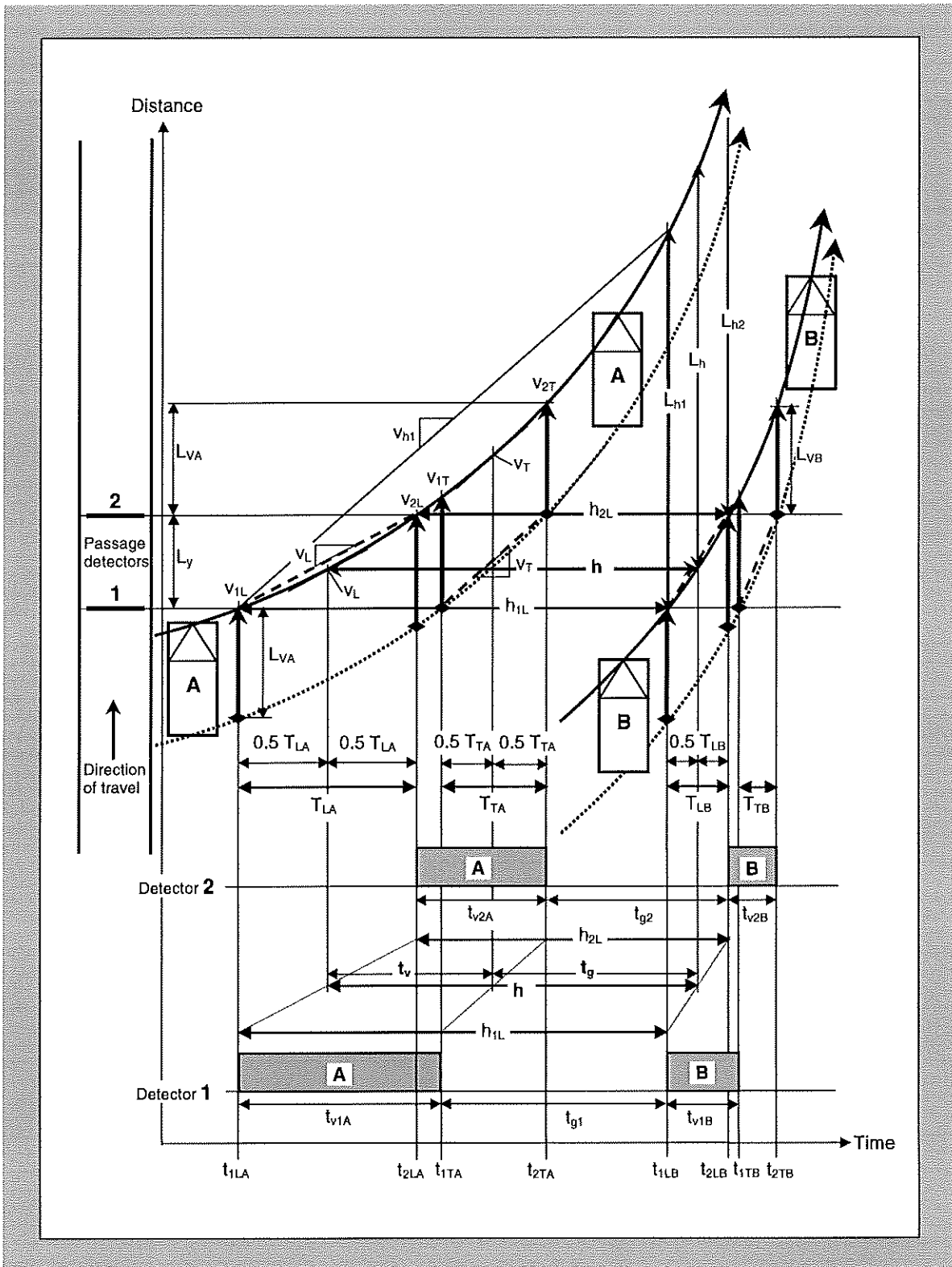


Figure 6.3 – Time-distance diagram explaining the measurement of traffic flow parameters with the two passage detectors: vehicles in acceleration

Using the raw data collected by the VDAS passage detection system, the following quantities are calculated (see *Figures 6.2 and 6.3*):

T_{LA} : travel time between Detectors 1 and 2 for the *leading end of vehicle A*

$$T_{LA} = t_{2LA} - t_{1LA} \quad (6.1)$$

T_{TA} : travel time between Detectors 1 and 2 for the *trailing end of vehicle A*

$$T_{TA} = t_{2TA} - t_{1TA} \quad (6.2)$$

T_{LB} : travel time between Detectors 1 and 2 for the *leading end of vehicle B*

$$T_{LB} = t_{2LB} - t_{1LB} \quad (6.3)$$

T_{TB} : travel time between Detectors 1 and 2 for the *trailing end of vehicle B*

$$T_{TB} = t_{2TB} - t_{1TB} \quad (6.4)$$

The speeds (km/h) based on time measurements for the leading and trailing ends of the vehicle are calculated from (given for vehicle A):

$$v_L = 3.6 L_y / T_{LA} \quad (6.5)$$

$$v_T = 3.6 L_y / T_{TA} \quad (6.6)$$

Headways (h), vehicle passage times (t_v) and gap times (t_g) for individual vehicles as measured at detectors 1 and 2 are calculated as follows:

$$h_{1L} = t_{1LB} - t_{1LA} \quad (6.7)$$

$$h_{2L} = t_{2LB} - t_{2LA} \quad (6.8)$$

$$t_{v1A} = t_{1TA} - t_{1LA} \quad (6.9)$$

$$t_{v2A} = t_{2TA} - t_{2LA} \quad (6.10)$$

$$t_{g1} = t_{1LB} - t_{1TA} \quad (6.11)$$

$$t_{g2} = t_{2LB} - t_{2TA} \quad (6.12)$$

Average headway, vehicle passage time, gap time and speed values are calculated as follows:

$$h = 0.5 (h_{1L} + h_{2L}) \quad (6.13)$$

$$t_v = 0.5 (t_{v1A} + t_{v2A}) \quad (6.14)$$

$$t_g = 0.5 (t_{g1} + t_{g2}) \quad (6.15)$$

$$v_a = 0.5 (v_L + v_T) \quad (6.16)$$

As seen in *Figure 6.3*, $h_{1L} = t_{v1A} + t_{g1}$, $h_{2L} = t_{v2A} + t_{g2}$, and $h = t_v + t_g$.

As discussed in *Section 5*, the headway and gap time parameters given by *Equations (6.13) and (6.15)* belong to the following vehicle (i.e. in front of vehicle B) since these parameters are observed when vehicle B arrives at the detection system. Therefore, these parameters are used in association with vehicle B in data analysis. However, the vehicle passage time from *Equation (6.14)* is associated with the leading vehicle (vehicle A) as it depends on the speed of vehicle A (v_L , v_T , v_A as shown in *Figures 6.2 and 6.3*).

Note that an arithmetic mean of the leading and trailing speeds is used. Assuming a constant acceleration rate during that part of the acceleration manoeuvre of the vehicle over the two-detector system, the average speed v_a represents the speed at mid-point in time between where speed v_L occurs (at time $t_{1LA} + 0.5 T_{LA}$) and speed v_T occurs (at time $t_{1TA} + 0.5 T_{TA}$).

An acceleration rate based on the assumption of constant acceleration can be estimated using the basic data as follows:

$$a = (v_T - v_L) / t_v \quad (6.17)$$

where t_v is the average vehicle passage time from *Equation (6.14)*, and v_L and v_T are the leading and trailing speeds from *Equations (6.5) and (6.6)*.

The constant acceleration rate estimate from *Equation (6.17)* could be used to obtain speeds v_{1L} , v_{2L} , v_{1T} , v_{2T} for the front of the vehicle at base times t_{1LA} , t_{2LA} , t_{1TA} , t_{2TA} as shown in *Figure 6.3*:

$$v_{1L} = v_L - 0.5 a T_{LA} \quad (6.18a)$$

$$v_{2L} = v_L + 0.5 a T_{LA} \quad (6.18b)$$

$$v_{1T} = v_T - 0.5 a T_{TA} \quad (6.18c)$$

$$v_{2T} = v_T + 0.5 a T_{TA} \quad (6.18d)$$

Therefore, $v_L = 0.5 (v_{1L} + v_{2L})$ and $v_T = 0.5 (v_{1T} + v_{2T})$ represent average speeds at mid-points of T_{LA} and T_{TA} times (however, the corresponding distances are not at the mid-point of the travel distance).

The two-detector passage detection system is thus used to measure individual vehicle headways and speeds. The system cannot measure vehicle *spacings* (L_h), i.e. the distance (m) between vehicles A and B, directly. As the headway and speed change while the two vehicles accelerate, the spacing between them also changes.

In *Figures 6.2 and 6.3*, spacing is seen to be measured in front of vehicle B (i.e. L_{h1} and L_{h2} as measured at times t_{1LB} and t_{2LB} belong to vehicle B), but this is related to the speed of the leading edge of vehicle A. As seen in *Figure 6.3*, the spacing values L_{h1} and L_{h2} correspond to headways at detectors 1 and 2 (h_{1L} , h_{2L}), and the average spacing L_h corresponds to the average headway (h), respectively. The corresponding speeds (vehicle A) are v_{1LA} , v_{2LA} and v_L .

The spacings can be estimated using the constant acceleration assumption:

$$L_{h1} = v_{h1} h_{1L} = (v_{1L} + 0.5 a h_{1L}) h_{1L} \quad (6.19a)$$

$$L_{h2} = v_{h2} h_{2L} = (v_{2L} + 0.5 a h_{2L}) h_{2L} \quad (6.19b)$$

$$L_h = v_h h = (v_L + 0.5 a h) h \quad (6.19c)$$

From *Equations (6.18a) and (6.18b)*, spacings at detectors 1 and 2 can also be expressed as:

$$L_{h1} = (v_L - 0.5 a T_{LA} + 0.5 a h_{1L}) h_{1L} \quad (6.20a)$$

$$L_{h2} = (v_L + 0.5 a T_{LA} + 0.5 a h_{2L}) h_{2L} \quad (6.20b)$$

7 QUEUE DISCHARGE MODELS

Various models to represent queue discharge characteristics at a signalised intersection as depicted in *Figure 7.1* were investigated during this research and exponential functions of queue discharge flow rate and speed were found to provide the most useful model. Bonneson (1992a,b) developed queue discharge headway and speed models which calculated the departure headway and speed as a function of the *vehicle position in queue*. Bonneson's headway model was not of particular use for the purpose of this study, but his model for speed as a function of the queued vehicle position provided a good exponential form.

Instead of using the vehicle position in queue, the queue discharge flow rate (headway) and speed models are expressed as a function of the *time since the start of green*. This provides simple yet powerful analytical models for the investigation of queue discharge characteristics at signalised intersections.

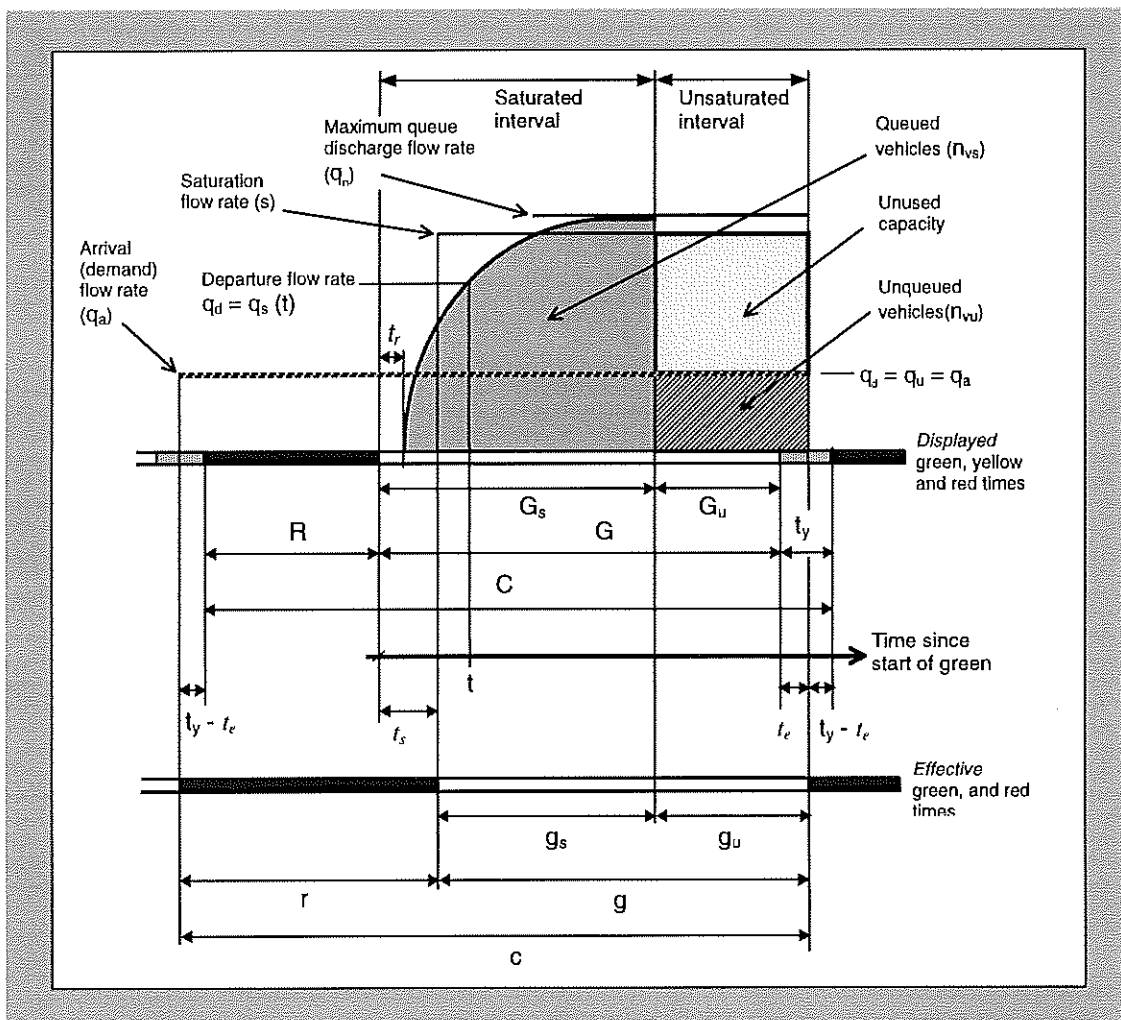


Figure 7.1 – Departures during the saturated and unsaturated portions of the green period with the exponential queue discharge model and saturation flow approximation shown

The readers interested in alternative model forms are referred to Akçelik, Roper and Besley (1999b) for a study of models for saturated freeway flows. Some of these models were found to give reasonable estimates for queue discharge flows at the signal stop line. However, comprehensive analyses were not carried out on alternative models since the exponential model was found to be more useful and satisfactory.

The exponential queue discharge speed and flow rate models are expressed as follows:

$$v_s = v_n (1 - e^{-m_v(t - t_r)}) \quad (7.1)$$

$$q_s = q_n (1 - e^{-m_q(t - t_r)}) \quad (7.2)$$

where

t = time since the start of the displayed green period (seconds),

t_r = start response time (a constant value) related to an average driver response time for the first vehicle to start moving at the start of the displayed green period (seconds),

v_s = queue discharge speed at time t (km/h),

v_n = maximum queue discharge speed (km/h),

m_v = a parameter in the queue discharge speed model,

q_s = queue discharge flow rate at time t (veh/h),

q_n = maximum queue discharge flow rate (veh/h), and

m_q = a parameter in the queue discharge flow rate model.

In *Equations (7.1) and (7.2)*, q_n and v_n are the parameters for the actual traffic mix including heavy vehicles although calibration results are for light vehicles (mainly cars) only. In *Figure 7.1*, q_a and q_d represent the arrival and departure flow rates, respectively. The departure flow rate is $q_d = q_s(t)$ during the *saturated* part of the green period, and $q_d = q_u = q_a$ during the *unsaturated* part of the green period.

The queue discharge headway at time t (h_s in seconds) and the cumulative queue discharge flow at time t (n_s in vehicles) models that correspond to *Equation (7.2)* are:

$$h_s = h_n / (1 - e^{-m_q(t - t_r)}) \quad (7.3)$$

$$\begin{aligned} n_s &= \int_{t_r}^t \left(\frac{q_s}{3600} \right) dt \quad (\text{for } t > t_r) \quad (7.4) \\ &= \frac{q_n}{3600} \left[(t - t_r) - \frac{1 - e^{-m_q(t - t_r)}}{m_q} \right] \end{aligned}$$

where h_n is the minimum queue discharge headway (seconds) and q_n is the maximum queue discharge flow rate (veh/h).

The headway and flow rate parameters are related through:

$$h = 3600 / q \quad (7.5a)$$

where q is the flow rate in veh/h and h is the headway in seconds.

Thus:

$$h_s = 3600 / q_s \quad (7.5b)$$

$$h_n = 3600 / q_n \quad (7.5c)$$

The following queue discharge speed-flow and flow-speed relationships can be derived from *Equations (7.1) and (7.2)*:

$$v_s = v_n [1 - (1 - q_s / q_n)^{m_v / m_q}] \quad (7.6a)$$

$$q_s = q_n [1 - (1 - v_s / v_n)^{m_q / m_v}] \quad (7.6b)$$

The vehicle spacing at time t during the queue discharge, L_{hs} (m/veh) can be calculated using the general relationship:

$$L_{hs} = v_s h_s / 3.6 = 1000 v_s / q_s \quad (7.7)$$

where v_s (km/h), q_s (veh/h) and h_s (s) are from *Equations (7.1) to (7.3)*.

Applying the boundary condition that speed is zero ($v_s = 0$) when the vehicle spacing during queue discharge equals the jam spacing ($L_{hs} = L_{hj}$), the parameters m_v and m_q are related through:

$$m_q = m_v \frac{L_{hn}}{L_{hj}} = 1000 m_v \frac{v_n}{q_n L_{hj}} \quad (7.8)$$

where L_{hj} is the average jam spacing (m/veh), and L_{hn} is the average spacing (m/veh) at the minimum queue discharge headway, or maximum queue discharge flow rate ($L_{hn} = v_n h_n / 3.6 = 1000 v_n / q_n$). Average jam spacing is the sum of average gap (space) length and average vehicle length for vehicles in a stationary queue ($L_{hj} = L_{sj} + L_v$).

Signal Timing Relationships

Relationships between displayed and effective red, green and cycle times are shown in *Figure 7.1*, and the formulae are given below.

$$g = G - t_s + t_e - t_b \quad (7.9)$$

$$r = R + t_s + t_y - t_e + t_b \quad (7.10)$$

$$C = R + G + t_y \quad (7.11)$$

$$c = r + g = C \quad (7.12)$$

$$G_s = g_s + t_s + t_b \quad (7.13)$$

$$G_u = G - G_s = g_u - t_e \quad (7.14)$$

$$g = g_s + g_u = G_s - t_s - t_b + G_u + t_e = G - t_s - t_b + t_e \quad (7.15)$$

where r , g , c are the effective red, green and cycle times; R , G , C are the displayed red, green and cycle times; g_s , g_u are the durations of the saturated and unsaturated intervals of the effective green period; G_s , G_u are the corresponding displayed green values; t_y is the yellow time; t_s , t_e are the start loss and end gain times; and t_b is the blocked green time, i.e. that part of the green period during which no vehicles can depart due to downstream queue interference, opposing vehicles, pedestrians, and so on (not shown in *Figure 7.1*).

Start and Departure Response Times, Queue Clearance and Arrival Wave Speeds, Start Loss and Acceleration Delay

Figure 7.2 shows vehicles accelerating from the queue at the start of the green period. This is an idealised diagram in that all vehicles accelerate in the same way with average acceleration characteristics assigned to each vehicle. Relationships among queue clearance wave speed, start and departure response times, start loss and acceleration delay parameters can be explained with the help of this diagram.

It is seen in *Figure 7.2* that, as the vehicles accelerate at the start of the green period and as the time since the start of the green period increases, the queue discharge headways measured at the VDAS detectors (h_s) reduce and the queue discharge speeds (v_s) increase. Eventually, vehicle speeds and headways measured at the two VDAS detector locations become steady and equal (approaching v_n and h_n).

As indicated in *Figure 7.2*, traditional traffic modelling simplifies this behaviour by projecting vehicle trajectories to the signal stop line, in effect, assuming instantaneous accelerations to the maximum queue departure speed (v_n) and departures at the maximum flow rate (q_n) (saturation flow rate, s), or with minimum departure headways (h_n). In this process, the first vehicle departing from the queue is also assigned the minimum headway, and the earlier part of the green period is considered to be a start loss (t_s). This can be explained through the following relationship between start loss, acceleration delay and the start response parameter (t_r) used in the exponential queue discharge models:

$$t_r = t_s + h_n - d_a \quad (7.16)$$

where d_a is the average acceleration delay calculated from:

$$d_a = t_a - 3.6 x_a / v_n \quad (7.17)$$

where t_a is the acceleration time (s), i.e. time it takes to accelerate from zero speed to the maximum queue discharge speed, v_n (km/h), x_a is the corresponding acceleration distance (m). Acceleration time and distance models given in the SIDRA user guide can be used to estimate these parameters (Akçelik and Besley 1999).

The queue clearance wave speed, v_x (km/h) corresponding to the minimum queue discharge headway (h_n) and the maximum queue discharge speed (v_n) as shown in *Figures 7.2 and 7.3* is given by:

$$v_x = v_n / (L_{hn} / L_{hj} - 1) = 3.6 L_{hj} / (h_n - 3.6 L_{hj} / v_n) \quad (7.18)$$

where $L_{hn} = v_n h_n / 3.6$ is the vehicle spacing (m) at the minimum queue discharge headway, and L_{hj} is the jam spacing (m).

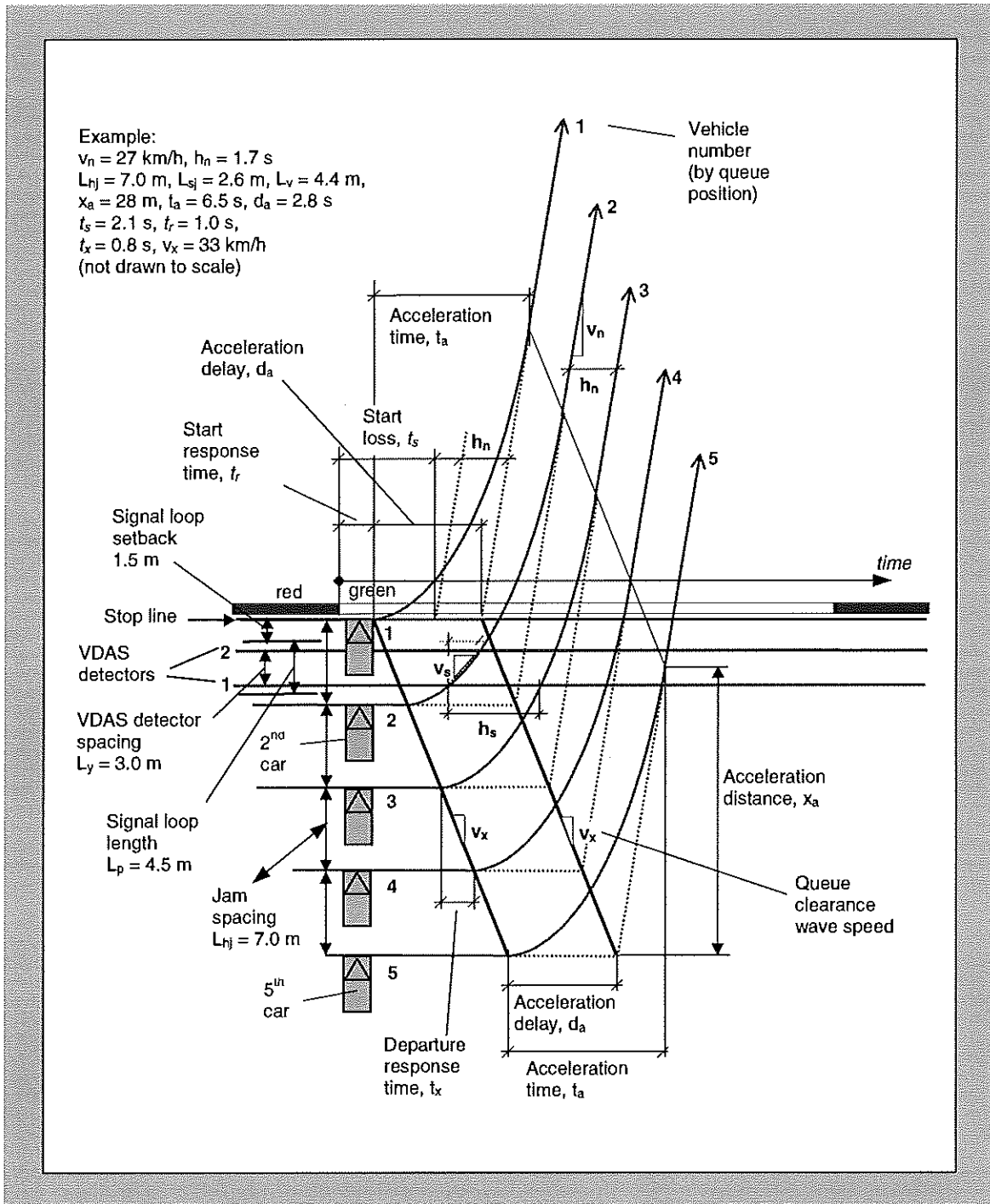


Figure 7.2 – Start and departure response times, queue clearance wave speed, start loss and acceleration delay

Departure Flows at the Signal Stop Line

To understand the difference between congested and uncongested traffic operations, it is important to distinguish between the *arrival (demand)* flow rate and the *departure* flow rate for a given traffic facility. As seen in *Figure 7.1*, the departure flow rate (q_d) measured at the signal stop line can be:

- (i) the departure flow rate ($q_d = q_s$) during the *saturated* part of green period (G_s or g_s), or
- (ii) the departure flow rate ($q_d = q_u = q_a$) during the *unsaturated* part of green period (G_u or g_u).

The departure flow rate during the saturated part of green period (q_s) is the queue discharge flow rate. This rate is seen to increase exponentially from zero at the start of the green period (after the start response time, t_r) to a maximum flow rate (q_n). Thus, q_s is a function of the time after the start of green, $q_s(t)$, as shown in *Figure 7.1*, and expressed by *Equation (7.2)*.

The departure flow rate after queue clearance (for unqueued vehicles) corresponds to the *arrival (demand)* flow rate measured under uninterrupted conditions at a point upstream of the back of queue, $q_d = q_u = q_a$. *Figure 7.1* depicts a constant (average) arrival flow rate (q_a) throughout the signal cycle. This represents the isolated intersection assumption in signal analysis methods.

A simple platooned arrivals model used in signal timing and performance analyses assumes two different arrival rates during the red and green periods (q_{ar} , q_{ag}). This can be specified using a known platoon arrival ratio, $P_A = q_{ag} / q_{ac}$ where q_{ac} is the arrival flow rate during the signal cycle. In the case of platooned arrivals, the departure flow rate during the unsaturated part of green period is $q_d = q_u = q_{ag} = P_A q_{ac}$. With non-platooned arrivals, $P_A = 1.0$ and $q_{ac} = q_{ag} = q_{ar} = q_a$. The reader is referred to Akçelik (1995b) for a detailed discussion of this subject.

Traditional methods of traffic signal analysis and control (Webster and Cobbe 1966, Akçelik 1981, AUSTROADS 1993, TRB 1998) approximate the queue discharge flow using a constant *saturation flow* rate, s , and the associated *start loss* and *end gain* time parameters (t_s , t_e), which are shown in *Figure 7.1*. These parameters are used to replace the displayed green, yellow and red times (G , t_y , R) with effective green and red times (g , r). The saturation flow approximation is based on obtaining the same number of (cumulative) vehicle departures from the queue as the area under the $q_s(t)$ curve for the period t_r to G_s . The average saturation flow rate (s) is very close to the maximum queue discharge flow rate (q_n) if the green period duration is sufficiently long. The derivation of average saturation flow, start loss and end gain parameters from the exponential queue discharge model using various definitions of saturation flow is discussed in *Section 12*.

While the well-established traditional methods are simpler to use, the use of the more realistic exponential queue discharge model is feasible using iterative methods through computer modelling. This would be beneficial in traffic signal analysis and control since the cycle capacity becomes more sensitive to the duration of the green period (i.e. capacity loss in short green periods would be better predicted).

The characteristic of the function representing the queue departure flow rate will change when there is downstream queue interference, i.e. when a downstream queue results in insufficient space for the departing vehicles to accelerate to full saturation speed. This could be represented by a reduced queue discharge flow rate and speed. This is discussed in *Section 11*.

In this report, the symbols q_n and s for maximum flow rate and saturation flow rate are used for the actual traffic mix including heavy vehicles. For a stream consisting of passenger car units (or light vehicles) only, the corresponding rates will be denoted by q_m and s_m . However, notations q_n and s are used in presenting the model calibration results (*Section 9*) and elsewhere in this report although the model calibration was conducted for conditions with light vehicles only.

Various relationships describing queue discharge characteristics at signalised intersections are given below.

Queue Clearance Time

The duration of the saturated part of the effective green period (queue clearance time) can be estimated from:

$$g_s = \frac{f_q y r}{1 - y} \quad \text{subject to } g_s \leq g \quad (7.23)$$

where

f_q = a factor that allows for (i) cycle-by-cycle variations in the value of the queue clearance time and (ii) effect of platooned arrivals,

y = flow ratio, i.e. the ratio of the arrival flow rate to saturation flow rate, $y = q_{ac} / s$ (for non-platooned arrivals, $y = q_a / s$), and

r = effective red time (seconds).

The factor f_q can be calculated using the SIDRA equations (Akçelik and Besley 1999):

$$f_q = PF_2 \quad \text{for fixed-time signals} \quad (7.24a)$$

$$f_q = PF_2 (1.08 - 0.1 (G/G_{max})^2) \quad \text{for actuated signals} \quad (7.24b)$$

subject to $(1.08 - 0.1 (G/G_{max})^2) \geq 1.0$

where

PF_2 = a progression factor for platooned arrivals generated by coordinated signals ($PF_2 = 1.0$ for random arrivals) (see Akçelik 1995b, Akçelik and Besley 1999),

G = displayed green time (seconds), and

G_{max} = maximum green time setting for actuated signals (seconds).

The duration of the unsaturated part of the effective green period (time after queue clearance time) can be calculated from:

$$g_u = g - g_s \quad (7.25)$$

The durations of the saturated and unsaturated parts of the green period (G_s , G_u) can be obtained using *Equations (7.13) and (7.14)*.

Number of Vehicles Departing During the Green Period

The following equation is a more general form of *Equation (7.4)* to calculate the number of vehicles that depart from the queue *during the interval t_1 to t_2* (n_{vT}):

$$\begin{aligned} n_{vT} &= \int_{t_1}^{t_2} (q_s / 3600) dt & (7.26) \\ &= \frac{q_n}{3600} \left[(t_2 - t_1) - \frac{e^{-m_q(t_1-t_r)} - e^{-m_q(t_2-t_1)}}{m_q} \right] \text{ for } t_r \leq t_1 \leq t_2 \leq G_s \end{aligned}$$

This equation applies for an interval after the start of the green period and before the end of the saturated part of the green period as indicated by the condition $t_r \leq t_1 \leq t_2 \leq G_s$. More specific forms of this equation are given below.

The number of vehicles that depart from the queue *during an initial interval 0 to t_i* , or effectively from t_r to t_i (n_{vi}), obtained from *Equation (7.26)* putting $t_1 = t_r$ and $t_2 = t_i$:

$$\begin{aligned} n_{vi} &= \int_{t_r}^{t_i} (q_s / 3600) dt & (7.27) \\ &= \frac{q_n}{3600} \left[(t_i - t_r) - \frac{1 - e^{-m_q(t_i-t_r)}}{m_q} \right] \text{ for } t_r \leq t_i \leq G_s \end{aligned}$$

Considering an unsaturated green period ($G_s < G$), the number of vehicles that depart from the queue *during the saturated part of the green period*, i.e. during the interval 0 to G_s , or effectively from t_r to G_s (n_{vs}), obtained from *Equation (7.26)* putting $t_1 = t_r$ and $t_2 = G_s$:

$$\begin{aligned} n_{vs} &= \int_{t_r}^{G_s} (q_s / 3600) dt & (7.28) \\ &= \frac{q_n}{3600} \left[(G_s - t_r) - \frac{1 - e^{-m_q(G_s-t_r)}}{m_q} \right] \end{aligned}$$

This is the number of queued vehicles during the green period.

Finding n_{vs} from *Equation (7.28)* requires an iterative method since G_s depends on the saturation flow as seen from *Equation (7.23)*. The basis of *Equation (7.23)* is the relationship $n_{vs} = n_r + q_{ar} R + q_{ag} G_s$ where n_r is the residual queue left over from the previous green time ($n_r = 0$ in *Equation 7.23*), q_{ar} is the arrival flow rate during the red period, and q_{ag} is the arrival flow rate during the green period. *Equation (7.23)* is obtained by using the saturation flow approximation:

$$n_{vs} = s g_s / 3600 \quad (7.28a)$$

where $g_s = G_s - t_s$ from *Equation (7.13)*. It is shown in *Section 12* that the values of average saturation flow and start loss depend on the duration of G_s . As a result *Equations (7.28) and (7.23)* need to be solved together using an iterative method. When G_s is sufficiently long, $s = q_n$ is obtained. This can be used to determine G_s from

Equation (7.23) without iterations, or this value of G_s can be used as an initial value in the iterative method.

The number of unqueued vehicles that depart *during the unsaturated part of the green period* is given by:

$$n_{vu} = q_u g_u / 3600 \quad (7.29)$$

where q_u is the flow rate (veh/h) during the unsaturated part of the green period ($q_u = q_{ag}$ for platooned arrivals, or $q_u = q_a$ for random arrivals), and g_u is the unsaturated part of the green period from *Equation (7.25)*.

The total number of vehicles that depart *during green period* (n_{vg}) is calculated differently for an unsaturated green period, i.e when the green period is not fully saturated ($G_s < G$), and for a fully saturated green period ($G = G_s$):

$$\begin{aligned} n_{vg} &= n_{vs} + n_{vu} && \text{for } G_s < G \\ &= n_{vs} + n_e && \text{for } G_s = G \end{aligned} \quad (7.30)$$

where n_{vs} and n_{vu} are calculated from *Equations (7.28) and (7.29)*, and n_e is the number of vehicles departing after the end of green period (during yellow and all-red clearance intervals).

When the saturation flow approximation is used, the number of vehicles that depart during a fully saturated effective green period ($g_s = g$) is given by:

$$n_{vg} = s g / 3600 \quad (7.31)$$

The *average departure flow rates* (veh/h) during the during the green period, q_{dg} and the signal cycle, q_{dc} can be calculated from:

$$q_{dg} = 3600 n_{vg} / g \quad (7.32)$$

$$q_{dc} = 3600 n_{vg} / c \quad (7.33)$$

where c is the cycle time (s) and g is the effective green time.

The *average departure headway* during the green period allowing for different departure headways during the saturated and unsaturated parts of the green period is given by:

$$h_{dg} = 3600 / q_{dg} = g / n_{vg} \quad (7.34)$$

The *capacity*, Q (veh/h) is obtained as an average departure flow rate per cycle considering fully saturated green periods ($Q = q_{dc}$ for $G_s = G$ and $G_u = 0$, or $g_s = g$ and $g_u = 0$). From *Equation (7.33)*:

$$Q = 3600 n_{vg} / c \quad (7.35)$$

With the saturation flow approximation, using n_{vg} from *Equation (7.31)*:

$$Q = s g / c \quad (7.36)$$

The *unused (spare) capacity* considering an undersaturated green period ($G_s < G$) as shown in *Figure 7.1* is $n_{vg} - (n_{vs} + n_{vu})$ where n_{vg} is for $G_s = G$. Using the saturation flow approximation, the unused capacity is $sg - (s g_s + q_u g_u) = (s - q_u) g_u$.

8 MODEL CALIBRATION METHOD

A key criterion in the calibration of the exponential queue discharge speed and flow models is the best prediction ability for low speed and low flow rate conditions. In particular, the decision regarding optimum loop length depends on these conditions (see *Section 14*). On the other hand, the calibration method is affected by lack of data at very low speeds and low flow rates. This is a result of the difficulty in measuring speed and headway for the first few vehicles in the queue. As a result, alternative calibration methods were developed during this research.

The calibration method described in this report differs from the iterative method used in the earlier stages of the study for calibrating the queue discharge flow rate model. Thus, the calibration results given in *Section 9* supersede the results given in the earlier report WD R 96/043 (Akçelik and Besley 1996). Instead, an inverse frequency weighted average value of the minimum headway (h_n) is determined. This parameter is then used in determining parameter m_q using jam spacings (L_{hj}) measured for each site as discussed in *Sections 2 and 4*.

As discussed by Messer and Bonneson (1997), higher frequency of headway observations at lower queue positions (with larger headways) may introduce a bias in determining the minimum queue departure headway (h_n). The method used here employs headways weighted by inverse frequency of the headways by queue position in order to avoid this bias.

Minimum departure headway and maximum departure flow rate parameters obtained using the calibration method *with and without weighting* are also given in *Section 9*.

All calibration results given in this report are for conditions with light vehicles (mainly cars) only. Data points for heavy vehicles as well as those with headways affected by heavy vehicles were removed from each data set for this purpose.

Standard Calibration Procedure

The standard calibration procedure used in this report is described below. The procedure is repeated in *Figure 8.1* due to its importance.

- (i) The average jam spacing value for light vehicles (L_{hjLV}) measured for each site is used.
- (ii) Non-linear regression analyses are carried out to determine parameters v_n and m_v in the queue discharge speed model (*Equation 7.1*).
- (iii) The minimum queue discharge headway (h_n) is determined as the average headway for vehicles excluding the headways of the first *five* queue positions. Headways are weighted by inverse frequency of the headways by queue position in order to avoid the bias due to the higher frequency of headways at lower queue positions. Thus, the weighting factor for each queue position is determined as the total number of data points for all queue positions divided by the number of data points for the given queue position.

(iv) Parameters q_n and m_q in the queue discharge flow rate model (*Equation 7.2*) are calculated from:

$$q_n = 3600 / h_n \quad (8.1)$$

$$m_q = m_v L_{hn} / L_{hj} \quad (8.2)$$

where h_n is from step (iii), v_n and m_v are from step (ii), and $L_{hj} = L_{hjLV}$ is from step (i), and L_{hn} is the vehicle spacing at minimum queue discharge headway calculated from:

$$L_{hn} = v_n h_n / 3.6 \quad (8.3)$$

The speed and headway data used for the main set of calibration results given in *Section 9* were v_a , i.e. average of leading and trailing speeds from *Equation (6.16)*, and h_{1L} , i.e. the headway measured at Detector 1 from *Equation (6.7)*. The start response time was $t_r = 0$ for all sites. This is calibration method 1 in *Table 8.1* which summarises the alternative calibration methods discussed below.

Non-linear regression analyses were carried out using the SPSS package (Norusis and SPSS 1993).

Alternative Calibration Methods

Alternative calibration methods are investigated using different headway and speed data derived from raw detector data (see *Section 6*) and different values of the start response time, t_r in the queue discharge model (from regression or a specified value).

Alternative calibration methods are applied to data from three sites only, namely sites 335 (Melbourne), 610 (Sydney) and 511 (Sydney). Sites 335 and 610 are right-turn traffic lanes with short green times, and Site 511 is a major through traffic lane with very long green time.

Alternative calibration methods tested using data for these sites are summarised in *Table 8.1*. For all methods listed in *Table 8.1*, spacing data were calculated using *Equations (6.19a to 6.19c)*, and the estimated spacings were calculated from *Equation (7.7)*.

In most cases, the standard calibration procedure described in *Figure 8.1* is used. However, methods 5, 7, 10, 12 and 14 differ from the procedure significantly. These methods are indicated by an asterisk in *Table 8.1*. For these methods:

- (i) the headway (flow rate) model parameters are determined from regression, and
- (ii) the jam spacing is *estimated* using parameters from regression.

The model parameters obtained through alternative calibration methods are given in *Section 9*. Figures showing measured and predicted queue discharge speeds, headways, flow rates and spacings for alternative calibration method 13 are given in *Appendix B*.

Step 1

Use the average jam spacing value measured for each site. In this study, average jam spacing for light vehicles ($L_{hj} = L_{hjLV}$) was used since model calibration was carried out for conditions with light vehicles (mainly cars) only.

Step 2

Carry out non-linear regression analyses to determine parameters v_n and m_v in the queue discharge speed model:

$$v_s = v_n (1 - e^{-m_v(t - t_f)})$$

Step 3

Determine the minimum queue discharge headway (h_n) as the average headway for vehicles excluding the headways of the first *five* queue positions. Use weighting by inverse frequency of the headways by queue position in order to avoid the bias due to the higher frequency of headways at lower queue positions. Calculate the weighting factor for each queue position from:

$$\text{weighting factor} = \frac{\text{total number of data points for all queue positions}}{\text{the number of data points for the given queue position}}$$

Step 4

To determine parameters q_n and m_q in the queue discharge flow rate model:

$$q_s = q_n (1 - e^{-m_q(t - t_f)})$$

calculate:

$$q_n = 3600 / h_n$$

$$m_q = m_v L_{hn} / L_{hj}$$

where h_n is from *Step 3*, v_n and m_v are from *Step 2*, and L_{hj} is from *Step 1*, and L_{hn} is the vehicle spacing at minimum queue discharge headway calculated from:

$$L_{hn} = v_n h_n / 3.6$$

Figure 8.1 – Standard procedure used for the calibration of exponential queue discharge speed and flow rate models

Table 8.1

Alternative methods for queue discharge model calibration

Calibration method number	Speed data, v	Headway data h	Start response time t_r	Jam spacing L_{hj}	Speed model parameters m_v, v_n	Headway model parameter h_n	Headway (flow) model parameter m_q
1	v_a	h_{1L}	$t_r = 0$ specified	Measured value specified	Speed model regression	Weighted average for queue pos. > 5	Calculated from $m_q = m_v L_{hn} / L_{hj}$
2	v_L	h	$t_r = 0$ specified	Measured value specified	Speed model regression	Weighted average for queue pos. > 5	Calculated from $m_q = m_v L_{hn} / L_{hj}$
3	v_{1L}	h_{1L}	$t_r = 0$ specified	Measured value specified	Speed model regression	Weighted average for queue pos. > 5	Calculated from $m_q = m_v L_{hn} / L_{hj}$
4	v_{1L}	h_{1L}	From speed model regression	Measured value specified	Speed model regression	Weighted average for queue pos. > 5	Calculated from $m_q = m_v L_{hn} / L_{hj}$
5 *	v_{1L}	h_{1L}	From speed model regression	Calculated from $L_{hj} = (m_v / m_q) L_{hn}$	Speed model regression	Headway model regression	Headway model regression
6	v_{1L}	h_{1L}	$t_r = 1.0$ specified	Measured value specified	Speed model regression	Weighted average for queue pos. > 5	Calculated from $m_q = m_v L_{hn} / L_{hj}$
7 *	v_{1L}	h_{1L}	$t_r = 1.0$ specified	Calculated from $L_{hj} = (m_v / m_q) L_{hn}$	Speed model regression	Headway model regression	Headway model regression
8	NOT USED						
9	v_L	h_{2L}	$t_r = 0$ specified	Measured value specified	Speed model regression	Weighted average for queue pos. > 5	Calculated from $m_q = m_v L_{hn} / L_{hj}$
10 *	v_L	h_{2L}	$t_r = 0$ specified	Calculated from $L_{hj} = (m_v / m_q) L_{hn}$	Speed model regression	Headway model regression	Headway model regression
11	v_L	h_{2L}	From speed model regression	Measured value specified	Speed model regression	Weighted average for queue pos. > 5	Calculated from $m_q = m_v L_{hn} / L_{hj}$
12 *	v_L	h_{2L}	From speed model regression	Calculated from $L_{hj} = (m_v / m_q) L_{hn}$	Speed model regression	Headway model regression	Headway model regression
13	v_L	h_{2L}	$t_r = 1.0$ specified	Measured value specified	Speed model regression	Weighted average for queue pos. > 5	Calculated from $m_q = m_v L_{hn} / L_{hj}$
14 *	v_L	h_{2L}	$t_r = 1.0$ specified	Calculated from $L_{hj} = (m_v / m_q) L_{hn}$	Speed model regression	Headway model regression	Headway model regression

* Methods 5, 7, 10, 12, 14 does not use the standard calibration procedure

v_a = average of leading and trailing speeds from Equation (6.16)

v_L = leading speed, v_L from Equation (6.5)

v_{1L} = projected speed at Detector 1 from Equation (6.18a)

h_{1L} = headway measured at Detector 1 from Equation (6.7)

h_{2L} = headway measured at Detector 2 from Equation (6.8)

h = average headway from Equation (6.13)

v_n = maximum queue discharge speed

h_n = minimum queue discharge headway

q_n = queue discharge maximum flow rate (calculated as $q_n = 3600/h_n$)

m_v = parameter in the queue discharge speed model

m_q = parameter in the queue discharge headway (flow rate) model

Data Aggregation

Initial investigation of speed and headway data for vehicles crossing the signal stop line involved all vehicles queued and unqueued. Data were analysed by combining data points combined across all signal cycles, aggregated on the basis of time after the start of green period (in 1-second intervals). This method has the shortcoming of combining saturated and unsaturated data points around the transition (end of queue) region since the saturation (queue clearance) time varies from cycle to cycle.

The queue discharge speed and flow relationships obtained using this method were mentioned briefly in Akçelik (1996). However, the maximum queue discharge flow rates (q_n) obtained from this method appeared to be too high, and the quality of the regressions for queue discharge flow rates appeared to be not as good as the quality of regressions for queue discharge speeds. This method was abandoned since better results were obtained using non-aggregated data, ensuring that queue discharge speed and flow rates for saturated green periods only are used in model calibration.

Figure 8.2 shows the aggregated speed and flow data as a function of the time since the start of the green period for Site Mel1 (Ferntree Gully Road and Stud Road). Figure 8.3 shows speed as a function of the flow rate for the same site. Mixed speed and flow data points in Figures 8.2 and 8.3 denote the points which, in the process of aggregation, included data from different cycles some with queued vehicles and some with unqueued vehicles.

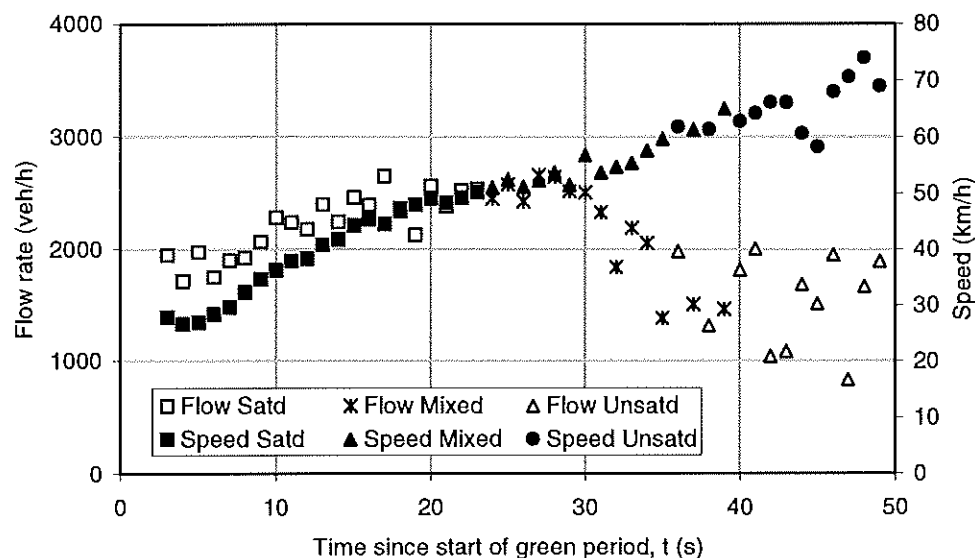


Figure 8.2 – Aggregated departure speed and flow data (1-sec averages) as a function of the time since the start of the green period for Site Mel1 (Ferntree Gully Rd and Stud Rd)

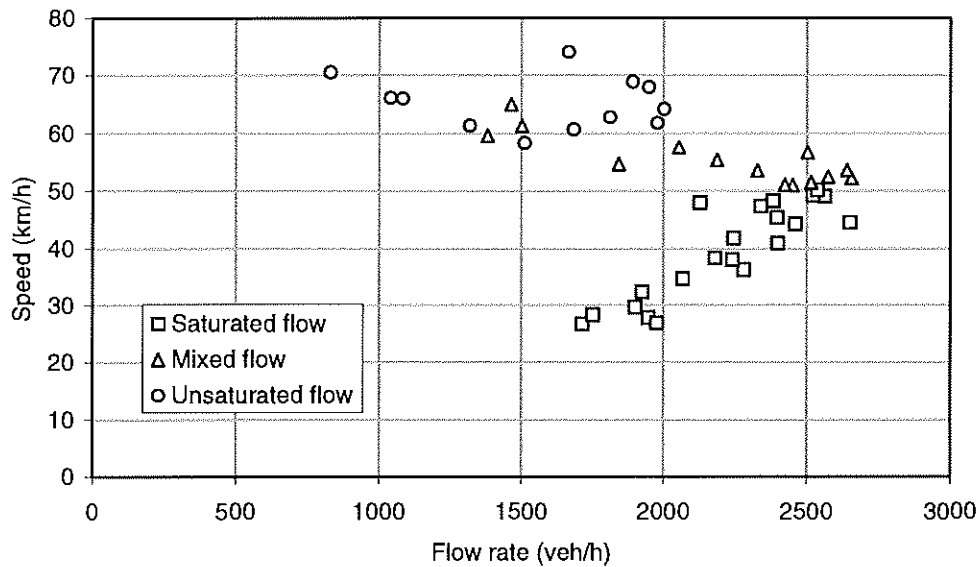


Figure 8.3 – Speed as a function of the departure flow rate for Site 1 (using the data shown in Figure 8.2)

Figures 8.2 and 8.3 are useful in showing the characteristics of departure flows at the signal stop line when both saturated and unsaturated portions of the green period are considered together. Calibration results for queue discharge (saturated flow) models are given in Section 9 while models representing unqueued (unsaturated) traffic flows are discussed in Section 10.

9 MODEL CALIBRATION RESULTS

Calibration Results for Queue Discharge Models For Sydney and Melbourne 1998 Sites

Sydney and Melbourne 1998 survey site characteristics are summarised in *Tables 3.1 and 3.2* in *Section 3*. Calibration results obtained using the procedure described in *Section 8* for Sydney and Melbourne 1998 survey sites are presented in *Tables 9.1 and 9.2*.

In addition to parameters v_n , m_v , h_n , q_n , and m_q , *Tables 9.1 and 9.2* give the speed limit that can be used as a free-flow speed (v_f), the ratio (v_f/v_n), jam spacing values for light and heavy vehicles ($L_{hj} = L_{hjLV}, L_{hjHV}$), spacing at maximum queue discharge flow speed (L_{hn}), ratio m_v/m_q , jam space (gap) length (L_{sj}), queue clearance wave speed (v_x), and the departure response time (t_x) for each site.

Confidence intervals of parameters v_n , m_v and q_n for each site are also given in *Tables 9.1 and 9.2*.

Tables 9.3 and 9.4 give the minimum departure headway and maximum departure flow rate parameters obtained using the standard calibration method described in *Section 8* with and without weighting.

Measured and predicted queue discharge speeds, flow rates, vehicle spacings and headways for all 1998 Sydney and Melbourne sites are shown in figures given in *Appendix B*. Spacing data seen in graphs given in *Appendix B* were calculated using *Equation (5.24)*, and the estimated spacings were calculated from *Equation (7.7)*.

Table 9.1

Parameters for the Queue Discharge Speed and Flow Models for SYDNEY 1998 Sites

Site	163	610	1081	413	511
Prop. HV in traffic stream	0.033	0.007	0.028	0.050	0.071
Prop. HV in jam queues	0.017	0.015	0.044	0.047	0.091
Measured L_{hj} (All veh.)	6.1	5.9	6.9	7.0	7.1
Measured L_{hjLV} (Cars only)	6.0	5.9	6.8	6.8	6.6
Calculated L_{hjHV} (HV only)	8.6	7.9	8.7	11.0	11.9
Sample size (Sat. periods)	452	188	1061	748	1615
Speed model					
R^2	0.53	0.48	0.61	0.38	0.63
v_n (km/h)	24.7	21.7	39.5	33.2	52.8
v_n 95% Confidence Interval	24.3 - 25.1	21.1 - 22.3	39.1 - 39.9	32.6 - 33.7	52.5 - 53.2
m_v	0.317	0.373	0.103	0.2	0.078
m_v 95% Confidence Interval	0.295 - 0.339	0.327 - 0.420	0.098 - 0.108	0.182 - 0.217	0.075 - 0.081
Headway and flow rate models					
h_n (s)	1.716	1.831	2.011	1.999	1.577
q_n (veh/h)	2098	1966	1790	1801	2283
q_n 95% Confidence Interval	2081 - 2114	1934 - 2000	1784 - 1797	1792 - 1810	2278 - 2289
m_q	0.621	0.698	0.334	0.542	0.273
Free-flow speed as the speed limit					
v_l (km/h)	60	60	60	60	70
v_n/v_l	0.41	0.36	0.66	0.55	0.75
Calculated parameters					
L_{hn} (m/veh)	11.8	11.0	22.1	18.4	23.1
m_v/m_q	0.510	0.535	0.308	0.369	0.285
L_{hj} (m/veh)	6.0	5.9	6.8	6.8	6.6
L_{sj} (m/veh) †	1.6	1.5	2.4	2.4	2.2
$v_x = v_n / (L_{hn} / L_{hj} - 1)$ (km/h)	25.7	24.9	17.6	19.4	21.1
$t_x = 3.6 L_{hj} / v_x$ (s)	0.84	0.85	1.39	1.26	1.13

† $L_{sj} = L_{hj} - L_v$ using $L_v = 4.4$ m.

Table 9.2

Parameters for the Queue Discharge Speed and Flow Models for MELBOURNE 1998 Sites

Site	121	335	3196	4273	849	456
Prop. HV in traffic stream	0.050	0.031	0.073	0.014	0.152	0.033
Prop. HV in jam queues	0.058	0.036	0.061	0.015	0.041	0.024
Measured L_{hj} (All veh.)	6.9	7.0	7.4	7.4	7.0	7.1
Measured L_{hjLV} (Cars only)	6.6	6.9	7.0	7.3	6.9	7.0
Calculated L_{hjHV} (HV only)	12.1	10.1	13.1	13.6	8.7	12.2
Sample size (Sat. periods)	309	588	635	632	972	626
Speed model						
R^2	0.43	0.5	0.44	0.67	0.76	0.83
v_n (km/h)	24.4	27.1	31.7	36.4	46.4	53.8
v_n 95% Confidence Interval	23.8 - 25.1	26.6 - 27.6	30.9 - 32.4	35.7 - 37.1	45.9 - 47.0	53.0 - 54.7
m_v	0.287	0.252	0.15	0.135	0.102	0.118
m_v 95% Confidence Interval	0.252 - 0.322	0.232 - 0.272	0.136 - 0.165	0.127 - 0.144	0.098 - 0.106	0.112 - 0.123
Headway and flow rate models						
h_n (s)	1.848	1.687	1.903	1.857	1.801	1.486
q_n (veh/h)	1948	2133	1892	1938	1999	2422
q_n 95% Confidence Interval	1931 - 1965	2121 - 2146	1882 - 1902	1927 - 1949	1990 - 2008	2410 - 2434
m_q	0.545	0.464	0.359	0.347	0.343	0.374
Free-flow speed as the speed limit						
v_t (km/h)	70	70	60	60	70	80
v_n/v_t	0.35	0.39	0.53	0.61	0.66	0.67
Calculated parameters						
L_{hn} (m/veh)	12.5	12.7	16.8	18.8	23.2	22.2
m_v/m_q	0.527	0.543	0.418	0.389	0.297	0.315
L_{hj} (m/veh)	6.6	6.9	7.0	7.3	6.9	7.0
L_{sj} (m/veh) †	2.2	2.5	2.6	2.9	2.5	2.6
$v_x = v_n / (L_{hn} / L_{hj} - 1)$ (km/h)	27.2	32.2	22.8	23.1	19.6	24.8
$t_x = 3.6 L_{hj} / v_x$ (s)	0.87	0.77	1.11	1.14	1.27	1.02

† $L_{sj} = L_{hj} - L_v$ using $L_v = 4.4$ m.

Table 9.3**Parameters for the Queue Discharge Headway and Flow Models
with and without headway weighting - SYDNEY 1998 Sites**

Site	163	610	1081	413	511
Without weighting					
h_n	1.719	1.848	2.044	2.001	1.621
q_n	2094	1948	1761	1799	2221
h_n - 95% Confidence Interval	1.664 - 1.775	1.715 - 1.981	1.996 - 2.093	1.942 - 2.060	1.588 - 1.654
With inverse frequency weighting by queue position					
h_n	1.716	1.831	2.011	1.999	1.577
q_n	2098	1966	1790	1801	2283
h_n - 95% Confidence Interval	1.703 - 1.730	1.800 - 1.862	2.003 - 2.018	1.989 - 2.009	1.573 - 1.580
No. of cases (queue position 6 and higher)	155	35	906	573	1525
Total sample size (all headways)	375	151	1022	705	1596

Table 9.4**Parameters for the Queue Discharge Headway and Flow Models
with and without headway weighting - MELBOURNE 1998 Sites**

Site	121	335	3196	4273	849	456
Without weighting						
h_n	1.778	1.704	1.875	1.961	1.789	1.517
q_n	2025	2113	1920	1836	2013	2373
h_n - 95% Confidence Interval	1.708 - 1.847	1.664 - 1.744	1.830 - 1.919	1.900 - 2.022	1.749 - 1.828	1.477 - 1.557
With inverse frequency weighting by queue position						
h_n	1.848	1.687	1.903	1.857	1.801	1.486
q_n	1948	2133	1892	1938	1999	2422
h_n - 95% Confidence Interval	1.832 - 1.864	1.677 - 1.698	1.892 - 1.913	1.847 - 1.868	1.793 - 1.809	1.479 - 1.494
No. of cases (queue position 6 and higher)	149	368	447	387	763	478
Total sample size (all headways)	271	526	591	566	920	588

Calibration Results for Melbourne 1996 Sites

The queue discharge model parameters for “Melbourne 1996” sites given in report WD R 96/043 (Akçelik and Besley 1996) were revised due to the improved calibration method applied to the Sydney and Melbourne 1998 data. Melbourne 1996 survey site characteristics are summarised in *Table 3.3 in Section 3*. The surveys were actually carried out during late 1993 to mid-1994, but are referred to by the year of the report.

The calibration results for Melbourne 1996 sites are given in *Table 9.5*. Note that Site Mel1 in *Table 9.5* is the same as Site 456 in *Table 9.2*. This provides an opportunity to compare results from surveys carried out at two different dates (although the survey method used in 1998 was more refined).

Melbourne 1996 sites are qualified as *isolated intersection* and *paired intersection* sites. Paired intersection sites are closely spaced relative to a downstream signalised intersection which affects the queue discharge characteristics at the survey site. However, signal cycles with any downstream queue interference (speed reduction or blockage due to the downstream queue at the survey lane) were not included in the calibration of models for the paired intersection sites (Mel2, Mel5 and Mel6). Thus, the model parameters represent the geometric and environmental conditions only rather than direct queue interference which is a function of demand levels and signal timing parameters. The effect of downstream queue interference is discussed in *Section 11*.

These results given in *Table 9.5* were obtained using a jam spacing of $L_{hjLV} = 7.0$ m specified for all sites as in WD R 96/043 although $L_{hjLV} = 7.2$ m was measured at site Mel7 during the initial stage of the study. Note that the value $L_{hjLV} = 7.0$ m was measured at Sites 456 and 3196, and L_{hjLV} values for other through lanes were 6.9 for Site 849 and 7.3 for Site 4273 (*Table 9.2*). The latter is likely to be due to the uphill grade. Therefore, $L_{hjLV} = 7.0$ m is seen to be a good value for the through lanes included in Melbourne 1996 surveys.

In addition to the calibration parameters v_n , m_v , h_n , q_n , and m_q , *Table 9.5* gives the speed limit that can be used as a free-flow speed (v_f), the ratio (v_f/v_n), jam spacing values for light and heavy vehicles ($L_{hj} = L_{hjLV}$, L_{hjHV}), spacing at maximum queue discharge flow speed (L_{hn}), ratio m_v/m_q , jam space (gap) length (L_{sj}), queue clearance wave speed (v_x), and the departure response time (t_x) for each site.

Confidence intervals of parameters v_n , m_v and q_n for each site are also given in *Table 9.5*.

Table 9.5

Parameters for the Queue Discharge Speed and Flow Models for MELBOURNE 1996 Sites

Site	Mel1	Mel3	Mel4	Mel7	Mel2	Mel5	Mel6
Isolated or paired intersection site	Isolated	Isolated	Isolated	Isolated	Paired	Paired	Paired
L_{hjL_v} (Cars only) used in calibration	7.0	7.0	7.0	7.0	7.0	7.0	7.0
Sample size (Sat. periods)	605	779	426	1025	337	200	262
Speed model							
R^2	0.73	0.596	0.707	0.754	0.232	0.154	0.416
v_n (km/h)	56.1	46.2	47.9	52.4	30.9	27.1	34.6
v_n 95% Confidence Interval	55.0 - 57.1	45.6 - 46.9	46.5 - 49.2	51.7 - 53.1	30.1 - 31.6	26.4 - 27.8	33.6 - 35.7
m_v	0.104	0.126	0.089	0.097	0.233	0.310	0.190
m_v 95% Confidence Interval	0.099 - 0.110	0.120 - 0.133	0.082 - 0.095	0.093 - 0.101	0.202 - 0.265	0.254 - 0.367	0.168 - 0.211
Headway and flow rate models							
h_n (s)	1.407	1.485	1.624	1.830	1.816	1.995	1.705
q_n (veh/h)	2558	2423	2217	1968	1982	1804	2112
q_n 95% Confidence Interval	2543 - 2573	2414 - 2433	2200 - 2233	1958 - 1977	1965 - 1999	1790 - 1819	2096 - 2128
m_q	0.326	0.343	0.275	0.369	0.519	0.665	0.445
Free-flow speed as the speed limit							
v_f (km/h)	80	80	60	80	60	60	80
v_n/v_f	0.70	0.58	0.80	0.66	0.52	0.45	0.43
Calculated parameters							
L_{hn} (m/veh)	21.9	19.1	21.6	26.6	15.6	15.0	16.4
m_v/m_q	0.319	0.367	0.324	0.263	0.449	0.466	0.427
L_{hj} (m/veh)	7.0 *	7.0 *	7.0 *	7.0 *	7.0 *	7.0 *	7.0 *
L_{sj} (m/veh) †							
$v_x = v_n / (L_{hn} / L_{hj} - 1)$ (km/h)	26.3	26.8	23.0	18.7	25.2	23.7	25.8
$t_x = 3.6 L_{hj} / v_x$ (s)	0.96	0.94	1.10	1.35	1.00	1.07	0.98

* Nominal values (jam spacing was not measured during these early surveys except at Mel7 site where $L_{hj} = 7.2$ m was measured).

† $L_{sj} = L_{hj} - L_v$ using $L_v = 4.4$ m.

Combined Sydney and Melbourne Results

Tables 9.6 and 9.7 present calibration results for all Sydney and Melbourne sites together, combining results for through lanes at isolated and paired intersection sites, and fully-controlled right-turn lanes at isolated sites. Average values of all parameters are also given for right-turn isolated, through isolated, through paired intersection, and all through sites.

The symbols used in Tables 9.6 and 9.7 are:

v_n	: maximum queue discharge speed (km/h)
q_n	: maximum queue discharge flow rate (veh/h)
m_v	: parameter in the queue discharge speed model
m_q	: parameter in the queue discharge flow rate model
m_v/m_q	: ratio of m_v to m_q
h_n	: minimum queue discharge headway (s)
v_f	: free-flow speed (km/h)
v_n/v_f	: ratio of the maximum queue discharge speed to the free-flow speed
L_{hjLV}	: jam spacing for light vehicles (m)
L_{hjHV}	: jam spacing for heavy vehicles (m)
t_{gn}	: gap time (s) at maximum queue discharge flow speed
t_{sn}	: space time (s) at maximum queue discharge flow speed
L_{hn}	: spacing (m) at maximum queue discharge flow speed
L_{hj}	: same as L_{hjLV}
L_{sj}	: jam space (gap) length calculated from $L_{sj} = L_{hj} - L_v$ using an average light vehicle length of $L_v = 4.4$ m
v_x	: average queue clearance wave speed (km/h)
t_x	: average departure response time (response time for the next vehicle in the queue to start moving) (s)

"Average site" values of parameters for right-turn isolated, through isolated, through paired intersection, and all through sites are calculated as follows:

- (i) calculate statistical averages for v_n , m_v , h_n , L_{hjLV} , L_{hjHV} , v_f ,
- (ii) calculate $q_n = 3600 / h_n$ where h_n is the average site value from (i), and calculate L_{hn} from Equation (5.50),
- (iii) calculate parameter m_q from Equation (7.8) using the parameter values from (i) and (ii),
- (iv) calculate parameters t_{gn} and t_{sn} from Equations (5.48) and (5.49), and calculate from Equations (7.18) and (7.19).

Table 9.6

Summary of queue discharge model parameters for all survey sites

Site	v_n (km/h)	q_n (veh/h)	m_v	m_q	m_v/m_q	h_n (s)	v_f (km/h)	v_n/v_f	L_{njLV} (m)	L_{njHV} (m)
Average values										
Right-turn (isolated) sites	24.5	2033	0.307	0.582	0.528	1.771	65	0.38	6.4	9.7
Through (isolated) sites	45.1	2086	0.118	0.369	0.321	1.725	69	0.65	6.9	11.3
Through (paired int.) sites	30.9	1958	0.244	0.550	0.444	1.839	67	0.46	7.0 *	
All Through sites	42.1	2057	0.145	0.427	0.340	1.750	69	0.61	7.0	11.3
Right-turn (isolated) sites										
TCS163 (1)	24.7	2098	0.317	0.621	0.510	1.716	60	0.41	6.0	8.6
TCS610	21.7	1966	0.373	0.698	0.534	1.831	60	0.36	5.9	7.9
TCS121	24.4	1948	0.287	0.545	0.527	1.848	70	0.35	6.6	12.1
TCS335	27.1	2133	0.252	0.464	0.543	1.687	70	0.39	6.9	10.1
Through (isolated) sites										
TCS1081 (2)	39.5	1790	0.103	0.334	0.308	2.011	60	0.66	6.8	8.7
TCS413	33.2	1801	0.200	0.542	0.369	1.999	60	0.55	6.8	11.0
TCS511	52.8	2283	0.078	0.273	0.286	1.577	70	0.75	6.6	11.9
TCS3196 (3)	31.7	1892	0.150	0.359	0.418	1.903	60	0.53	7.0	13.1
TCS4273 (4)	36.4	1938	0.135	0.347	0.389	1.857	60	0.61	7.3	13.6
TCS849	46.4	1999	0.102	0.343	0.297	1.801	70	0.66	6.9	8.7
TCS456	53.8	2422	0.118	0.374	0.316	1.486	80	0.67	7.0 *	12.2
Mel1	56.1	2558	0.104	0.326	0.319	1.407	80	0.70	7.0 *	
Mel3	46.2	2423	0.126	0.343	0.367	1.485	80	0.58	7.0 *	
Mel4	47.9	2217	0.089	0.275	0.324	1.624	60	0.80	7.0 *	
Mel7	52.4	1968	0.097	0.369	0.263	1.830	80	0.66	7.0 *	
Through (paired intersection) sites										
Mel2	30.9	1982	0.233	0.519	0.449	1.816	60	0.52	7.0 *	
Mel5	27.1	1804	0.310	0.665	0.466	1.995	60	0.45	7.0 *	
Mel6	34.6	2112	0.190	0.445	0.427	1.705	80	0.43	7.0 *	

* Nominal values (jam spacing was not measured during these early surveys except at Mel7 site where $L_{nj} = 7.2$ m was measured).

- (1) Data for AM and PM peak periods combined
- (2) 9 per cent uphill grade
- (3) Shared through and left turn (15 per cent left turn)
- (4) 6 per cent uphill grade

Table 9.7

Further queue discharge model parameters for all survey sites

Site	v_n (km/h)	q_n (veh/h)	m_v/m_q	h_n (s)	$t_{gn} \dagger$ (s)	$t_{sn} \dagger$ (s)	L_{hn} (m)	L_{hj} (m)	L_{sj} (m)	v_x (km/h)	t_x (s)
Average values											
Right-turn (isolated) sites	24.5	2033	0.528	1.771	1.12	0.46	12.0	6.4	2.0	27.3	0.84
Through (isolated) sites	45.1	2086	0.321	1.725	1.37	1.02	21.6	6.9	2.5	21.3	1.17
Through (paired int.) sites	30.9	1958	0.444	1.839	1.33	0.80	15.8	7.0 *	2.6	24.7	1.02
All Through sites	42.1	2057	0.340	1.750	1.37	0.99	20.4	7.0	2.6	21.7	1.15
Right-turn (isolated) sites											
TCS163 (1)	24.7	2098	0.510	1.716	1.07	0.42	11.8	6.0	1.6	25.7	0.84
TCS610	21.7	1966	0.534	1.831	1.10	0.35	11.0	5.9	1.5	24.9	0.85
TCS121	24.4	1948	0.527	1.848	1.20	0.53	12.5	6.6	2.2	27.2	0.87
TCS335	27.1	2133	0.543	1.687	1.10	0.51	12.7	6.9	2.5	32.2	0.77
Through (isolated) sites											
TCS1081 (2)	39.5	1790	0.308	2.011	1.61	1.20	22.1	6.8	2.4	17.6	1.39
TCS413	33.2	1801	0.369	1.999	1.52	1.03	18.4	6.8	2.4	19.4	1.26
TCS511	52.8	2283	0.286	1.577	1.28	0.97	23.1	6.6	2.2	21.1	1.13
TCS3196 (3)	31.7	1892	0.418	1.903	1.40	0.89	16.8	7.0	2.6	22.7	1.11
TCS4273 (4)	36.4	1938	0.389	1.857	1.42	0.98	18.8	7.3	2.9	23.1	1.14
TCS849	46.4	1999	0.297	1.801	1.46	1.11	23.2	6.9	2.5	19.6	1.27
TCS456	53.8	2422	0.316	1.486	1.19	0.89	22.2	7.0 *	2.6	24.8	1.02
Mel1	56.1	2558	0.319	1.407	1.12	0.84	21.9	7.0 *	2.6	26.3	0.96
Mel3	46.2	2423	0.367	1.485	1.14	0.79	19.1	7.0 *	2.6	26.8	0.94
Mel4	47.9	2217	0.324	1.624	1.29	0.95	21.6	7.0 *	2.6	23.0	1.10
Mel7	52.4	1968	0.263	1.830	1.53	1.22	26.6	7.0 *	2.6	18.7	1.35
Through (paired intersection) sites											
Mel2	30.9	1982	0.449	1.816	1.30	0.78	15.6	7.0 *	2.6	25.2	1.00
Mel5	27.1	1804	0.466	1.995	1.41	0.81	15.0	7.0 *	2.6	23.6	1.07
Mel6	34.6	2112	0.427	1.705	1.25	0.78	16.4	7.0 *	2.6	25.8	0.98

* Nominal values (jam spacing was not measured during these early surveys except at Mel7 site where $L_{hj} = 7.2$ m was measured).

† For t_{gn} , t_{sn} , and L_{sj} : Detection zone length is $L_p = 4.5$ m, and average vehicle length is $L_v = 4.4$ m

All parameters in this table are for light vehicles (cars) only.

- (1) Data for AM and PM peak periods combined
- (2) 9 per cent uphill grade
- (3) Shared through and left turn (15 per cent left turn)
- (4) 6 per cent uphill grade

The results show that queue discharge characteristics for through and right-turn movements differ significantly, and there are also significant differences between through lanes at isolated sites and paired intersection sites. Considering average values of parameters for all through and right-turn sites, maximum queue discharge flow rates for right-turn sites are similar to those for isolated through sites.

Lower L_{hj} , L_{hn} , L_{sj} , v_n , v_n/v_f , t_x parameters, and higher m_v , m_q , m_v/m_q and v_x are observed for right-turn sites. Lower jam spacing and lower departure response time (higher queue clearance speed) at right-turn sites help to achieve low queue discharge headways, therefore high maximum flow rates. Higher $m_v / m_q (= k_n / k_j)$ means that the maximum flow rate in the speed-density curve is achieved later.

Parameters for through movements at paired intersection sites are between the through (isolated) and right turn (isolated) site values although lower maximum flow rates are observed at these sites (see *Section 11* for further discussion on paired intersection sites).

Although sites 413 and 3196 are isolated through sites, their queue discharge characteristics appear to be closer to the paired intersection sites (e.g. low v_n , high m_v). This is related to site 413 having a CBD character and site 3196 being a shared left-turn and through traffic lane at a small intersection in a suburban shopping centre environment. In particular, it is noted that short downstream distance (140 m) for site 413 is consistent with this result.

It is often stated in the literature that saturation flow rate may decrease with time, especially in the case of long green times (e.g. Teply and Jones 1991, Teply, et al. 1995). There was no sign of this at any site as evident from figures given in *Appendix B*. In particular, no drop in saturation flow rate or saturation speed is observed at site 511 where the average green time is 120 s (average cycle time 160 s). Only at site 610 (right-turn with short green time), the queue discharge flow rate is observed to peak around 10 s after the start of the green period, and then drops slightly.

For comparison with the results given in *Tables 9.6 and 9.7*, Bonneson (1992a) reported a jam spacing of $L_{hj} = 7.9$ m/veh measured under US conditions. This is about 1.0 m larger than the Australian values found in this study. Niittymäki and Pursula (1997) reported gap times at maximum queue discharge flow rate (or at saturation headway), t_{gn} in the range 1.1 and 1.3 s, start response times in the range 0.9 to 1.0 s, and queue discharge headways in the range 1.7 and 2.0 s observed in Finland. These parameter values are consistent with the values seen in *Tables 9.6 and 9.7*.

It is seen from *Table 9.7* that v_x is in the range 18 to 32 km/h and t_x is in the range 0.8 to 1.4 s. These values are consistent with the response times of 1.0 to 1.3 s and a response wave speed of 28.5 km/h reported by Bonneson (1992a).

Relationships between various queue discharge model parameters are shown in *Figures 9.1 to 9.3* including linear trendline and associated regression equations that may be useful for practical purposes (see *Section 16* for further discussion).

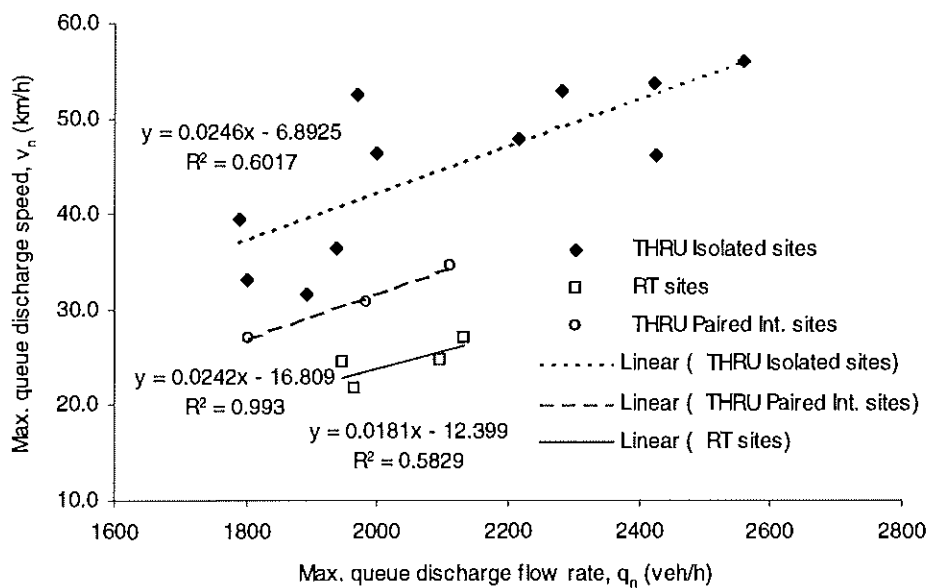


Figure 9.1 – Relationship between maximum queue discharge speed, v_n and maximum queue discharge flow rate, q_n

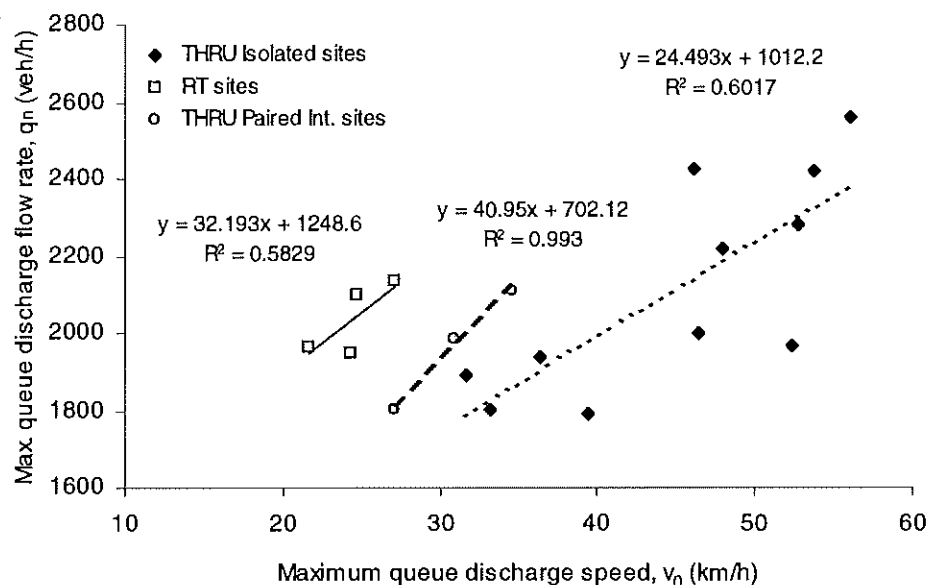


Figure 9.2 – Relationship between maximum queue discharge flow rate, q_n and maximum queue discharge speed, v_n

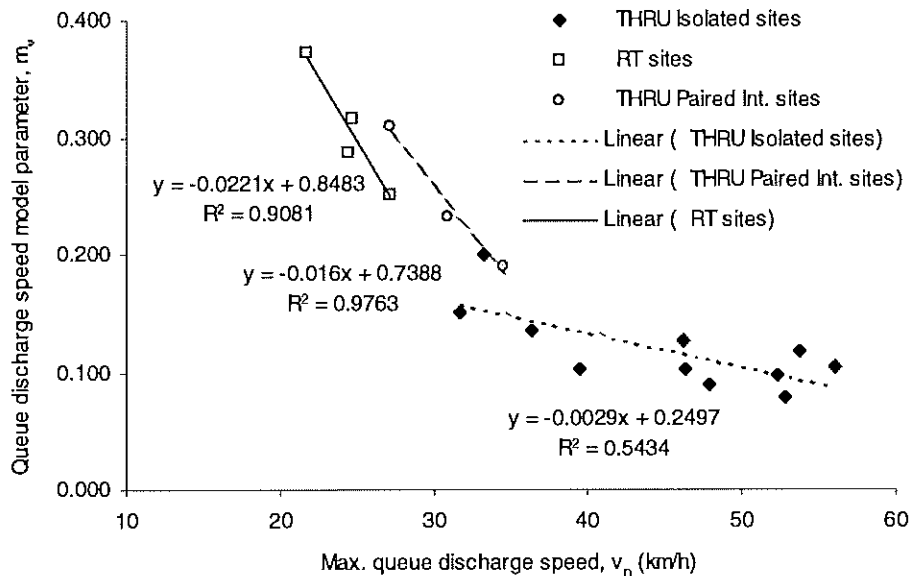


Figure 9.3 – Relationship between queue discharge speed model parameter, m_v , and maximum queue discharge speed, v_n for different site types

Results for Alternative Calibration Methods

Alternative calibration methods were also investigated using different headway and speed data derived from raw detector data and different values of the start response time, t_r , as discussed in *Section 8*.

Alternative calibration methods were applied to 1998 data from three sites only, namely sites 335 (Melbourne), 610 and 511 (Sydney). Sites 335 and 610 are right-turn traffic lanes with short green times, and Site 511 is a major through traffic lane with very long green time. For these sites, data were further processed to eliminate a few outliers (data points with very high or very low headway or speed values). Therefore, the results for the "original calibration method (method 1)" differ slightly from those reported above (summarised in *Tables 9.6 and 9.7*).

Tables 9.8 to 9.10 summarise model parameters obtained from alternative calibration methods for sites 335, 610 and 511 allowing for comparison of model parameters obtained from alternative methods.

Figures showing measured and predicted queue discharge speeds, headways, flow rates and spacings for alternative calibration method 13 are given in *Appendix B*.

The following conclusions are drawn from the findings summarised in *Tables 9.8 to 9.10*.

- (i) The headway regression method used to determine the headway (flow rate) model parameters results in estimated jam spacing (L_{hj}) values that are significantly greater than the measured values. Correct prediction of this parameter is very important for model accuracy, and particularly in its implications for the optimum loop length as discussed in *Section 14*. Therefore this method is not preferred, thus confirming the standard calibration procedure that employs the measured jam spacing (*Figure 8.1*).
- (ii) Determining the start response time parameter of the queue discharge model freely from speed model regression gave acceptable results (in the range 0.7 to 1.6 s) for the right-turn lane sites (335 and 610), but gave a negative value for the through lane site (511). It is difficult to estimate this parameter from regressions reliably due to lack of data at low speeds at the start of the green period. The use of a specified value of $t_r = 1.0$ s appears to be reasonable.
- (iii) Alternative methods using different speed and headway variables derived from raw detector data using the standard calibration method (using the measured jam spacing) gave close results although some improvements were obtained in queue discharge speed, headway and flow rate predictions. For a given site, the ratio m_v/m_q , which is the parameter in the speed-flow model, does not vary significantly for alternative calibration methods that use the measured jam spacing. This is a satisfactory result, in that the speed – flow and space time – speed relationships and the optimum loop length values indicate low sensitivity to the method used (assuming the calibration procedure using the measured jam spacing). This is further discussed in *Section 14*.
- (iv) Although alternative calibration methods using measured jam spacings give similar results in terms of the resulting speed - flow and space time - speed relationships and the optimum loop length values, it is recommended that calibration method 13 is used in future data analyses. This method uses the standard calibration procedure with a specified start response time value of $t_r = 1.0$ s, and employs the speed based on the leading end of the vehicle (v_L) and headways measured at Detector 2 (h_{2L}). This method improves the queue discharge headway prediction at low speeds, particularly for right-turn sites where the queue discharge speeds are low.

The calibration results given in this section are based on the definition of headway and spacing parameters from the *front* of the leading vehicle to the *front* of the following vehicle. Alternatively, headway and spacing parameters may be measured from the *back* of the leading vehicle to the *back* of the following vehicle (see *Figures 5.5 and 5.6* in *Section 5*). Limited analysis of parameters using the latter method indicated that the difference between the two methods would not affect the conclusions of this report.

Table 9.8

**Model parameters obtained from alternative calibration methods for Site 335
(right-turn traffic lane: Doncaster Rd and Blackburn Rd, Melbourne)**

Calibration method number	Jam spacing	Start lag	Max. queue discharge speed	Speed model parameter	Min. queue discharge headway	Max. queue discharge flow rate	Headway (flow) model parameter	Parameter for speed – flow model
	L_{hj}	t_r	v_n	m_v	h_n	q_n	m_q	m_v / m_q
1	6.9	0	27.39	0.2434	1.6528	2178	0.4435	0.549
2	6.9	0	28.80	0.1845	1.6473	2185	0.3523	0.524
3	6.9	0	28.92	0.1808	1.6528	2178	0.3479	0.520
4	6.9	0.68	28.35	0.2141	1.6528	2178	0.4039	0.530
5 *	12.5	0.68	28.35	0.2141	1.6099	2236	0.2179	0.982
6	6.9	1.0	28.10	0.2339	1.6528	2178	0.4373	0.535
7 *	12.5	1.0	28.10	0.2339	1.6237	2217	0.2365	0.989
8	NOT USED							
9	6.9	0	29.43	0.1596	1.6416	2193	0.3104	0.514
10 *	9.8	0	29.43	0.1596	1.6144	2230	0.2149	0.743
11	6.9	1.62	28.11	0.2356	1.6416	2193	0.4377	0.538
12 *	9.8	1.62	28.11	0.2356	1.6601	2169	0.3117	0.756
13	6.9	1.0	28.61	0.1997	1.6416	2193	0.3776	0.529
14 *	9.8	1.0	28.61	0.1997	1.6417	2193	0.2655	0.752

* Methods 5, 7, 10, 12, 14 does not use the standard calibration procedure

Table 9.9

**Model parameters obtained from alternative calibration methods for Site 610
(right-turn traffic lane: Military Rd and Murdoch St, Sydney)**

Calibration method number	Jam spacing	Start lag	Max. queue discharge speed	Speed model parameter	Min. queue discharge headway	Max. queue discharge flow rate	Headway (flow) model parameter	Parameter for speed – flow model
	L_{hj}	t_r	v_n	m_v	h_n	q_n	m_q	m_v / m_q
1	5.9	0	21.33	0.3868	1.8642	1931	0.7241	0.534
2	5.9	0	22.58	0.2985	1.8562	1939	0.5892	0.507
3	5.9	0	24.20	0.2291	1.8642	1931	0.4865	0.471
4	5.9	1.12	22.69	0.3547	1.8642	1931	0.7063	0.502
5 *	11.4	1.12	22.69	0.3547	1.8292	1968	0.3575	0.992
6	5.9	1.0	22.84	0.3365	1.8642	1931	0.6744	0.499
7 *	11.2	1.0	22.84	0.3365	1.8245	1973	0.3462	0.972
8	NOT USED							
9	5.9	0	23.31	0.2389	1.8483	1948	0.4844	0.493
10 *	7.5	0	23.31	0.2389	1.8517	1944	0.3837	0.622
11	5.9	1.37	22.13	0.3717	1.8483	1948	0.7159	0.519
12 *	8.2	1.37	22.13	0.3717	1.8704	1925	0.5208	0.714
13	5.9	1.0	22.44	0.3244	1.8483	1948	0.6335	0.512
14 *	7.9	1.0	22.44	0.3244	1.8650	1930	0.4747	0.683

* Methods 5, 7, 10, 12, 14 does not use the standard calibration procedure

Table 9.10

**Model parameters obtained from alternative calibration methods for Site 511
(through traffic lane: General Holmes Drive and Bestic St, Sydney)**

Calibration method number	Jam spacing	Start lag	Max. queue discharge speed	Speed model parameter	Min. queue discharge headway	Max. queue discharge flow rate	Headway (flow) model parameter	Parameter for speed – flow model
	L_{hj}	t_r	v_n	m_v	h_n	q_n	m_q	m_v / m_q
1	6.6	0	52.80	0.0778	1.6115	2234	0.2788	0.279
2	6.6	0	52.87	0.0753	1.6097	2236	0.2696	0.279
3	6.6	0	52.94	0.0724	1.6115	2234	0.2599	0.278
4	6.6	-3.70	53.63	0.0564	1.6115	2234	0.2050	0.275
5 *	9.3	-3.70	53.63	0.0564	1.6040	2244	0.1444	0.390
6	6.6	1.0	52.75	0.0786	1.6115	2234	0.2811	0.280
7 *	7.1	1.0	52.75	0.0786	1.6126	2232	0.2628	0.299
8	NOT USED							
9	6.6	0	52.94	0.0732	1.6080	2239	0.2622	0.279
10 *	7.0	0	52.94	0.0732	1.6094	2237	0.2464	0.297
11	6.6	-4.61	53.76	0.0542	1.6080	2239	0.1973	0.275
12 *	8.7	-4.61	53.76	0.0542	1.6037	2245	0.1499	0.362
13	6.6	1.0	52.76	0.0794	1.6080	2239	0.2835	0.280
14 *	6.4	1.0	52.76	0.0794	1.6111	2234	0.2934	0.271

* Methods 5, 7, 10, 12, 14 does not use the standard calibration procedure

10 UNINTERRUPTED FLOW MODELS FOR SIGNALISED INTERSECTIONS

Various speed-flow-density models considered for the uninterrupted flow region that applies to the unsaturated part of the green period are described below. These models apply to all uninterrupted flow conditions, e.g. as observed on freeways and mid-block sections of arterial roads.

Alternative model forms described in Akçelik, Roper and Besley (1999b) for unsaturated freeway flows are also suitable for unsaturated flows (after queue clearance) at the signal stop line. However, a comprehensive study of the application of these models to unsaturated flows at signalised intersections was not undertaken due to data limitations and because this was not the main objective of this research. The main limitation was the quantity of data since the unsaturated part of the green period represented a small portion of time at the survey sites. This is because efficient signal control avoids prolonged intervals after queue clearance. There was also a lack of data for flow rates below about 500 veh/h (corresponding to headways above 7 s).

A limited study of four models was undertaken during the early stage of this research using data from site Mel7. With reference to *Figure 5.8 in Section 5*, Models 1 and 2 apply to region A, Model 3 applies to both regions A and B ($v = v_u$ or v_s), and Model 4 applies to regions A and C. These models are identical to those used for the freeway study (Akçelik, Roper and Besley 1999b).

The heavy vehicle data (including the following vehicle data) were eliminated as in the case of queue discharge flow data. Various methods of data aggregation were tried. The best method appeared to be using non-aggregated flow rates and speeds using data for vehicles that depart during the period from 6 seconds after the last queued vehicle departs to the start of the red period. Furthermore, data representing flow rates above the upper 95th percentile value of the maximum queue discharge flow rate were eliminated considering that these represented bunched vehicles in the uninterrupted traffic stream. This method differs significantly from most speed-flow studies that aggregate data into 5 to 15-minute intervals.

The models are described below. In all models, v_u (km/h) is the uninterrupted speed, i.e. the speed during the unsaturated part of the green period (after queue clearance) as observed at the signal stop line (km/h), and q_u is the associated flow rate (veh/h). For further discussion on these models, refer to (Akçelik, Roper and Besley 1999b).

Model 1:

$$v_u = v_f + b_1 (q_u / 1000)^{p_2} \quad (10.1)$$

subject to $p_2 > 0$ and $b_1 < 0$

where v_u (km/h) is the speed, q_u (veh/h) is the flow rate, v_f (km/h) is the free-flow speed, and b_1 , p_2 are constants related through:

$$b_1 = -(v_f - v_n) / (q_n / 1000)^{p_2} \quad (10.2)$$

where v_n (km/h) is the speed at maximum flow rate, q_n (veh/h) is the maximum flow rate.

The model can be expressed in the following form for calibration purposes:

$$v_u = v_f - (v_f - v_n) (q/q_n)^{p_2} \quad (10.3)$$

subject to $p_2 > 0$

Model 2:

$$q_u = q_n [1 - ((v_u - v_n) / (v_f - v_n))^{p_2}] \quad (10.4)$$

subject to $p_2 > 0$

where q_u (veh/h) is the flow rate, q_n (veh/h) is the maximum flow rate, v_u (km/h) is the speed, v_n (km/h) is the speed at maximum flow rate, v_f (km/h) is the free-flow speed, and p_2 is a constant:

The speed-flow function corresponding to *Equation (10.4)* is:

$$v_u = v_n [1 + (v_f/v_n - 1) (1 - q_u/q_n)^{1/p_2}] \quad (10.5)$$

subject to $p_2 > 0$

Model 3:

This model covers both unsaturated and saturated conditions as a single model.

$$q_u = 1000 v / [L_{hj} + p_1 v_u / (1 - v_u / v_f)^{p_2}] \quad (10.6)$$

subject to $p_1 > 0$ and $p_2 > 0$

where q_u (veh/h) is the flow rate, v_u (km/h) is the speed, v_f (km/h) is the free-flow speed, L_{hj} (m/veh) is the jam density, and p_1 , p_2 are constants related through:

$$p_1 = [(L_{hn} - L_{hj}) (1 - v_n / v_f)^{p_2}] / v_n \quad (10.7)$$

where v_n (km/h) is the speed at maximum flow rate, L_{hn} (m/veh) is the spacing at maximum flow rate calculated from:

$$L_{hn} = 1000 v_n / q_n \quad (10.8)$$

where q_n (veh/h) is the maximum flow rate.

From *Equation (10.7)*, jam spacing is:

$$L_{hj} = L_{hn} - [p_1 v_n / (1 - v_n / v_f)^{p_2}] \quad (10.9)$$

The model can be expressed in the following form for calibration purposes:

$$q_u = 1000 / [(L_{hj} / v_u) + (1000 / q_n - L_{hj} / v_n) ((1 - v_n / v_f) / (1 - v_u / v_f))^{p_2}] \quad (10.10)$$

subject to $p_2 > 0$

A useful method to derive the fundamental speed-flow-density relationships is to start by modelling vehicle spacing as a function of speed as discussed in detail by Lay (1979, 1985) who showed that this approach is well related to driver behaviour (reaction times, stopping distances, out-of-lane factors, and so on). Lay (1979) proposed a polynomial spacing-speed model which produced all desirable characteristics of a speed-flow relationship except one condition: speeds exceeded the free-flow speed as the flows

approached zero in Region A in *Figure 5.8* in *Section 5* ($v_u > v_f$ when $q = 0$). Model 3 given here is based on the following spacing-speed relationship that satisfies this condition:

$$L_h = L_{hj} + p_1 v_u / (1 - v_u / v_f)^{p_2} \quad (10.11)$$

subject to $p_1 > 0$ and $p_2 > 0$

In Model 3, parameter p_1 is related to driver reaction times (including out-of-lane effects) and determines the extra spacing required under low to medium flow conditions in Region A. Parameter p_2 is important in determining the characteristics of the speed-flow model for conditions around the maximum flow rate and in Region B.

Model 4:

This is based on a function described by Akçelik (1991), and is used in the SIDRA software package for uninterrupted traffic flows (Akçelik and Besley 1999). It can be used as a general travel time (cost) function for all types of interrupted and uninterrupted traffic facilities for traffic planning purposes. In a recent study, the model was found to give desirable characteristics for traffic assignment purposes, and was found to give satisfactory estimates of travel speeds under US conditions (Dowling, Singh and Cheng 1998).

Model 4 is a general time-dependent model that applies to both unsaturated and oversaturated conditions (applies to regions A and C in *Figure 5.8* in *Section 5*). For oversaturated conditions (demand flow rate larger than the maximum flow rate), it requires demand flow rates rather than flow rates measured by detectors. Therefore, for calibration purposes under this project, this model was applied to unsaturated conditions only (speed less than the speed at maximum flow rate).

The model is expressed as:

$$v_u = v_f / \{1 + 0.25 v_f T_f [z + \text{sqrt}(z^2 + m_c x / (q_n T_f))]\} \quad (10.12)$$

where v (km/h) is the speed, v_f (km/h) is the free-flow speed, T_f (h) is the duration of the analysis period, m_c is a constant and

$$z = x - 1 \quad (10.13a)$$

$$x = q_u / q_n \quad (10.13b)$$

where q_u (veh/h) is the flow rate, q_n (veh/h) is the maximum flow rate.

Parameter m_c is related to other parameters through:

$$m_c = 16 q_n (v_f/v_n - 1)^2 / (v_f^2 T_f) \quad (10.14)$$

where v_n (km/h) is the speed at maximum flow rate.

The spacing at maximum flow rate, L_{hn} (m/veh) is calculated from:

$$L_{hn} = 1000 v_n / q_n \quad (10.15)$$

The model can be expressed in the following form for calibration purposes:

$$v_u = v_f / \{1 + 0.25 v_f T_f [z + \text{sqrt}(z^2 + (16 (q_u/q_n) (v_f/v_n - 1)^2 / (v_f T_f)^2))]\} \quad (10.16)$$

where $z = (q_u/q_n) - 1$.

Calibration Results for Unsaturated Flows

The calibration results for Models 1, 2, 3 and 4 for Site 7 are given in *Table 10.1*. The preferred parameter values for each model are shown in bold italic, and the corresponding model predictions and speed-flow data are shown in *Figures 10.1 to 10.4*. For this site, the maximum queue discharge flow rate, $q_n = 2038$ veh/h and the corresponding speed, $v_n = 52.2$ km/h were used (as determined during the earlier stage of the study) as a condition for the speed-flow relationship for unsaturated flows.

For Model 1, after analysing the results of initial regressions using SPSS (Norusis and SPSS 1993), parameter $p_2 = 3$ was set and two different methods were used to estimate parameters v_f and b_1 as shown in *Table 10.1*.

For Model 2, cases with $v_u < v_n$ need to be excluded from regression analysis. The model did not produce a satisfactory method of estimating v_f . Exclusion of low speed cases ($v_u < v_n$) biased the v_f estimate. Parameter p_2 was estimated by specifying a value of v_f as seen in *Table 10.1*.

For Model 3, cases with $v_u > v_f$ need to be excluded from the regression analyses. As a result, it is not possible to use this model to estimate v_f . *Table 10.1* gives the regression and calculated results obtained by specifying $v_f = 70$ km/h and $L_{hj} = 7.0$ m/veh.

For Model 4, several methods were used for regression analyses to determine appropriate values of parameters v_f , m_c and T_f as seen in *Table 10.1*.

Generally, it was found that all models tended to imply lower free-flow speeds than the speed limit (about 5 to 15 km/h smaller). It is emphasised that the free-flow speed is simply a model parameter estimated for best fit for the overall speed-flow relationship rather than the best estimate of a free-flow speed.

Table 10.1

*Calibration results for speed-flow models 1, 2, 3 and 4 for unsaturated flows
(Site Mel7: Ferntree Gully Road and Scoresby Road)*

MODEL 1							
	v_f (km/h)	b_1	p_2	R^2	95% confid. interval of v_f	v_n	v_n / v_f
Estimate v_f, b_1, p_2	75.7	-9.11	1.1	0.26	57.3 - 94.0	55.8	0.74
Specify $p_2 = 3.0$, estimate v_f, b_1	69.0	-1.82	3.0	0.23	66.6 - 71.5	53.6	0.78
Specify $p_2 = 3.0$, estimate v_f , calculate b_1	69.4	-2.03	3.0	0.22	67.2 - 71.7	52.2*	0.75
MODEL 2							
	v_f (km/h)	p_2		R^2	95% confid. interval of v_f	v_n	v_n / v_f
Estimate v_f, p_2	142.9	0.45		0.23	61.1 - 224.7	52.2*	0.37
Specify $v_f = 70.0$, estimate p_2	70.0	0.62		NS	NA	52.2*	0.75
Specify $v_f = 75.0$, estimate p_2	75.0	1.30		NS	NA	52.2*	0.70
MODEL 3							
	v_f (km/h)	p_1	p_2	R^2	95% confid. interval of v_f	v_n	v_n / v_f
Specify $v_f = 70.0$, estimate p_1, p_2	70.0	0.39	0.21	0.25	NA	43.2	0.62
Specify $v_f = 70.0$, calculate p_1, p_2	70.0	0.30	0.13	0.25	NA	52.2*	0.75
MODEL 4							
	v_f (km/h)	m_c	T_f	R^2	95% confid. interval of v_f	v_n	v_n / v_f
Specify $T_f = 1.0$ h, estimate v_f, m_c	65.6	1.15	1.0	0.04	63.4 - 67.8	47.2	0.72
Specify $T_f = 1.0$ h, estimate v_f , calculate m_c	65.2	0.48	1.0	0.04	63.1 - 67.3	52.2*	0.80
Specify $T_f = 0.25$ h, estimate v_f , calculate m_c	67.8	2.53	0.25	0.13	65.3 - 70.4	52.2*	0.77
Estimate v_f, T_f , calculate m_c	69.9	5.98	0.13	0.14	66.5 - 73.2	52.2*	0.75

* From the exponential queue discharge model: $v_n = 52.2$ km/h, $q_n = 2038$ veh/h.

For Model 3, $L_{hj} = 7.0$ m/veh.

NA: Not applicable, NS: Not significant

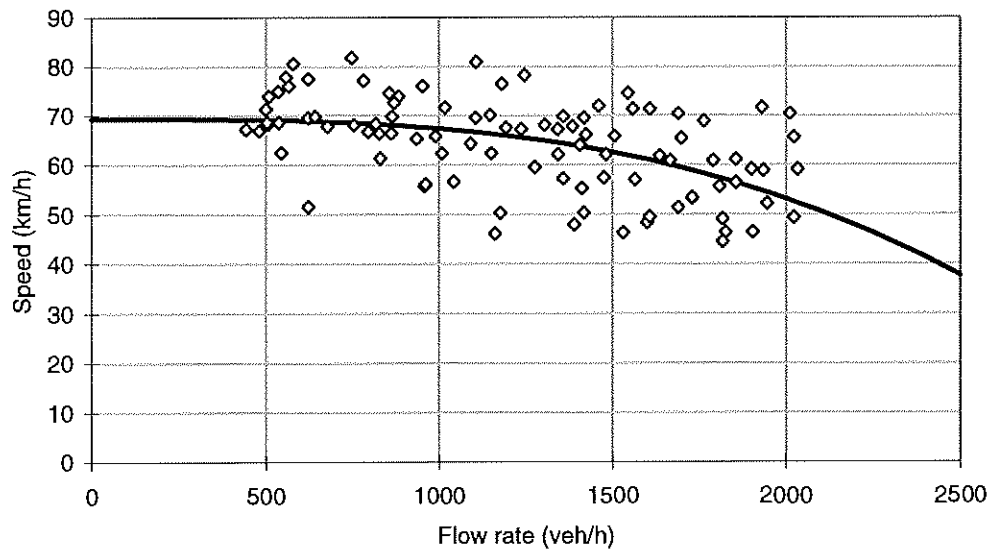


Figure 10.1 – Unsaturated speed-flow data and Model 1 predictions for Site 7 (Ferntree Gully Road and Scoresby Road)

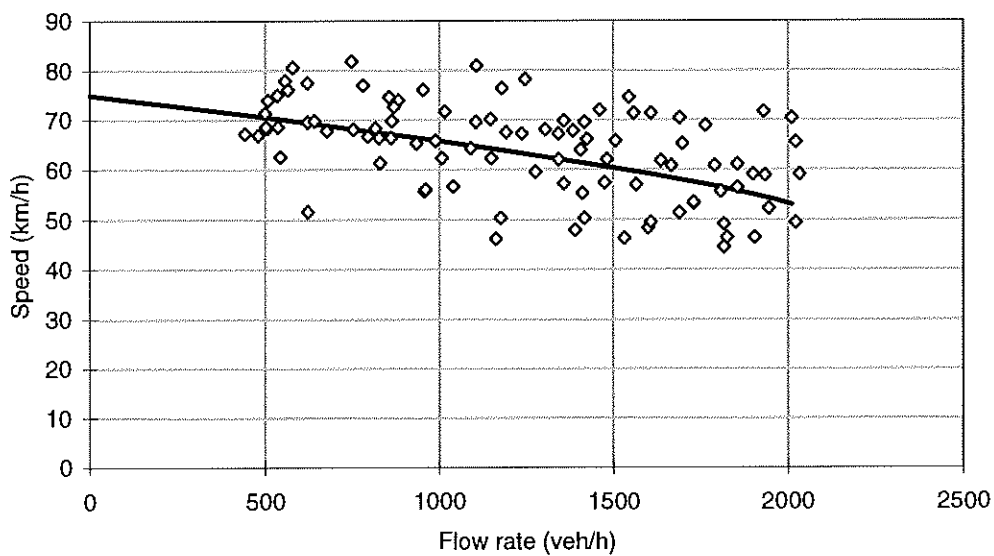


Figure 10.2 – Unsaturated speed-flow data and Model 2 predictions for Site 7 (Ferntree Gully Road and Scoresby Road)

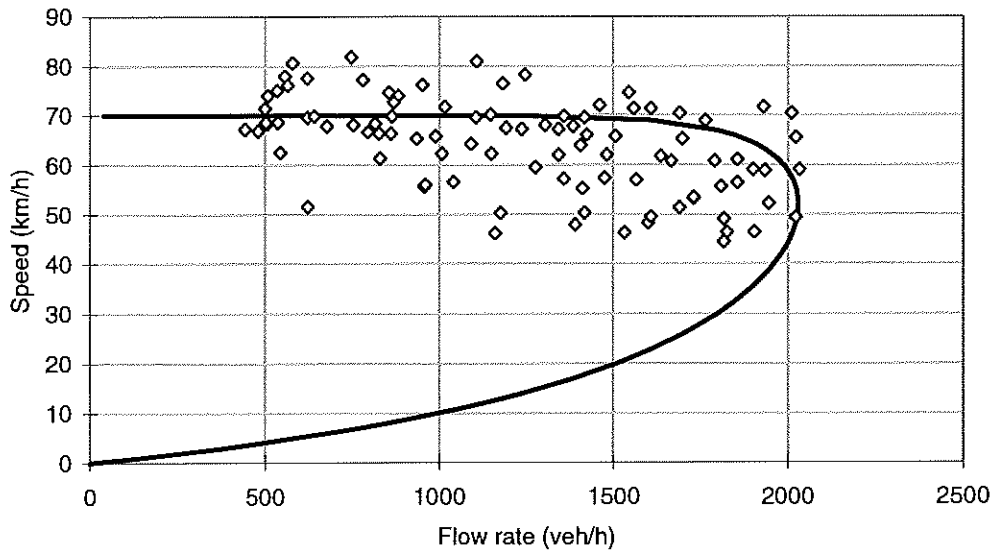


Figure 10.3 – Unsaturated speed-flow data and Model 3 predictions for Site 7 (Ferntree Gully Road and Scoresby Road)

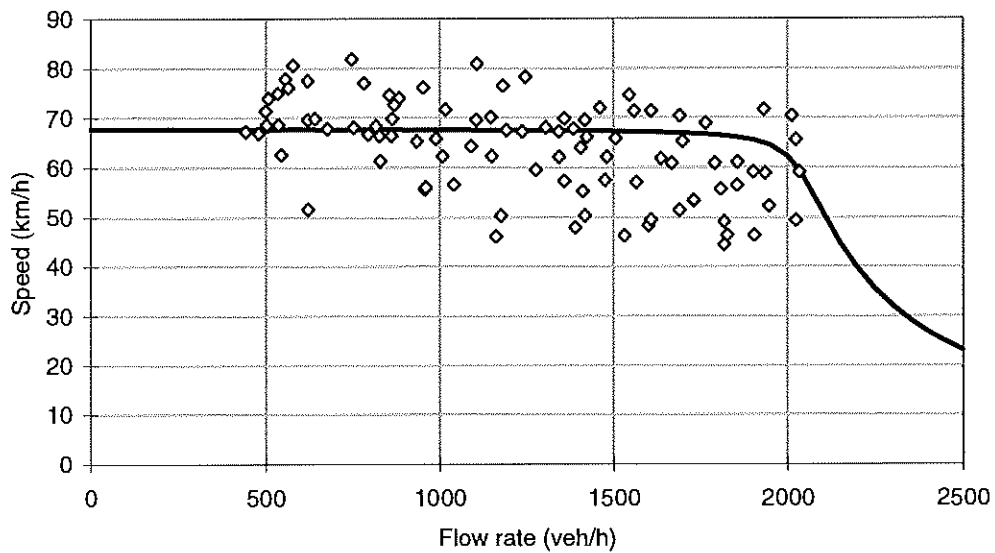


Figure 10.4 – Unsaturated speed-flow data and Model 4 predictions for Site 7 (Ferntree Gully Road and Scoresby Road)

11 DOWNSTREAM QUEUE INTERFERENCE AT PAIRED INTERSECTIONS

The term *paired intersection* is used for closely spaced intersections with queuing within the intersection area (on internal approaches). Examples of paired intersections include diamond interchanges, closely-spaced intersections, staggered T junctions, and large intersections with internal queuing, e.g. due to a wide median. The intersection pair is either regulated from a single traffic signal controller on a common cycle length using built-in offsets achieved through special phasing arrangements, or from two separate controllers which are coordinated as part of a wider signal coordination system.

An important issue in modelling paired intersections is the queue interaction effects between the two intersections since, in many instances, the presence of a downstream queue may inhibit the normal saturation flow rate at the upstream intersection (Roughail and Akçelik 1991, 1992; Johnson and Akçelik 1992).

As seen in *Tables 9.5 to 9.7* in *Section 9* summarising calibration results for the exponential queue discharge flow rate and speed models, sites Mel2, Mel5 and Mel6 are paired intersections. The model parameters for these sites are significantly different from those for isolated through traffic sites:

- (i) maximum queue departure flow rates, speeds at maximum flow and spacings at maximum flow (q_n , v_n , L_{hn}) are lower,
- (ii) parameters m_q , and m_v are higher indicating quicker acceleration to the maximum speed and achievement of the maximum flow rate sooner,

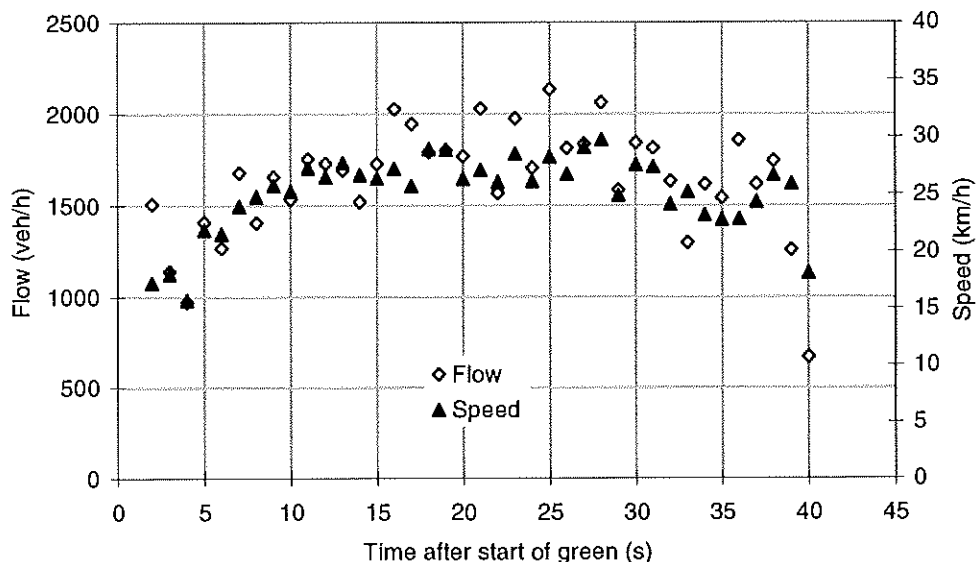


Figure 11.1 – Reduction in queue discharge flow rate and speed as a result of downstream queue interference at site Mel5 (Pedestrian Crossing on Canterbury Road)

- (iii) maximum flow rate in the speed-density curve is achieved later ($k_n / k_j = m_v / m_q =$ average value of 0.45 against 0.33 for isolated through traffic sites), and
- (iv) the ratio of maximum queue discharge speed to the free-flow speed is smaller (an average value of 0.44 against 0.60 for isolated through traffic sites).

Queue discharge model parameters for paired intersection sites were derived using data points not affected by queue interference. This was determined both visually and by calculating the standard deviations of speed and headway and choosing the points up to a time when the standard deviations increased markedly.

Conditions that provided sufficient data for queue interference analysis were observed only at site Mel5 (Pedestrian Crossing on Canterbury Road, East Camberwell). *Figure 11.1* shows the reduction in queue discharge flow rate and speed after about 25 seconds since the start of green at this site. The downstream queues were formed by the vehicles departing from the upstream signal stopped by downstream pedestrian signals actuated by heavy pedestrian flows. This provided good data for analysing queue interaction.

To examine the effects of downstream queue interference on queue discharge speed, distance to the back of the downstream queue (L_{dq}) was determined for each data point. The ratio of the observed speed (v_r) to the speed predicted by the exponential queue discharge speed model (v_s) was calculated. The speed (v_s) calculated from *Equation 7.1* using the calibration parameters for site Mel5 in *Tables 9.5 to 9.7* represented the expected speeds without downstream queue interference.

As seen in *Figures 11.2 and 11.3*, the speeds were affected when the distance to the back of queue became less than about 30 to 40 m. The ratios $v_r / v_s > 1$ observed in *Figure 11.2* could be explained partly by speeding up of vehicles in order to make it into the downstream section before speed reductions due to the downstream queue interference take effect, and partly because v_r is a measured speed with statistical variations whereas v_s is a predicted average speed. No attempt was made to model the observed cases of $v_r / v_s > 1.0$.

The following model provided a reasonable general relationship between the ratio v_r / v_s and the distance to the back of queue (L_{dq}) for site Mel5:

$$v_r / v_s = 1 - e^{-0.09 L_{dq}} \quad (11.1)$$

where v_r is the queue discharge speeds reduced due to downstream queue interaction, and L_{dq} is in metres. The model was calibrated using non-linear regression method. The values of v_r / v_s predicted using *Equation (11.1)* are plotted in *Figures 11.2 and 11.3*. The model predicts $v_r / v_s = 0.97$ at $L_{dq} = 40$ m.

Thus, the reduced queue discharge speed at time t since the start of the green period (v_r) can be calculated from:

$$v_r = v_s (1 - e^{-0.09 L_{dq}}) \quad (11.2)$$

where v_s is the queue discharge speed at time t since the start of the green period without any downstream queue effect as given by *Equation (7.1)*.

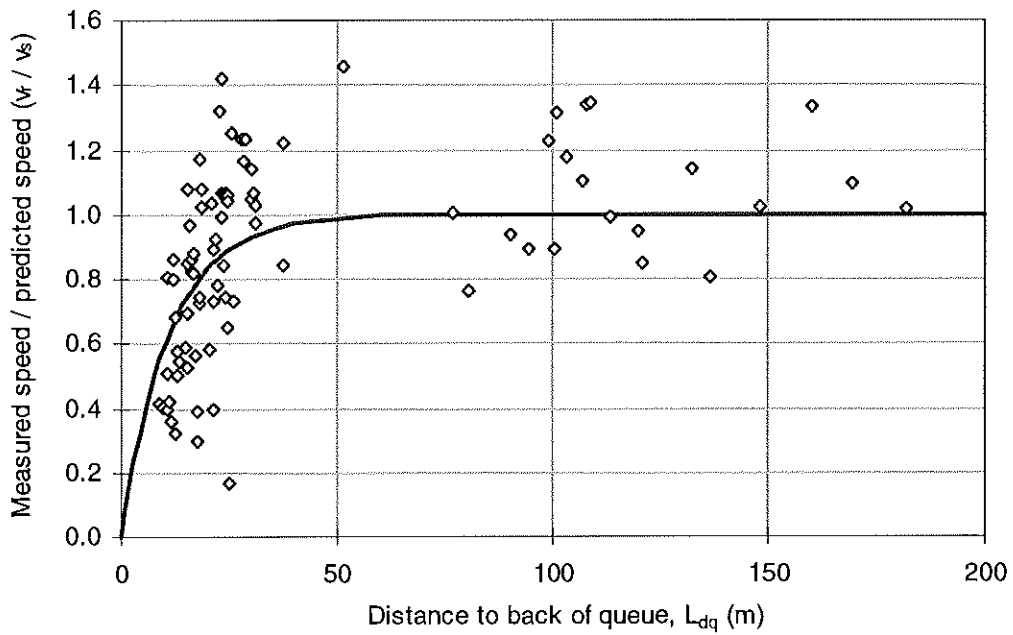


Figure 11.2 – Effect of the distance to the back of downstream queue on speed at site Mel5

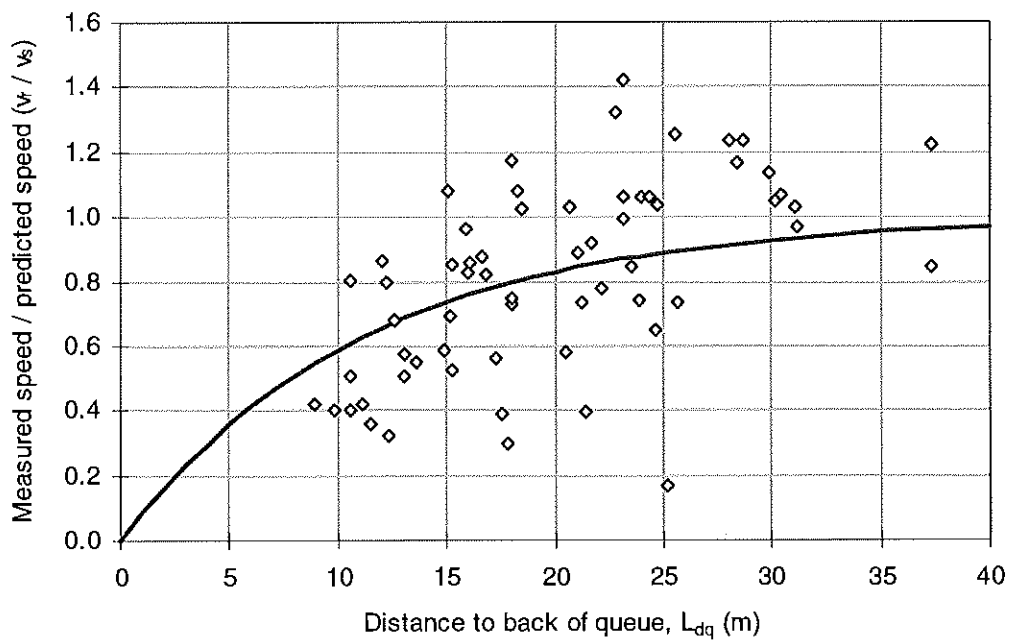


Figure 11.3 – Speed reduction as a function of the distance to the back of downstream queue at site Mel5

The corresponding reduced flow rate, q_r can then be calculated using the following equation based on *Equation (7.6b)*:

$$q_r = q_n [1 - (1 - v_r / v_n)^{m_q / m_v}] \quad (11.3)$$

In the case of site Mel6, the distances to the back of the downstream queue were generally greater than 60 m, and no queue interference effects were observed. There was insufficient data for detailed modelling of queue interaction effects at this site.

Although based on a small number of sites, the results indicate that the downstream queue interference occurs only when the distance to the back of queue is very small. For all practical purposes, it could be concluded that queue interaction occurs only when the downstream queue storage space is fully occupied.

The finding that the downstream queue interference occurs only when the distance to the back of queue is very small is supported by the fact that the distance to the back of downstream queue includes the intersection negotiation distance which can be of the order of 15 m at a small intersection (4 lanes across the intersection). Our preliminary observations at other sites were consistent with this finding. Similar results have been reported by Prosser and Dunne (1994) based on surveys in Sydney.

12 SATURATION FLOW, START LOSS AND END GAIN

The traditional queue discharge models for traffic signals (Webster and Cobbe 1966, Akçelik 1981, Teply, et al. 1995, TRB 1998) use a constant queue discharge flow rate called *saturation flow rate* and the associated *start loss* and *end gain* times to convert the displayed green time to an *effective green time*. Capacity and performance (delay, queue length) models are based on the use of effective green time and saturation flow rate.

Relationships between effective and displayed green times (g, G), start loss and end gain times (t_s, t_e), and durations of the saturated and unsaturated parts of the green period as effective and displayed green times ($g_s, g_u; G_s, G_u$) are given in *Section 7*.

In this section, the derivation of the saturation flow (s), start loss (t_s) and end gain time (t_e) parameters from the exponential queue discharge flow model is discussed. Different "measurement methods" (or "definitions") to derive the saturation flow and the associated start loss and gain parameters are discussed. The dependence of the start loss and end gain times on the saturation flow definition is emphasised. For further discussion on different methods of determining the saturation flow, the reader is referred to Teply and Jones (1991).

Average saturation speeds consistent with the method to determine the saturation flow can also be derived from the exponential queue discharge speed model (see *Section 13*).

General equations for determining the saturation flow rate, start loss and end gain times are:

$$s = \frac{3600(n_{vs} - n_{vi})}{G_s - t_i} \quad (12.1)$$

$$t_s = t_i - \frac{3600n_{vi}}{s} \quad (12.2)$$

$$t_e = \frac{3600n_e}{s} \quad (12.3)$$

where n_{vs} is the total number of vehicles departing from the queue during the saturated part of the green period (t_r to G_s), n_{vi} is the number of vehicles departing from the queue during an initial interval (0 to t_i), and n_e is the number of vehicles that depart after the end of the green period, i.e. during the terminating intergreen time (yellow and all-red intervals).

Using the exponential queue discharge flow model, values of n_{vs} and n_{vi} can be calculated from *Equations (7.28) and (7.27)*, respectively.

The following methods for determining saturation flows and the associated start loss and end gain values are considered:

- (i-a) HCM method (TRB 1998, Chapter 9, Appendix IV): average queue departure flow rate during the saturated part of green period excluding the first 4 vehicles ($n_{vi} = 4$).
- (i-b) A variation to the HCM method: average queue departure flow rate during the saturated part of green period excluding the first 5 vehicles ($n_{vi} = 5$).
- (ii) ARR 123 method (Akçelik 1981, Appendix E): average queue departure flow rate during the saturated part of the green period excluding the vehicles departing during the first 10 seconds ($t_i = 10$).
- (iii) Zero start loss and end gain method ($t_s = 0$, $t_e = 0$): average queue departure flow rate during the saturated part of the green period including all vehicles that depart at the start of the green period but excluding any vehicles that depart after the end of the green period.
- (iv-a) SCATS MF method: average queue departure flow rate during a fully-saturated green period including all vehicles that depart during the green period and after the green period but averaging over the green time plus terminating intergreen time (zero start loss, and end gain time = intergreen time, $t_s = 0$, $t_e = I_t = t_y + t_{ar}$).
- (iv-b) A variation to the SCATS MF method: as for (iv-a) but averaging over the green time plus yellow time (zero start loss, and end gain time = yellow time, $t_s = 0$, $t_e = t_y$).

Data for the analysis of saturation flow, start loss and end gain times for all sites are given in *Table 12.1*. The values of s , t_s and t_e calculated for different methods using *Equations (12.1) to (12.3)* are given in *Tables 12.2 and 12.3*.

The saturation flow (s) obtained from *Method (i-b)* corresponds to the maximum queue discharge flow rate (q_n) obtained from model calibration in using $n_{vi} = 5$ vehicles in the initial period. However, the value of s calculated using *Method (i-b)* differs slightly from q_n since it is derived analytically using the queue discharge flow model.

In *Methods (i-a) and (i-b)*, the values of t_i that give $n_{vi} = 4.0$ and $n_{vi} = 5.0$ are found by trial and error using *Equation (7.27)*, and n_{vs} is calculated for the interval t_i to G_s using *Equation (7.28)*. The values of t_i and n_{vs} ($G_s = G$) are given in *Table 12.1*.

It should also be noted that the q_n parameter for the exponential model was calculated from the minimum departure headway (h_n) which was obtained as the average headway with weighting based on inverse frequency of the headways by queue position (see *Section 8*). Generally, saturation flow measurement methods do not use headway weighting, and as a result are biased due to the higher frequency of headways at lower queue positions (the HCM method is affected by this bias). The saturation flow rate measured without any weighting by queue position would be lower than the queue discharge flow rate obtained using headway weighting by queue position. Comparison of *Method (i-a)* and *Method (i-b)* is useful for investigating the sensitivity to the number of vehicles excluded (four vs five).

Table 12.1

Data for the analysis of saturation flow rates, start loss and end gain times

Site	L_{hj} (m)	t_x (s)	v_n (km/h)	q_n (veh/h)	m_q	c (s)	G (s)	G_{max} (s)	t_i ($n_{vi}=4$)	t_i ($n_{vi}=5$)	n_{vi} ($t_i =$ 10 s)	n_{vs} ($G_s =$ G)	n_{vs} ($G_s =$ G_{max})
Average values													
Right-turn (isolated) sites	6.4	0.84	24.5	2033	0.582	136	17	30	8.8	10.6	4.7	8.8	15.8
Through (isolated) sites	6.9	1.17	45.1	2086	0.369	129	56	72	9.5	11.3	4.3	30.6	40.1
Through (paired int.) sites	7.0 *	1.02	30.9	1958	0.550	129	59	82	9.2	11.0	4.5	31.1	43.8
All Through sites	7.0	1.15	42.1	2057	0.427	129	56	74	9.4	11.1	4.4	30.8	41.0
Right-turn (isolated) sites													
TCS163 (1)	6.0	0.84	24.7	2098	0.621	144	13	30	8.5	10.2	4.9	6.6	16.5
TCS610	5.9	0.85	21.7	1966	0.698	149	13	20	8.8	10.6	4.7	6.3	10.1
TCS121	6.6	0.87	24.4	1948	0.545	139	20	40	9.2	11.1	4.4	9.8	20.7
TCS335	6.9	0.77	27.1	2133	0.464	112	23	29	8.9	10.6	4.7	12.4	15.9
Through (isolated) sites													
TCS1081 (2)	6.8	1.39	39.5	1790	0.334	131	64	81	11.0	13.0	3.5	30.3	38.8
TCS413	6.8	1.26	33.2	1801	0.542	140	60	82	9.8	11.8	4.1	29.1	40.1
TCS511	6.6	1.13	52.8	2283	0.273	160	120	125	9.7	11.4	4.2	73.8	76.9
TCS3196 (3)	7.0	1.11	31.7	1892	0.359	120	32	43	10.3	12.3	3.8	15.4	21.1
TCS4273 (4)	7.3	1.14	36.4	1938	0.347	109	43	66	10.2	12.1	3.9	21.6	34.0
TCS849	6.9	1.27	46.4	1999	0.343	130	52	59	10.0	11.9	4.0	27.3	31.1
TCS456	7.0 *	1.02	53.8	2422	0.374	140	36	55	8.5	10.0	5.0	22.4	35.2
Mel1	7.0 *	0.96	56.1	2558	0.326	158	43	58	8.5	10.0	5.0	28.4	39.0
Mel3	7.0 *	0.94	46.2	2423	0.343	131	59	82	8.7	10.3	4.8	37.7	53.2
Mel4	7.0 *	1.10	47.9	2217	0.275	130	67	80	9.9	11.6	4.1	39.0	47.0
Mel7	7.0 *	1.35	52.4	1968	0.369	75	35	59	10.0	11.8	4.0	17.7	30.8
Through (paired intersection) sites													
Mel2	7.0 *	1.00	30.9	1982	0.519	138	33	45	9.2	11.0	4.5	17.1	23.7
Mel5	7.0 *	1.07	27.1	1804	0.665	129	102	148	9.5	11.5	4.3	50.4	73.4
Mel6	7.0 *	0.98	34.6	2112	0.445	121	42	54	9.0	10.8	4.6	23.3	30.4

* Nominal values (jam spacing was not measured during these early surveys except at Mel7 site where $L_{hj} = 7.2$ m was measured).

All parameters in this table are for light vehicles (cars) only.

- (1) Data for AM and PM peak periods combined. G is average of green times observed during AM and PM peak periods. G_{max} is observed during the PM peak period.
- (2) 9 per cent uphill grade
- (3) Shared through and left turn (15 per cent left turn)
- (4) 6 per cent uphill grade

For the ARR 123 method, the value of n_{vi} is calculated with $t_i = 10$ in *Equation (7.27)*, and n_{vs} is calculated for the interval t_i to G_s using *Equation (7.28)*. The values of n_{vi} ($t_i = 10$ s) and n_{vs} ($G_s = G$) are given in *Table 12.1*. It is seen that the value of $t_i = 10$ s represents a good choice as a value that gives n_{vi} between 4 and 5 vehicles.

Method (iii) further simplifies the saturation flow measurement by eliminating the start loss and end gain times. This gives a saturation flow based on zero start loss and zero end gain definition, s_o ($t_s = t_e = 0$, therefore $g = G$). This is derived using $t_i = 0$ and $n_{vi} = 0$, n_{vs} is calculated using *Equation (7.28)*, effectively for the interval t_r to G_s , and n_e is included in the saturation flow calculation:

$$s_o = \frac{3600(n_{vs} + n_e)}{G_s} \quad (12.4)$$

$$= \frac{q_m \left[(G_s - t_r) - \frac{1 - e^{-m_q(G_s - t_r)}}{m_q} \right] + 3600n_e}{G_s}$$

For *Methods (i) to (iii)*, saturation flows are calculated using average values of green time observed at each site as fully saturated green time ($G_s = G$). On the other hand, $G_s = G_{max}$ is used for *Methods (iv-a) and (iv-b)* using the values of maximum green time observed at each site.

Table 12.1 gives the average green and cycle times and maximum green times (G , c , G_{max}) observed at each site (also see *Tables 4.3 to 4.5* in *Section 4*), the average site values of G , c , G_{max} for the right-turn, through (isolated) and through (paired intersection) sites, and the values of n_{vs} calculated using $G_s = G$ and $G_s = G_{max}$.

For site 163, queue discharge flow and speed models were calibrated using data for AM and PM peak periods combined. Therefore, for the analysis presented here, G and c in *Table 12.1* are the average green and cycle times observed during AM and PM peak periods, and G_{max} is the higher value observed during the PM peak period.

The saturation flow (s_{MF}) from *Method (iv-a)* corresponds to the SCATS maximum flow (MF) parameter in terms of its definition. It is emphasised that the SCATS system uses complicated filtering algorithms to measure MF on line, and therefore caution should be used when comparing s_{MF} with MF values measured by SCATS. See *Section 13* for further discussion on this parameter.

For *Method (iv-a)*, $t_i = 0$ and $n_{vi} = 0$ are used as in *Method (iii)*, therefore $t_s = 0$, and n_{vs} is calculated using *Equation (7.28)*, effectively for the interval t_r to G_s . For this method $G_s = G_{max}$ is used, and s_{MF} is calculated to include the effect of n_e :

$$s_{MF} = \frac{3600(n_{vs} + n_e)}{G_{max} + I_t} \quad (12.5)$$

$$= \frac{q_m \left[(G_{max} - t_r) - \frac{1 - e^{-m_q(G_{max} - t_r)}}{m_q} \right] + 3600n_e}{G_{max} + I_t}$$

where q_m is the maximum queue discharge flow rate for a traffic stream consisting of passenger car units (light vehicles) only.

Since s_{MF} includes the effect of n_e , the end gain time equals the terminating intergreen time, $t_e = I_t = t_y + t_{ar}$ so that the effective green time is calculated correctly ($g_{max} = G_{max} + I_t$ and $s_{MF} g_{max} / 3600 = n_{vs} + n_e$).

Method (iv-b) provides a variation to the s_{MF} method by obtaining the average saturation flow over $G_{max} + t_y$ rather than $G_{max} + I_t$:

$$s_{MF} = \frac{3600(n_{vs} + n_e)}{G_{max} + t_y} \quad (12.6)$$

In this case, the end gain time equals the yellow time, $t_e = t_y$ so that the effective green time is calculated correctly ($g_{max} = G_{max} + t_y$ and $s_{MF} g_{max} / 3600 = n_{vs} + n_e$).

In the study presented in this section, $t_r = 0$ s, $I_t = 6$ s, $t_y = 4$ s, and $n_e = 1.5$ veh were used for all cases.

It is seen from the results given in *Tables 12.2 and 12.3* and comparisons shown in *Figures 12.1 to 12.6* that *Methods (i-a), (i-b) and (ii)* produce saturation flows that are very close to the maximum queue discharge flow rate (*Figure 12.1*). *Method (iii)* saturation flows are reasonably close to the maximum queue discharge flow rate but this is seen to be a less precise method (*Figure 12.2*). In particular, this method gives higher saturation flows for right turn sites.

Methods (iv-a) and (iv-b) give lower saturation flows (about 10 % and 7 % respectively) as seen in *Figures 12.3 and 12.4*. However, cycle capacities calculated using maximum green times ($s g_{max}$ where $g_{max} = G_{max} - t_s + t_e$) are almost identical for all saturation flow methods since differences in saturation flows are compensated by differences in start loss and end gain times. This is seen clearly from *Figure 12.5* for the ARR 123 method, and *Figure 12.6* for the s_{MF} method.

The saturation flow rate in cumulative average format used by the Canadian capacity guide for signalised intersections (Teply, et al. 1995) presents a further alternative for saturation flow measurement. This can be calculated as (n_s / t) using n_s from *Equation (7.4) in Section 7*. The value of (n_s / t) is less than the queue discharge flow rate q_s from *Equation (7.2)* for any finite value of t . The cumulative saturation flow format used by the Canadian capacity guide implies a zero-start loss value ($t_s = 0$) although *Figure 1-28* of the guide indicates a shift at the start of the effective green period relative to the displayed green period.

Alternative saturation flow methods discussed in this section emphasise the importance of start loss and end gain times as an integral part of the saturation flow definition. Therefore, saturation flows must be used with start loss and end gain times defined and measured consistently.

It is also important to note that start loss and end gain times are significantly different for different site types. In particular for the controlled right-turn and paired intersection through sites, start loss values are about 1.0 s shorter, consistent with lower jam spacing and departure response times (*Table 12.2*).

Table 12.2

Saturation flow rates, start loss and end gain times obtained using various methods to determine saturation flow: HCM and ARR 123 Methods

Site	q _n (veh/h)	HCM Method (n _{vl} = 4)			HCM Method (n _{vl} = 5)			ARR 123 Method (t _i = 10)		
		s (veh/h)	t _s (s)	t _e (s)	s (veh/h)	t _s (s)	t _e (s)	s (veh/h)	t _s (s)	t _e (s)
Average values										
Right-turn (isolated) sites	2033	2029	1.7	2.7	2029	1.7	2.7	2032	1.7	2.7
Through (isolated) sites	2086	2083	2.6	2.6	2084	2.6	2.6	2083	2.6	2.6
Through (paired int.) sites	1958	1957	1.8	2.8	1957	1.8	2.8	1958	1.8	2.8
All Through sites	2057	2059	2.4	2.6	2060	2.4	2.6	2056	2.3	2.6
Right-turn (isolated) sites										
TCS163 (1)	2098	2094	1.6	2.6	2096	1.6	2.6	2096	1.6	2.6
TCS610	1966	1965	1.4	2.7	1965	1.4	2.7	1965	1.4	2.7
TCS121	1948	1946	1.8	2.8	1947	1.8	2.8	1946	1.8	2.8
TCS335	2133	2128	2.1	2.5	2130	2.1	2.5	2130	2.1	2.5
Through (isolated) sites										
TCS1081 (2)	1790	1787	2.9	3.0	1789	2.9	3.0	1786	2.9	3.0
TCS413	1801	1801	1.8	3.0	1801	1.8	3.0	1801	1.8	3.0
TCS511	2283	2278	3.4	2.4	2280	3.5	2.4	2278	3.4	2.4
TCS3196 (3)	1892	1886	2.7	2.9	1889	2.7	2.9	1885	2.7	2.9
TCS4273 (4)	1938	1933	2.8	2.8	1935	2.8	2.8	1933	2.8	2.8
TCS849	1999	1995	2.8	2.7	1997	2.9	2.7	1995	2.8	2.7
TCS456	2422	2412	2.5	2.2	2416	2.6	2.2	2416	2.6	2.2
Mel1	2558	2544	2.8	2.1	2549	2.9	2.1	2549	2.9	2.1
Mel3	2423	2416	2.8	2.2	2419	2.8	2.2	2418	2.8	2.2
Mel4	2217	2208	3.4	2.4	2211	3.5	2.4	2208	3.4	2.4
Mel7	1968	1963	2.6	2.8	1965	2.7	2.7	1963	2.6	2.8
Through (paired intersection) sites										
Mel2	1982	1981	1.9	2.7	1981	1.9	2.7	1981	1.9	2.7
Mel5	1804	1804	1.5	3.0	1804	1.5	3.0	1804	1.5	3.0
Mel6	2112	2109	2.2	2.6	2111	2.2	2.6	2110	2.2	2.6

All parameters in this table are for light vehicles (cars) only.

- (1) Data for AM and PM peak periods combined. G is average of green times observed during AM and PM peak periods. G_{max} is observed during the PM peak period.
- (2) 9 per cent uphill grade
- (3) Shared through and left turn (15 per cent left turn)
- (4) 6 per cent uphill grade

Table 12.3

Saturation flow rates, start loss and end gain times obtained using various methods to determine saturation flow: zero start loss and end gain, and SCATS MF methods

Site	Q _n (veh/h)	Zero Start Loss and End Gain Method			SCATS MF Method ($t_e = I_t$)			SCATS MF Method ($t_e = t_y$) (variation)		
		s (veh/h)	t _s (s)	t _e (s)	s (veh/h)	t _s (s)	t _e (s)	s (veh/h)	t _s (s)	t _e (s)
Average values										
Right-turn (isolated) sites	2033	2144	0	0	1745	0	6.0	1849	0	4.0
Through (isolated) sites	2086	2082	0	0	1922	0	6.0	1973	0	4.0
Through (paired int.) sites	1958	1989	0	0	1846	0	6.0	1889	0	4.0
All Through sites	2057	2068	0	0	1911	0	6.0	1960	0	4.0
Right-turn (isolated) sites										
TCS163 (1)	2098	2254	0	0	1804	0	6.0	1911	0	4.0
TCS610	1966	2165	0	0	1612	0	6.0	1746	0	4.0
TCS121	1948	2039	0	0	1734	0	6.0	1812	0	4.0
TCS335	2133	2168	0	0	1790	0	6.0	1899	0	4.0
Through (isolated) sites										
TCS1081 (2)	1790	1791	0	0	1667	0	6.0	1706	0	4.0
TCS413	1801	1836	0	0	1702	0	6.0	1741	0	4.0
TCS511	2283	2258	0	0	2156	0	6.0	2189	0	4.0
TCS3196 (3)	1892	1896	0	0	1663	0	6.0	1734	0	4.0
TCS4273 (4)	1938	1934	0	0	1774	0	6.0	1825	0	4.0
TCS849	1999	1991	0	0	1808	0	6.0	1865	0	4.0
TCS456	2422	2392	0	0	2166	0	6.0	2240	0	4.0
Mel1	2558	2501	0	0	2280	0	6.0	2354	0	4.0
Mel3	2423	2395	0	0	2239	0	6.0	2291	0	4.0
Mel4	2217	2177	0	0	2031	0	6.0	2080	0	4.0
Mel7	1968	1970	0	0	1787	0	6.0	1844	0	4.0
Through (paired intersection) sites										
Mel2	1982	2030	0	0	1780	0	6.0	1852	0	4.0
Mel5	1804	1830	0	0	1751	0	6.0	1774	0	4.0
Mel6	2112	2128	0	0	1912	0	6.0	1978	0	4.0

All parameters in this table are for light vehicles (cars) only.

- (1) Data for AM and PM peak periods combined. G is average of green times observed during AM and PM peak periods. G_{max} is observed during the PM peak period.
- (2) 9 per cent uphill grade
- (3) Shared through and left turn (15 per cent left turn)
- (4) 6 per cent uphill grade

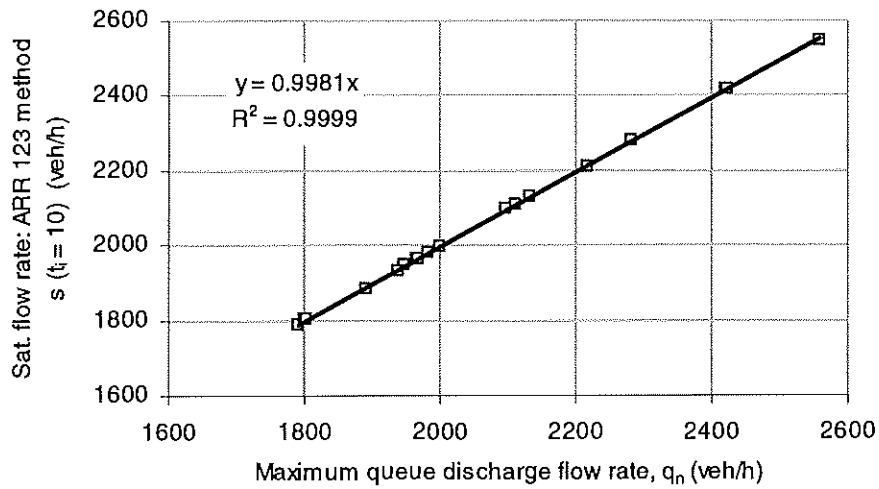


Figure 12.1 – Comparison of saturation flow, s ($t_i = 10$ s) using Method (ii) (ARR 123 method) with the maximum queue discharge flow rate, q_n (similar results are observed for the HCM method)

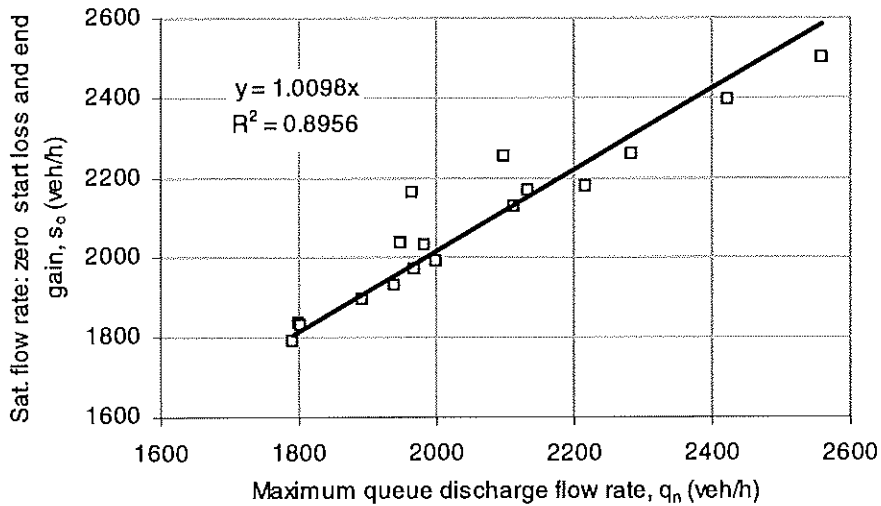


Figure 12.2 – Comparison of saturation flow, s_o (zero start loss and end gain method) with the maximum queue discharge flow rate, q_n

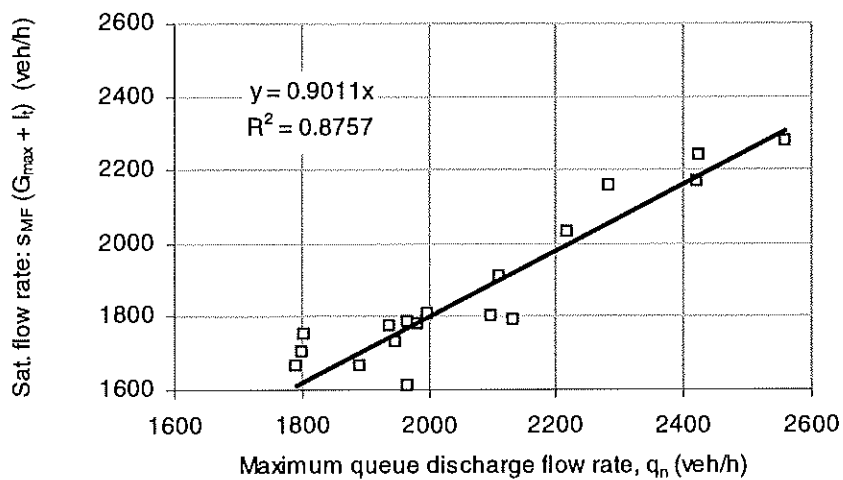


Figure 12.3 – Comparison of saturation flow, s_{MF} (SCATS MF definition) with the maximum queue discharge flow rate, q_n

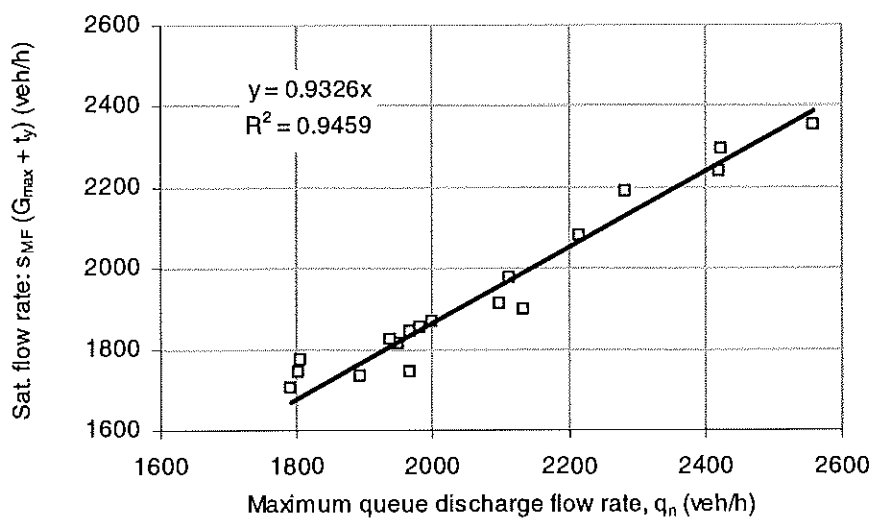


Figure 12.4 – Comparison of saturation flow, s_{MF} (a variation to the SCATS MF definition) with the maximum queue discharge flow rate, q_n

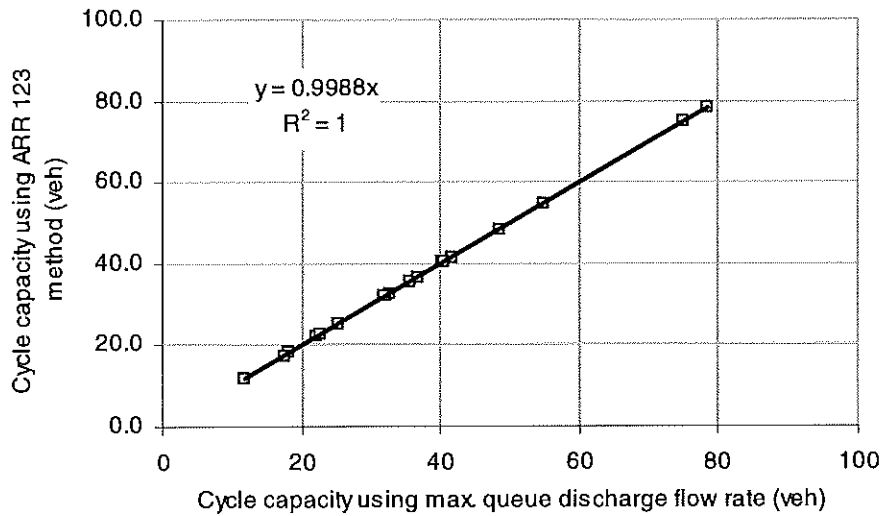


Figure 12.5 – Comparison of cycle capacity ($s g_{max}$) using the ARR 123 method with the cycle capacity using maximum queue discharge flow rate, q_n

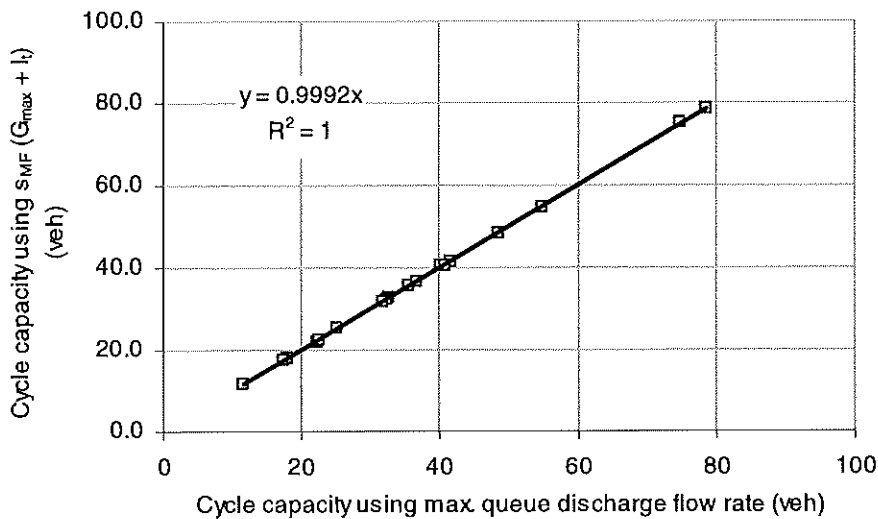


Figure 12.6 – Comparison of cycle capacity ($s g_{max}$) using s_{MF} (SCATS MF definition) with the cycle capacity using maximum queue discharge flow rate, q_n

Heavy Vehicle Effect on Saturation Flows

The results of saturation flow analysis given in this section and the queue discharge model calibration results given in *Section 9* gave saturation flows ($s = s_m$) and maximum queue discharge flow rates ($q_n = q_m$) for light vehicles (mainly passenger cars). Strictly speaking, symbols q_n are s are used for the overall traffic stream including light and heavy vehicles, and the corresponding symbols for light vehicles are q_m and s_m (pcu/h).

The maximum queue discharge flow rates for the actual traffic mix and passenger cars only (q_m, q_n), and the saturation flow rates for the actual traffic mix and for passenger cars only (s, s_m) are related through:

$$q_n = q_m / f_c \quad (12.7)$$

$$s = s_m / f_c \quad (12.8)$$

where f_c is the traffic composition factor given by:

$$f_c = 1 + p_{HV} (f_{HV} - 1) \quad (12.9)$$

where f_{HV} is a heavy vehicle factor for saturation flow purposes, and p_{HV} is the proportion of heavy vehicles in the traffic stream.

The heavy vehicle factor, f_{HV} is typically in the range 1.5 to 2.0 veh/pcu. The SIDRA software package uses $f_{HV} = 1.65$ for through traffic (see Akçelik and Besley 1999).

Variations in Saturation Flows and Start Loss Values at a Given Site

Limited analysis of cycle-by-cycle variations in minimum queue discharge headway (h_n), cycle capacities ($s_{g_{max}}$) and space time (t_s) at a given site were carried out. For this purpose, the required variables were calculated for each cycle as follows (subscript j indicates the j th signal cycle). This analysis was carried out for signal cycles with light vehicles only.

The minimum queue discharge headway for each cycle (h_{nj}) was calculated as the average headway between vehicles departing from the queue after the first five vehicles. Time for the first 5 vehicles to depart (t_{ij}) was determined for each cycle for calculating the start loss time. The maximum queue discharge speed (v_{nj}) was determined using non-linear regression for the exponential queue discharge model. The largest value of G observed at the site was used as the maximum green time (G_{max}). For detector space time calculations, a detection zone length of $L_p = 4.5$ m and an average vehicle length of $L_v = 4.4$ m were used for all cycles at all sites.

Saturation flow (veh/h):

$$s_j = 3600 / h_{nj} \quad (12.10)$$

Start loss:

$$t_{sj} = t_{ij} - 5 h_{nj} \quad (12.11)$$

End gain:

$$t_{ej} = 3600 n_c / s_j \quad (12.12)$$

Maximum cycle capacity:

$$s_j g_{\max j} = s_j (G_{\max} - t_{sj} + t_{ej}) \quad (12.13)$$

Detector space time at maximum queue discharge flow (see *Section 5*):

$$t_{snj} = h_{nj} - \frac{3.6 (L_p + L_v)}{v_{nj}} \quad (12.14)$$

Of particular interest is the variance to mean ratio of cycle capacity:

$$I_{sg} = \text{var} (s_j g_{\max j}) / \text{mean} (s_j g_{\max j}) \quad (12.15)$$

The variance to mean ratio of cycle capacity is relevant to modelling the effect of randomness in departure flows for predicting traffic performance (delay, queue length and queue move-up rate) for signalised intersections. Although this parameter is included in basic theoretical treatment of delay modelling (Tarko and Rajaraman 1998), it has not been used explicitly in most delay models used in practice. Some coordinated signal delay models allow for filtering/metering of departure flows for saturated cycles at the upstream intersection, thus reducing the amount of randomness. For example, see the US Highway Capacity Manual (TRB 1998) and the SIDRA User Guide (Akçelik and Besley 1999). This may lead to the prediction of zero delays at the downstream intersection when the upstream intersection is oversaturated since the effect of variations in cycle capacity is ignored. An understanding of the values of this parameter at real-life intersections helps with improved modelling of the coordinated signal performance in particular.

Cycle-by-cycle variance analysis was carried out for sites 335 (Melbourne), 413 (Sydney), 511 (Sydney), 3196 (Melbourne), and 849 (Melbourne). The results are summarised in *Table 12.4*. Note that average values of minimum queue discharge headway (h_n) and detector space time at minimum queue discharge headway (t_{sn}) differ from the average values given in *Section 9* (see *Table 9.7*) particularly because of the way headway is calculated using headway weighting by queue position in the standard calibration procedure (*Section 8*).

Distributions of h_{nj} , $s_j g_{\max j}$ and t_{snj} varied considerably from site to site. Distributions for sites 335 (right turn movement with short green time) and 511 (through movement with very long green time) are given in *Figures 12.7 to 12.12*.

It is seen from *Table 12.4* that the variance to mean ratio of cycle capacity (I_{sg}) for the five survey sites is in the range 0.08 to 0.34. It appears that 0.10 is a typical value for isolated sites. Interestingly, a high value of 0.34 was observed at the CBD site 413, suggesting that further attention needs to be paid to this parameter for coordinated signal modelling.

Table 12.4

Analysis of cycle by cycle variations in minimum queue discharge headway (h_n), cycle capacity (g_{max}), detector space time at minimum queue discharge headway (t_{sn}), and other parameters

	h_n (s)	s (veh/h)	t_i (s)	t_s (s)	t_e (s)	G_s (s)	G (s)	s g_{max} (veh)	v_n (km/h)	t_{sn} (s)	I_{sg}
Site 335											0.08
Mean	1.70	2133	9.44	0.92	2.55	19.1	23.9	17	29.5	0.57	
Std Dev.	0.167	206	0.94	1.35	0.25	4.5	3.1	1.2	8.0	0.26	
Variance	0.028	42308	0.88	1.82	0.06	20.2	9.5	1.4	63.5	0.07	
85th percentile	1.88	2290	10.39	2.29	2.82	23	27	19	33.4	0.79	
98th percentile	2.03	2599	11.64	3.65	3.05	26	29	21	41.4	1.16	
Site 413											0.34
Mean	2.02	1805	9.88	-0.21	3.03	34.4	59.5	41	35.6	1.09	
Std Dev.	0.224	194	1.35	1.69	0.34	14.8	9.2	3.7	6.0	0.30	
Variance	0.050	37494	1.83	2.87	0.11	219.6	84.8	14.0	36.1	0.09	
85th percentile	2.23	2026	11.30	1.43	3.35	53	70	45	41.7	1.36	
98th percentile	2.54	2175	12.88	3.74	3.82	63	75	47	48.3	1.76	
Site 511											0.10
Mean	1.62	2226	10.05	1.95	2.43	35.5	120.4	78	52.9	1.01	
Std Dev.	0.07	91	1.30	1.41	0.10	22.9	4.7	2.9	2.9	0.08	
Variance	0.00	8250	1.70	2.00	0.01	524.1	21.6	8.1	8.2	0.01	
85th percentile	1.71	2315	11.58	3.49	2.57	65	124	81	55.3	1.07	
98th percentile	1.73	2324	12.61	4.64	2.59	79	125	81	57.0	1.14	
Site 3196											0.10
Mean	1.93	1885	10.89	1.27	2.89	26.0	31.4	23	33.8	0.94	
Std Dev.	0.177	166	1.39	1.82	0.27	5.7	4.3	1.5	7.1	0.25	
Variance	0.031	27713	1.92	3.30	0.07	32.6	18.3	2.2	50.7	0.06	
85th percentile	2.08	2063	12.30	2.74	3.12	30	35	25	39.0	1.18	
98th percentile	2.28	2139	13.87	5.27	3.41	37	42	25	53.1	1.50	
Site 849											0.12
Mean	1.78	2028	10.33	1.41	2.68	32.7	51.8	33	46.6	1.08	
Std Dev.	0.136	149	0.79	1.05	0.20	12.6	2.6	2.0	6.9	0.15	
Variance	0.019	22124	0.62	1.10	0.04	158.3	6.6	4.0	47.2	0.02	
85th percentile	1.91	2197	11.27	2.30	2.86	49	53	35	52.0	1.23	
98th percentile	2.17	2280	11.71	2.83	3.25	51	56	36	60.9	1.34	

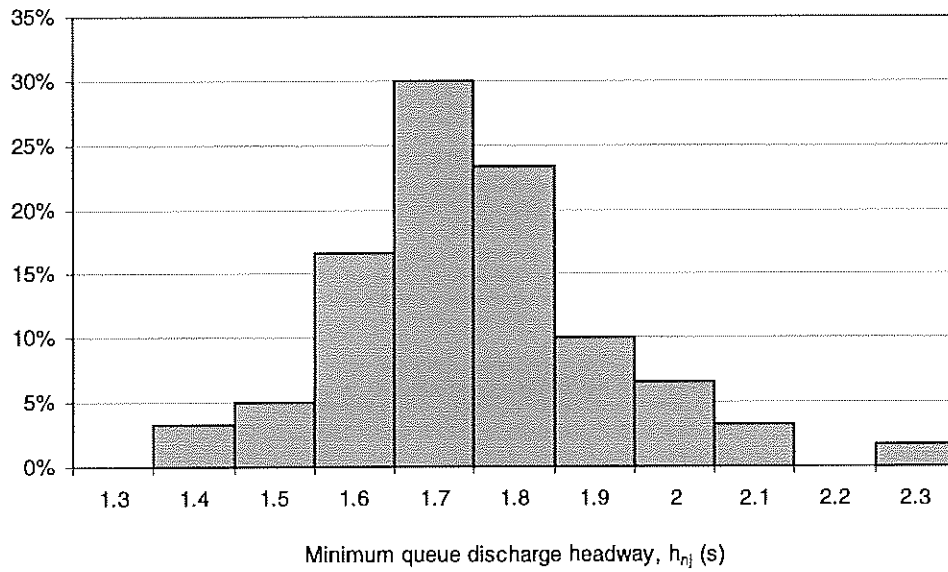


Figure 12.7 – Distribution of cycle-by-cycle values of the minimum queue discharge headway, h_{nj} at Site 335 (right turn movement with short green time)

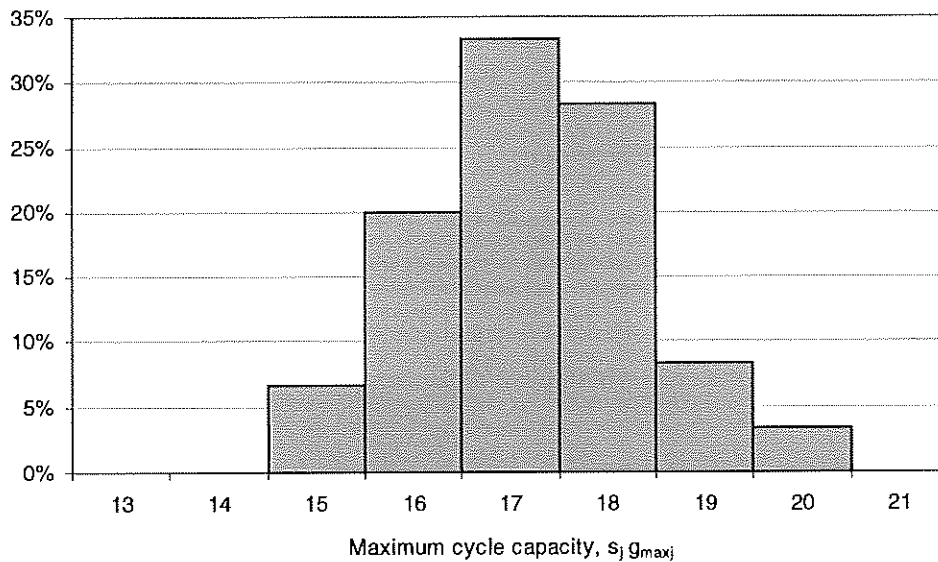


Figure 12.8 – Distribution of cycle-by-cycle values of the maximum cycle capacity, $s_j g_{maxj}$ at Site 335 (right turn movement with short green time)

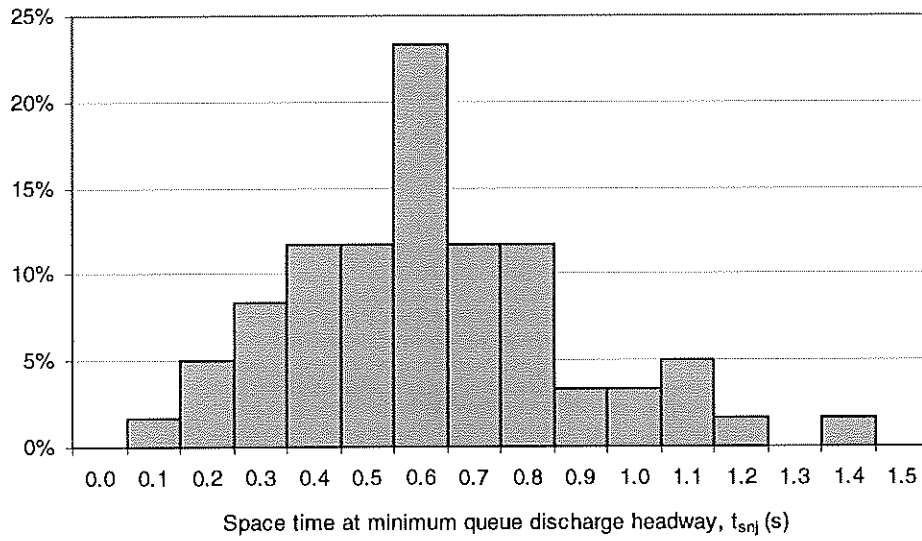


Figure 12.9 – Distribution of cycle-by-cycle values of the space time at maximum queue discharge flow, t_{snj} at Site 335 (right turn movement with short green time)

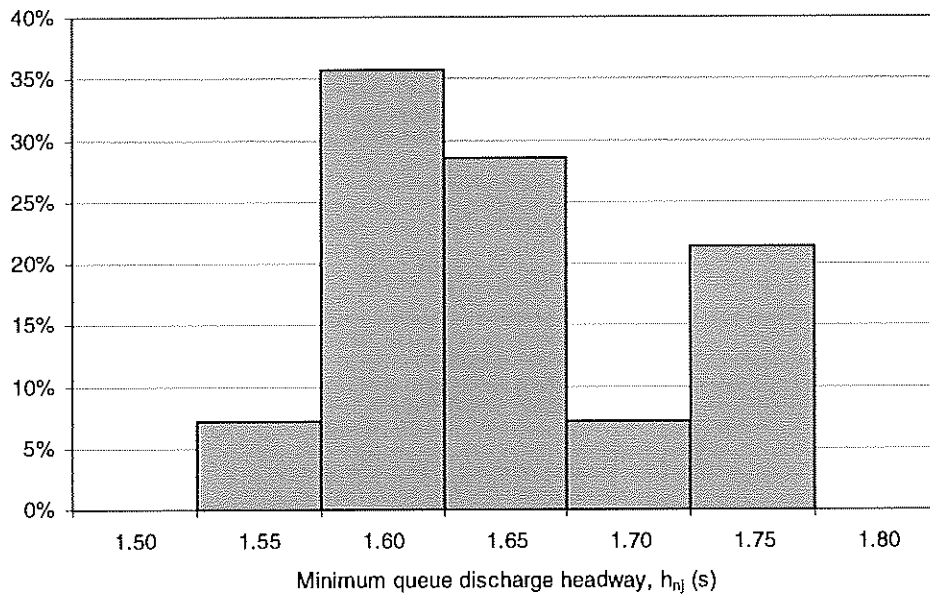


Figure 12.10 – Distribution of cycle-by-cycle values of the minimum queue discharge headway, h_{nj} at Site 511 (through movement with very long green time)

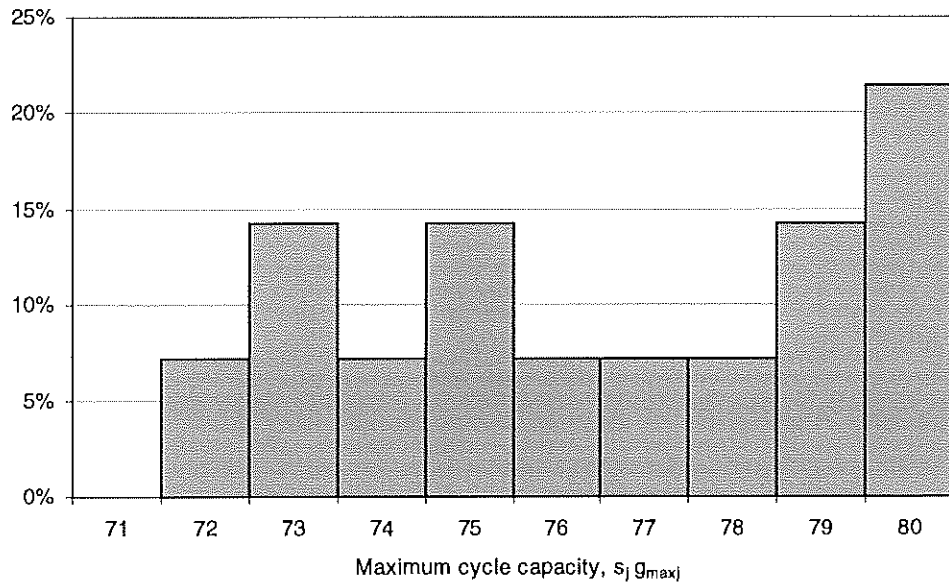


Figure 12.11 – Distribution of cycle-by-cycle values of the maximum cycle capacity, $s_j g_{maxj}$ at Site 511 (through movement with very long green time)

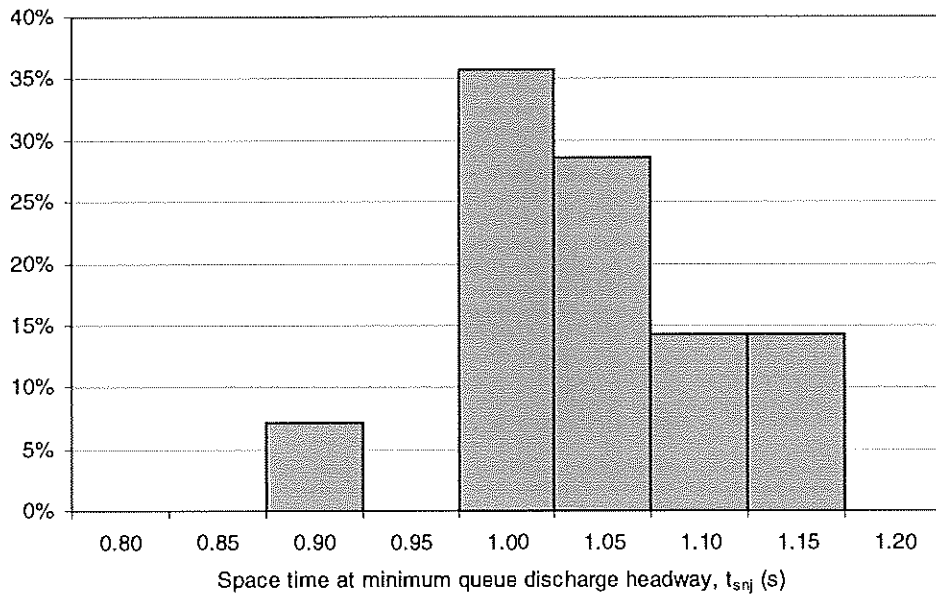


Figure 12.12 – Distribution of cycle-by-cycle values of the space time at maximum queue discharge flow, t_{snj} at Site 511 (through movement with very long green time)

13 SCATS CONTROL PARAMETERS

In this section, SCATS control parameters MF (maximum flow), HW (headway time at maximum flow), KP (occupancy time at maximum flow) and DS (degree of saturation) are compared with their analytical counterparts derived from queue discharge models presented in previous sections.

The purpose is to demonstrate the validity of fundamental relationships with reference to established control parameters used in practice. This information would be useful in understanding the SCATS system, and in the validation of analytical and simulation models used for the analysis of SCATS operation (Lowrie 1982, 1984, 1990; Fehon and Moore 1982).

The SCATS method determines the MF, HW, KP and DS parameters from on-line measurements using a complicated procedure. This includes a filtering process to determine the maximum flow and occupancy (MF and KP), and the corresponding space time is then used in determining DS on a cycle by cycle basis. The analytical parameters corresponding to these SCATS control parameters are s_{MF} (saturation flow estimate based on the SCATS MF method as discussed in *Section 12*), t_{oMF} (occupancy time corresponding to s_{MF}), and x (degree of saturation), respectively. The analytical parameter corresponding to the space time at SCATS maximum flow is t_{sMF} . These estimates can be compared with the SCATS-reported MF, HW, KP and DS parameters to assess how well these parameters correspond to each other.

It is emphasised that such a comparison does not represent a one to one correspondence between the SCATS-reported and analytical parameters. This is because the SCATS on-line feedback system applies a complex set of rules to determine these parameters by considering values measured cycle by cycle whereas the corresponding analytical parameters are average values obtained for limited survey periods. Nevertheless, such a comparison is useful to determine if the calibrated models have reasonable prediction abilities.

MF, HW and KP Parameters

The SCATS parameters MF (maximum flow), HW (headway time at maximum flow) and KP (occupancy time at maximum flow) reported by the SCATS system for the survey days at Sydney and Melbourne 1998 sites are given *Tables 4.1 and 4.2* in *Section 4*.

Formulae for calculating analytical parameters corresponding to the SCATS parameters MF, HW, KP and the space time (HW – KP) are given below. These parameters are calculated for traffic conditions that generate maximum queue departure flow. Thus, they are derived assuming light vehicles (cars) only, and using a fully saturated maximum green time ($G_s = G_{max}$).

From (Equation 12.5) in Section 12, the analytical parameter corresponding to the MF parameter (s_{MF}) is given by:

$$s_{MF} = \frac{q_m \left[(G_{\max} - t_r) - \frac{1 - e^{-m_q(G_{\max} - t_r)}}{m_q} \right] + 3600n_e}{G_{\max} + I_t} \quad (13.1)$$

where q_m is the maximum queue discharge flow rate (per hour) for a traffic stream consisting of passenger car units (light vehicles) only, G_{\max} is the maximum green time, I_t is the terminating intergreen time, and n_e is the number of vehicles that depart during the terminating intergreen period.

The headway at maximum flow is:

$$h_{MF} = 3600 / s_{MF} \quad (13.2)$$

The analytical parameter corresponding to the KP parameter, average detector occupancy time (t_{oMF}) at s_{MF} and the related detector space time (t_{sMF}) can be calculated from:

$$t_{oMF} = 3.6 (L_{vm} + L_p) / v_{MF} \quad \text{subject to } t_{oMF} \leq h_{MF} \quad (13.3)$$

$$t_{sMF} = h_{MF} - t_{oMF} \quad \text{subject to } t_{sMF} \geq 0 \quad (13.4)$$

where L_{vm} is the average vehicle length for passenger car units (m/pcu), L_p is the effective detection zone length (m), and v_{MF} is the average speed corresponding to s_{MF} :

$$v_{MF} = \frac{v_m \left[(G_{\max} + t_{em} - t_r) - \frac{1 - e^{-m_q(G_{\max} + t_{em} - t_r)}}{m_q} \right]}{G_{\max} + t_{em}} \quad (13.5)$$

where v_m is the maximum queue discharge speed for a traffic stream consisting of passenger car units (light vehicles) only, and t_{em} is the end gain based on the maximum queue discharge flow rate for a traffic stream consisting of passenger car units (light vehicles) only:

$$t_{em} = 3600 n_e / q_m \quad (13.6)$$

The average speed v_{MF} used for occupancy time calculation is obtained by averaging over the interval 0 to $G_{\max} + t_{em}$. This allows for occupancy times during intervals 0 to t_r and G_{\max} to $(G_{\max} + t_{em})$. The latter allows for the departure of n_e vehicles at the queue discharge speed predicted by the exponential model at that time. Since there are no vehicles departing during $(G_{\max} + t_{em})$ to $(G_{\max} + I_t)$, this interval is not included in the calculation of occupancy time, implying no occupancy (i.e. $I_t - t_{em}$ = space time) through the use of Equation (13.4).

Table 13.1

SCATS parameters MF, HW, KP and (HW – KP) and the corresponding Analytical Parameters Based on Calibrated Models for Sydney and Melbourne 1998 Sites

Site		Reported by SCATS				Analytical parameters					
		MF	HW	KP	HW – KP	s_{MF}	h_{MF}	$G_{max} + t_{em}$	v_{MF}	t_{oMF}	t_{sMF}
Right-turn (isolated) sites											
163	Syd	1895	1.90	1.27	0.63	1804	2.00	32.6	22.3	1.44	0.56
610	Syd	1579	2.28	1.54	0.74	1612	2.23	22.7	19.1	1.67	0.56
121	Mel	1925	1.87	1.26	0.61	1734	2.08	42.8	22.4	1.43	0.65
335	Mel	1915	1.88	1.24	0.64	1790	2.01	31.5	23.7	1.35	0.66
Through (isolated) sites											
1081	Syd	1818	1.98	0.96	1.02	1667	2.16	84.0	34.9	0.92	1.24
413	Syd	1714	2.10	1.19	0.91	1702	2.12	85.0	31.2	1.03	1.09
511	Syd	2156	1.67	0.75	0.92	2156	1.67	127.4	47.5	0.67	1.00
3196	Mel	1905	1.89	0.91	0.98	1663	2.16	45.9	27.1	1.18	0.98
4273	Mel	1827	1.97	na	na	1774	2.03	68.8	32.5	0.99	1.04
849	Mel	2034	1.77	0.76	1.01	1808	1.99	61.7	39.0	0.82	1.17
456	Mel	2236	1.61	0.76	0.85	2166	1.66	57.2	45.8	0.70	0.96

na: not available

The SCATS parameters MF, HW, KP and (HW – KP) as well as the analytically derived parameters s_{MF} , h_{MF} , t_{oMF} , and t_{sMF} , respectively, are given in Table 13.1. The values given in the table were calculated using measured G_{max} values given in Tables 4.3 and 4.4 for each site, with $I_t = 6$ s, $n_e = 1.5$ veh, $L_{vm} = 4.4$ m, and $L_p = 4.5$ m. Note that all calibration results are for light vehicles (cars) only, and therefore $v_m = v_n$, $q_m = q_n$ are used in Equations (13.1) to (13.6) for results in Table 13.1.

Figures 13.1 to 13.3 show the correspondence between SCATS-reported parameters MF, KP and space time (HW – KP) and the analytical parameters s_{MF} , t_{oMF} and t_{sMF} with linear trendlines indicating good correspondence given basic differences between the measurement and estimation methods.

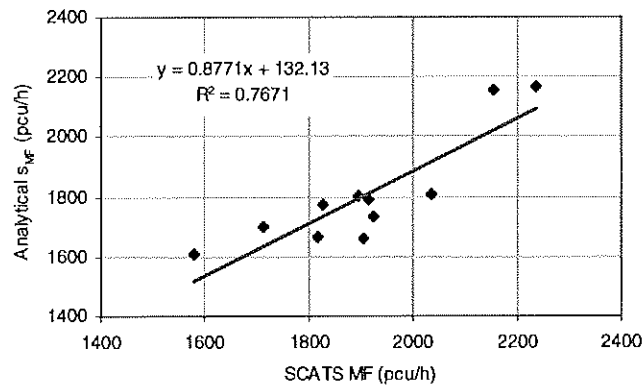


Figure 13.1 - Correspondence between SCATS-reported maximum flow parameter MF and the analytical parameter s_{MF} for Sydney and Melbourne 1998 sites

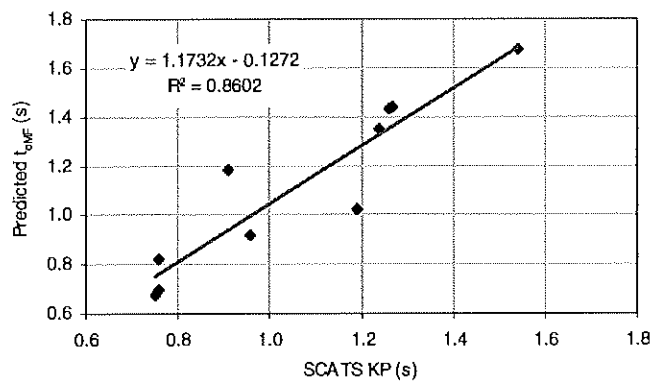


Figure 13.2 - Correspondence between SCATS-reported occupancy parameter KP and the analytical parameter t_{oMF}

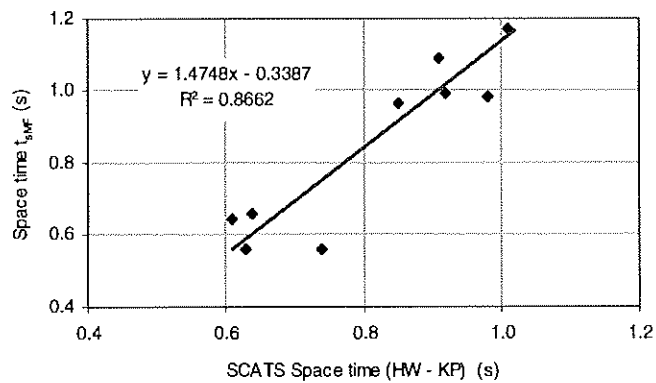


Figure 13.3 - Correspondence between SCATS-reported space time and the analytical parameter t_{sMF}

DS Parameter

The SCATS DS parameter is the basic strategic control parameter in the operation of the SCATS dynamic signal control system including the control of an isolated intersection. The DS parameter is defined as "the ratio of the effectively used green time to the total available green time", and is formulated in terms of presence loop occupancy and volume data measured by the system. Lowrie (1982, 1990) qualifies the SCATS DS parameter as "analogous to degree of saturation". In this section, an estimate of the DS parameter is calculated using the saturation flow and saturation speed estimates derived from the exponential queue discharge flow and speed models. This allows a discussion of the DS parameter in relation to the *degree of saturation* used in the traditional traffic signal analysis methods (Akçelik 1981, TRB 1998, Webster and Cobbe 1966).

The SCATS method determines the DS parameter from cycle by cycle measurements. The *DS estimate* given here is an analytical construct as an average value that does not directly relate to the DS parameter measured by SCATS. The emphasis in the discussion presented here is the on *meaning* of the DS parameter rather than the measured DS parameter and its role on actual SCATS operations which is outside the scope of this report. The SCATS method also applies various adjustments to the basic DS parameter for use in its signal timing algorithms. These adjustments will be ignored in discussing the basic meaning of the DS parameter as a performance measure.

The definition of the SCATS DS parameter as the ratio of the effectively used green time to the total available green time (Lowrie 1982, 1990) can be expressed as:

$$DS = (g_{DS} - T_s + n_{vg} t_{sMF}) / g_{DS} \quad (13.7)$$

where

g_{DS} = effective green time for the purpose of estimating SCATS DS, which is the sum of the displayed green time and the terminating intergreen time ($G + I_t$):

T_s = total space time during the green period including both saturated and unsaturated intervals ($T_s = \text{sum}(t_{si})$ where t_{si} is the space time of the i th vehicle that departs during the green period,

n_{vg} = number of vehicles that depart during the green period calculated from *Equation (7.30)*, and

t_{sMF} = average space time at SCATS MF calculated from *Equation (13.4)*

The total space time, T_s , can be calculated using the average space times during queue clearance (t_{ssa}) and after queue clearance (t_{su}):

$$T_s = n_{vs} t_{ssa} + n_{vu} t_{su} \quad (13.8)$$

where n_{vs} and n_{vu} are the numbers of vehicles that depart during the saturated and unsaturated parts of the green period calculated from *Equations (7.28) and (7.29)*, and t_{ssa} and t_{su} are the average space times during the saturated and unsaturated parts of the green period calculated from:

$$t_{ssa} = h_{sa} - t_{osa} \quad \text{subject to } t_{ssa} \geq 0 \quad (13.9)$$

$$t_{osa} = 3.6 (L_v + L_p) / v_{sa} \quad \text{subject to } t_{osa} \leq h_{sa} \quad (13.10)$$

$$v_{sa} = \frac{v_n \left[(G_s - t_r) - \frac{1 - e^{-m_q(G_s - t_r)}}{m_q} \right]}{G_s - t_r} \quad (13.11)$$

$$t_{su} = h_u - t_{ou} \quad \text{subject to } t_{su} \geq 0 \quad (13.12)$$

$$t_{ou} = 3.6 (L_v + L_p) / v_u \quad \text{subject to } t_{ou} \leq h_u \quad (13.13)$$

$$h_{sa} = 3600 / q_{sa} \quad (13.14)$$

$$q_{sa} = n_{vs} / G_s \quad (13.15)$$

$$h_u = 3600 / q_u \quad (13.16)$$

where

t_{osa} and t_{ssa} are the average occupancy and space times during the saturated part of the green period,

t_{ou} and t_{su} are the average occupancy and space times during the unsaturated part of the green period,

$L_v + L_p$ is the sum of vehicle and detection zone lengths,

v_{sa} is the average speed during the saturated part of the green period,

G_s is the duration of the saturated part of the green period,

t_r is the start response time,

v_u is the average speed during the unsaturated part of the green period, which can be calculated from *Equation (10.12)*,

h_{sa} and h_u are the average departure headways during the saturated and unsaturated parts of the green period,

q_{sa} is the average flow rate during the saturated part of the green period determined using n_{vs} (total number of vehicle departures during the saturated part of the green period) from *Equation (7.28)*, or for simpler analysis, the saturation flow rate can be used for this purpose ($q_{sa} = s$),

q_u is the average departure flow rate during the unsaturated part of the green period determined as $q_u = q_a$ (the average arrival flow rate), or with platooned arrivals, q_u is the average arrival flow rate during the green period ($q_u = q_{ag}$).

Parameters in *Equations (13.8) to (13.16)* are calculated for the actual traffic mix. The maximum queue discharge speed for the actual traffic mix can be calculated from:

$$v_n = v_m [1 - (1 - f_{vHV}) p_{HV}] \quad (13.17)$$

where v_m is the maximum queue discharge speed for a traffic stream consisting of passenger car units only (km/h), f_{vHV} is a speed factor for heavy vehicles ($f_{vHV} \leq 1$ so that the heavy vehicle speed is less than the passenger car speed) and p_{HV} is the proportion of heavy vehicles in the traffic stream.

For the effect of heavy vehicles on queue discharge flow rates, see *Equations (12.7) to (12.9)* in *Section 12*.

For improved estimates of the average space time during the saturated part of the green time (t_{ssa}), and therefore the total space time (T_s) for use in calculating DS, it may be desirable to allow for zero space times due to low speeds at the start of the green period. For this purpose, the first 5 to 10 seconds of the displayed green period could be ignored. If this method is adopted, it should also be applied to the estimation of the average space time at SCATS Maximum Flow (t_{sMF}).

For comparison with the SCATS DS estimate, the traditional *degree of saturation* parameter (Akçelik 1981, TRB 1998, Webster and Cobbe 1966) is calculated from:

$$x = q_a / Q = q_a c / s g \quad (13.18)$$

where q_a is the demand (arrival) flow rate (veh/s), Q is the capacity from *Equation (7.36)*, g is the effective green time (s), c is the cycle time (s), and s is the saturation flow rate (veh/s) calculated from *Equation (12.1)*.

The percentage difference between the DS estimate from *Equation (13.7)* and the degree of saturation from *Equation (13.18)* can be calculated from:

$$\text{DIF}\% = 100 (\text{DS} / x) - 1 \quad (13.19)$$

It is emphasised that DS in *Equations (13.7) and (13.19)* is an estimate of the basic DS parameter, not the DS value measured by the real-life SCATS system.

Example for Comparison of SCATS DS and Traditional Degree of Saturation

An example is given in *Table 13.2* comparing the SCATS DS estimate with the traditional degree of saturation (x) using the queue discharge characteristics and signal timing data for the average through (isolated) site (data given in *Tables 9.6, 9.7 and 12.1 to 12.3*; also see *Table 15.1* in *Section 15*).

The traffic stream is assumed to consist of light vehicles only. The average vehicle length is $L_v = 4.4$ m, and the detection zone length is $L_p = 4.5$ m. Actuated signal control method is assumed (affects the calculation of the queue clearance time).

The arrival (demand) flow rate is varied to obtain low x , medium x , high x and oversaturated ($x > 1$) conditions. Arrival flow rates (q_a), flow ratios ($y = q_a / s$), and the saturated and unsaturated parts of the green period (g_s , g_u) calculated from *Equations (7.13), (7.14) and (7.23) to (7.25)* are given in *Table 13.2*.

The data for this example are as follows:

- Queue discharge parameters: $v_n = 45.1$ (km/h), $q_n = 2086$ (veh/h), $m_v = 0.118$, $m_q = 0.369$, $h_n = 1.725$ (s), $v_f = 69$ (km/h).
- Signal timings: $G = 56$, $G_{\max} = 72$ s, $c = 129$ s (*Table 12.1*). Intergreen, yellow and all-red times: $I_t = 6$ s, $t_y = 4$ s, $t_{ar} = 2.0$ s. Therefore $g_{DS} = 62$ s.
- Number of vehicles departing after the green period, $n_e = 1.5$ veh.
- Saturation flow, start loss and end gain times calculated using the ARR 123 method: $s = 2083$, $t_s = 2.6$, $t_e = 2.6$ s (see *Method (ii)* results in *Table 12.2*).

- Using the start loss and end gain values above, effective green time is $g = 56 - 2.6 + 2.6 = 56.0$ s, the effective maximum green time is $g_{\max} = 72 - 2.6 + 2.6 = 72.0$ s, effective red time is $r = 129 - 56 = 73$ s.
- The analytical parameters corresponding to SCATS MF and KP parameters calculated from *Equations (13.1) to (13.6)*: $s_{MF} = 1923$ pcu/h, $h_{MF} = 1.872$ s, $G_{\max} + t_{em} = 74.6$ s, $t_{oMF} = 0.80$ s, and $t_{sMF} = 1.07$ s. For this example, the uninterrupted travel speed, v_u is kept constant at $v_u = v_f = 69$ km/h. Therefore, the corresponding occupancy time is constant, $t_{ou} = 0.46$ s. The space time for uninterrupted flow varies with the varying demand flow rate (given in *Table 13.2*).
- The green time ratio is $u = g / c = 56 / 129 = 0.434$.
- Since isolated signals, $PF_2 = 1.0$.
- Since actuated signals, the factor in the queue clearance formula, $f_q = 1.08 - 0.1 \times (56 / 72)^2 = 1.02$.
- Capacity from *Equation (7.36)*: $Q = 2083 \times 56 / 129 = 904$ veh/h.

The results given in *Table 13.2* indicate that the correspondence between the SCATS DS estimate and the traditional degree of saturation is reasonably good. The difference decreases as the DS and x values increase towards the capacity value. Larger differences at low degrees of saturation are less important since the rate of change in traffic performance (delay, queue length, etc) is much less at low to medium degrees of saturation. Generally higher differences were found for the average right-turn site.

Table 13.2

SCATS DS estimate and traditional degree of saturation using queue discharge characteristics for the average through site with varying demand flow rates

Case	q_a	g_s	g_u	v_{sa}	q_{sa}	t_{ssa}	t_{su}	T_s	n_{vg}	DS	x	DIF%
Low x	542	26.2	29.8	32.3	1890	0.91	6.17	41.5	19.6	0.670	0.600	11.6 %
Medium x	678	36.0	20.0	35.3	1940	0.95	4.85	38.0	24.6	0.811	0.750	8.2 %
High x	813	47.7	8.3	37.6	1974	0.97	3.96	34.2	29.5	0.958	0.900	6.4 %
Oversat.	922	56.0	0	38.3	1985	0.98	3.44	31.7	32.4	1.049	1.020	2.9 %

14 DETECTION ZONE LENGTH AND GAP SETTING

14.1 Optimum Detection Zone Length

An optimum detection zone length (L_p) is sought in terms of the best ability to detect traffic variables relevant to adaptive control. For the purpose of this discussion, the effective detection zone length will be considered to be approximately the same as the detector loop length (see *Section 5* for a discussion on detection zone length).

Lowrie (1984) discussed the choice of loop length considering the relationships between vehicle speed, gap length and space time (v , L_s and t_s). AUSTROADS (1993) Guide to Traffic Signals discusses the relationship between density and space time as a function of the detection zone length (k , t_s , L_p) for selecting an appropriate loop length. The results presented here update the relationships given in AUSTROADS (1993) with current data.

For SCATS control, *vehicle counts* (n_{vg}) and *space time* (t_s) are used in deriving the SCATS DS (degree of saturation) parameter as discussed in *Section 13*. Space time also corresponds to the "gap setting" or "unit extension time setting" in traditional actuated signal control that uses presence detection (Akçelik 1995a). It will be shown that the corresponding distance-based parameter *gap (space) length* (L_s) is an important parameter in determining the optimum loop length.

As discussed in *Section 5*, space time is the duration of the time between the detection of two consecutive vehicles when the presence detection zone is not occupied. Gap length is the distance between two consecutive vehicles measured from the back end of the leading vehicle to the front end of the following vehicle.

Space time - speed relationships for detection zone lengths in the range $L_p = 0.5$ m to 6.0 m for average right-turn (isolated), through (isolated) and through (paired intersection) sites, as well as the corresponding gap length - speed and spacing - speed relationships are shown in *Figures 14.1 to 14.6*. Note that spacing equals gap length plus vehicle length ($L_h = L_s + L_v$).

Desired characteristics of the space time variable for determining optimum loop length can be explained in terms of space time - speed relationship:

- (i) non-zero space time values should be obtained at low speeds, and at the same time,
- (ii) a single speed value should be obtained for each given space time.

These can be observed from the space time - speed graphs (*Figures 14.1, 14.3 and 14.5*, and the figures in *Appendix C*).

Thus, the optimum length for a loop is one that is as short as possible but not so short as to result in a double valued space-time relationship. To determine the optimum loop length, a limiting (low) speed value (v_o) that gives zero space time ($t_s = 0$) can be chosen. The limiting speed must be as low as possible so that the range of speeds 0 to v_o is as small as possible. A detection zone length above the optimum value ($L_p > L_{po}$) increases this range. On the other hand, a detection zone length below the optimum value ($L_p < L_{po}$) may give two speed values for a given space time as seen from the space time - speed graphs.

The limiting speed (v_o) needs to be selected conservatively since, if v_o is too low, the loop length may be too short under adverse driving conditions (e.g. wet weather or darkness). This is because the gap lengths (L_s) may increase and speeds decrease under adverse conditions, resulting in a sharp increase in space time at low speeds (see *Equation 5.22* in *Section 5*), and therefore leading to a double valued speed – space time relationship. This is also supported by the possibility of higher space times considering the cycle by cycle variations in queue discharge characteristics as discussed in *Section 12*.

On the other hand, the condition when zero space time ($t_s = 0$) occurs is caused by the gap length being less than the effective detection zone length, or loop length being too long ($L_s < L_p$) as seen in *Figure 14.7*. As a result, the "bridging" effect occurs, i.e. the time when the front end of the following vehicle (B) enters the detection zone occurs before the time when the rear end of the leading vehicle (A) exits the detection zone ($t_{LB} < t_{TA}$). It is seen that this leads to overlapping of detector occupancy times for vehicles A and B (shown as t_{oAB}), and hence zero space time ($t_s = 0$). A shorter loop length is selected to minimise this condition, in contrast with the choice of a longer loop considering adverse conditions. Other advantages of a shorter loop length are lower cost and better sensitivity.

The space time - speed and gap length - speed relationships for *Figures 14.1 to 14.6*, and the figures in *Appendix C* were derived as follows.

From *Equations (5.22) and (5.23)*, the space time - speed relationship is:

$$t_s = h - t_o = \frac{3600}{q} - \frac{3.6(L_p + L_v)}{v} \quad (14.1)$$

where h is the headway (s), q is the flow rate (veh/h), v is the speed (km/h), L_p is the detection zone length (m) and L_v is the average vehicle length (m).

From *Equation (5.24)*, the gap length is:

$$L_s = L_h - L_v = \frac{1000v}{q} - L_v \quad (14.2)$$

where L_h is the spacing (m), q is the flow rate (veh/h), v is the speed (km/h), and L_v is the average vehicle length (m).

A two-piece speed-flow model is used similar to the models used in the recent freeway traffic flow study (Akçelik, Roper and Besley 1999b). The model is implemented in an Excel application. The flow rate is varied and the corresponding speed values are calculated using:

- (i) for speeds below the maximum queue discharge speed ($v \leq v_n$), the queue discharge speed - flow relationship given by *Equation (7.6a)* in *Section 7* (using parameters from calibration results), and
- (ii) for speeds above the maximum queue discharge speed ($v > v_n$), Akçelik's time-dependent speed - flow model for uninterrupted flow conditions (*Model 4* in *Section 10*).

Then, using the calculated speed values, the space time and gap length are determined from *Equations (14.1) and (14.2)*.

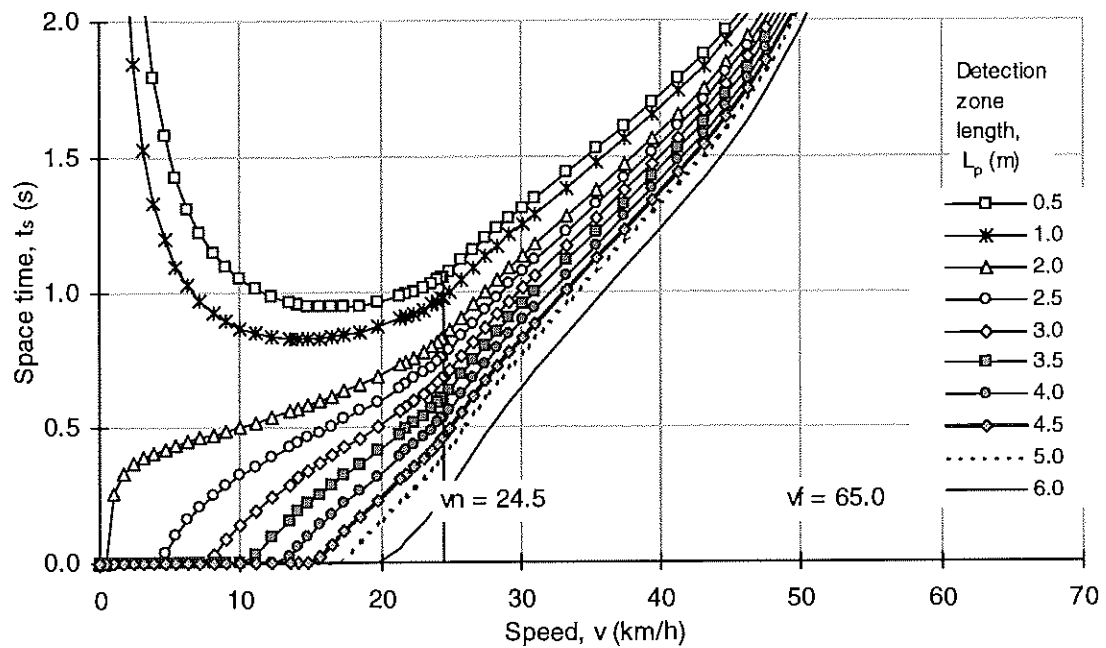


Figure 14.1 – Space time – speed relationships as a function of the detection zone length for an average right-turn (isolated) site

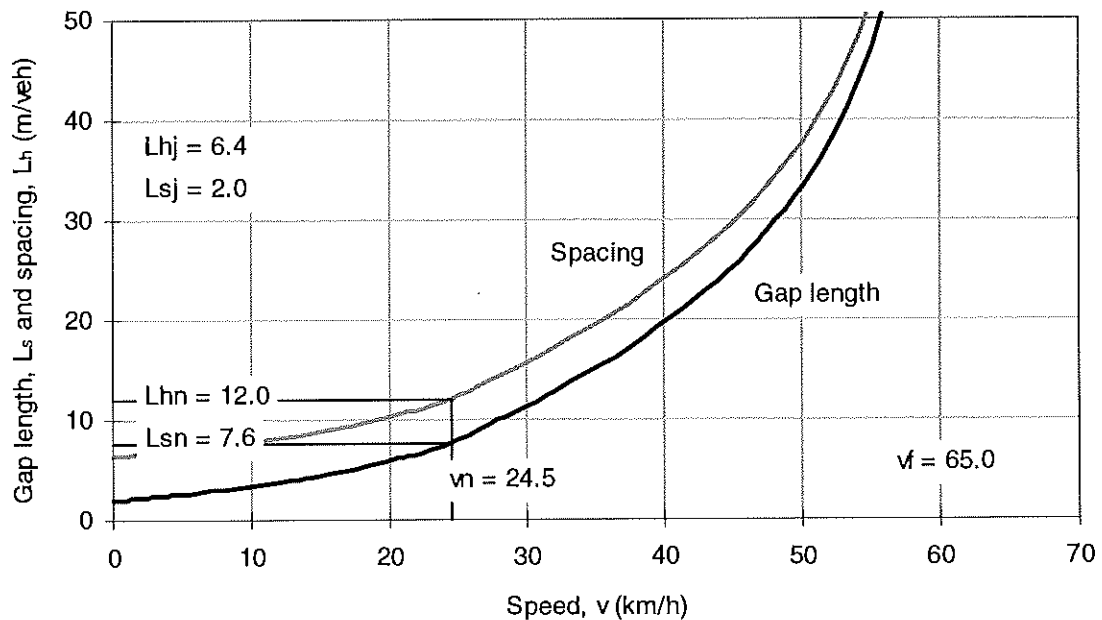


Figure 14.2 – Gap length – speed and spacing – speed relationships for an average right-turn (isolated) site

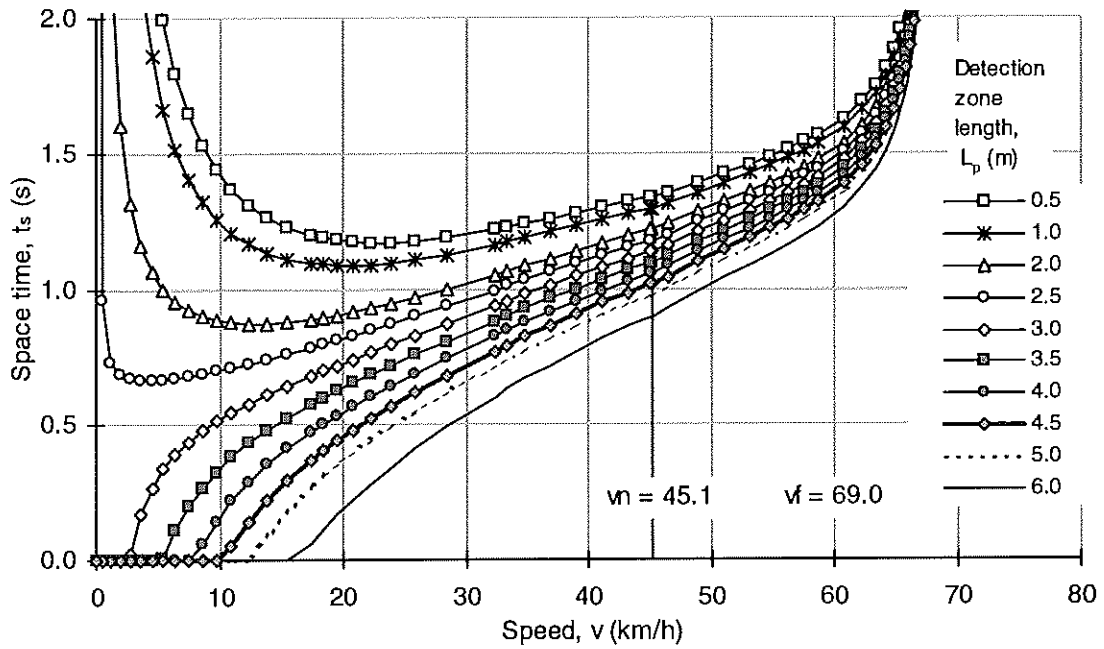


Figure 14.3 – Space time – speed relationships as a function of the detection zone length for an average through (isolated) site

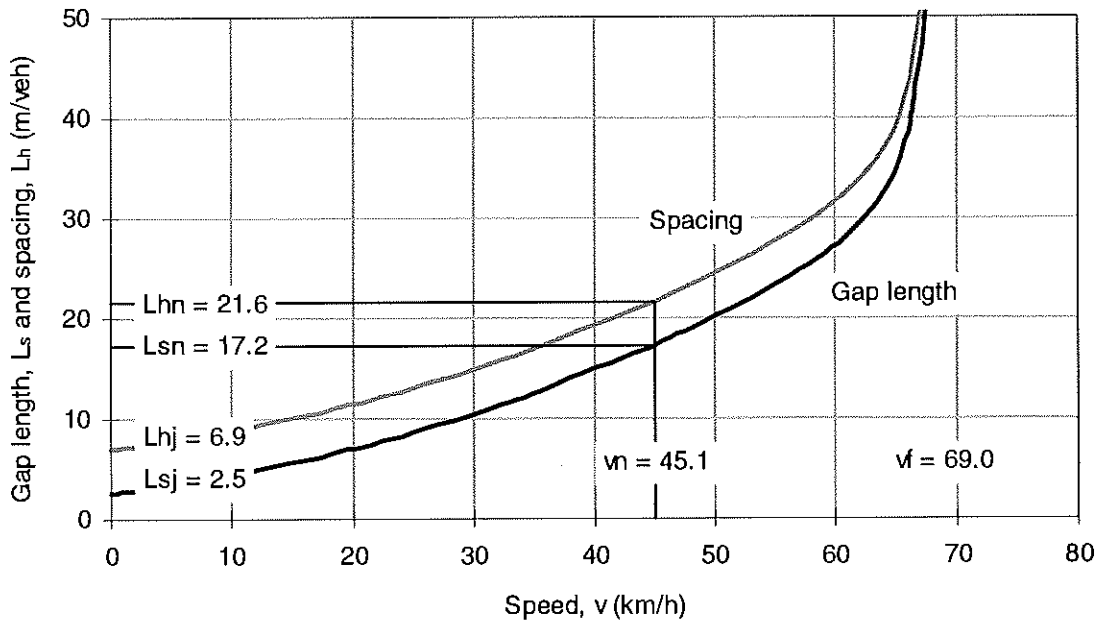


Figure 14.4 – Gap length – speed and spacing – speed relationships for an average through (isolated) site

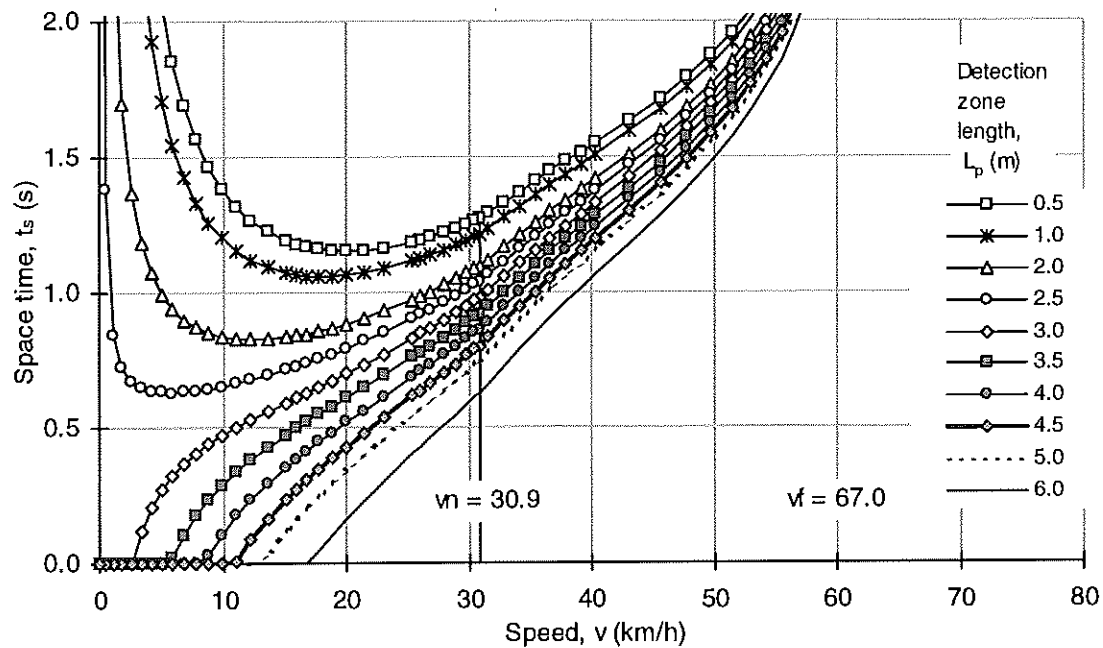


Figure 14.5 – Space time – speed relationships as a function of the detection zone length for an average through (paired intersection) site

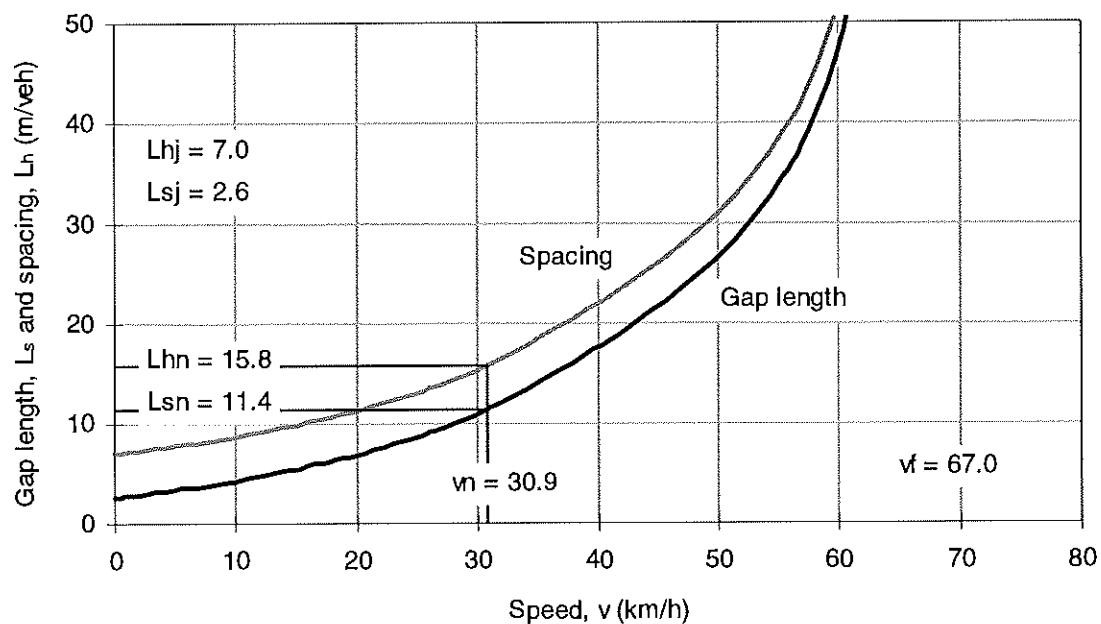


Figure 14.6 – Gap length – speed and spacing – speed relationships for an average through (paired intersection) site

For the analysis of optimum detection zone length, the queue discharge model is the relevant one, and the speed - flow model for uninterrupted conditions does not have any effect on the optimal value.

For the space time - speed and gap length - speed graphs given in this section and *Appendix C*, an average vehicle length of $L_v = 4.4$ m was used. This was found in a recent freeway study (Akçelik, Roper and Besley 1998b). Examples of actual cars with a length close to this average value (in the range 4.2 to 4.5 m) are Ford Laser, Holden Nova, Hyundai Lantra, Mazda 323, Mercedes-Benz C240, Nissan Coupe, Subaru Impreza, Toyota Corolla and Volvo V40, also Jeep Cherokee. In the time-dependent speed-flow model, an analysis period of $T_f = 1$ h was used.

For optimum detection zone length for a chosen limiting speed (L_{p0}) at $t_s = 0$, it is seen from *Equation (3.1.4)* that vehicle spacing must satisfy the condition $L_h = L_{p0} + L_v$. This means that the optimum loop length must satisfy $L_{p0} = L_h - L_v$. Since $L_h - L_v = L_s$ is the gap length, the optimum loop length (L_{p0}) at the limiting speed (v_0) equals the gap length at that speed (L_{sv_0}):

$$L_{p0} = L_{sv_0} \quad (14.3)$$

As an absolute limit from an analytical perspective, an optimum loop length for zero speed (jam) conditions (L_{p0} at $v_0 = 0$) is considered. Under these conditions, the minimum value of gap length, i.e. the *jam gap length*, $L_{s0} = L_{sj}$ is relevant:

$$L_{p0} = L_{sj} = L_{hj} - L_v \quad (14.4)$$

where L_{hj} is the jam spacing and L_v is the average vehicle length.

Jam spacing for survey sites (cars only) are in the range $L_{hj} = 5.9$ to 7.3 m. Using an average car length of $L_v = 4.4$ m, this means that $L_{p0} = 1.5$ to 2.9 m is found as an absolute limit for the optimum loop length.

This shows the importance of the use of correct value of jam spacing (L_{hj}) for the purpose of optimum detection zone length. The model calibration procedure based on the use of measured jam spacing values rather than the values predicted from regression is used for this reason (see *Section 8*).

Jam gap length may increase under adverse driving conditions. Therefore, the limiting speed for determining the optimum detection zone length should not be too low as this would result in a double valued speed - space time relationship. In view of this, two speed values ($v_0 = 5$ km/h and 10 km/h) are chosen for the analysis presented here. Optimum loop lengths based on these speeds are given by:

$$L_{p5} = L_{s5} = L_{h5} - L_v \quad (14.5)$$

$$L_{p10} = L_{s10} = L_{h10} - L_v \quad (14.6)$$

where L_v is the average vehicle length, L_{p5} and L_{p10} are the optimum loop lengths, L_{s5} and L_{s10} are the gap lengths, and L_{h5} and L_{h10} are the spacings at the chosen speeds of 5 and 10 km/h.

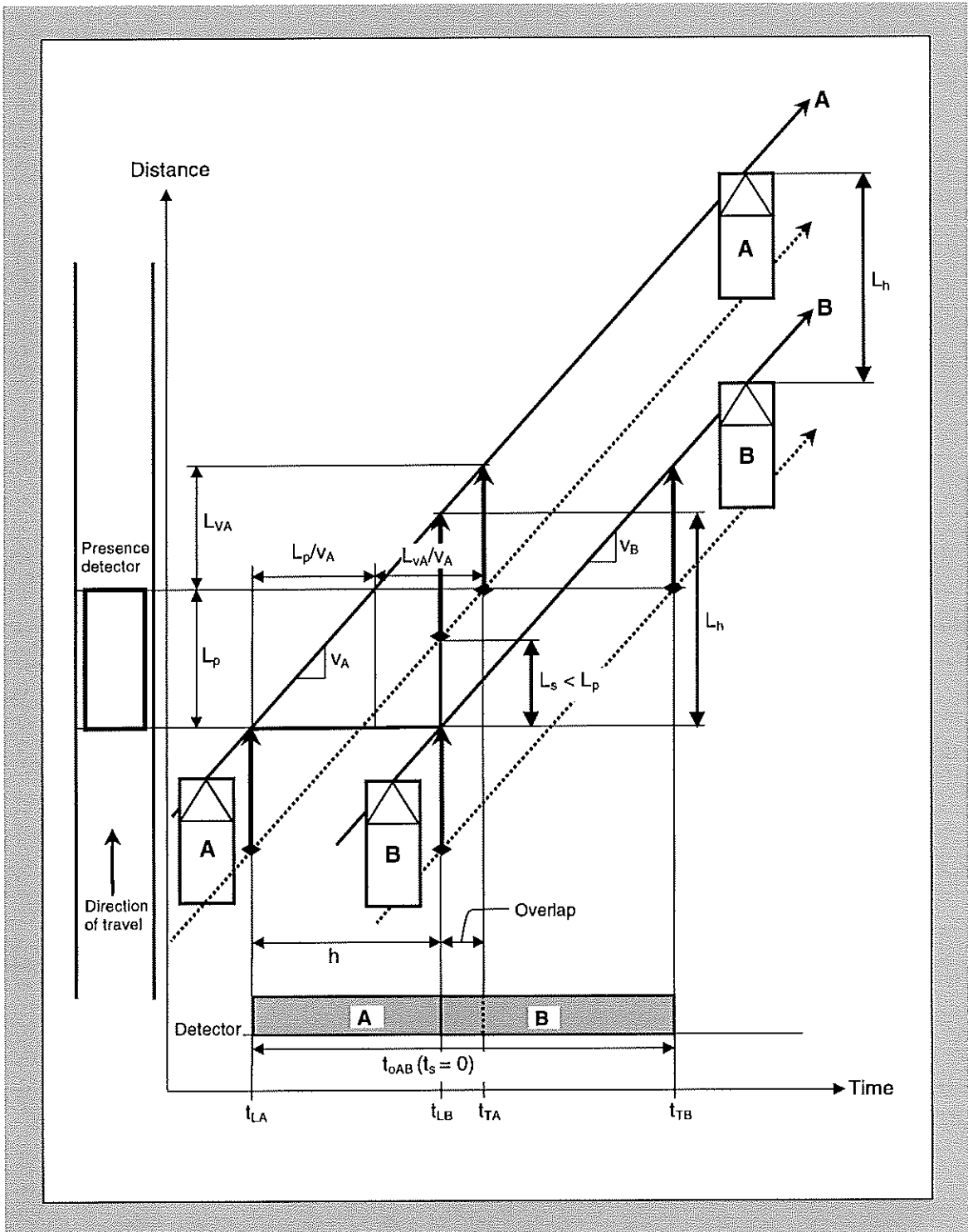


Figure 14.7 – Time-distance diagram explaining the case of zero space time with presence detection (constant speeds)

Table 14.1 summarises various queue discharge model parameters for individual sites and for various “average sites”. The parameters in Table 14.1 are: maximum queue discharge speed (v_n), maximum queue discharge flow rate (q_n), minimum queue discharge headway (h_n), space time at maximum flow (t_{sn}), spacing at maximum flow (L_{hn}), queue discharge speed-flow model parameter (m_v/m_q), measured jam spacing (L_{hj}), and the predicted spacings at $v_o = 5$ and 10 km/h (L_{s5} and L_{s10}). Spacings (L_{h5} , L_{h10}) were calculated from Equation (5.24) using the model parameters for each site.

Table 14.2 gives the optimum detection zone lengths for chosen limiting speed values of $v_o = 0, 5$ and 10 km/h (L_{p0} , L_{p5} and L_{p10}) for individual survey sites as well as average right turn and through traffic sites. These are calculated from Equations (14.4) to (14.6) using $L_v = 4.4$ m.

Results for three sites (610, 335 and 511) obtained using queue discharge model parameters from alternative calibration methods are given in Table 14.3. Alternative methods for queue discharge model calibration are described in Section 8.

Figures 14.8 to 14.11 show the relationships between the optimum detection zone length based on the chosen limiting speed of $v_o = 10$ km/h (L_{p10}) and queue discharge model parameters v_n , q_n , L_{hn} and m_v/m_q . Similar results are obtained for the limiting speed of $v_o = 5$ km/h (L_{p5}).

Figures 14.12 and 14.13 show the relationships between the optimum detection zone lengths (L_{p5} and L_{p10}) and the jam gap length, L_{sj} . Figures 14.14 and 14.15 show the relationships between the optimum detection zone lengths (L_{p5} and L_{p10}) and the jam spacing, L_{hj} . Figures 14.12 to 14.15 include exponential trendlines indicating strong relationships between the optimum detection zone lengths (L_{p5} and L_{p10}) and the jam gap length (L_{sj}) and jam spacing (L_{hj}) parameters.

The following conclusions are drawn from the results given in Tables 14.2 and 14.3 and Figures 14.8 to 14.15.

- (i) The **optimum detection zone length** appears to be independent of the maximum queue discharge speed (v_n), the maximum flow rate (q_n) and the spacing at maximum flow (L_{hn}). There seems to be a linear decreasing relationship between the optimum loop length and the speed-flow model parameter m_v/m_q . The maximum queue discharge speed and the spacing at maximum flow may have some affect on the optimum loop length for right-turn lanes, but it is not possible to establish this due to the small number of right-turn sites surveyed.
- (ii) The optimum detection zone length is clearly related to **jam gap length** ($L_{sj} = L_{hj} - L_v$) as expected from the relationships discussed above. The following exponential regression models (see Figures 14.12 and 14.13) can be used to determine the optimum loop length when more detailed analysis is not possible:

$$L_{p5} = 1.3 e^{0.39 L_{sj}} \quad (14.7)$$

$$L_{p10} = 1.9 e^{0.33 L_{sj}} \quad (14.8)$$

Table 14.1

Queue discharge model parameters including measured jam spacings and the predicted vehicle spacings at the queue discharge speeds of 5 and 10 km/h

Site	v_n (km/h)	q_n (veh/h)	h_n (s)	$t_{sn} \dagger$ (s)	L_{hn} (m)	m_v/m_q	L_{hj} (m)	L_{h5} (m)	L_{h10} (m)
Average values									
Right-turn (isolated) sites	24.5	2036	1.77	0.46	12.0	0.527	6.4	7.0	7.8
Through (isolated) sites	45.1	2117	1.70	0.99	21.3	0.334	6.9	7.8	8.8
Through (paired Int.) sites	30.9	1966	1.83	0.79	15.7	0.449	7.0	7.8	8.7
All Through sites	42.1	2085	1.73	0.97	20.2	0.368	7.0	7.8	8.8
Right-turn (isolated) sites									
TCS163	24.7	2098	1.72	0.42	11.8	0.510	6.0	6.7	7.5
TCS610	21.7	1966	1.83	0.35	11.0	0.534	5.9	6.6	7.4
TCS121	24.4	1948	1.85	0.53	12.5	0.527	6.6	7.3	8.1
TCS335	27.1	2133	1.69	0.51	12.7	0.543	6.9	7.5	8.2
Through (isolated) sites									
TCS1081	39.5	1790	2.01	1.20	22.1	0.308	6.8	7.9	9.1
TCS413	33.2	1801	2.00	1.03	18.4	0.369	6.8	7.8	8.9
TCS511	52.8	2283	1.58	0.97	23.1	0.286	6.6	7.4	8.4
TCS3196	31.7	1892	1.90	0.89	16.8	0.418	7.0	7.8	8.9
TCS4273	36.4	1938	1.86	0.98	18.8	0.389	7.3	8.2	9.2
TCS849	46.4	1999	1.80	1.11	23.2	0.297	6.9	7.9	9.0
TCS456	53.8	2422	1.49	0.89	22.2	0.316	7.0 *	7.8	8.6
Mel1	56.1	2558	1.41	0.84	21.9	0.319	7.0 *	7.7	8.5
Mel3	46.2	2423	1.49	0.79	19.1	0.367	7.0 *	7.7	8.5
Mel4	47.9	2217	1.62	0.95	21.6	0.324	7.0 *	7.8	8.8
Mel7	52.4	1968	1.83	1.22	26.6	0.263	7.0	8.0	9.2
Through (paired intersection) sites									
Mel2	30.9	1982	1.82	0.78	0.449	0.449	7.0 *	7.8	8.7
Mel5	27.1	1804	2.00	0.81	0.466	0.466	7.0 *	7.8	8.8
Mel6	34.6	2112	1.70	0.78	0.427	0.427	7.0 *	7.7	8.6

* Nominal values (jam spacing was not measured during these early surveys except at Mel7 site).

† t_{sn} is for a detection zone length of $L_p = 4.5$ m.

Table 14.2

Optimum detection zone length (loop length) values based on the chosen speeds of 0, 5 and 10 km/h

Site	Site description	City	L _{po} based on v _o = 0 km/h	L _{p5} based on v _o = 5 km/h	L _{p10} based on v _o = 10 km/h
	Average values				
	Right-turn (isolated) sites		2.0	2.6	3.4
	Through (isolated) sites		2.5	3.4	4.4
	Through (paired intersection) sites		2.6	3.4	4.3
	All Through sites		2.6	3.4	4.4
	Right-turn (isolated) sites				
TCS163	Pacific Hwy and Mowbray Rd in Chatswood.	Sydney	1.6	2.3	3.1
TCS610	Military Rd and Murdoch St in Cremorne.	Sydney	1.5	2.2	3.0
TCS121	Maroondah Hwy and Mitcham Rd in Mitcham.	Melbourne	2.2	2.9	3.7
TCS335	Doncaster Rd and Blackburn Rd in East Doncaster.	Melbourne	2.5	3.1	3.8
	Through (isolated) sites				
TCS1081	Lilyfield Rd and James St in Lilyfield. 9% uphill grade.	Sydney	2.4	3.5	4.7
TCS413	Broadway and City Rd. in Broadway.	Sydney	2.4	3.4	4.5
TCS511	General Holmes Dve and Bestic St in Kyeemagh.	Sydney	2.2	3.0	4.0
TCS3196	Middleborough Rd and Highbury Rd in East Burwood. Shared through plus left-turn lane.	Melbourne	2.6	3.4	4.5
TCS4273	Toorak Rd and Tooronga Rd in Hawthorn East. 6% uphill grade.	Melbourne	2.9	3.8	4.8
TCS849	Canterbury Rd and Mitcham Rd in Vermont.	Melbourne	2.5	3.5	4.6
TCS456	Ferntree Gully Rd and Stud Rd in Scoresby.	Melbourne	2.6	3.4	4.2
Mel1	Ferntree Gully Rd and Stud Rd in Scoresby.	Melbourne	2.6	3.3	4.1
Mel3	South Eastern Arterial and Burke Rd in Glen Iris.	Melbourne	2.6	3.3	4.1
Mel4	Canterbury Rd and Middleborough Rd in Box Hill.	Melbourne	2.6	3.4	4.4
Mel7	Ferntree Gully Rd and Scoresby Rd in Knoxfield.	Melbourne	2.6	3.6	4.8
	Through (paired intersection) sites				
Mel2	Kooyong Rd and Dandenong Rd in Armadale.	Melbourne	2.6	3.4	4.3
Mel5	Pedestrian Crossing on Canterbury Rd in East Camberwell.	Melbourne	2.6	3.4	4.4
Mel6	Boronia Rd and Wantirna Rd in Wantirna.	Melbourne	2.6	3.3	4.2

$$L_{po(0)} = L_{sj} = L_{hj} - L_v$$

$$L_{po(5)} = L_{s(5)} = L_{h(5)} - L_v$$

$$L_{po(10)} = L_{s(10)} = L_{h(10)} - L_v$$

As discussed at the start of this section, the jam gap length may increase under adverse traffic conditions (e.g. rain). *Equations (14.7) and (14.8)* indicate that the optimum loop length should be increased with this in mind. For example, if the jam gap length is increased from 2.5 m to 3.0 m, L_{p5} increases from 3.4 m to 4.2 m.

Ideally jam gap length should be measured in real-life situations. However it is easier to measure the jam spacing as in the surveys reported under this project. In this case, the jam gap length can be calculated from $L_{sj} = L_{hj} - L_v$ assuming an average vehicle length. It is important that the average vehicle length used to calculate the jam gap length represents the population of vehicles in the survey. Using cars (or *light vehicles*) only helps to determine the jam gap length (gap length between vehicles in queue during the red signal). This is useful since the jam gap length (L_{sj}) and the gap length values at low speeds (L_{s5} , L_{s10}) are fairly independent of the vehicle size.

Heavy vehicles increase vehicle spacings due to longer vehicle length but the gap lengths are not increased as dramatically. Although it is possible that heavy vehicles have some impact on the jam gap length and gap length values at low speeds (L_{sj} , L_{s5} , L_{s10}), the overall impact on these parameters, therefore on the optimum loop length, would be minimal with low heavy vehicle percentages. If the overall jam gap length increases significantly due to a large percentage of heavy vehicles in the traffic stream, then the optimum loop length could be increased proportionately. However, further research is recommended on the effect of heavy vehicles on jam gap length.

- (iii) It appears that it is possible to reduce the current loop length of 4.5 m used with the SCATS system to about 3.5 m for *through traffic lanes* and 3.0 m *right-turn lanes* under green arrow control. This is based on a chosen limiting speed of 5 km/h. On this basis, the range of optimum loop length for through traffic lanes is 3.0 to 3.8 m, with an average value of 3.4 m, considering all through traffic sites. There was no obvious difference between through sites in Sydney and Melbourne although the number of sites in Sydney is too small to arrive at a firm conclusion regarding this.

Considering all right-turn traffic sites, the range of optimum loop length is 2.2 to 3.1 m, with an average value of 2.6 m. The optimum loop length is shorter for the two right-turn sites in Sydney (2.2 and 2.3 m) and larger for the two right-turn sites in Melbourne (2.9 and 3.1 m). This is in line with the corresponding jam spacing values observed at the two Sydney sites (5.9 and 6.0 m) and at the two Melbourne sites (6.6 and 6.9 m).

Further data from a larger number of sites would be useful to arrive at a more conclusive result about the appropriate level of safety margin in determining the optimum loop length.

- (iv) From *Table 14.3*, it is seen that optimum loop length values obtained using queue discharge speed and flow models based on *alternative calibration methods* (*Section 8*) are essentially the same. This is valid for the calibration methods that use the standard calibration procedure that employs the measured jam spacing value. The methods that estimate the jam spacing using parameters from headway model regression (calibration methods 5, 7, 10, 12, 14 in *Sections 8 and 9*) are not appropriate since they overestimate the jam spacing significantly.

Table 14.3

Optimum detection zone length (loop length) values based on the chosen speeds of 0, 5 and 10 km/h using alternative calibration methods for three sites

Site description and calibration method	L_{p0} based on $v_0 = 0$ km/h	L_{p5} based on $v_0 = 5$ km/h	L_{p10} based on $v_0 = 10$ km/h
Right-turn (isolated) site TCS610: Military Rd and Murdoch St in Cremorne, Sydney			
Calibration Method 1 (main results)	1.5	2.2	3.0
Alternative Calibration Method 9: $v_L, h_{2L}, t_0 = 0$	1.5	2.2	3.2
Alternative Calibration Method 13: $v_L, h_{2L}, t_0 = 1.0$	1.5	2.2	3.1
Right-turn (isolated) site TCS335: Doncaster Rd and Blackburn Rd in East Doncaster, Melbourne			
Calibration Method 1 (main results)	2.5	3.1	3.8
Alternative Calibration Method 9: $v_L, h_{2L}, t_0 = 0$	2.5	3.1	3.8
Alternative Calibration Method 13: $v_L, h_{2L}, t_0 = 1.0$	2.5	3.1	3.8
Through (isolated) site: TCS511 General Holmes Dve and Bestic St in Kyeemagh, Sydney			
Calibration Method 1 (main results)	2.2	3.0	4.0
Alternative Calibration Method 9: $v_L, h_{2L}, t_0 = 0$	2.2	3.1	4.1
Alternative Calibration Method 13: $v_L, h_{2L}, t_0 = 1.0$	2.2	3.1	4.1

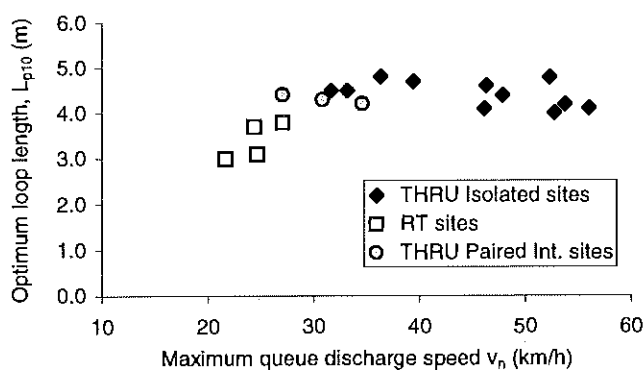


Figure 14.8 – Optimum loop length based on the chosen limiting speed value of 10 km/h, L_{p10} as a function of maximum queue discharge speed, v_n

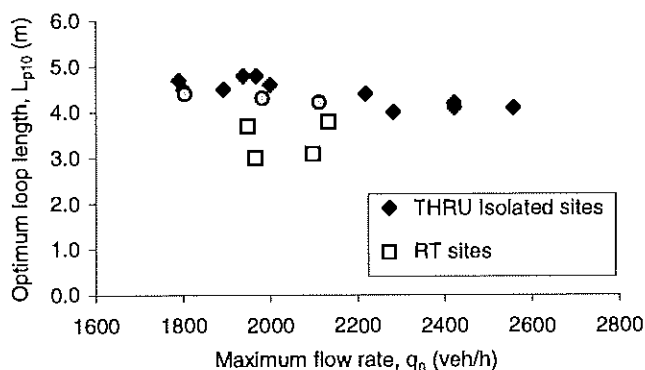


Figure 14.9 – Optimum loop length based on the chosen limiting speed value of 10 km/h, L_{p10} as a function of maximum queue discharge flow rate, q_n

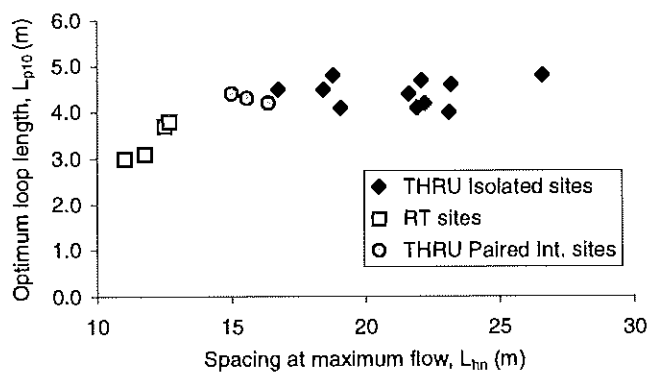


Figure 14.10 – Optimum loop length based on the chosen limiting speed value of 10 km/h, L_{p10} as a function of spacing at maximum queue discharge flow, L_{fn}

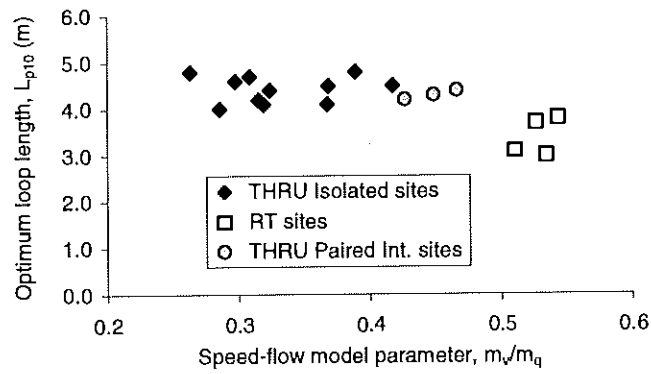


Figure 14.11 – Optimum loop length based on the chosen limiting speed value of 10 km/h, L_{p10} as a function of speed-flow model parameter, m_v/m_q

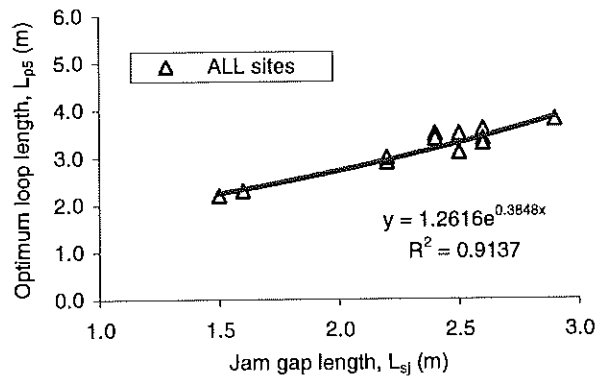


Figure 14.12 – Optimum loop length based on the chosen limiting speed value of 5 km/h, L_{p5} as a function of jam gap length, L_{sj}

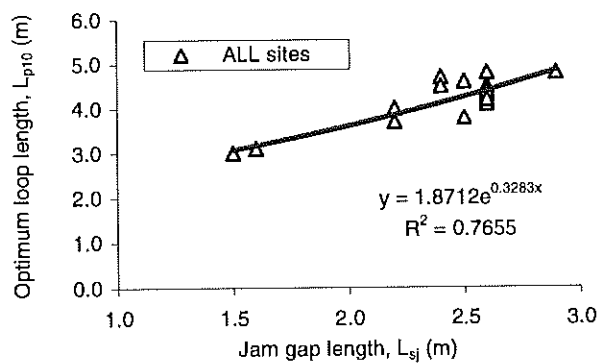


Figure 14.13 – Optimum loop length based on the chosen limiting speed value of 10 km/h, L_{p10} as a function of jam gap length, L_{sj}

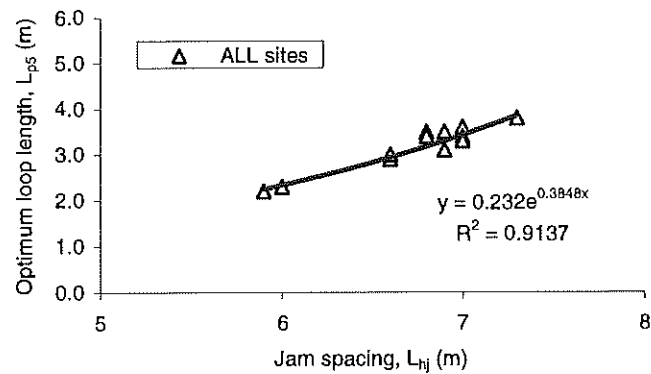


Figure 14.14 – Optimum loop length based on the chosen limiting speed value of 5 km/h, L_{p5} as a function of jam spacing, L_{hj}

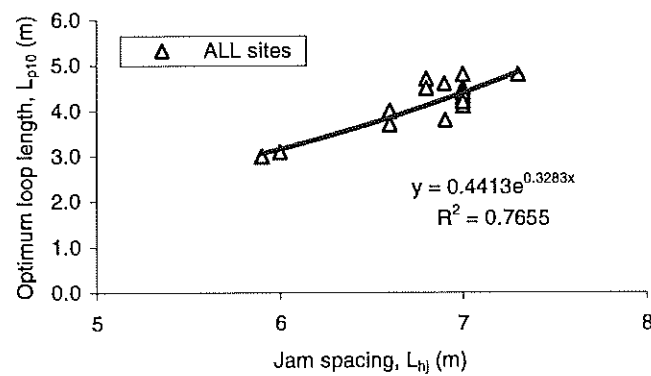


Figure 14.15 – Optimum loop length based on the chosen limiting speed value of 10 km/h, L_{p10} as a function of jam spacing, L_{hj}

14.2 Gap Setting

Information about the space time – speed – detection zone length relationships can be used to develop guidance for appropriate *gap setting* (unit extension time setting) values for traditional vehicle-actuated control as well as SCATS control. A survey of Australian vehicle-actuated control practice showed that gap settings (e_s) used in practice were in the range 2.5 to 4.0 s for through traffic and 2.0 to 4.0 s for right-turn traffic (Akçelik 1995a). These settings were associated with a loop length of 4.0 or 4.5 m used generally except in Queensland where loop lengths of 1.8 – 3.0 m (gap setting in the range 3.0 – 4.0 s) were used.

For efficient control with small cycle times, the gap setting should be as small as possible while ensuring that gap change (green period termination due to measured space time exceeding the gap setting) does not occur during the saturated part of the green period. Therefore, the gap setting can be related to the space time at maximum queue discharge (saturation) flow, t_{sn} . The results of surveys in Sydney and Melbourne summarised in *Table 14.1* show that space times at maximum queue discharge flow (t_{sn}) are much lower than the gap settings used in practice (calculated for a detection zone length of 4.5 m). Values of t_{sn} are in the range 0.78 to 1.22 s for through sites (average 1.0 s), and in the range 0.35 to 0.53 s for right-turn sites (average 0.5 s). This is consistent with the low minimum queue discharge headways (h_n) and high saturation flow rates (q_n) for both right-turn and through traffic lanes.

However, considering the cycle-by-cycle variation of queue discharge parameters at a given site, a factor should be applied to the t_{sn} value to determine an appropriate gap setting value. For example:

$$e_s = f_e t_{sn} \quad (14.9)$$

where e_s is the gap setting as a space time value (s), and t_{sn} is the space time at maximum queue discharge flow (s), and f_e is the variational factor.

Results given in *Table 12.4* in *Section 12* show that the 98th percentile space time at maximum flow (t_{sn}) can be as high as twice the average value as observed at the right-turn site 335, and as low as 13 per cent higher than the average value as observed at the through traffic site 511. An appropriate value of f_e chosen conservatively could be in the range 1.5 to 2.0.

Table 14.4 gives t_{sn} values for detection zone lengths of 2.0 m, 3.0 m, 4.0 m, 4.5 m and 6.0 m, and the corresponding gap setting values based on *Equation (14.9)* using a conservative factor value of $f_e = 2.0$. The results are given for individual survey sites as well as average right-turn and through traffic sites. For through traffic sites, $e_s = 1.6$ to 2.4 s (average 2.0 s), and for right-turn sites, $e_s = 0.8$ to 1.1 s (average 0.9 s) are obtained with a loop length of 4.5 m. The results indicate that shorter gap settings could be used compared with the current practice, especially for fully controlled right-turn phases.

Table 14.4

Space time (t_{sn}) at maximum queue discharge flow for selected detection zone length values (L_p), and the corresponding gap settings (e_s)

	Space time, t_{sn} (s) for detection zone length, L_p (m)					Gap setting, e_s (s) for detection zone length, L_p (m)				
	$L_p =$	2.0	3.0	4.0	4.5	6.0	2.0	3.0	4.0	4.5
Average values										
Right-turn (isolated) sites	0.83	0.68	0.53	0.46	0.24	1.66	1.36	1.07	0.92	0.48
Through (isolated) sites	1.21	1.14	1.06	1.02	0.90	2.43	2.27	2.11	2.03	1.79
Through (paired Int.) sites	1.09	0.98	0.86	0.80	0.63	2.18	1.95	1.72	1.60	1.25
All Through sites	1.20	1.12	1.03	0.99	0.86	2.40	2.23	2.06	1.98	1.72
Right-turn (isolated) sites										
TCS163	0.78	0.64	0.49	0.42	0.20	1.57	1.27	0.98	0.84	0.40
TCS610	0.77	0.60	0.44	0.35	0.11	1.54	1.21	0.87	0.71	0.21
TCS121	0.90	0.76	0.61	0.53	0.31	1.81	1.51	1.22	1.07	0.63
TCS335	0.84	0.70	0.57	0.50	0.31	1.67	1.41	1.14	1.01	0.61
Through (isolated) sites										
TCS1081	1.43	1.34	1.25	1.20	1.06	2.86	2.67	2.49	2.40	2.13
TCS413	1.31	1.20	1.09	1.03	0.87	2.61	2.39	2.18	2.07	1.74
TCS511	1.14	1.07	1.00	0.97	0.87	2.28	2.14	2.01	1.94	1.74
TCS3196	1.18	1.06	0.95	0.89	0.72	2.35	2.13	1.90	1.78	1.44
TCS4273	1.22	1.13	1.03	0.98	0.83	2.45	2.25	2.05	1.95	1.66
TCS849	1.30	1.23	1.15	1.11	0.99	2.61	2.45	2.30	2.22	1.99
TCS456	1.06	0.99	0.92	0.89	0.79	2.12	1.98	1.85	1.78	1.58
Mel1	1.00	0.93	0.87	0.84	0.74	1.99	1.86	1.74	1.67	1.48
Mel3	0.99	0.91	0.83	0.79	0.67	1.97	1.82	1.66	1.58	1.35
Mel4	1.14	1.07	0.99	0.96	0.84	2.29	2.14	1.99	1.91	1.68
Mel7	1.39	1.32	1.25	1.22	1.12	2.78	2.64	2.51	2.44	2.23
Through (paired intersection) sites										
Mel2	1.07	0.95	0.84	0.78	0.60	2.14	1.91	1.67	1.56	1.21
Mel5	1.14	1.01	0.88	0.81	0.61	2.29	2.02	1.76	1.63	1.23
Mel6	1.04	0.94	0.83	0.78	0.62	2.08	1.87	1.66	1.56	1.25

Space times (t_{sn}) are based on average vehicle length of $L_v = 4.4$ m

Gap settings are calculated from $e_s = 2.0 t_{sn}$

These results are based on parameters obtained for traffic in a single lane assuming separate detection of traffic in each lane. For a traffic stream consisting of several lanes, the analysis should be applied to the critical lane for the movement. If vehicles in several lanes are detected together, the space times will be shorter due to the overlapping of vehicle entry and exit times in and out of the detection zone that covers a number of lanes. Therefore, the suggestion of using shorter gap settings for efficient operation is still valid in this case.

On the other hand, there are other reasons for using longer gap settings in practice. For example, a larger gap setting may be preferred for minor actuated movements at an intersection controlled by coordinated actuated signals. This would help to avoid undue gapping out of minor signal phases in order to preserve signal offsets that achieve best traffic progression.

15 FUNDAMENTAL RELATIONSHIPS AT THE SIGNAL STOP LINE – AN EXAMPLE

In this section, the following figures are given for an example case:

- (i) the predicted flow rate, headway, speed, vehicle spacing and gap length, detector occupancy time and space time values as a function of the time since the start of the green period (*Figures 15.1 to 15.6*), and
- (ii) the relationships between traffic flow variables flow rate, headway, speed, vehicle spacing and gap length, detector occupancy time and space time, density, and time and space occupancy ratios (*Figures 15.7 to 15.20*).

All figures use the exponential queue discharge model parameters for the average through (isolated). The parameters are summarised in *Table 15.1* (from *Tables 9.6 and 9.7* given in *Section 9*).

For the uninterrupted travel conditions, Model 4 described in *Section 10* is used with parameters $T_f = 0.50$ h and $m_c = 4.2$.

Traffic stream is assumed to consist of cars only ($L_v = 4.4$ m /veh). Detection zone length is $L_p = 4.5$ m.

Table 15.1

Queue discharge model parameters used for the examples given in this section (data for the average through isolated site described in Section 9)

v_n (km/h)	q_n (veh/h)	m_v	m_q	m_v/m_q	h_n (s)	v_l (km/h)	v_r/v_l	O_{ln}	
45.1	2086	0.118	0.369	0.321	1.725	69	0.65	41.2 %	
t_{gn}^* (s)	t_{sn}^* (s)	L_{hn} (m)	L_{hj} (m)	L_{sj}^* (m)	k_n (veh/km)	k_j (veh/km)	k_r/k_j	O_{sn}	O_{sj}
1.35	0.99	21.3	6.9	2.5	47	150	0.324	20.4 %	63.4 %

* For t_{gn} , t_{sn} , and L_{sj} : Detection zone length is $L_p = 4.5$ m, and average vehicle length is $L_v = 4.4$ m

For the figures in group (i), the saturated and unsaturated parts of the green period were determined assuming the following values of signal timing and traffic parameters. Actuated signal control method is assumed.

- Signal timings observed for the average through isolated site: $G = 56$, $G_{\max} = 72$ s, $c = 129$ s (*Table 12.1*).
- Intergreen, yellow and all-red times: $I_t = 6$ s, $t_y = 4$ s, $t_{ar} = 2.0$ s.
- Number of vehicles departing after the green period, $n_e = 1.5$ veh.
- Saturation flow, start loss and end gain times calculated using the ARR 123 method: $s = 2083$, $t_s = 2.6$, $t_e = 2.6$ s (see *Method (ii)* results in *Table 12.2*).
- Using the start loss and end gain values above, effective green time is $g = 56 - 2.6 + 2.6 = 56.0$ s, the effective maximum green time is $g_{\max} = 72 - 2.6 + 2.6 = 72.0$ s, effective red time is $r = 129 - 56 = 73$ s.
- The green time ratio is $u = g / c = 56 / 129 = 0.434$.
- Arrival flow rate is $q_a = 720$ veh/h
- The flow ratio is $y = 720 / 2083 = 0.3456$
- Since isolated signals, $PF_2 = 1.0$.
- Since actuated signals, the factor in the queue clearance formula, $f_q = 1.08 - 0.1 \times (56 / 72)^2 = 1.02$.
- The saturated part of green period from *Equation (7.23)* is $g_s = 1.02 \times 0.3456 \times 73 / (1 - 0.3456) = 39.3$ s, and the unsaturated part of the green period is $g_u = 56.0 - 39.3 = 16.7$ s. From *Equations (7.13) and (7.14)*, $G_s = 39.3 + 2.6 = 41.9$ s, $G_u = 16.7 - 2.6 = 14.1$ s.
- Capacity from *Equation (7.36)*: $Q = 2083 \times 56 / 129 = 904$ veh/h.
- Degree of saturation: $x = q_a / Q = 720 / 904 = 0.796$.

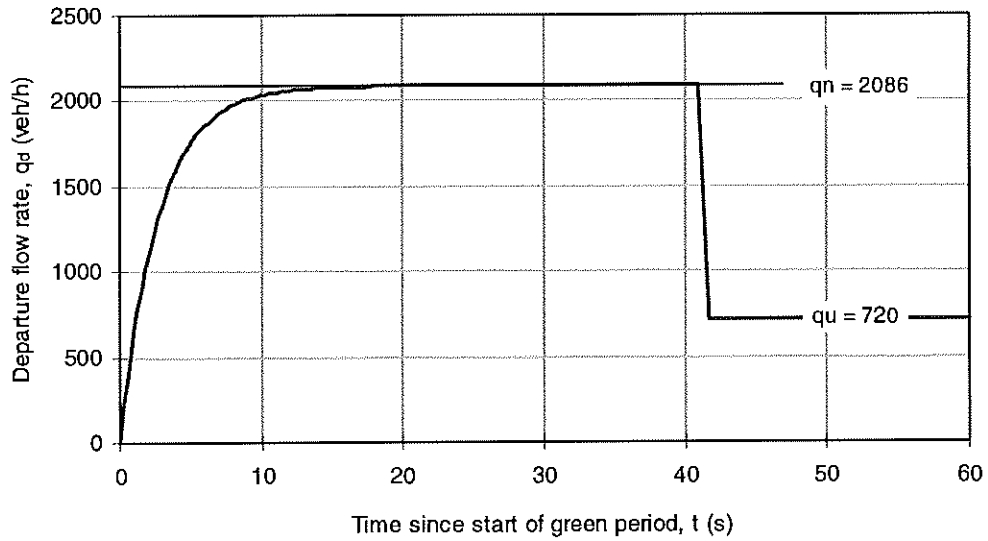


Figure 15.1 – Departure flow rates for saturated and unsaturated parts of the green period (an example using average through isolated site parameters)

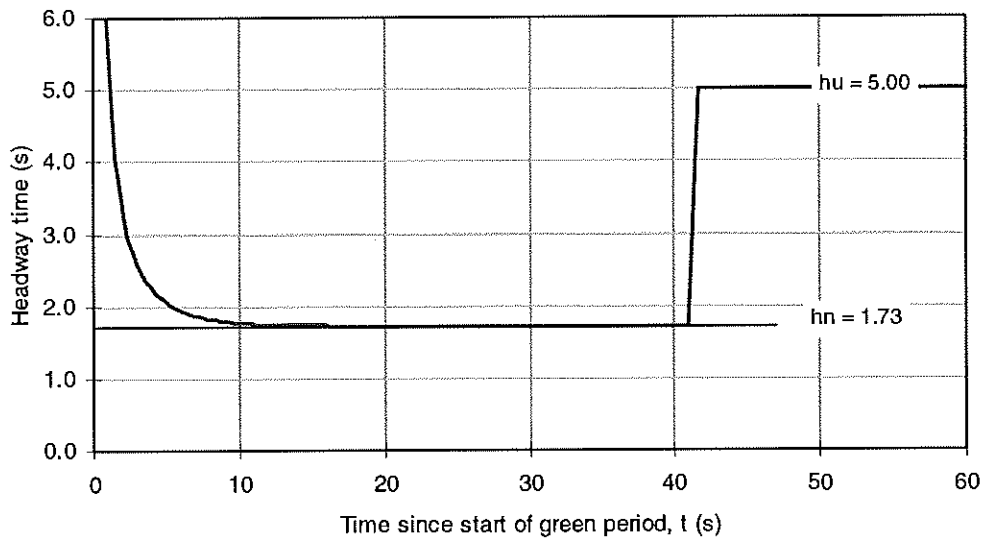


Figure 15.2 – Departure headways for saturated and unsaturated parts of the green period (an example using average through isolated site parameters)

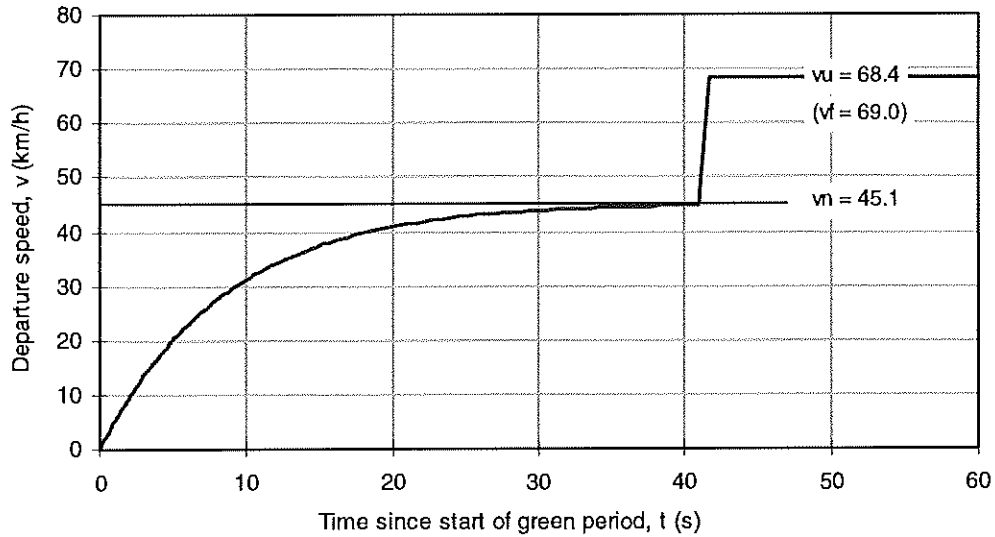


Figure 15.3 – Departure speeds for saturated and unsaturated parts of the green period (an example using average through isolated site parameters)

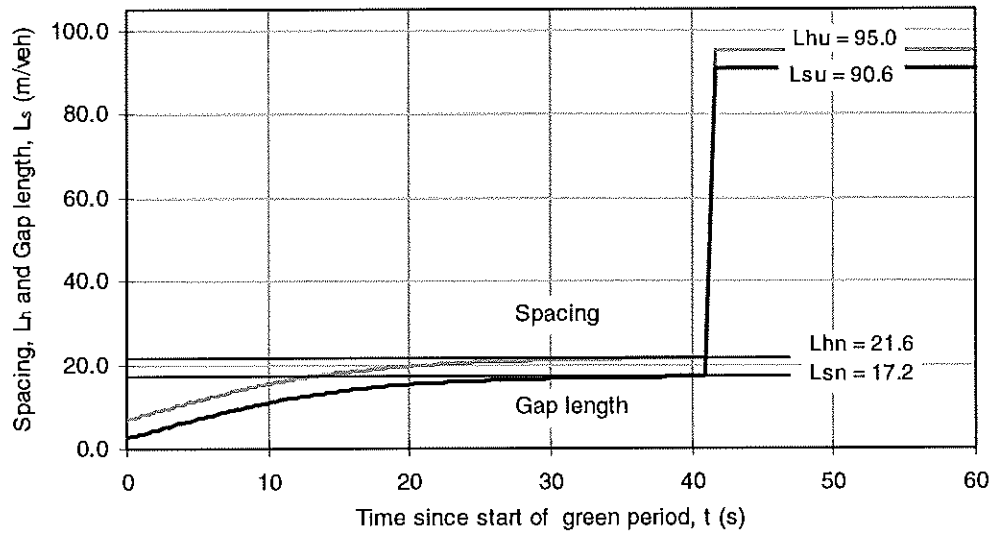


Figure 15.4 – Vehicle spacings and gap lengths for saturated and unsaturated parts of the green period (an example using average through isolated site parameters)

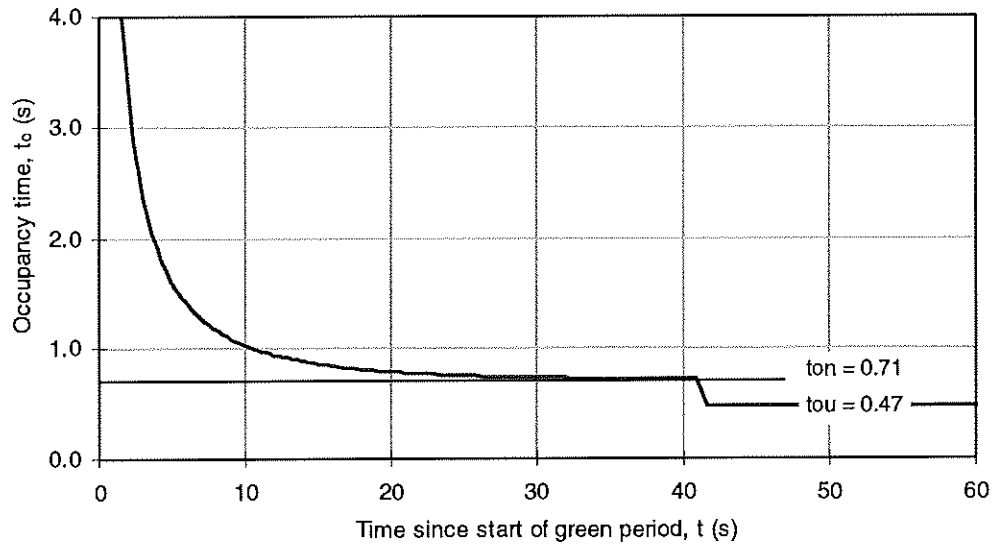


Figure 15.5 – Occupancy time for saturated and unsaturated parts of the green period (an example using average through isolated site parameters)

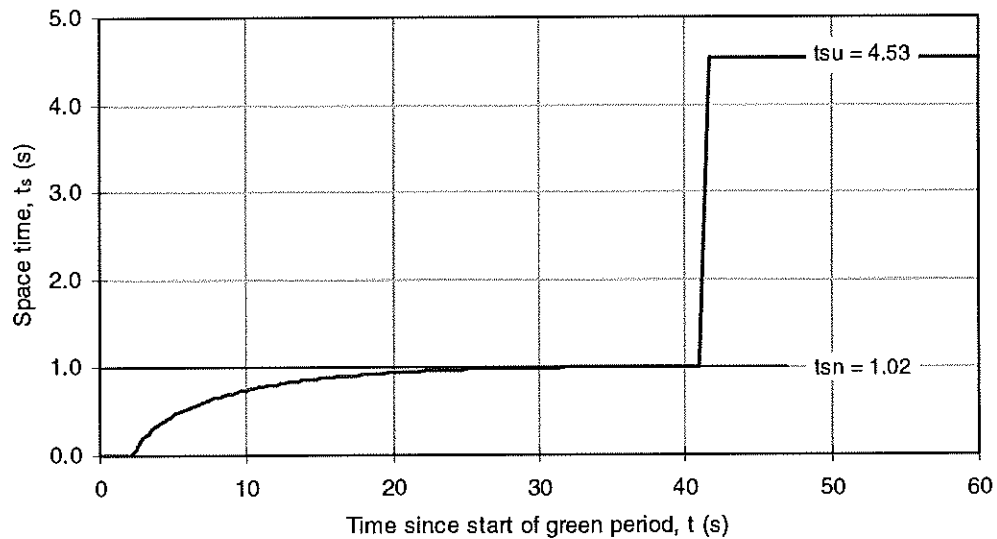


Figure 15.6 – Space time for saturated and unsaturated parts of the green period (an example using average through isolated site parameters)

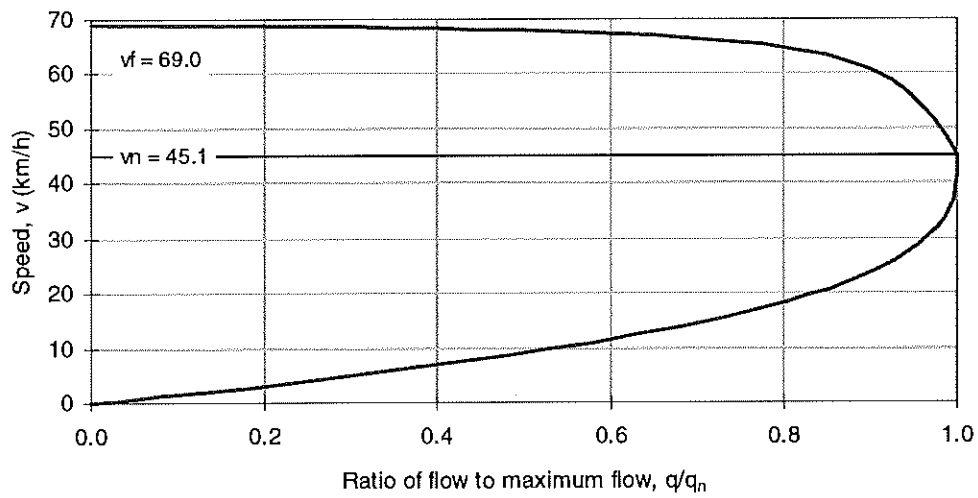


Figure 15.7 – Speed as a function of the ratio of flow rate to the maximum flow rate (an example using average through isolated site parameters)

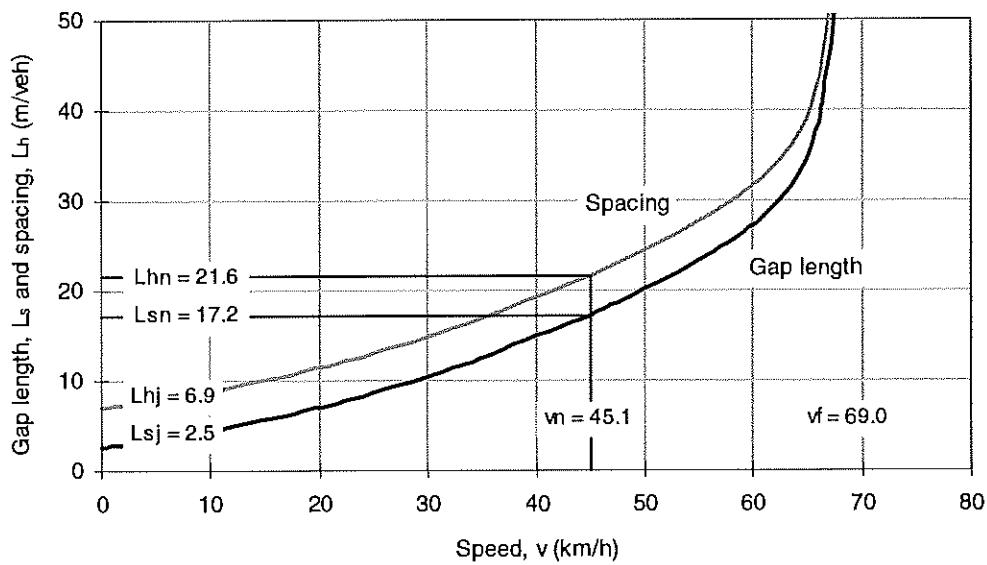


Figure 15.8 – Spacing and gap length as a function of speed (an example using average through isolated site parameters)

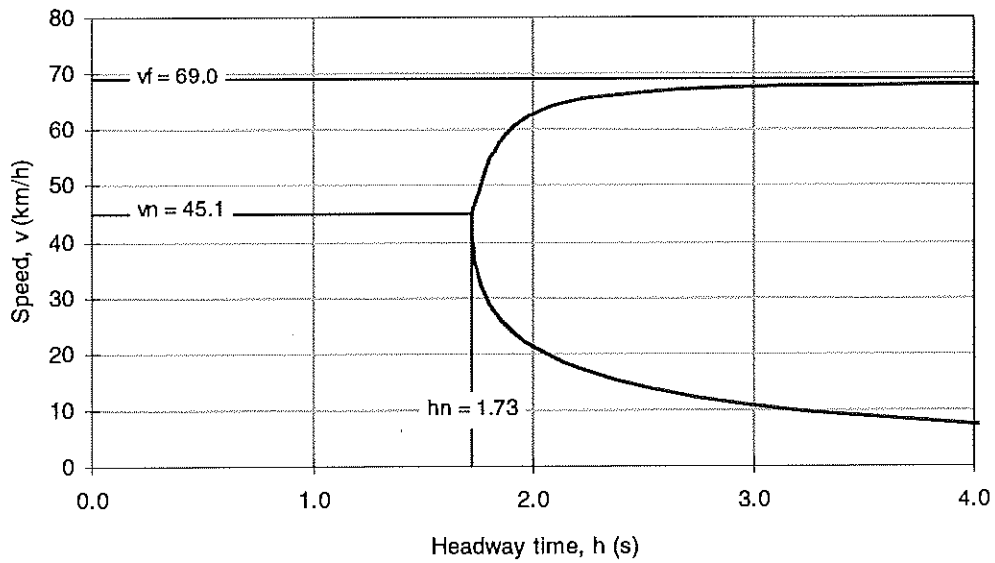


Figure 15.9 – Speed as a function of headway time
 (an example using average through isolated site parameters)

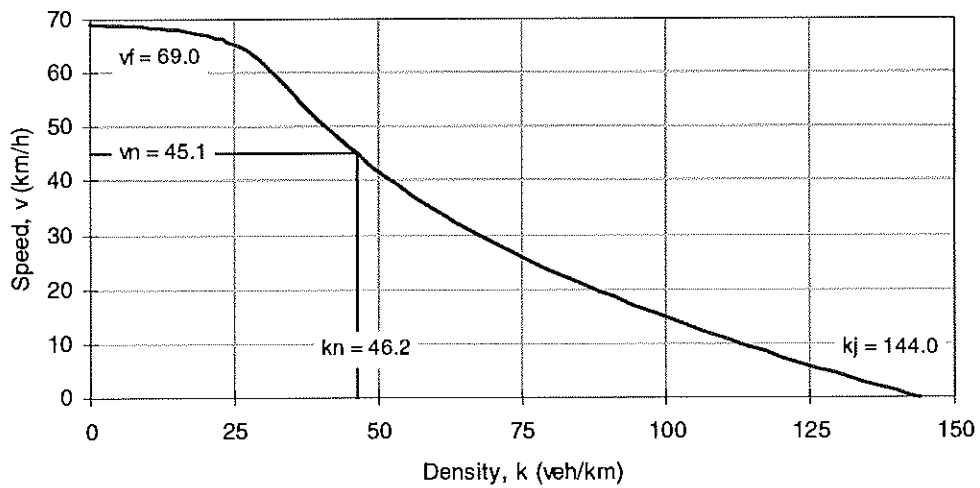
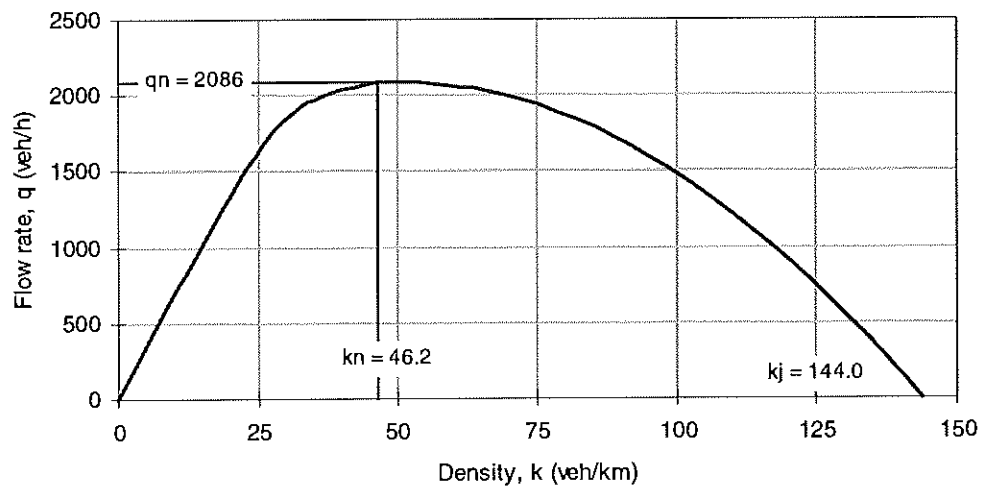
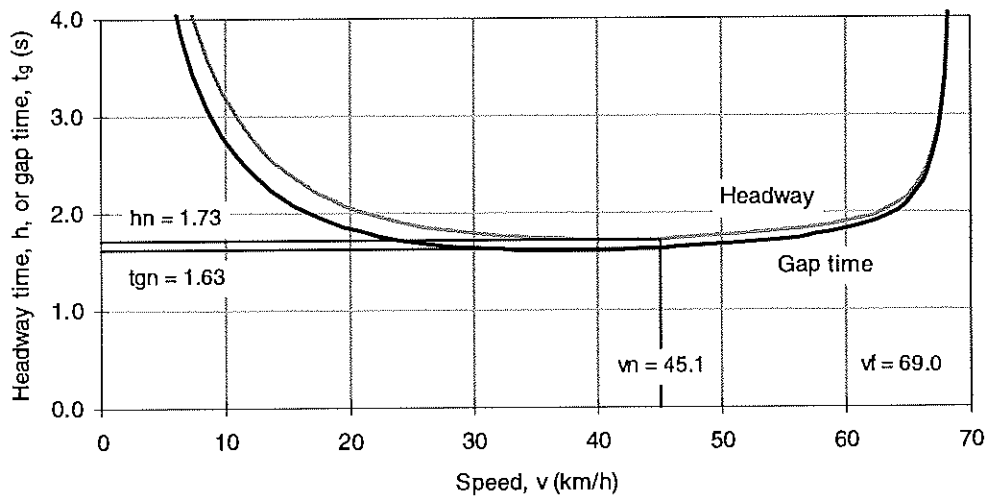


Figure 15.10 – Speed as a function of density
 (an example using average through isolated site parameters)



*Figure 15.11 – Flow rate as a function of density
(an example using average through isolated site parameters)*



*Figure 15.12 – Headway and gap time as a function of speed
(an example using average through isolated site parameters)*

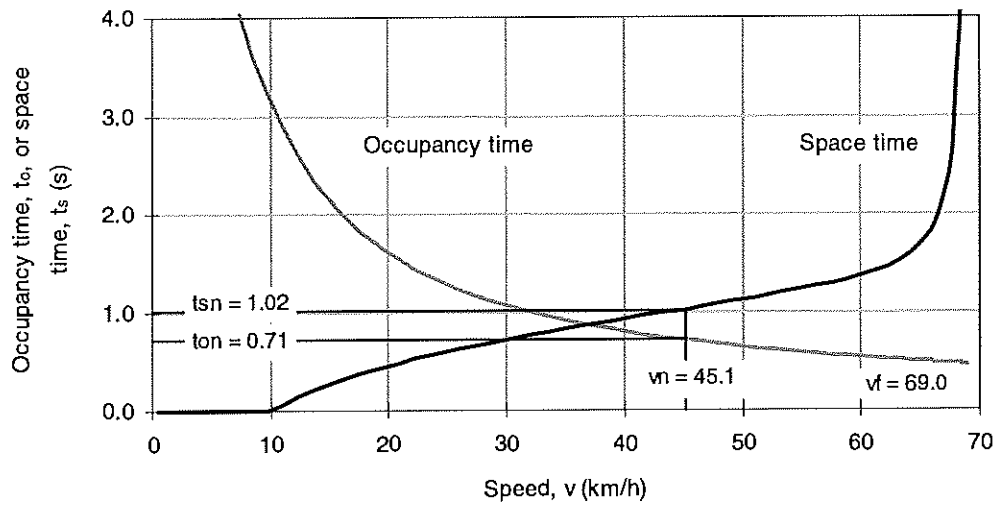


**Figure 15.13 – Occupancy and space time as a function of speed
 (an example using average through isolated site parameters)**

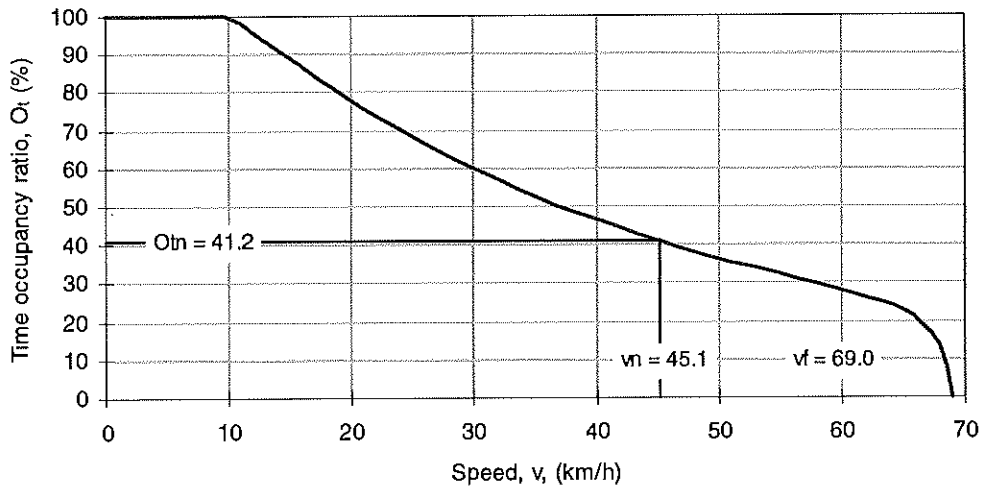


**Figure 15.14 – Time occupancy ratio as a function of speed
 (an example using average through isolated site parameters)**

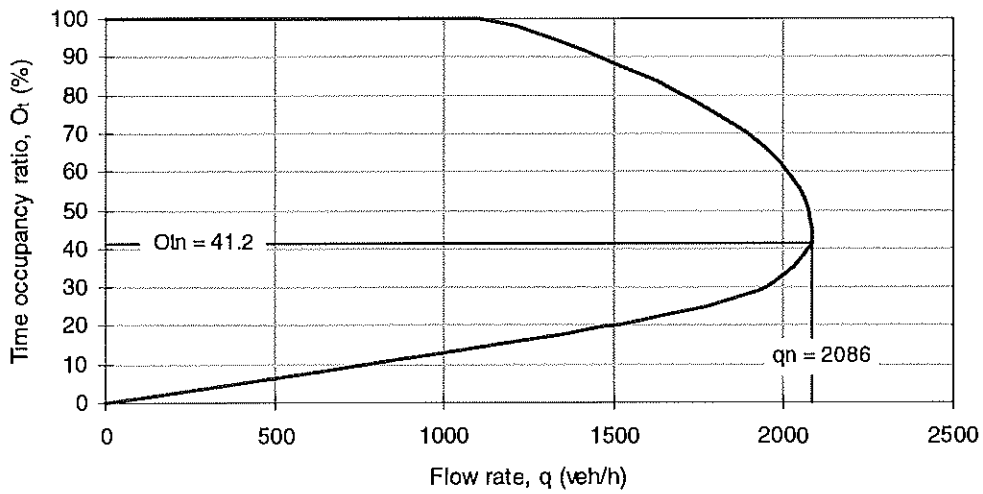


Figure 15.15 – Time occupancy ratio as a function of flow rate (an example using average through isolated site parameters)

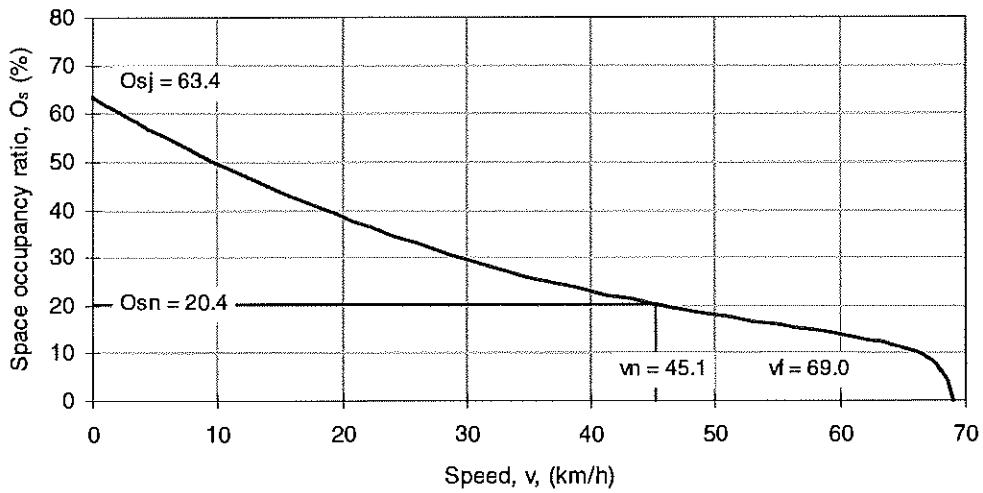


Figure 15.16 – Space occupancy ratio as a function of speed (an example using average through isolated site parameters)

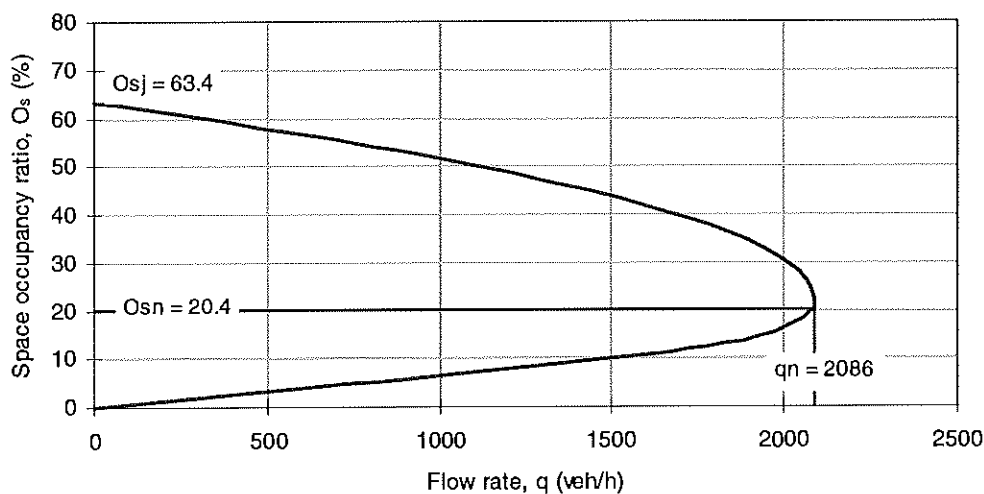


Figure 15.17 – Space occupancy ratio as a function of flow rate (an example using average through isolated site parameters)

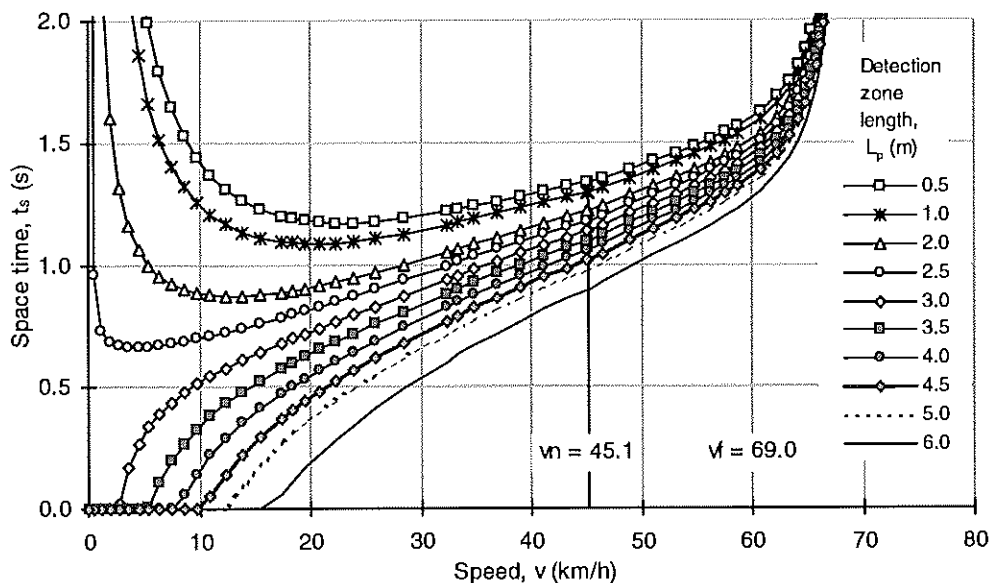


Figure 15.18 – The relationship between space time and speed as a function of the detection zone length (an example using average through isolated site parameters)

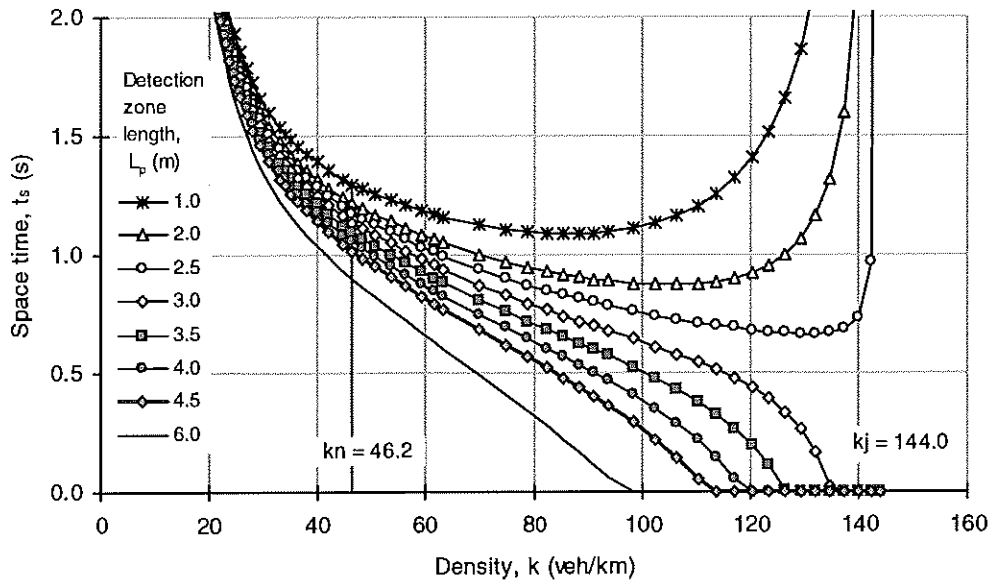


Figure 15.19 – The relationship between space time and density as a function of the detection zone length (an example using average through isolated site parameters)

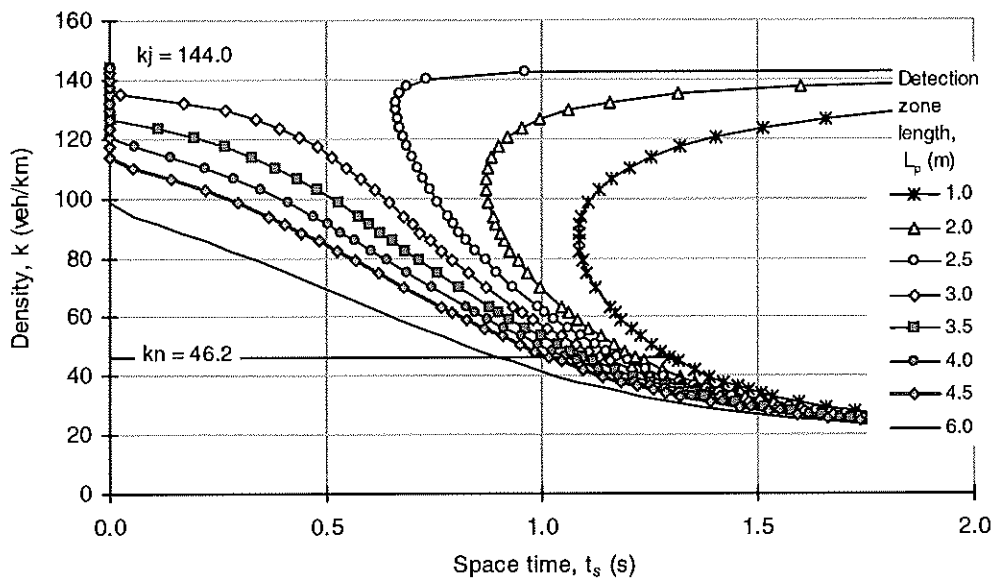


Figure 15.20 – The relationship between density and space time as a function of the detection zone length (an example using average through isolated site parameters)

16 USEFUL RELATIONSHIPS FOR PRACTICE

This section presents various relationships for use in applying the findings of this research in practice. These relationships are based on the material presented in previous sections.

Equations are presented for determining queue discharge model parameters. Ideally, all relevant traffic parameters should be measured in the field. However, when this is not possible, the required parameters can be estimated using the relationships given below.

Simple equations are given to determine optimum loop length and gap setting values.

In this section, the maximum queue discharge flow rate parameter will be treated as equivalent to the saturation flow rate ($q_n \approx s$) as this is appropriate for practical purposes. The terms "maximum queue discharge flow rate" and "saturation flow rate", as well as "maximum queue discharge speed" and "saturation speed" will be used interchangeably.

Maximum Queue Discharge Speed

The maximum queue discharge speed, or saturation speed (v_n) can be measured by driving through the intersection or estimated using a known saturation flow rate.

The saturation speed can be measured by driving through the intersection in the lane of interest, and recording the queue discharge speed when crossing the signal stop line. For this purpose, departure must be from the queue after stopping behind vehicles that have already queued in the lane of interest. The queue position must be at least the sixth vehicle position, but around the tenth and following queue positions are preferred.

When saturation flow rate is known either through field surveys, or through an established estimation method (e.g. Akçelik 1981, TRB 1998), the saturation speed can be estimated using the following regression equations based on model calibration results given in *Section 9* (see *Figure 9.1*).

For through (isolated) movements:

$$v_n = 0.025 s - 6.9 \quad (16.1)$$

For through (paired intersection) movements:

$$v_n = 0.024 s - 16.8 \quad (16.2)$$

For right-turn (isolated) movements:

$$v_n = 0.018 s - 12.4 \quad (16.3)$$

where v_n is the saturation speed in km/h, s is the saturation flow rate in veh/h.

Estimating the Saturation Flow Rate by Measuring the Saturation Speed

When resources are not available to measure the saturation flow rate through field surveys, a simple method can be used to obtain a rough estimate of saturation flow rate by measuring the maximum queue discharge speed (v_n) as described above. The following regression equations based on model calibration results given in *Section 9* are used for this purpose (see *Figure 9.2*).

For through movements at isolated intersections:

$$s = 1012 + 24.5 v_n \quad (16.4)$$

For through movements at paired (closely spaced) intersections, or intersections in CBD-type areas:

$$s = 702 + 41.0 v_n \quad (16.5)$$

For right-turn movements at isolated intersections:

$$s = 1249 + 32.2 v_n \quad (16.6)$$

where s is the saturation flow rate (or maximum queue discharge flow rate, $q_n \approx s$) in veh/h, and v_n is the saturation speed in km/h.

Measuring the Saturation Flow Rate, Start Loss and End Gain

The saturation flow rate, as an approximation to the maximum queue discharge flow rate ($s \approx q_n$), can be measured using one of the two established survey methods, namely the ARR 123 method (Akçelik 1981), or the HCM method (TRB 1998). These methods were described in detail in *Section 12*. The following modified version of the HCM method is recommended for use in practice. An example for the application of the method is shown in *Figure 16.1*.

In each signal cycle (j th cycle), starting with the green period, record the time when the *fifth* vehicle crosses the stop line (t_{ij}) and the last vehicle from the queue crosses the stop line (G_{sj}). Thus, t_{ij} is the duration of the initial interval and G_{sj} is the duration of the saturated part of the green period in the j th cycle. This method excludes the first *five* vehicles departing from the queue ($n_{vi} = 5$) unlike the HCM method which excludes the first four vehicles. The last vehicle departing from the queue may have joined the queue during the green period as shown in *Figures 2.3 and 2.4* in *Section 2* (the HCM method uses the last vehicle in queue when the signals turn green).

Count the number of vehicles departing from the queue during the saturated part of the green period (n_{vsj}) starting when the signals turn green and stopping when the last vehicle from the queue departs. Thus, n_{vsj} vehicles depart in G_{sj} seconds, $n_{vi} = 5$ vehicles depart during the initial interval, t_{ij} , and $(n_{vsj} - n_{vi})$ vehicles depart in $(G_{sj} - t_{ij})$ seconds.

If the green period is fully saturated ($G_{sj} = G_j$), the last vehicle from the queue departs at the end of the green period (when signals change to yellow). Count the number of vehicles departing during the yellow and all-red clearance period only during fully saturated green periods (n_{ej}).

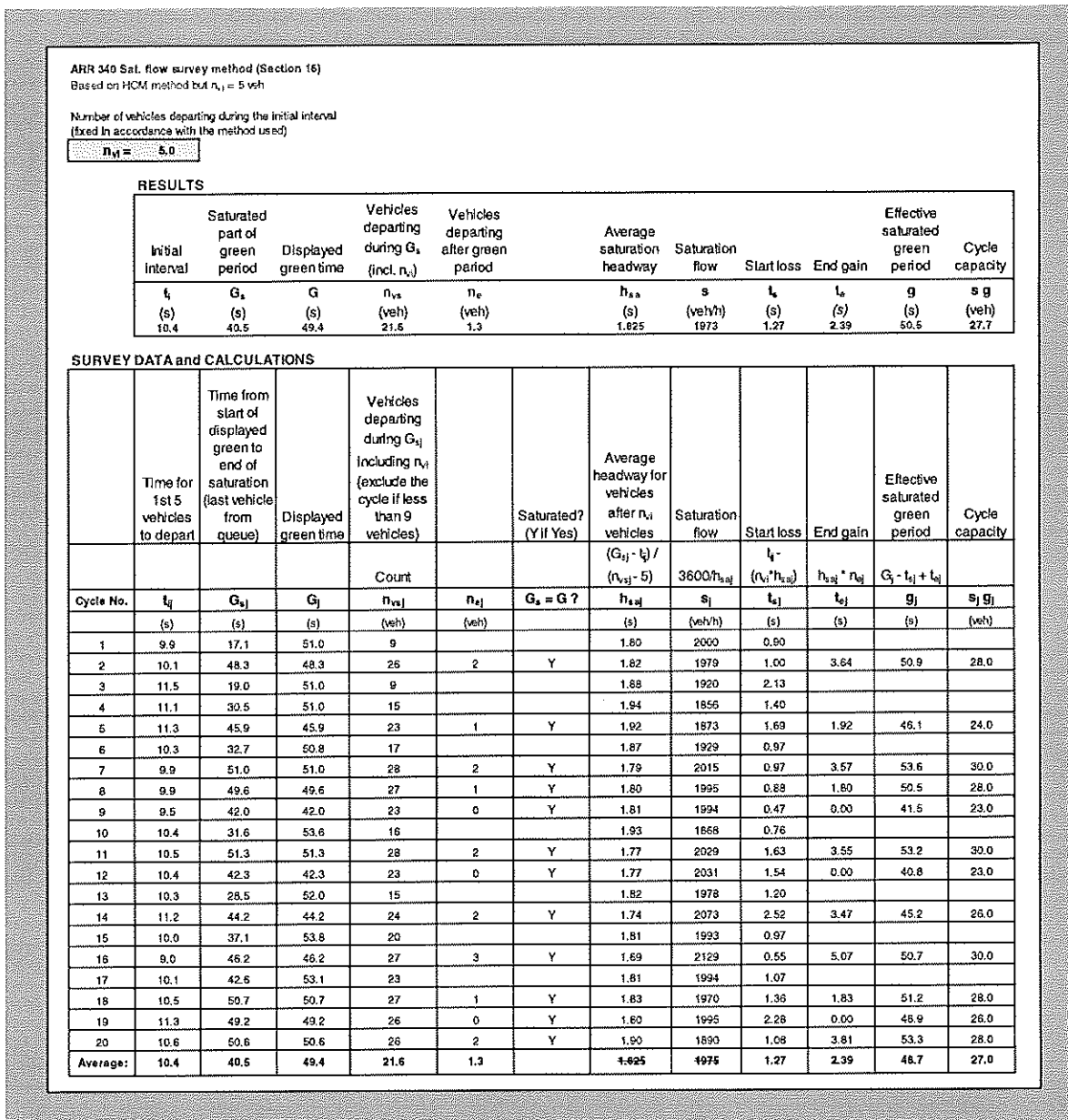


Figure 16.1 – Measurement of saturation flow rate, start loss and end gain times (an example)

For a given (jth) signal cycle, calculate the average saturation headway in s/veh (h_{saj}) and the corresponding saturation flow rate in veh/h (s_j) from:

$$h_{saj} = (G_{sj} - t_{ij}) / (n_{vsj} - n_{vi}) \tag{16.7a}$$

$$s_j = 3600 / h_{saj} \tag{16.7b}$$

where $n_{vi} = 5$ ($n_{vi} = 4$ in the original HCM method).

Considering all signal cycles observed, calculate the average saturation headway (h_{sa}) and the corresponding saturation flow rate (s) from:

$$h_{sa} = (G_s - t_i) / (n_{vs} - n_{vi}) \quad (16.8a)$$

$$s = 3600 / h_{sa} \quad (16.8b)$$

where the average values of the saturated part of the green period (G_s), vehicles departing during G_s , and duration of the initial interval (t_i) are calculated from:

$$G_s = (\Sigma G_{sj}) / n_c \quad (16.8c)$$

$$t_i = (\Sigma t_{ij}) / n_c \quad (16.8d)$$

$$n_{vs} = (\Sigma n_{vsj}) / n_c \quad (16.8e)$$

where n_c is the number of signal cycles observed and summations are over all signal cycles observed.

It is recommended that only signal cycles with $n_{vsj} \geq 9$ veh are used in determining the average saturation headway and the saturation flow rate using above equations. Thus, the minimum required number of vehicles departing after the initial interval (during $G_{sj} - t_{ij}$) is 4 vehicles. HCM recommends at least 15 signal cycles for a statistically significant value of saturation flow rate.

Note that the saturation flow rate obtained from *Equation (16.8b)* differs slightly from the HCM (TRB 1998) method of finding a statistical average of saturation flow rates for individual cycles:

$$s = (\Sigma s_j) / n_c \quad (16.9)$$

where n_c is the number of signal cycles and s_j is the saturation flow rate in the j th cycle from *Equation (16.7b)*.

Equation (16.8b) is recommended over *Equation (16.9)* for consistency between saturation flow, start loss and end gain parameters.

For a given (j th) signal cycle, the start loss and end gain parameters can be calculated from:

$$t_{sj} = t_{ij} - n_{vi} h_{saj} \quad (16.10)$$

$$t_{ej} = 3600 n_{ej} / s_j = h_{saj} n_{ej} \quad (16.11)$$

where $n_{vi} = 5$ veh, h_{saj} is calculated from *Equation (16.7a)* and n_{ej} is the number of vehicles departing during the yellow and all-red clearance interval. The end gain parameter is calculated for fully saturated cycles only.

Considering all signal cycles:

$$t_s = t_i - n_{vi} h_{sa} \quad (16.12)$$

$$t_e = 3600 n_e / s = h_{sa} n_e \quad (16.13)$$

where $n_{vi} = 5$ veh, h_{sa} is the average saturation headway from *Equation (16.8a)*, t_i is the average value of the initial interval from *Equation (16.8d)*, n_e is the average number of vehicles departing during the yellow and all-red clearance period calculated from:

$$n_e = (\sum n_{ej}) / n_{cs} \quad (16.14)$$

where n_{cs} is the number of fully saturated signal cycles.

Exponential Queue Discharge Speed Model Parameter m_v

This parameter can be estimated from the following regression equations based on model calibration results given in *Section 9* (see *Figure 9.3*).

For through (isolated) movements:

$$m_v = 0.25 - 0.003 v_n \quad (16.15)$$

For through (paired intersection) movements:

$$m_v = 0.74 - 0.016 v_n \quad (16.16)$$

For right-turn (isolated) movements:

$$m_v = 0.85 - 0.022 v_n \quad (16.17)$$

where v_n is the maximum queue discharge speed in km/h.

Exponential Queue Discharge Flow Model Parameter m_q

Calculate the m_q parameter from:

$$m_q = 1000 m_v v_n / (q_n L_{hj}) \quad (16.18)$$

where v_n is the maximum queue discharge speed in km/h, q_n is maximum queue discharge flow rate (saturation flow rate, $s \approx q_n$) in veh/h and L_{hj} is the jam density in metres.

Jam Spacing and Gap Length (L_{hj} , L_{sj}):

Jam density (L_{hj}) and jam gap length (L_{sj}) are important parameters that should be measured in the field wherever possible. For this purpose, record the number and type of stationary (queued) vehicles in a given distance from the signal stop-line, e.g. 90 m. For short lanes, count the number of vehicles in the short lane space. Use the vehicle queue spacing survey form given in *Section 2* (*Figure 2.9*).

Determine the jam spacing for light vehicles (L_{hjLV}) using data from queues where no heavy vehicles are present. Calculate the jam spacing for heavy vehicles (L_{hjHV}) from:

$$L_{hjHV} = [L_{hj} - (1 - p_{HV}) L_{hjLV}] / p_{HV} \quad (16.19)$$

where L_{hj} is the average jam spacing for all traffic in queue, and p_{HV} is the proportion of heavy vehicles in queue.

If it is not possible to measure the jam spacing, use the following values (default values based on average jam spacings given in *Table 9.6* in *Section 9*):

- Through traffic lanes: 7.0 m per light vehicle, 11.5 m per heavy vehicle.
- Right-turn traffic lanes: 6.5 m per light vehicle, 11.0 m per heavy vehicle.

Assuming average vehicle lengths of 4.4 m and 8.8 m per light vehicle and heavy vehicle, respectively, the above jam density values imply jam gap lengths of $L_{sj} = 2.5$ m for through traffic lanes and $L_{sj} = 2.0$ m for fully-controlled right-turn traffic lanes.

Other Parameters

Once parameters h_n , q_n , v_n , L_{hj} , m_v and m_q are established, a complete set of fundamental relationships for queue discharge behaviour at traffic signals can be obtained, useful for general traffic analysis as well as adaptive control purposes.

Additional parameters at maximum queue discharge flow and at jam conditions including spacing, gap length, density, time and space occupancy ratios, gap time, vehicle passage time, occupancy time and space time (L_{sj} , L_{sn} , k_j , k_n , O_{tj} , O_{tn} , O_{sj} , O_{sn} , t_{gn} , t_{vn} , t_{on} , t_{sn}) can be calculated using *Equations (5.41) to (5.54) in Section 5*.

Saturation Headway, Departure Response time and Start Loss

The following relationships from *Section 7* (see *Figures 7.2 and 7.3*) are useful in explaining the basic parameters that determine the minimum queue discharge headway (h_n in seconds), therefore the maximum queue discharge flow rate or saturation flow rate ($q_n \approx s$ in veh/h):

$$h_n = t_x + 3.6 L_{hj} / v_n \quad (16.20)$$

$$q_n = 3600 / (t_x + 3.6 L_{hj} / v_n) \quad (16.21)$$

where t_x is the queue departure response time for the next vehicle in the queue to start moving (s), v_n is the maximum queue discharge speed (km/h) and L_{hj} is the jam spacing (m).

Equation (16.20) indicates that the minimum queue discharge headway, or saturation headway, is the sum of queue departure response time and the time to travel the jam spacing distance at the maximum queue discharge speed.

Thus, when h_n , v_n and L_{hj} are known, parameter t_x can be determined from:

$$t_x = h_n - 3.6 L_{hj} / v_n \quad (16.22)$$

where t_x and h_n are in seconds, L_{hj} is in meters and v_n is in km/h.

The queue clearance wave speed (v_x in km/h) can be calculated using the queue departure response time:

$$v_x = 3.6 L_{hj} / t_x = 3.6 L_{hj} / (h_n - 3.6 L_{hj} / v_n) \quad (16.23)$$

Survey results summarised in *Table 9.7 in Section 9* indicate that t_x is in the range 0.8 to 0.9 for right-turn traffic sites and 0.9 to 1.4 s for through traffic sites, and v_x is in the range 25 to 32 km/h for right-turn traffic sites and 18 to 27 km/h for through traffic sites.

Equation (7.22) given in *Section 7* can be used for determining the arrival (queue formation) wave speed (v_y) which varies with the arrival flow rate.

The start loss time used to convert displayed green time to effective green time is explained through the following relationship (see *Figures 7.2 and 7.3 in Section 7*):

$$t_s = t_r + d_a - h_n \quad (16.24)$$

where t_r is the start response time, h_n is the minimum queue discharge headway, and d_a is the average acceleration delay calculated from:

$$d_a = t_a - 3.6 x_a / v_n \quad (16.25)$$

where t_a is the acceleration time (s), i.e. time it takes to accelerate from zero speed to the maximum queue discharge speed, v_n (km/h), and x_a is the corresponding acceleration distance (m). Acceleration time and distance models given in the SIDRA user guide can be used to estimate these parameters (Akçelik and Besley 1999).

Since the start loss can be determined in association with the saturation flow measurement method, and the acceleration delay can be calculated from *Equation (16.25)*, the start response time can be calculated from:

$$t_r = t_s + h_n - d_a \quad (16.26)$$

However, there are difficulties in determining t_r due to uncertainties in acceleration model characteristics. Further research is needed on this subject.

Optimum Loop Length

An optimum detection zone length, approximately equal to the loop length (L_p), is sought in terms of the best ability to detect traffic variables relevant to adaptive control. For this purpose, the relationship between space time (t_s) and speed (v_s) as a function of the loop length can be used.

The optimum detection zone length can be determined as the length at which the space time equals zero ($t_s = 0$) at a selected low (limiting) speed value (v_o). The limiting speed must be as low as possible so that the range of speeds 0 to v_o is as small as possible. The detection zone length above the optimum value ($L_p > L_{p0}$) increases this range. On the other hand, the detection zone length below the optimum value ($L_p < L_{p0}$) may give two speed values for a given space time as seen from the space time - speed graphs.

The limiting speed (v_o) needs to be selected conservatively since, if v_o is too low, the loop length may be too short under adverse traffic conditions (e.g. driving in rain and darkness). On the other hand, the condition when zero space time ($t_s = 0$) occurs is caused by the gap length being less than the effective detection zone length, or loop length being too long ($L_s < L_p$).

As a result, the "bridging" effect occurs, i.e. the time when the front end of the following vehicle enters the detection zone occurs before the time when the rear end of the leading vehicle exits the detection zone. A shorter loop length is selected to minimise this condition, in contrast with the choice of a longer loop considering adverse conditions. Other advantages of a shorter loop length are lower cost and better sensitivity.

As discussed in *Section 14*, the optimum detection zone length is clearly related to the **jam gap length** ($L_{sj} = L_{hj} - L_v$ where L_{hj} is the jam spacing and L_v is the average vehicle length). The following regression equations (see *Figures 14.12 and 14.13*) can be used

to determine the optimum loop length when more detailed analysis using space time - speed - loop length relationships is not possible:

$$L_{p5} = 1.26 e^{0.385 L_{sj}} \quad (16.27)$$

$$L_{p10} = 1.87 e^{0.328 L_{sj}} \quad (16.28)$$

Ideally jam gap length should be measured in real-life situations. However, it is easier to measure the jam spacing. In this case, the jam gap length can be calculated from $L_{sj} = L_{hj} - L_v$ assuming an average vehicle length.

As discussed above, the jam gap length may increase under adverse driving conditions (e.g. rain). *Equations (16.27) and (16.28)* indicate that the optimum loop length should be increased with this in mind. For example, if the jam gap length is increased from 2.5 m to 3.0 m, L_{p5} increases from 3.4 m to 4.2 m.

Gap Setting

Information about the space time - speed - detection zone length relationships can be used to develop guidance for appropriate gap setting (unit extension time setting) values for traditional vehicle-actuated control as well as SCATS control (see *Section 14* for a detailed discussion). Gap settings (e_s) in the range 2.5 to 4.0 s for through traffic and 2.0 to 4.0 s for right-turn traffic are used in Australian practice (Akçelik 1995a).

For efficient control with small cycle times, the gap setting should be as small as possible. Therefore, the gap setting can be related to the space time at maximum queue discharge (saturation) flow, t_{sn} . Considering the cycle-by cycle variation of queue discharge parameters at a given site, a factor should be applied to the t_{sn} value to determine an appropriate gap setting value:

$$e_s = f_e t_{sn} \quad (16.29)$$

where e_s is the gap setting as a space time value (s), f_e is the variational factor, and t_{sn} is the space time at maximum queue discharge flow ($q_n \approx s$):

$$t_{sn} = h_n - (L_p + L_v) / v_n \quad (16.30)$$

where $h_n = 3600 / q_n$ is the minimum queue discharge headway (seconds), v_n is the minimum queue discharge speed (km/h), L_p and L_v are the detection zone length and vehicle length (m).

Considering cycle-by-cycle variations in space time values (*Section 12*), an appropriate value of f_e chosen conservatively could be in the range 1.5 to 2.0.

Using a conservative value of $f_e = 2.0$, gap setting values of $e_s = 1.6$ to 2.4 s (average 2.0 s) for through traffic sites, $e_s = 0.8$ to 1.1 s (average 0.9 s) for right-turn sites are obtained with a loop length of 4.5 m. The results indicate that shorter gap settings could be used compared with the current Australian practice, especially for fully controlled right-turn phases.

On the other hand, there are other reasons for using longer gap settings in practice. For example, a larger gap setting may be preferred for minor actuated movements at an intersection controlled by coordinated actuated signals in order to preserve signal offsets that achieve best traffic progression.

17 CONCLUSION

Useful relationships for use in practice based on the findings of this study, including survey methods to measure saturation flow and saturation speed, simple regression equations to estimate queue discharge characteristics and determine optimum loop length and signal gap setting are given in *Section 16*.

General findings about queue discharge models are summarised and recommendations for further work are given in this section.

The results of detailed analysis of *queue discharge characteristics* at signalised intersections show that the characteristics of through and right-turn movements differ significantly, and there are also significant differences between through lanes at isolated sites and paired (closely spaced) intersection sites.

Maximum queue discharge flow rates for right-turn sites are found to be similar to those for isolated through sites. Lower jam spacing and lower departure response time (higher queue clearance speed) at right-turn sites help to achieve low queue discharge headways, therefore high maximum flow rates. Parameters for through movements at paired intersection sites are between the through (isolated) and right turn (isolated) site values although lower maximum flow rates are observed at these sites.

The exponential queue discharge flow (headway) and speed models presented in this report are found satisfactory in view of:

- (i) ability to derive a complete set of fundamental relationships for queue discharge behaviour at traffic signals, useful for general traffic analysis as well as adaptive control purposes (*Section 7*);
- (ii) reasonableness (compared with current knowledge and overseas data) of predicted queue discharge parameters, namely speed, flow rate, headway, spacing, gap (space) length, density, time and space occupancy ratios, gap time, vehicle passage time, occupancy time and space time, as well as implied optimum loop length (*Sections 9, 12, 14*);
- (iii) consistency of relative values of model parameters for through (isolated), through (paired intersection) and fully-controlled right turn (isolated) sites;
- (iv) consistency of saturation flow rate, start loss and end gain values derived from the exponential queue discharge flow model with those used in traditional signal analysis (*Section 12*); and
- (v) a reasonable match between the SCATS parameters MF (maximum flow), HW (headway at maximum flow), KP (occupancy time at maximum flow) and the space time (HW – KP), and the corresponding analytical estimates, as well as the ability to relate the SCATS DS parameter to the traditional degree of saturation parameter (*Section 13*).

It is often stated in the literature that saturation flow rate may decrease with time, especially in the case of long green times (e.g. Teply and Jones 1991, Teply, et al. 1995). The survey results presented in this report do not support this except in the case of downstream queue interference as evident from figures given in *Appendix B*.

Additional analysis for *uninterrupted flow conditions* at signalised intersections, as relevant to conditions after queue clearance (unsaturated part of the green period), indicates that speed – flow - density models for these conditions are consistent with general models for uninterrupted conditions (*Section 10*). Alternative models were assessed, and Akçelik's (1991) speed-flow model was recommended for this purpose. This model complements the exponential queue discharge models for saturated conditions, thus allowing for a complete analysis of traffic flow conditions at signalised intersections. This is demonstrated through the example given in *Section 15*. The findings also support the general explanation of the relationship between speed-flow functions for interrupted and uninterrupted flow conditions presented in *Section 5*.

Queue discharge model parameters for *paired (closely-spaced) intersection* sites were derived using data points not affected by queue interference. The model parameters for these sites are found to be significantly different from those for isolated through traffic sites (*Section 9*). In summary, maximum queue departure flow rates, speeds at maximum flow and spacings at maximum flow are lower, and queue discharge flow and speed model parameters m_q and m_v are higher indicating quicker acceleration to the maximum speed and achieving the maximum flow rate sooner.

Although based on a small number of paired intersection sites, analysis of conditions with downstream queue interference indicate that the downstream queue interference occurs only when the distance to the back of queue is very small (*Section 11*). For all practical purposes, it is concluded that queue interaction occurs when the downstream queue storage space is fully occupied. If required, equations given in *Section 11* can be used to calculate reduced queue discharge speed and flow rate as a function of the distance to the back of queue. Effectively, the equations reduce the queue discharge speed and flow rate only for distances below 30 to 40 m.

Analyses of *cycle-by-cycle variations* in minimum queue discharge headway, cycle capacities and space time at maximum flow at a given site (carried out for five sites) indicated that distributions of these parameters varied considerably from site to site (*Section 12*). For example, the 98th percentile space time at maximum flow can be as high as twice the average value, as observed at site 335 (right turn movement with short green time), and as low as 13 per cent higher than the average value, as observed at the site 511 (through movement with very long green time).

Of particular interest is the *variance to mean ratio of cycle capacity* which is important in modelling the effect of randomness in departure flows for predicting traffic performance (delay, queue length and queue move-up rate) for signalised intersections. Although this parameter is included in basic theoretical treatment of delay modelling, it has not been used explicitly in most delay models used in practice. Some coordinated signal delay models allow for filtering/metering of departure flows for saturated cycles at the upstream intersection, thus reducing the amount of randomness. For example, see the US Highway Capacity Manual (TRB 1998) and the SIDRA User Guide (Akçelik and Besley 1999). This may lead to the prediction of zero delays at the downstream intersection when the upstream intersection is oversaturated since the effect of variations in cycle capacity is ignored.

Analysis results for the five survey sites show that the variance to mean ratio of cycle capacity was in the range 0.08 to 0.34. It appears that 0.10 is a typical value for isolated sites. Interestingly, a high value of 0.34 was observed at the CBD site 413, suggesting that further attention needs to be paid to this parameter for coordinated signal modelling.

During this research, extensive effort has gone into fine-tuning the data analysis and calibration methods to improve the *headway and speed predictions at low speeds*. This is due to the lack of data at very low speeds and low flow rates related to the measurement of speed and headway for the first few vehicles in the queue at the start of the green period. Although the queue discharge models were generally satisfactory, there were several cases where the predicted headway and flow rate values for low speeds were not entirely satisfactory. This was particularly observed for the sites with low values of maximum queue discharge speed, which applied to most right-turn sites.

The data collection method and queue discharge models were investigated in detail, developing *alternative calibration methods* to derive queue discharge model parameters using different values of headway and speed variables obtained from raw detector data (*Section 8*). The use of measured jam spacing vs the jam spacing estimated using model parameters from headway regression was considered. The start response time was introduced into the exponential queue discharge headway and speed models as a result of this effort (*Section 7*). Alternative calibration methods were applied to data from three sites, namely Site 335 (Melbourne), Site 610 (Sydney) and Site 511 (Sydney). The following conclusions are drawn from the findings given in *Section 9*.

- (i) The headway regression method results in estimated jam spacing values that are significantly greater than the measured values. Correct prediction of this parameter is very important for the space time - speed relationships and the optimum loop length as discussed in *Section 14*. Therefore this method is not preferred, thus confirming the calibration procedure that employs the measured jam spacing (*Section 8*).
- (ii) Determining the start response time parameter freely from speed model regression gave acceptable results for the right-turn lane sites (335 and 610), but gave a negative value for the through lane site (511). The use of a specified value of 1.0 s appeared to be reasonable.
- (iii) Alternative methods using different speed and headway variables derived from raw detector data using the standard calibration method (with the measured jam spacing) gave close results although some improvements were obtained in queue discharge speed, headway and flow rate predictions. For a given site, the ratio m_v/m_q , which is the parameter in the speed-flow model, does not vary significantly for alternative calibration methods that use the measured jam spacing. This is a satisfactory result, in that the speed - flow and space time - speed relationships and the optimum loop length values indicate low sensitivity to the method used (assuming the calibration procedure using the measured jam spacing).
- (iv) Although alternative calibration methods using measured jam spacings give similar results in terms of the resulting speed - flow and space time - speed relationships and the optimum loop length values, it is recommended that calibration method 13 is used in future data analyses.

Method 13 uses the standard calibration procedure with a specified start response time of 1.0 s, and employs the speed based on the leading end of the vehicle and headways measured at the downstream detector. This method improves the queue discharge headway prediction at low speeds, particularly for right-turn sites where the queue discharge speeds are low.

Diagrams showing *space time - speed - detection zone length* relationships for average through (isolated and paired intersection) and average right turn (isolated) sites are given in *Section 14*, and diagrams showing the relationships for individual sites are given in *Appendix C*. These relationships are used for determining *optimum loop (detection zone) length* for adaptive control purposes.

For the dual purpose of counting vehicles and measuring space time, the optimum length for a loop is one that is as short as possible but not so short as to result in a double valued space-time relationship. Vehicle counts and space times are both used by the SCATS control system, and the space time measurement is relevant to traditional actuated control. To determine the optimum loop length, a limiting (low) speed value that gives zero space time can be chosen. Three limiting speeds are considered for this purpose, namely 0, 5 and 10 km/h. It is shown that the optimum loop length equals the gap length at the limiting speed. Choosing a speed above zero provides an increased loop length so to allow for increased jam gap length under adverse driving conditions (e.g. wet weather). Tables summarising queue discharge model parameters and presenting the optimum loop length results for individual sites and for "average" right-turn and through traffic sites are given in *Section 14*.

The following conclusions are drawn regarding optimum loop length for adaptive control.

- (i) The optimum detection zone length appears to be independent of the maximum queue discharge speed, the maximum flow rate and the spacing at maximum flow. There seems to be a linear decreasing relationship between the optimum loop length and the speed-flow model parameter m_v/m_q . The maximum queue discharge speed and the spacing at maximum flow may have some effect on the optimum loop length for right-turn lanes, but it is not possible to establish this due to the small number of right-turn sites surveyed.
- (ii) The optimum detection zone length is clearly related to *jam gap length* as summarised in *Section 16*. *Heavy vehicles* increase vehicle spacings due to longer vehicle length but the gap lengths are not increased as dramatically. Although it is possible that heavy vehicles have some impact on the jam gap length and gap length values at low speeds, the overall impact on these parameters, therefore on the optimum loop length, would be minimal with low heavy vehicle percentages. If the overall jam gap length increases significantly due to a large percentage of heavy vehicles in the traffic stream, then the optimum loop length could be increased proportionately. However, further research is recommended on the effect of heavy vehicles on jam gap length.
- (iii) It appears that it is possible to reduce the current loop length of 4.5 m used with the SCATS system to about 3.5 m for *through traffic lanes* and 3.0 m *right-turn lanes* under green arrow control. This is based on a chosen limiting speed of 5 km/h. On this basis, the range of optimum loop length for through traffic lanes

is 3.0 to 3.8 m, with an average value of 3.4 m, considering all through traffic sites. There was no obvious difference between through sites in Sydney and Melbourne although the number of sites in Sydney is too small to arrive at a firm conclusion regarding this.

Considering all right-turn traffic sites, the range of optimum loop length is 2.2 to 3.1 m, with an average value of 2.6 m. The optimum loop length is shorter for the two right-turn sites in Sydney (2.2 and 2.3 m) and larger for the two right-turn sites in Melbourne (2.9 and 3.1 m). This is in line with the corresponding jam spacing values observed at the two Sydney sites (5.9 and 6.0 m) and at the two Melbourne sites (6.6 and 6.9 m).

Further data from a larger number of sites would be useful to arrive at a more conclusive result about the appropriate level of safety margin in determining the optimum loop length.

- (iv) Optimum loop length values obtained using queue discharge speed and flow models based on *alternative calibration methods* are essentially the same. This is valid for the methods that use the standard calibration procedure that employs the measured jam spacing value. The methods that estimate the jam spacing using parameters from headway model regression are not appropriate since they overestimate the jam spacing significantly.

The results given in this report are based on the definition of headway and spacing parameters from the *front* of the leading vehicle to the *front* of the following vehicle. Alternatively, headway and spacing parameters may be measured from the *back* of the leading vehicle to the *back* of the following vehicle (see *Figures 5.5 and 5.6 in Section 5*). Limited analysis of parameters using the latter method indicated that the difference between the two methods would not affect the conclusions of this report.

Recommendations for future research

Based on the findings of this study, the following are the recommendations for further research.

- (i) The database for queue discharge models and optimum loop length results has relatively few points, particularly for right-turn and paired intersection sites. Therefore, further surveys are recommended at paired (closely-spaced) intersection and CBD type intersection sites.

Right-turn traffic lanes surveyed in this study included single right-turn lanes only. Surveys at dual right-turn lane sites are recommended with a view to establishing differences in queue discharge parameters of the inside and outside lanes. This should include the consideration of separation distance from the right-turn movement from opposite direction under "diamond" turn arrangements. The effect of signal phasing (leading vs lagging turn arrow), turn radius, and angle of turn on queue discharge model parameters could also be investigated.

An investigation of the effect of the distance to the downstream intersection on queue discharge model parameters (without the effect of downstream queue interference) is recommended for paired intersection and CBD type intersection sites.

Surveys described in this report were carried out mostly during morning and afternoon peak periods. It would be useful to conduct surveys during day off-peak (business) periods at selected sites where morning and afternoon peak period surveys were carried out. The purpose of these additional surveys would be to investigate differences between peak and off-peak traffic characteristics.

Similarly, conducting surveys at the same site under adverse light and weather conditions (dark, rainy) would be useful in order to determine impact of such adverse conditions on queue discharge parameters. These surveys could be limited to the assessment of effects on jam spacing (or jam gap length) since this parameter is the main factor in optimum loop length determination.

- (ii) The survey method used during this study is very comprehensive and costly. Simple survey methods to measure saturation flow and saturation speed described in *Section 16* could be used to extend the data base.
- (iii) Regression equations given in *Section 16* for use in practice can be improved by extending the data base through further surveys.
- (iv) Heavy vehicle effects should be analysed, particularly with a view to the effect on jam spacing and jam gap length.
- (v) A simple procedure for use in practice can be developed to enable traffic engineers to determine optimum loop length for through and right-turn lanes. The procedure should require collection of minimal amount of data. For this purpose regression equations could be developed for use when a parameter is not known. The simplest method would be the use of reliable regression equations (based on a large database and structured to cover different site characteristics) to determine the optimum loop length from jam gap length (or jam spacing), similar to the method summarised in *Section 16*.

Cycle-by-cycle variations of the minimum queue discharge headway, the cycle capacity, and the space time at maximum queue discharge flow should be investigated further. In particular, investigation of the *variance to mean ratio of cycle capacity* is recommended since this is important in modelling traffic performance (delay, queue length and queue move-up rate) for signalised intersections, especially for coordinated signals.

- (vi) The exponential queue discharge speed model implies a non-linear decreasing acceleration model with the maximum acceleration rate at the start of the acceleration manoeuvre. The acceleration time (time to accelerate to the maximum queue discharge headway) implied by the model is large because of the exponential nature of the model. Adjusting the model parameter m_v to obtain decreased acceleration times results in too sharp an increase compared with measured speed - time data. Further research on acceleration characteristics at the signal stop line would be useful considering an S-shaped speed - time model such as the model described by Akçelik and Biggs (1987). However, the exponential queue discharge speed model is simpler to use and appears to be adequate for the purpose of this study.

REFERENCES

- AKÇELİK, R. (1981). *Traffic Signals: Capacity and Timing Analysis*. Research Report ARR No. 123 (6th reprint: 1995). ARRB Transport Research Ltd, Vermont South, Australia.
- AKÇELİK, R. (1991). Travel time functions for transport planning purposes: Davidson's function, its time-dependent form and an alternative travel time function. *Australian Road Research* 21 (3), pp. 49–59.
- AKÇELİK, R. (1995a). *Signal Timing Analysis for Vehicle-Actuated Control*. Working Paper No. WD TE 95/007. ARRB Transport Research Ltd, Vermont South, Australia.
- AKÇELİK, R. (1995b). *Extension of the Highway Capacity Manual Progression Factor Method for Platooned Arrivals*. Research Report ARR No. 276. ARRB Transport Research Ltd, Vermont South, Australia.
- AKÇELİK, R. (1996). Relating flow, density, speed and travel time models for uninterrupted and interrupted traffic. *Traffic Engineering and Control* 37(9), pp. 511-516.
- AKÇELİK, R. (1997). Fundamental traffic variables in adaptive control and the SCATS DS parameter. *Proc. Third International Conference of ITS Australia (ITSA 97), Brisbane (CD)*.
- AKÇELİK, R. (1998). *Interchange Capacity and Performance Model for HCM 2000*. Technical Note. ARRB Transport Research Ltd, Vermont South, Australia.
- AKÇELİK, R. and BESLEY, M. (1996) *Fundamental Traffic Flow Relationships at Signalised Intersection Stop-Line*. Working Paper No. WD R 96/043. ARRB Transport Research Ltd, Vermont South, Australia.
- AKÇELİK, R. and BESLEY M. (1999). *SIDRA 5 User Guide (for version 5.2)*. ARRB Transport Research Ltd, Vermont South, Australia.
- AKÇELİK, R. and BIGGS, D.C. (1987). Acceleration profile models for vehicles in road traffic. *Transportation Science*, 21(1), pp. 36-54.
- AKÇELİK, R. and ROPER, R. (1998) *Fundamental Relationships for Adaptive Control: Survey Method*. Working Paper No. WD R 98/015. ARRB Transport Research Ltd, Vermont South, Australia.
- AKÇELİK, R., ROPER, R. and BESLEY M. (1998). *Fundamental Relationships for Adaptive Control: Survey Results for Sydney and Melbourne Sites*. Working Paper No. WD R 98/041. ARRB Transport Research Ltd, Vermont South, Australia.
- AKÇELİK, R., ROPER, R. and BESLEY M. (1999a). *Fundamental Relationships for Adaptive Control: Further Data Analysis and Optimum Loop Length*. Contract Report RC 7057. ARRB Transport Research Ltd, Vermont South, Australia.

- AKÇELİK, R., ROPER, R. and BESLEY M. (1999b). *Fundamental Relationships for Freeway Traffic Flows*. Research Report ARR 341. ARRB Transport Research Ltd, Vermont South, Australia.
- AUSTROADS (1988). *Traffic Surveys*. Guide to Traffic Engineering Practice, Part 3. Association of Australian State Road and Traffic Authorities, Sydney.
- AUSTROADS (1993). *Traffic Signals – A Guide to the Design of Traffic Signal Installations*. Guide to Traffic Engineering Practice, Part 7. Association of Australian State Road and Traffic Authorities, Sydney.
- BONNESON, J.A. (1992a). Modeling queued driver behaviour at signalised junctions. *Transportation Research Record* 1365, pp. 99-107.
- BONNESON, J.A. (1992b). Study of headway and lost time at single-point urban interchanges. *Transportation Research Record* 1365, pp. 30-39.
- BTCE (BUREAU OF TRANSPORT AND COMMUNICATIONS ECONOMICS) (1996). *Traffic Congestion and Road-User Charges in Australian capital Cities*. BTCE Report No. 92. Australian Government Publishing Service, Canberra.
- DOWLING, R.G., SINGH, R. and CHENG, W.W.K. (1998). The accuracy and performance of improved speed-flow curves. *Road and Transport Research* 7(2), pp. 36-51.
- DREW, D.R. (1968). *Traffic Flow Theory and Control*. McGraw-Hill, New York.
- FEHON, K.J. and MOORE, S.E. (1982). Dynamic control of a medium sized traffic signal network. *Proc. ARRB 11th* , 11 (4), pp. 85-93. ARRB Transport Research Ltd, Vermont South, Australia.
- JOHNSON, B. and AKÇELİK, R. (1992). Review of analytical software for applicability to paired intersections. *Proc. 16th ARRB Conf.* 16 (5), pp. 347-367. ARRB Transport Research Ltd, Vermont South, Australia.
- LAY, M.G. (1979). *A Speed-Flow Relationship Based on Recent Driver-Vehicle Data*. Internal Report AIR 000-126. ARRB Transport Research Ltd, Vermont South, Australia.
- LAY, M.G. (1985). *Source Book for Australian Roads (3rd Edition)*. ARRB Transport Research Ltd, Vermont South, Australia.
- LESCHINSKI, R.E. (1994). Evaluation of inductive loops for bicycle detection. *Proc. ARRB Transport Research 17th Conf.* 17 (5), pp. 119-131. ARRB Transport Research Ltd, Vermont South, Australia.
- LESCHINSKI, R. and ROPER, R. (1993). *VDAS Manual (VDAS 2000 and 3000 Vehicle Counter and Classifier)*. ARRB Transport Research Ltd, Vermont South, Australia.

- LOWRIE, P. (1982). The Sydney Coordinated Adaptive Traffic System - principles, methodology, algorithms. *Proc. International Conference on Road Traffic Signalling*. Institution of Electrical Engineers, London, pp. 67-70.
- LOWRIE, P. (1984). *Estimation of green time utilisation at traffic signals*. Technical Note (unpublished). Roads and Traffic Authority of New South Wales, Sydney.
- LOWRIE, P. (1990). *SCATS - A Traffic Responsive Method of Controlling Urban Traffic*. Roads and Traffic Authority of New South Wales, Sydney.
- LOWRIE, P. (1996). Freeway ramp metering systems. Paper presented at the *ITE Inaugural Regional Conference Transport and Livable Cities*, Melbourne. Roads and Traffic Authority of New South Wales, Sydney.
- MAY, A.D. (1990). *Traffic Flow Fundamentals*. Prentice-Hall, Englewood Cliffs, N.J.
- MESSER, C.J. and BONNESON, J.A. (1997). *Capacity Analysis of Interchange Ramp Terminals*. Final Report for National Cooperative Highway Research Program Project 3-47. Texas A & M Research Foundation TAMURF 7241. Texas, USA.
- MORRIS, D.J., DEAN, K.G. and HULSCHER, F.R. (1984). Development of an optimum loop configuration. *Proc. ARRB 12th Conf.* 12 (5), pp. 26-33. ARRB Transport Research Ltd, Vermont South, Australia.
- NIITTYMÄKI, J. and PURSULA, M. (1997). Saturation flows at signal-group-controlled traffic signals. *Transportation Research Record* 1572, pp. 24-32.
- NORUSIS, M.J. and SPSS Inc. (1993). *SPSS for Windows Advanced Statistics*, Release 6.0. SPSS Inc., Chicago.
- PROSSER, N. and DUNNE, M. (1994). A procedure for estimating movement capacities at signalised paired intersections. In: *Proceedings of the Second International Symposium on Highway Capacity*, Sydney, 1994 (Edited by R. Akçelik), Volume 2, pp. 473-492. ARRB Transport Research Ltd, Vermont South, Australia.
- ROUPHAIL, N.M. and AKÇELIK, R. (1991). *Paired Intersections: Initial Development of Platooned Arrival and Queue Interaction Models*. Working Paper WD TE 91/010. ARRB Transport Research Ltd, Vermont South, Australia.
- ROUPHAIL, N.M. and AKÇELIK, R. (1992). A preliminary model of queue interaction at signalised paired intersections. *Proc. 16th ARRB Conf.* 16 (5), pp. 325-345. ARRB Transport Research Ltd, Vermont South, Australia.
- RTA NSW (1991). *Traffic Signal Operation*. Manual RTA-TC-106. Roads and Traffic Authority of New South Wales, Sydney.
- TARKO, A. and RAJARAMAN, G. (1998). Effect of metering, splitting and merging on control delays in signalized networks.. In: *Proc. Third International Symposium on Highway Capacity*, Copenhagen, 1998 (Edited by R. Rysgaard), Volume 2, pp. 1007-1025. Road Directorate, Denmark.

TEPLY, S., ALLINGHAM, D.I., RICHARDSON, D.B. and STEPHENSON, B.W. (1995). *Canadian Capacity Guide for Signalised Intersections*. Institute of Transportation Engineers District 7 - Canada. 2nd edition.

TEPLY, S. and JONES, A.M. (1991). Saturation flow: Do we speak the same language? *Transportation Research Record* 1320, pp. 144-153.

TRANSPORTATION RESEARCH BOARD (1975). *Traffic Flow Theory*. Special Report 165. National Research Council, Washington, D.C., U.S.A.

TRANSPORTATION RESEARCH BOARD (1998). *Highway Capacity Manual*. Special Report 209 (Third edition: "1997 version"). National Research Council, Washington, D.C., U.S.A.

WARDROP, J.G. (1965). Experimental speed-flow relations in a single lane. In: Almond, J. (Ed.), *Proceedings of the Second International Symposium on the Theory of Road Traffic Flow*, London, 1963. OECD, Paris, pp. 104-109.

WEBSTER, F.V. and COBBE, B.M. (1966). *Traffic Signals*. HMSO, London.

APPENDIX A

SCATS Intersection Geometry and Phasing Diagrams for Sydney and Melbourne 1998 Survey Sites

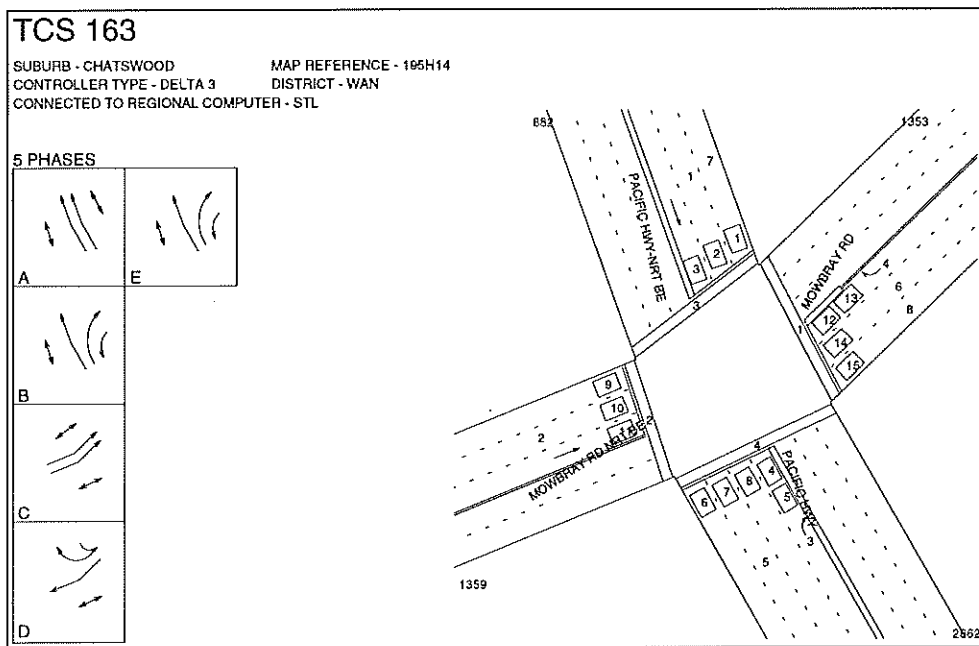


Figure A.1 – SCATS intersection geometry and phasing diagrams for Site 163: Pacific Highway - Mowbray Rd (Chatswood, Sydney) - right-turn lane (Lane 4) on Pacific Highway South approach

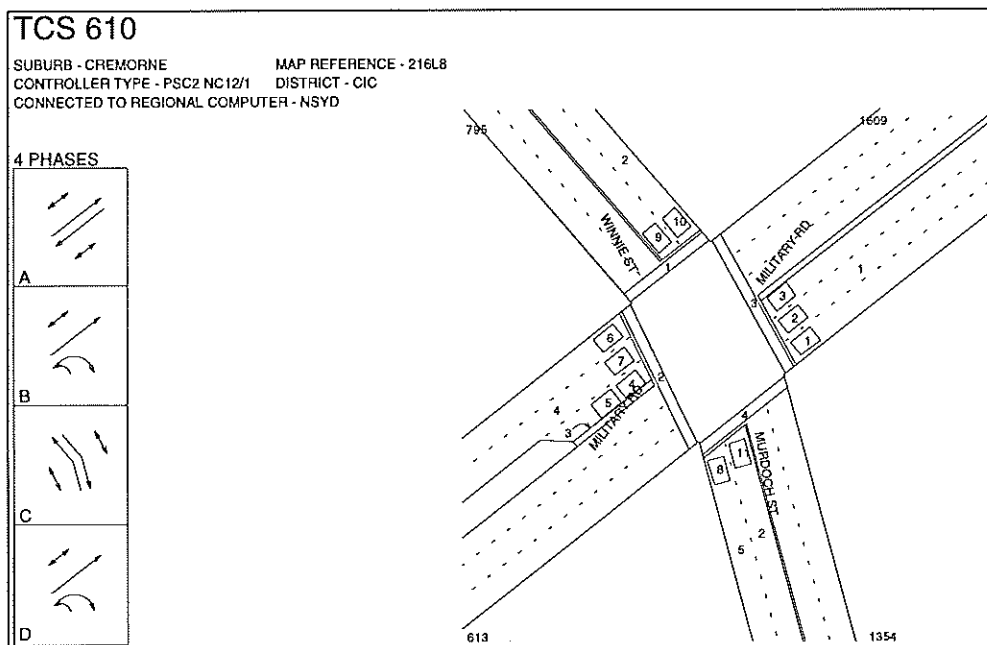
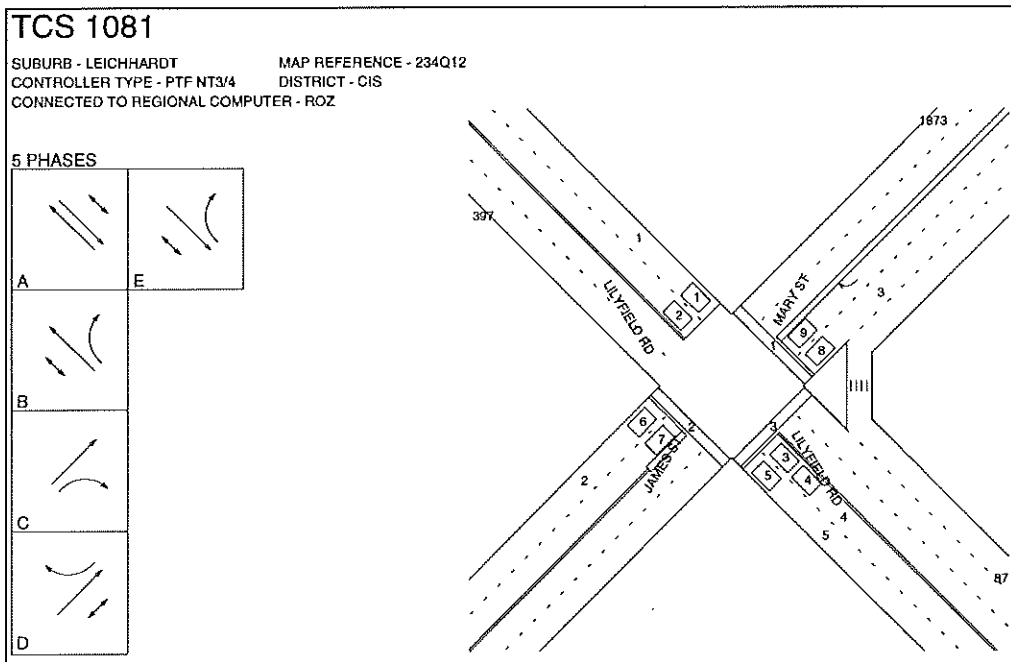
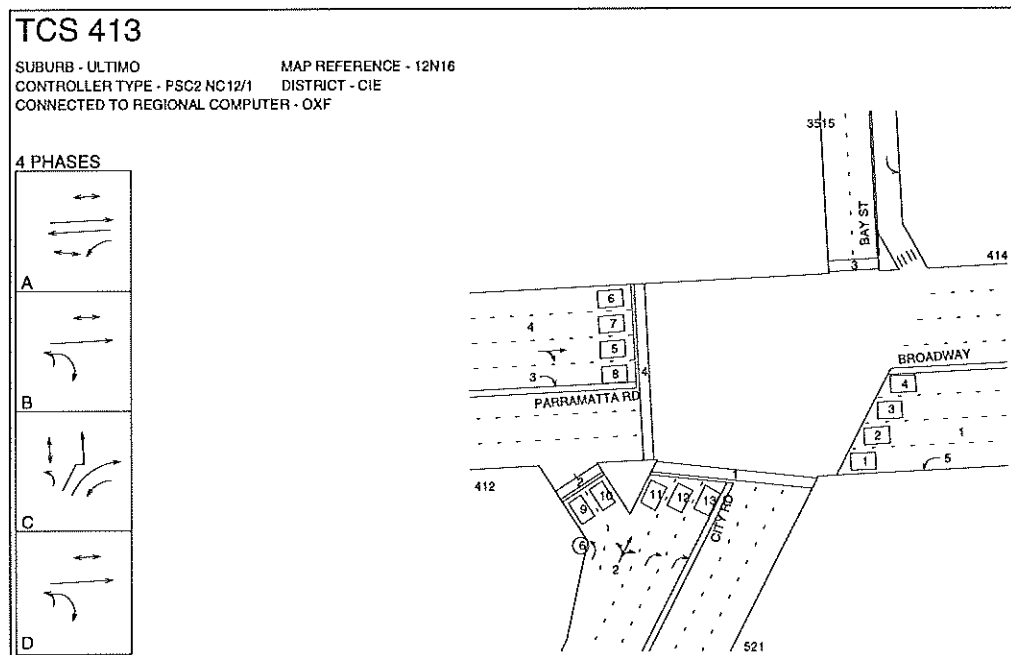


Figure A.2 – SCATS intersection geometry and phasing diagrams for Site 610: Military Road - Murdoch Street (Cremorne, Sydney) - right-turn lane (Lane 3) on Military Road West approach



**Figure A.3 – SCATS intersection geometry and phasing diagrams for Site 1081:
 Lilyfield Road - Mary Street - James Street (Lilyfield, Sydney) -
 through lane (Lane 2) on Lilyfield Road Northwest approach**



**Figure A.4 – SCATS intersection geometry and phasing diagrams for Site 413:
 Broadway - City Road (Ultimo, Sydney) -
 through lane (Lane 3) on Broadway East approach**

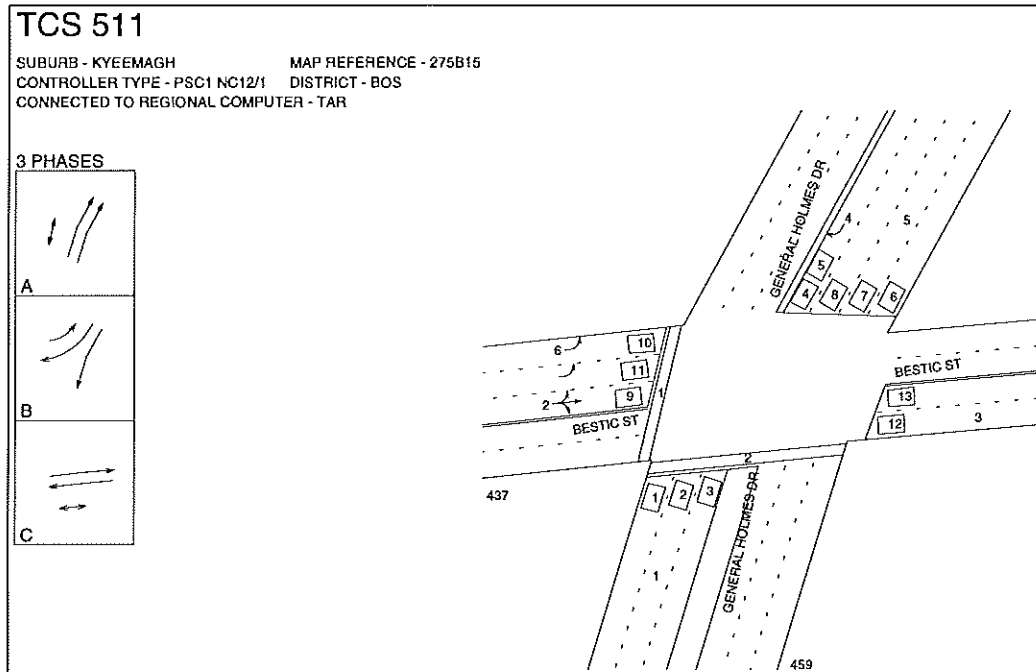


**Figure A.5 – SCATS intersection geometry and phasing diagrams for Site 511:
General Holmes Drive - Bestic Street (Kyeemagh, Sydney) -
through lane (Lane 2) on General Holmes Drive South approach**

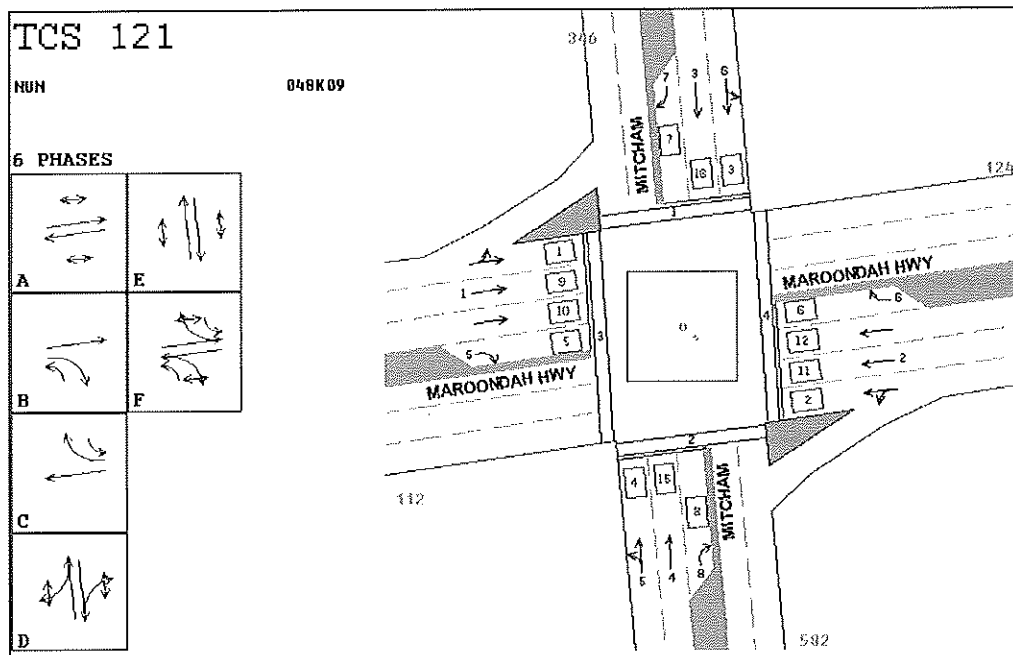


Figure A.6 – SCATS intersection geometry and phasing diagrams for Site 121: Maroondah Highway - Mitcham Road (Mitcham, Melbourne) - right-turn lane (Lane 4) on Maroondah Highway East approach

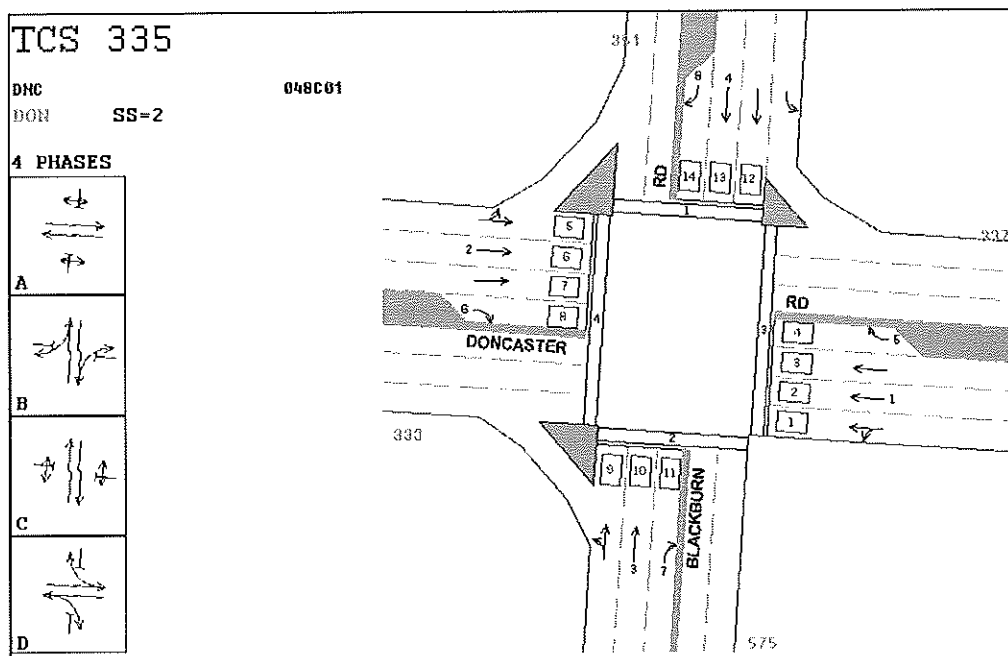


Figure A.7 – SCATS intersection geometry and phasing diagrams for Site 335: Doncaster Road - Blackburn Road (East Doncaster, Melbourne) - right-turn lane (Lane 4) on Doncaster Road East approach

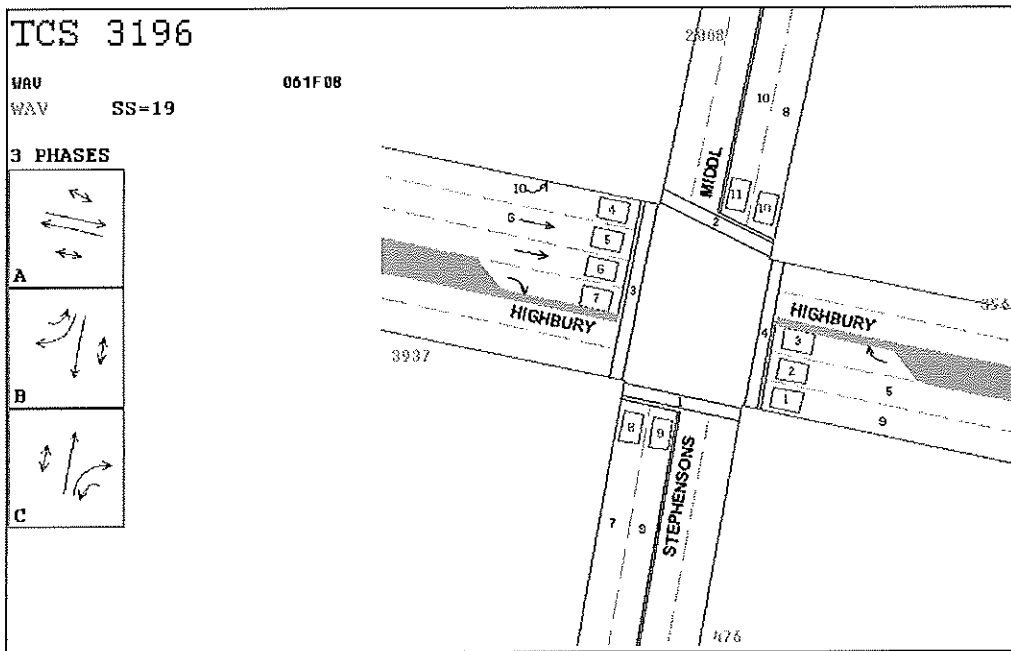


Figure A.8 – SCATS intersection geometry and phasing diagrams for Site 3196: Middleborough Road - Highbury Road (East Burwood, Melbourne) - through and left-turn lane (Lane 1) on Middleborough Road North approach

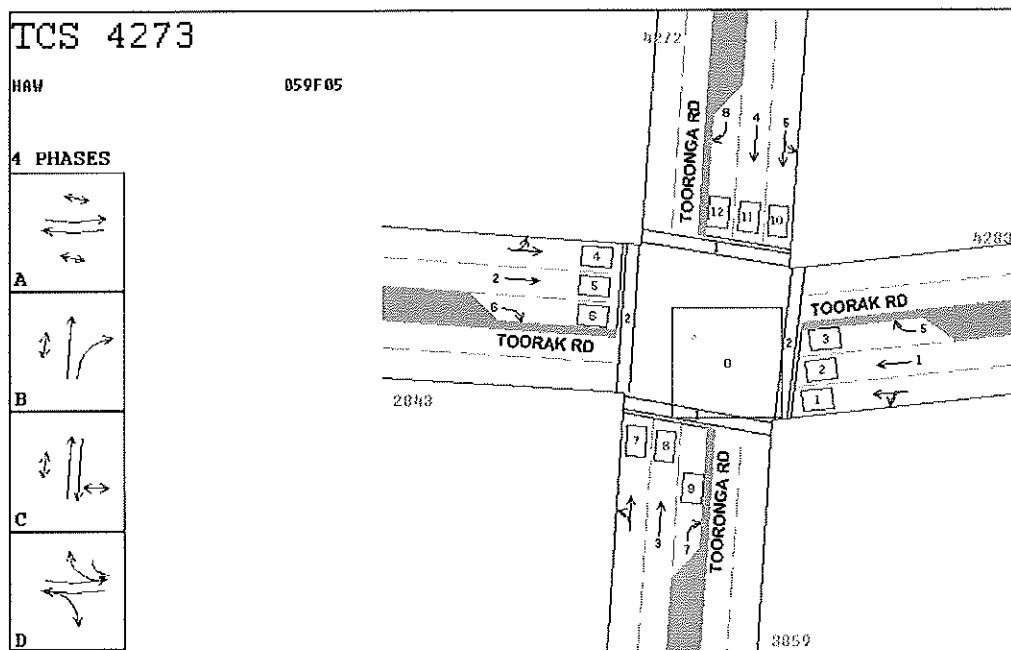


Figure A.9 – SCATS intersection geometry and phasing diagrams for Site 4273: Toorak Road - Toorong Road (Hawthorn East, Melbourne) - through lane (Lane 2) on Toorak Road West approach

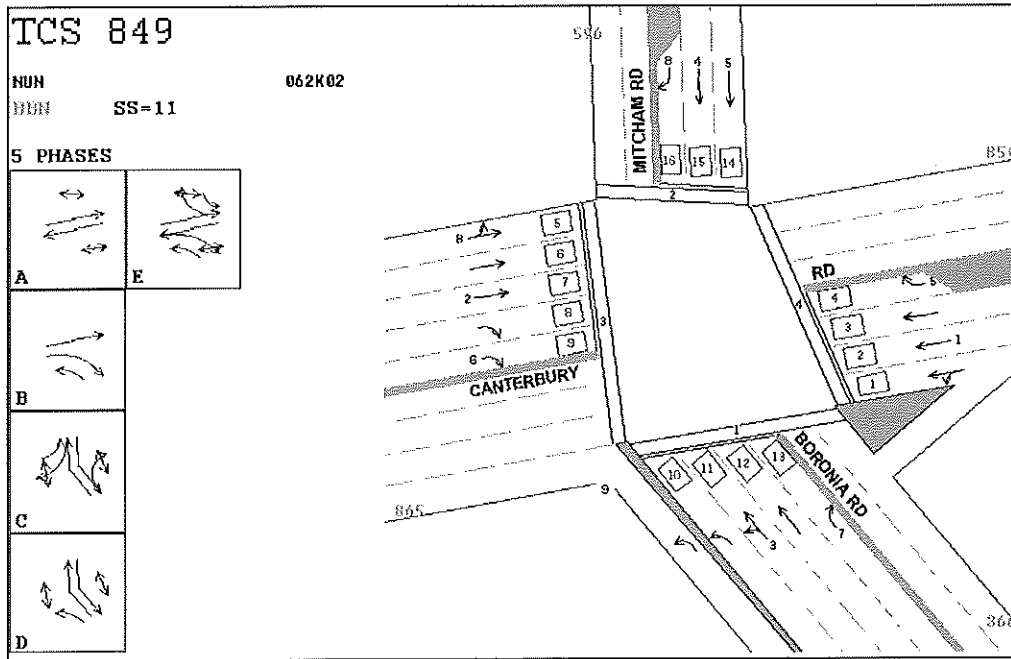


Figure A.10 – SCATS intersection geometry and phasing diagrams for Site 849: Canterbury Road - Mitcham Road (Vermont, Melbourne) - through lane (Lane 2) on Canterbury Road West approach

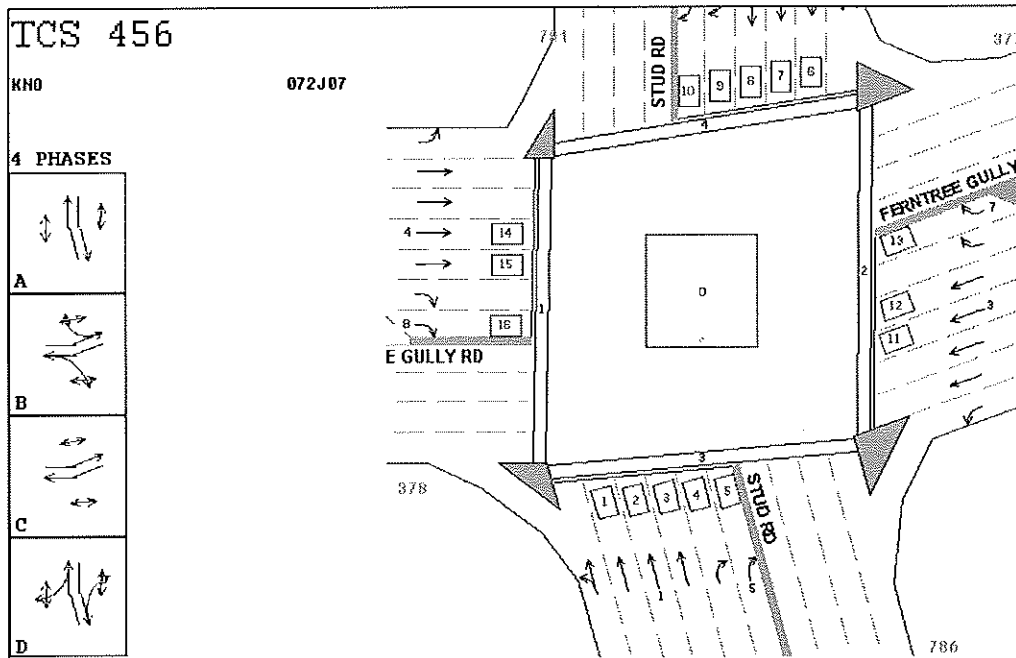


Figure A.11 – SCATS intersection geometry and phasing diagrams for Site 456: Ferntree Gully Road - Stud Road (Scoresby, Melbourne) - through lane (Lane 4) on Ferntree Gully Road West approach

APPENDIX B

Figures Showing Measured and Predicted Queue Discharge Speeds, Headways, Spacings and Flow Rates for Sydney and Melbourne 1998 Survey Sites

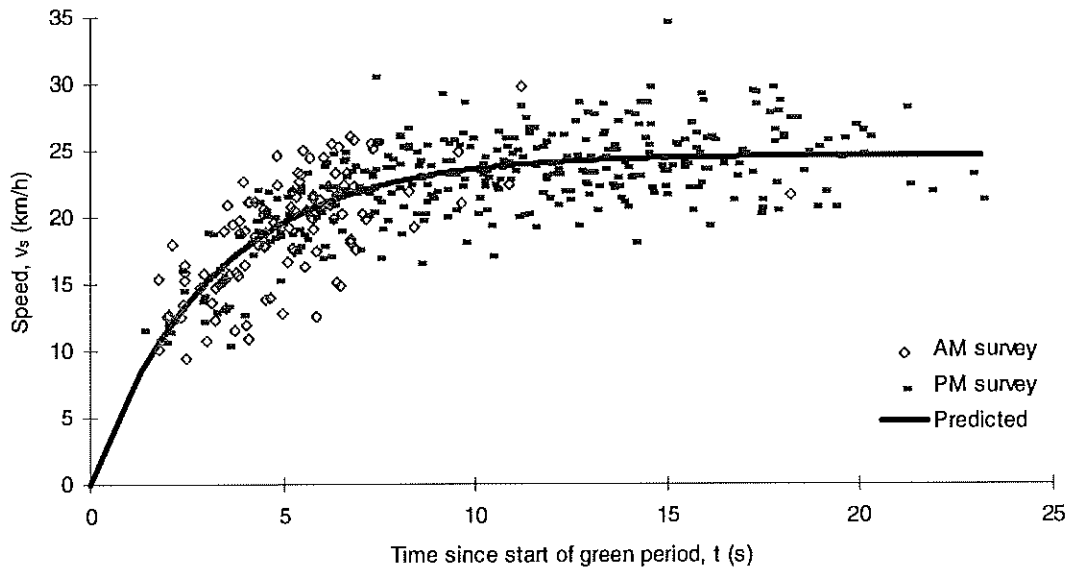
**Site 163: Pacific Hwy and Mowbray Rd in Chatswood, Sydney
(Right-Turn Isolated)**

Figure B.1a – Measured and predicted queue discharge speeds for Site 163

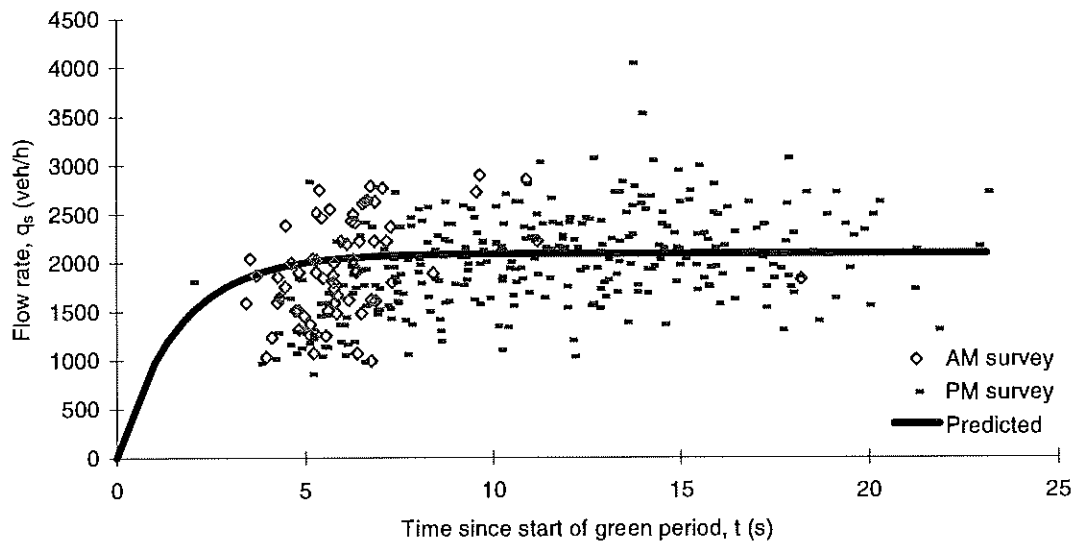


Figure B.1b – Measured and predicted queue discharge flow rates for Site 163

**Site 163: Pacific Hwy and Mowbray Rd in Chatswood, Sydney
(Right-Turn Isolated)**

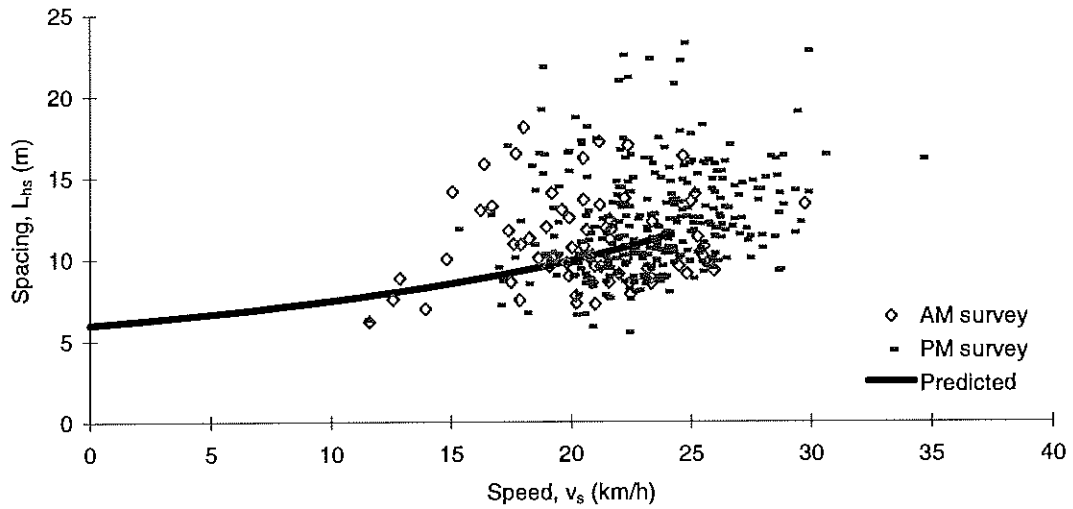


Figure B.1c – Vehicle spacing as a function of queue discharge speed for Site 163

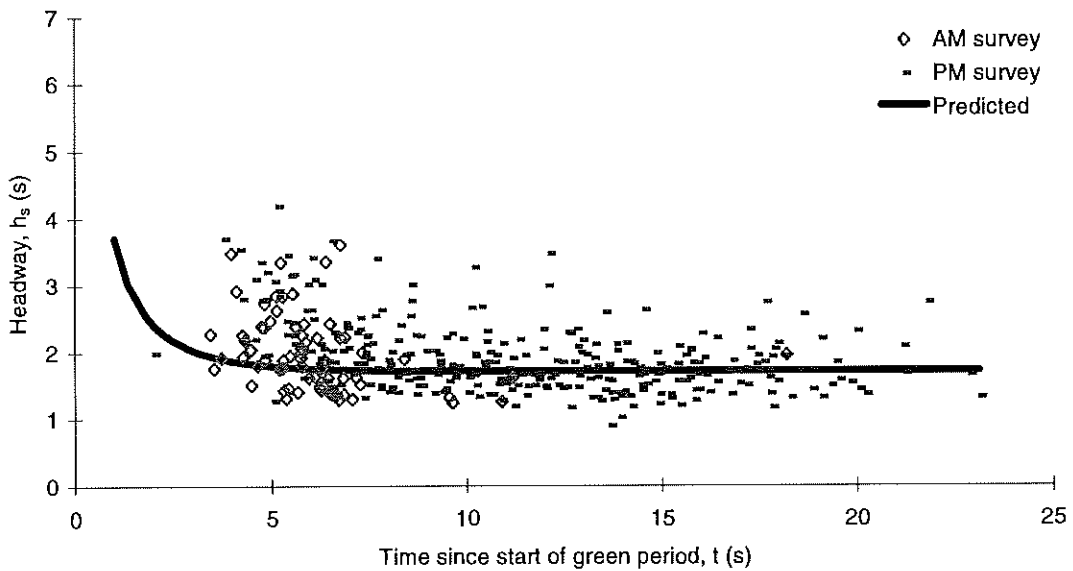


Figure B.1d – Measured and predicted queue discharge headways for Site 163

**Site 610: Military Rd. and Murdoch St. in Cremorne, Sydney
(Right-Turn Isolated)**

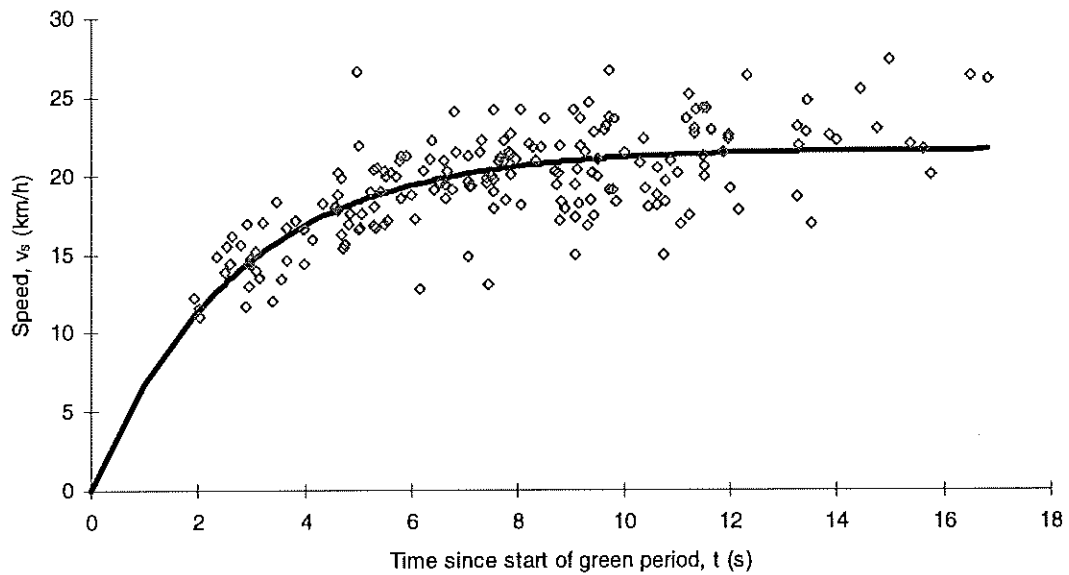


Figure B.2a – Measured and predicted queue discharge speeds for Site 610

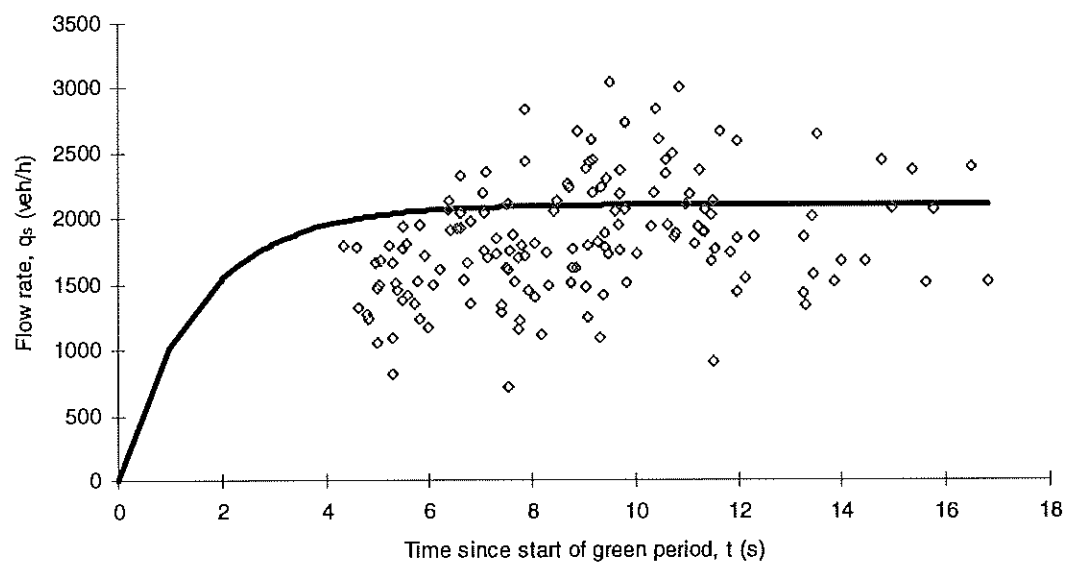


Figure B.2b – Measured and predicted queue discharge flow rates for Site 610

**Site 610: Military Rd. and Murdoch St. in Cremorne, Sydney
(Right-Turn Isolated)**

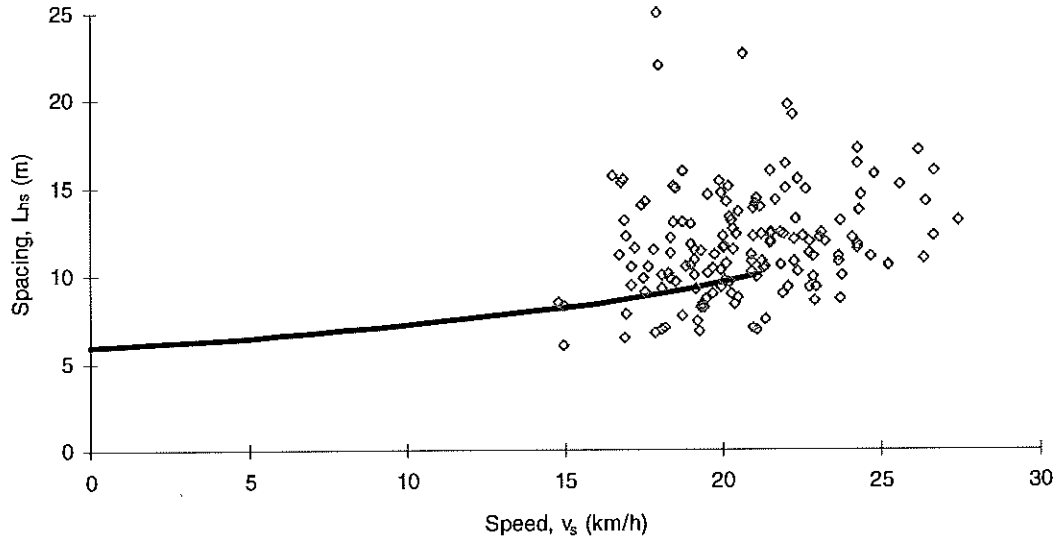


Figure B.2c – Vehicle spacing as a function of queue discharge speed for Site 610

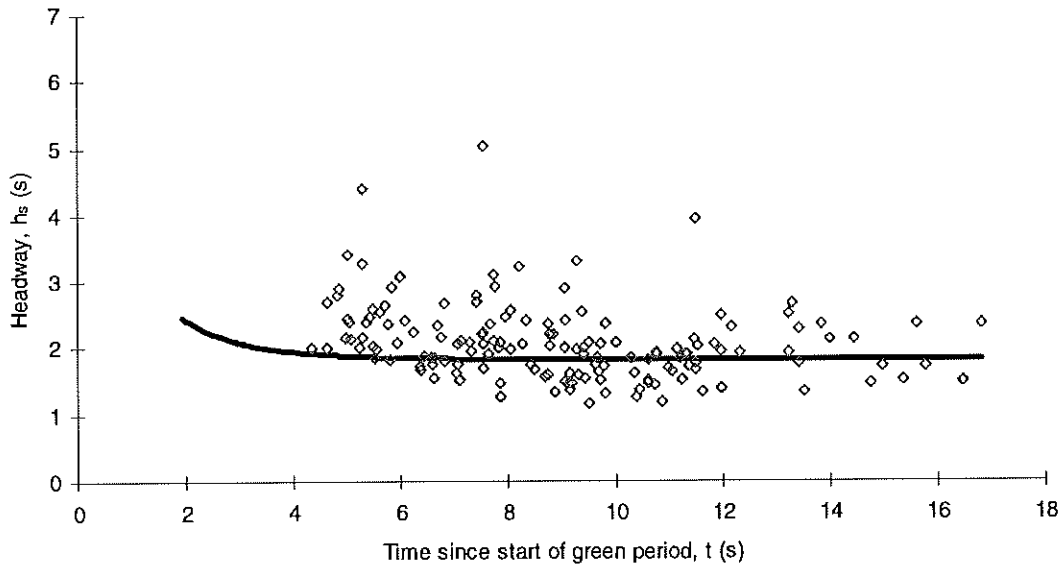


Figure B.2d – Measured and predicted queue discharge headways for Site 610

**Site 1081: Lilyfield Rd. and James St. in Lilyfield, Sydney
(Through Isolated)**

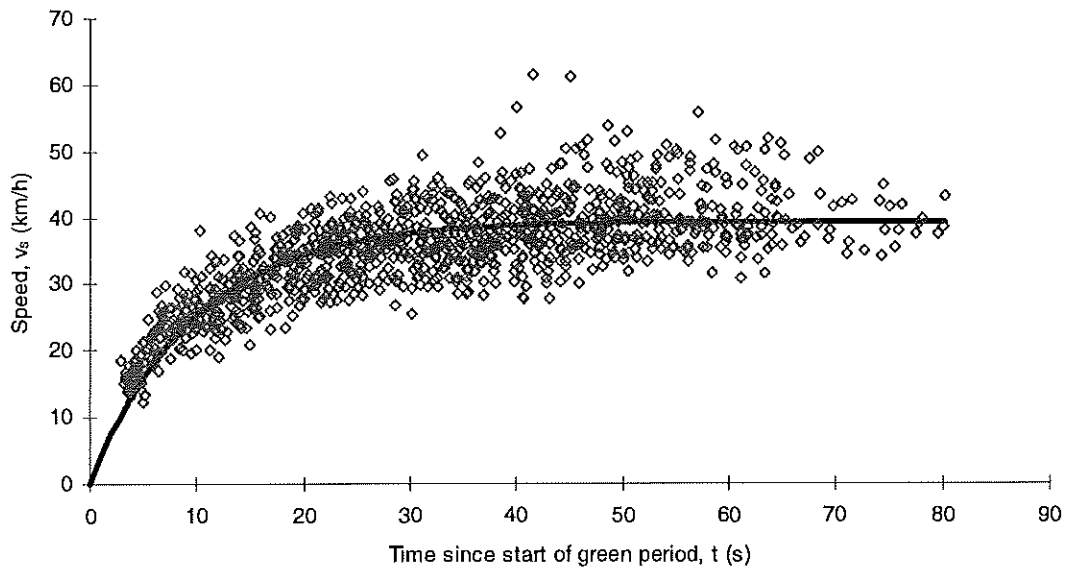


Figure B.3a – Measured and predicted queue discharge speeds for Site 1081

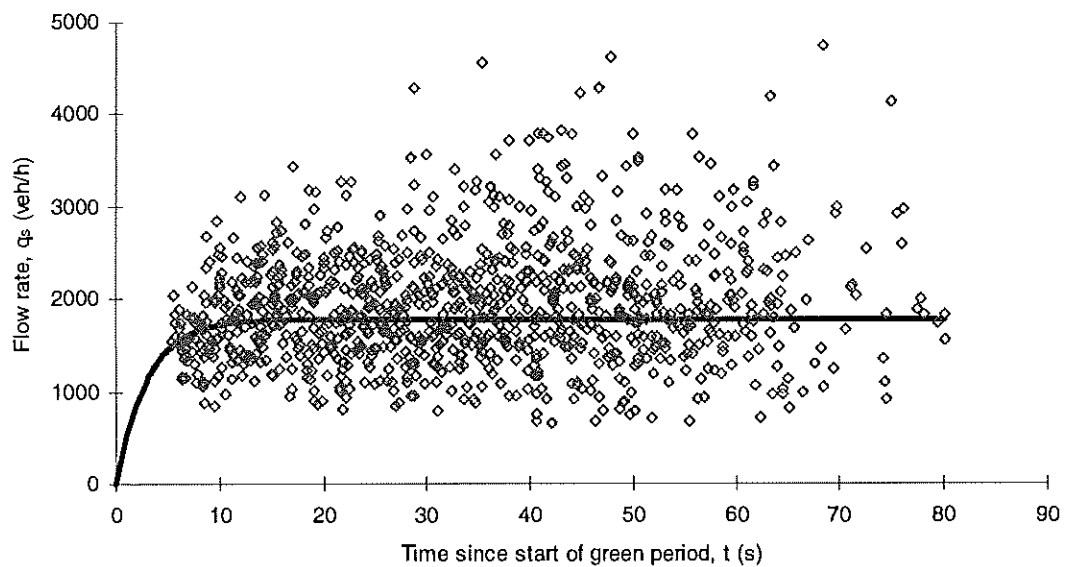


Figure B.3b – Measured and predicted queue discharge flow rates for Site 1081

**Site 1081: Lilyfield Rd. and James St. in Lilyfield, Sydney
(Through Isolated)**

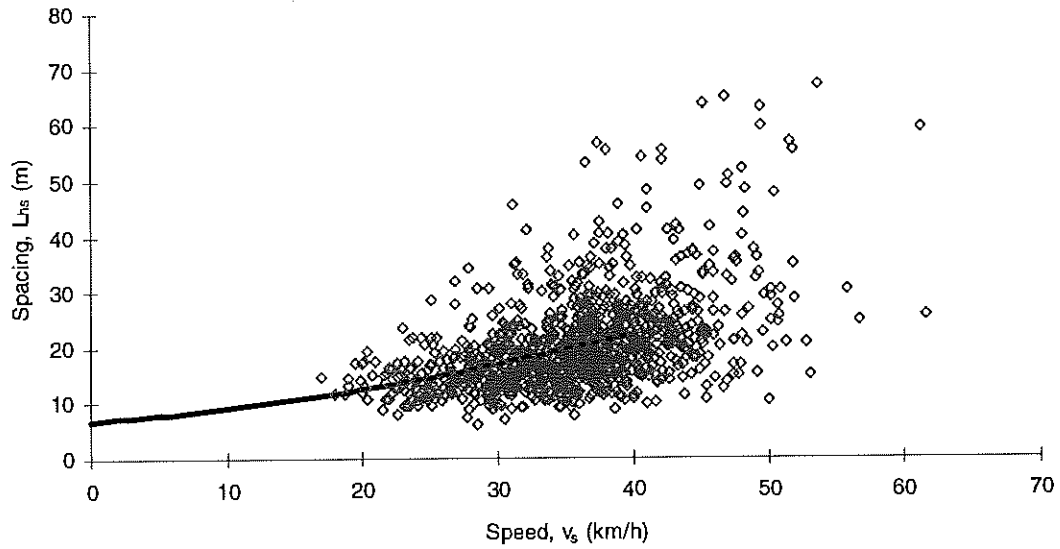


Figure B.3c – Vehicle spacing as a function of queue discharge speed for Site 1081

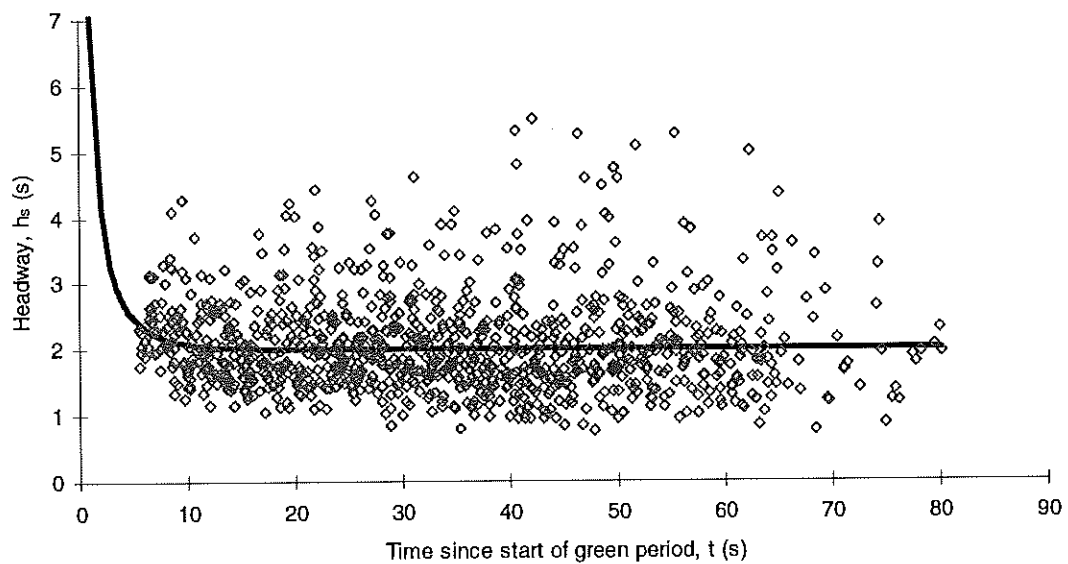


Figure B.3d – Measured and predicted queue discharge headways for Site 1081

**Site 413: Broadway and City Rd. in Broadway, Sydney
(Through Isolated)**

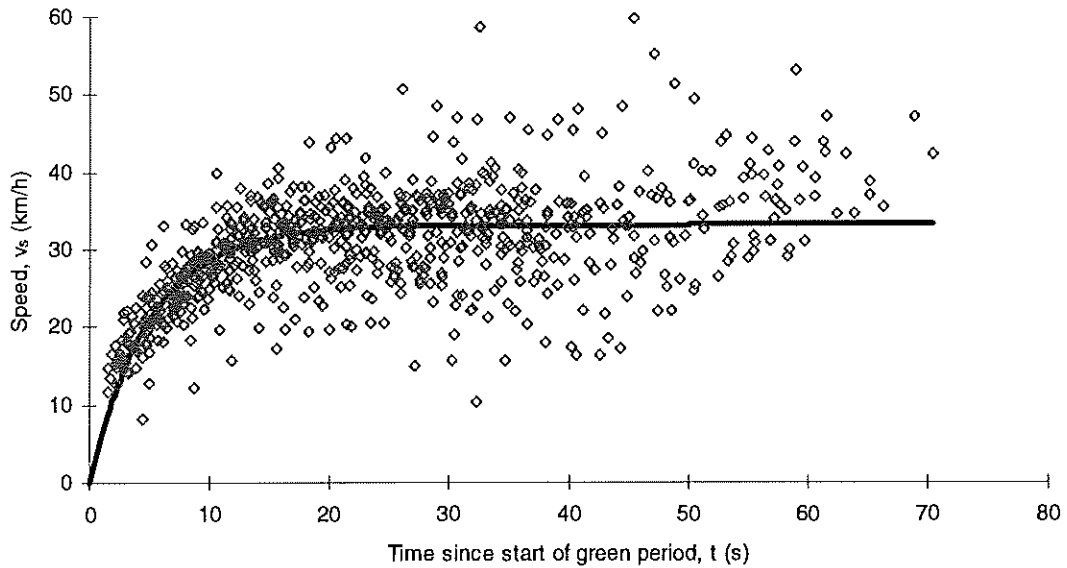


Figure B.4a – Measured and predicted queue discharge speeds for Site 413

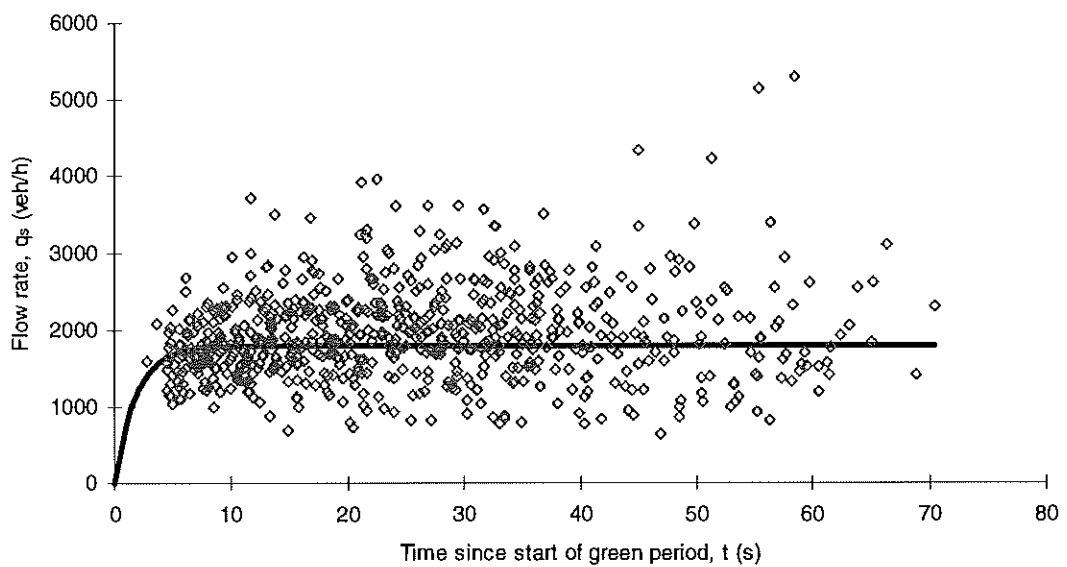


Figure B.4b – Measured and predicted queue discharge flow rates for Site 413

**Site 413: Broadway and City Rd. in Broadway, Sydney
(Through Isolated)**

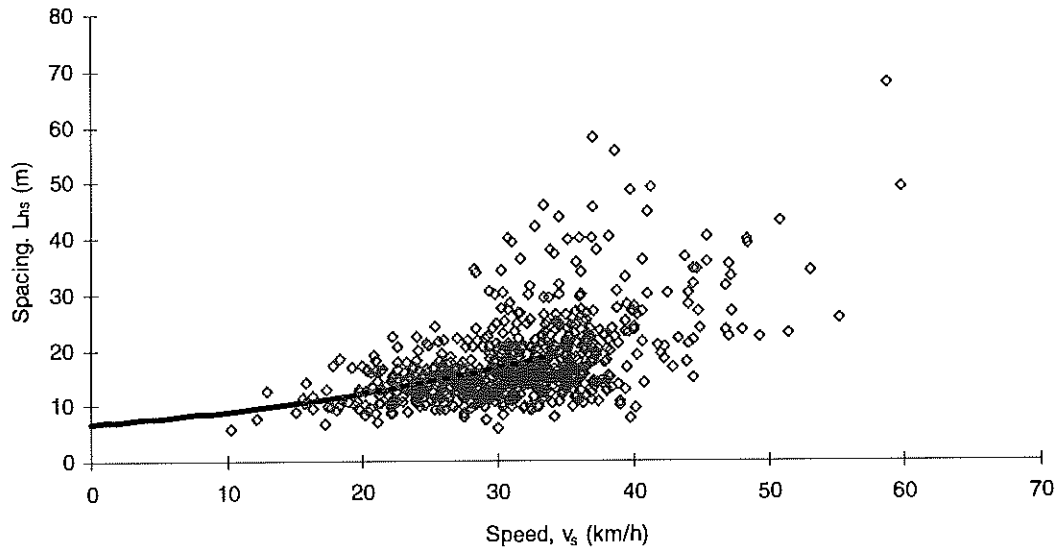


Figure B.4c – Vehicle spacing as a function of queue discharge speed for Site 413

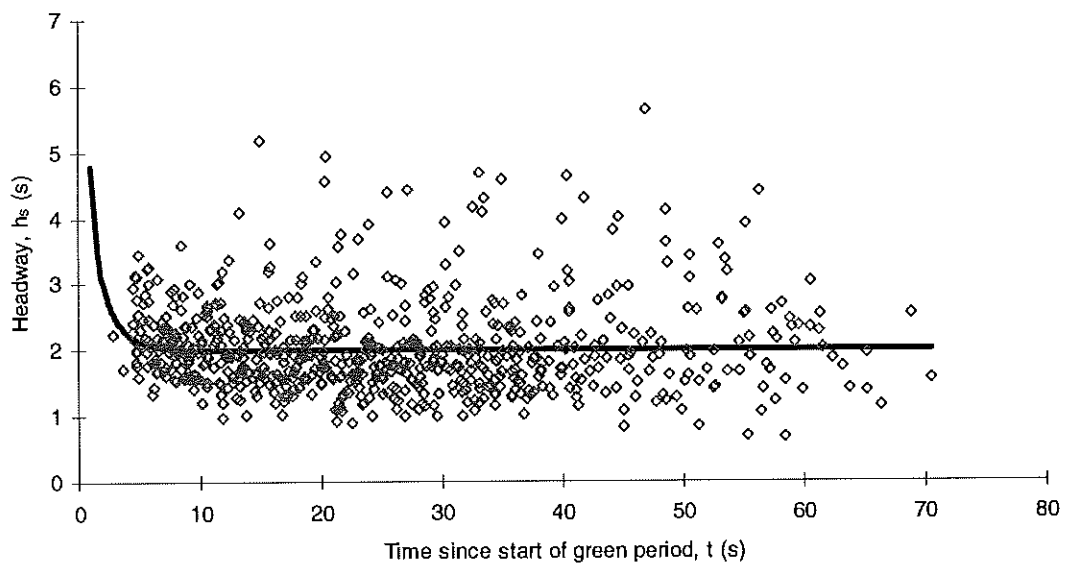


Figure B.4d – Measured and predicted queue discharge headways for Site 413

**Site 511: General Holmes Dve and Bestic St. in Kyeemagh, Sydney
(Through Isolated)**

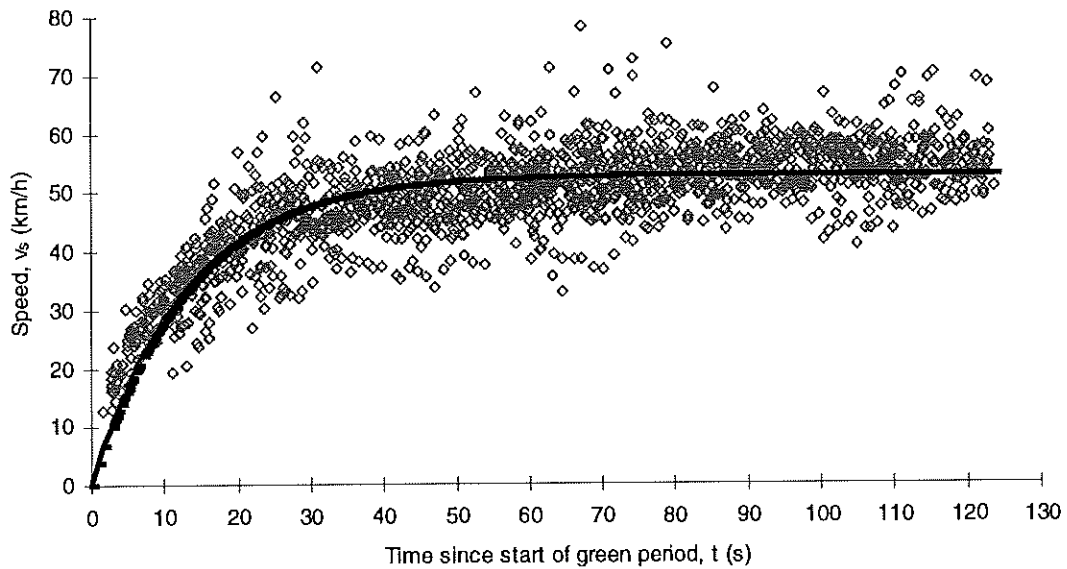


Figure B.5a – Measured and predicted queue discharge speeds for Site 511

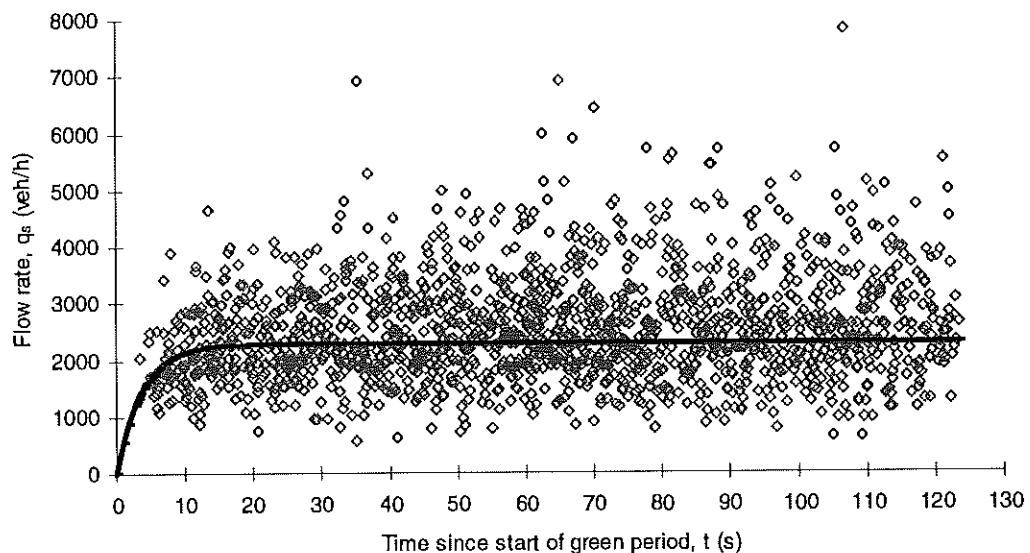


Figure B.5b – Measured and predicted queue discharge flow rates for Site 511

**Site 511: General Holmes Dve and Bestic St. in Kyeemagh, Sydney
(Through Isolated)**

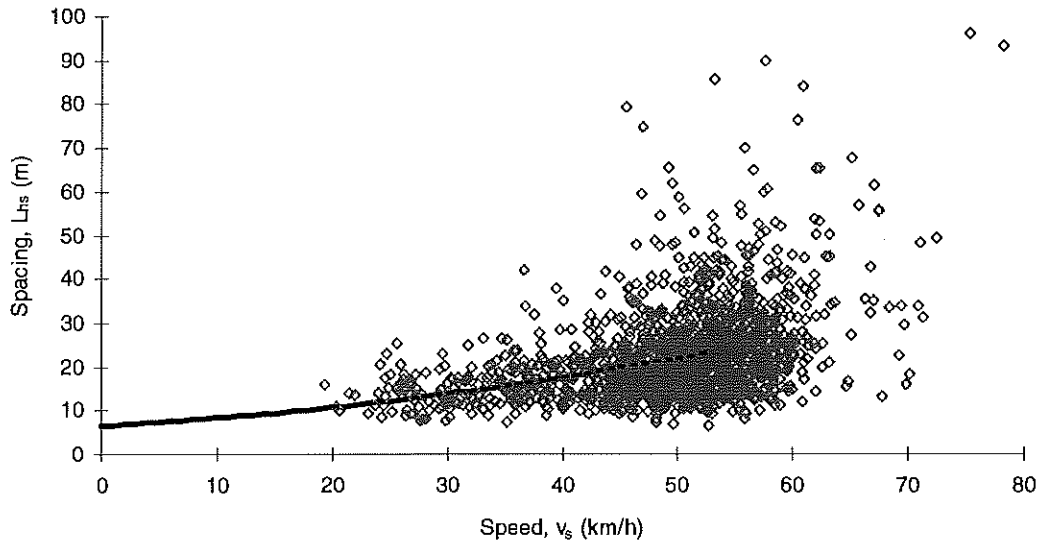


Figure B.5c – Vehicle spacing as a function of queue discharge speed for Site 511

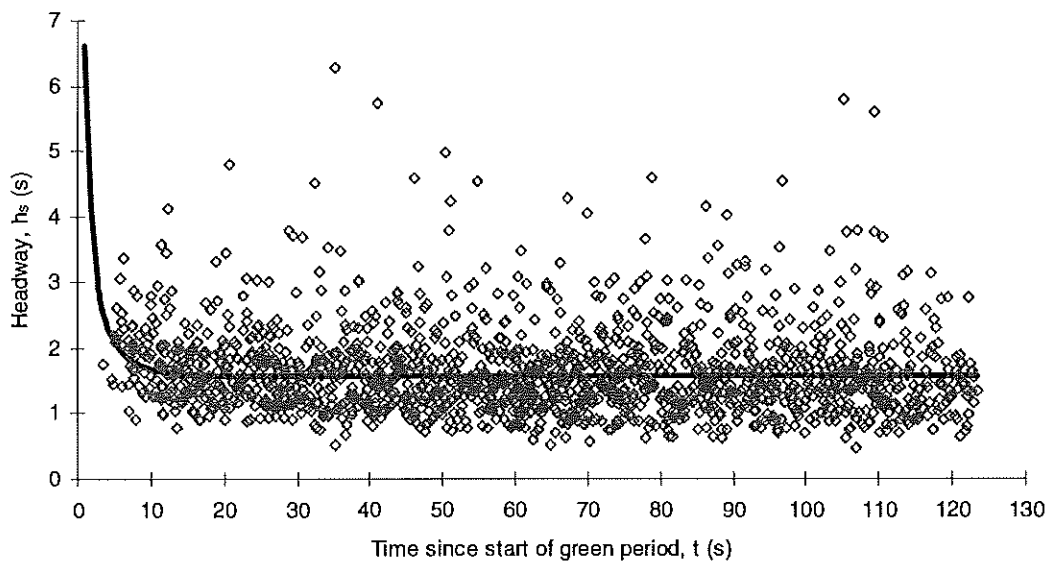


Figure B.5d – Measured and predicted queue discharge headways for Site 511

**Site 121: Maroondah Hwy and Mitcham Rd in Mitcham, Melbourne
(Right-Turn Isolated)**

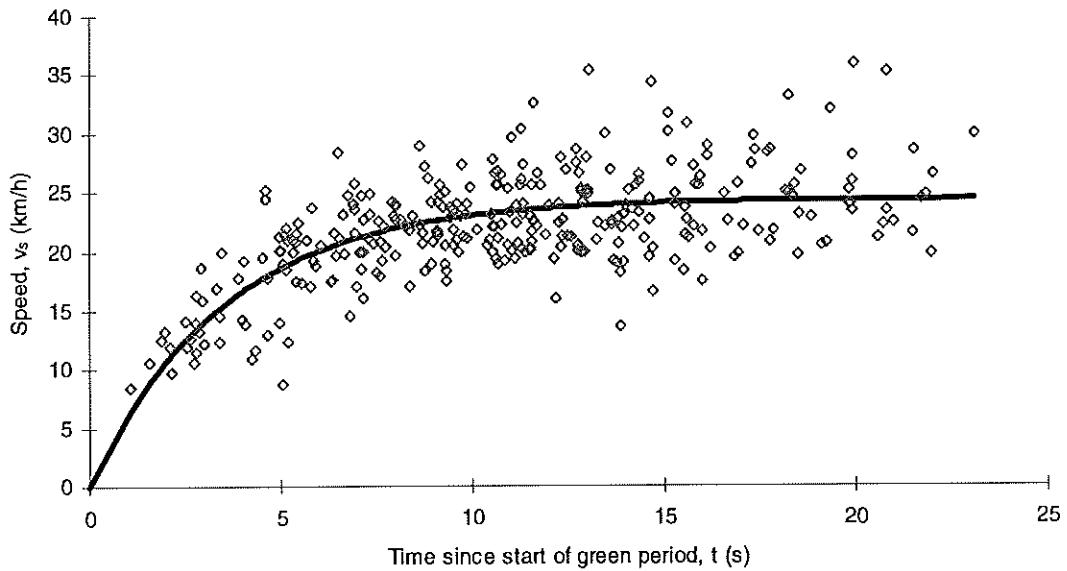


Figure B.6a – Measured and predicted queue discharge speeds for Site 121

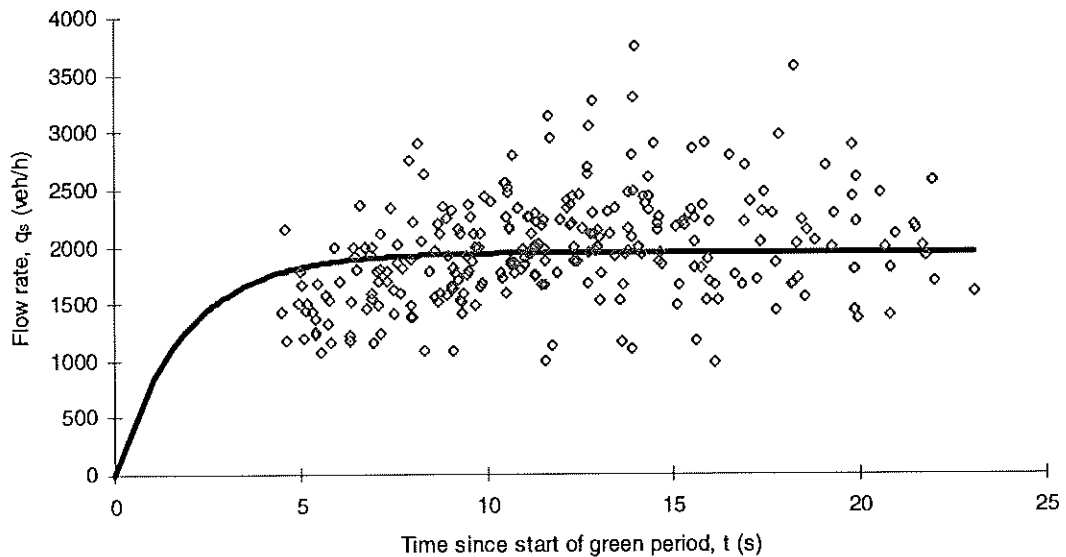


Figure B.6b – Measured and predicted queue discharge flow rates for Site 121

**Site 121: Maroondah Hwy and Mitcham Rd in Mitcham, Melbourne
(Right-Turn Isolated)**

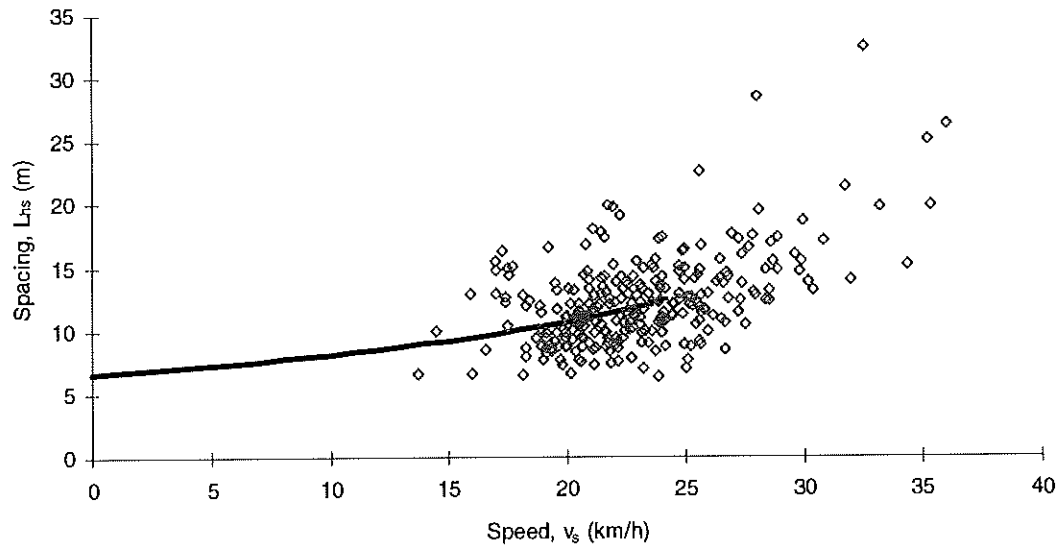


Figure B.6c – Vehicle spacing as a function of queue discharge speed for Site 121

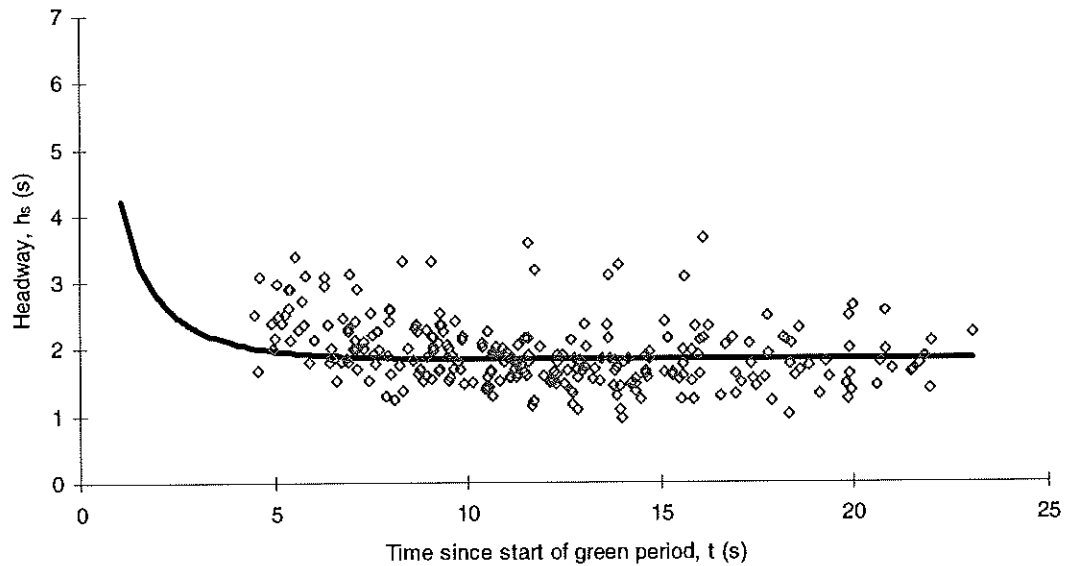


Figure B.6d – Measured and predicted queue discharge headways for Site 121

**Site 335: Doncaster Rd and Blackburn Rd in East Doncaster, Melbourne
(Right-Turn Isolated)**

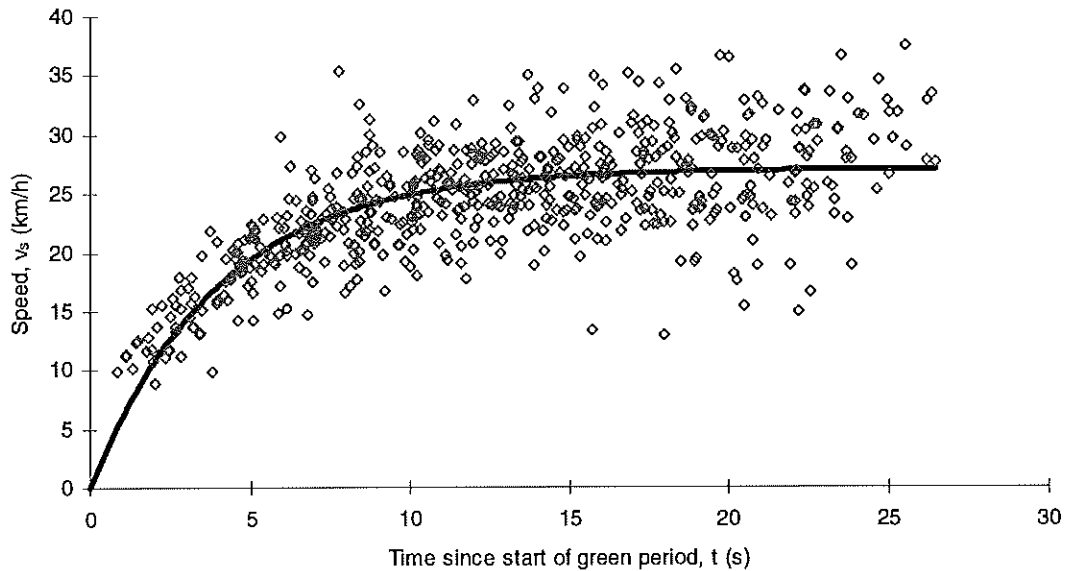


Figure B.7a – Measured and predicted queue discharge speeds for Site 335

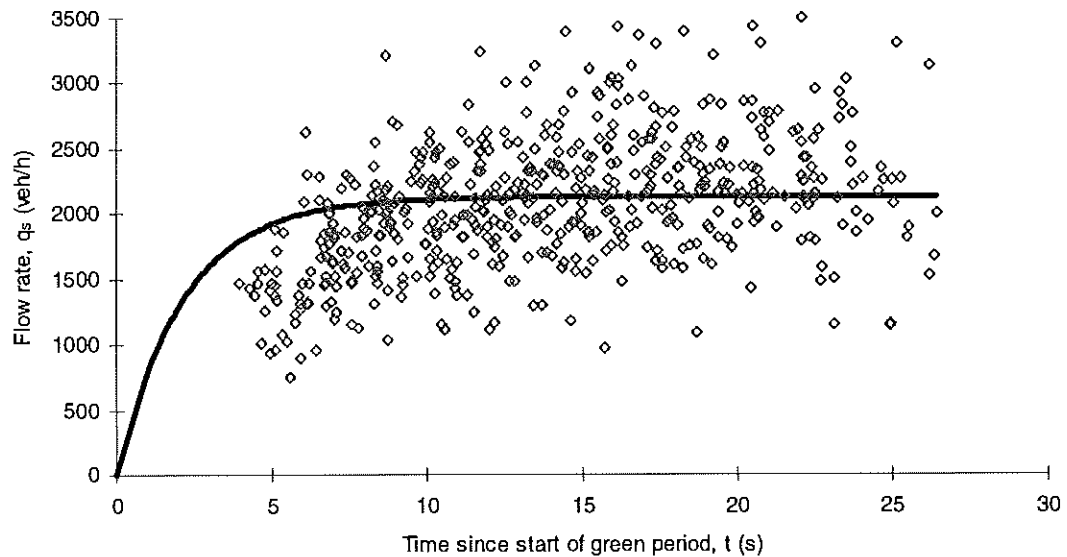


Figure B.7b – Measured and predicted queue discharge flow rates for Site 335

**Site 335: Doncaster Rd and Blackburn Rd in East Doncaster, Melbourne
(Right-Turn Isolated)**

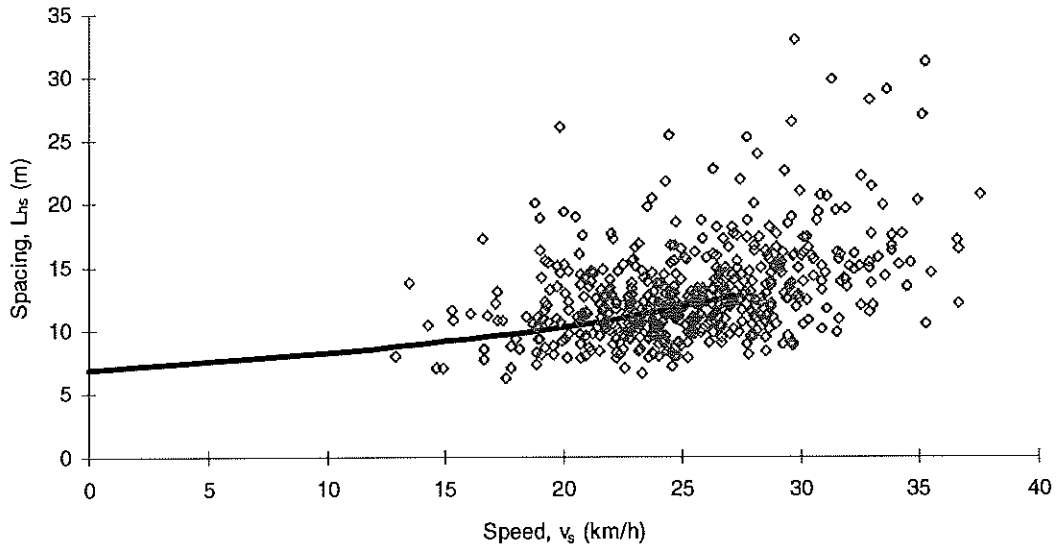


Figure B.7c – Vehicle spacing as a function of queue discharge speed for Site 335

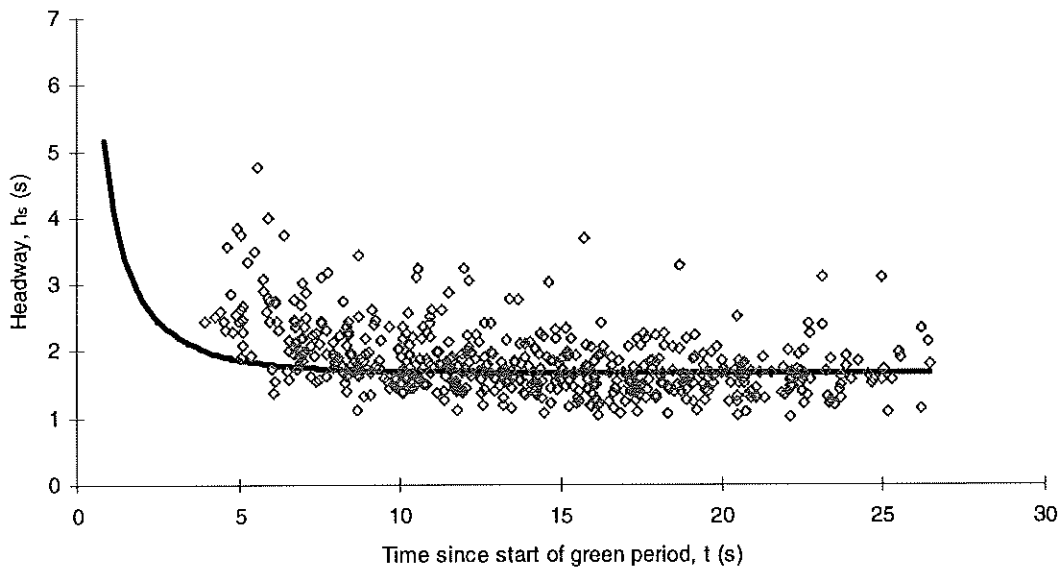


Figure B.7d – Measured and predicted queue discharge headways for Site 335

**Site 3196: Middleborough Rd and Highbury Rd in East Burwood, Melbourne
(Through Isolated)**

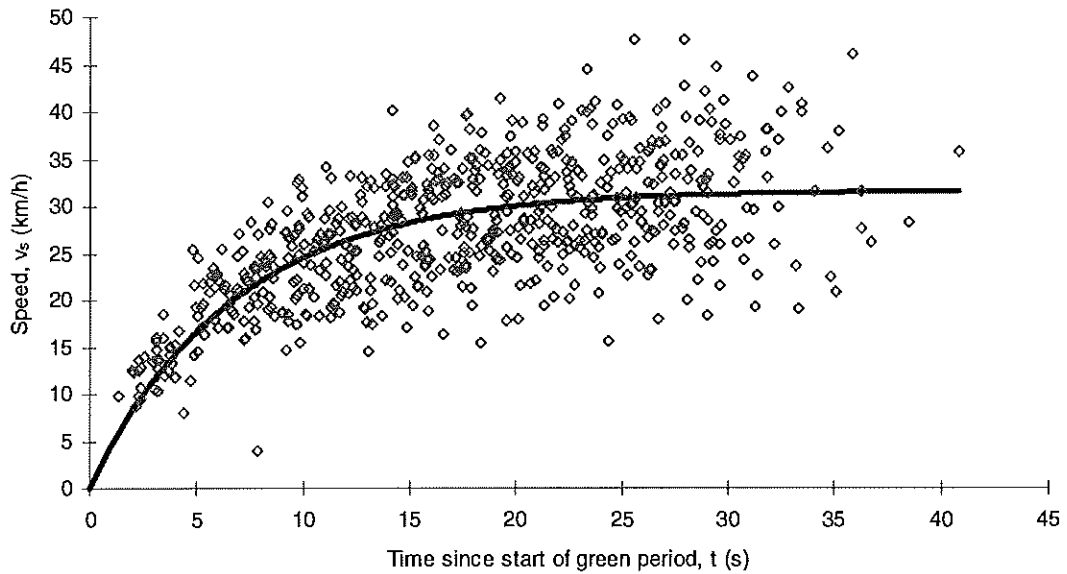


Figure B.8a – Measured and predicted queue discharge speeds for Site 3196

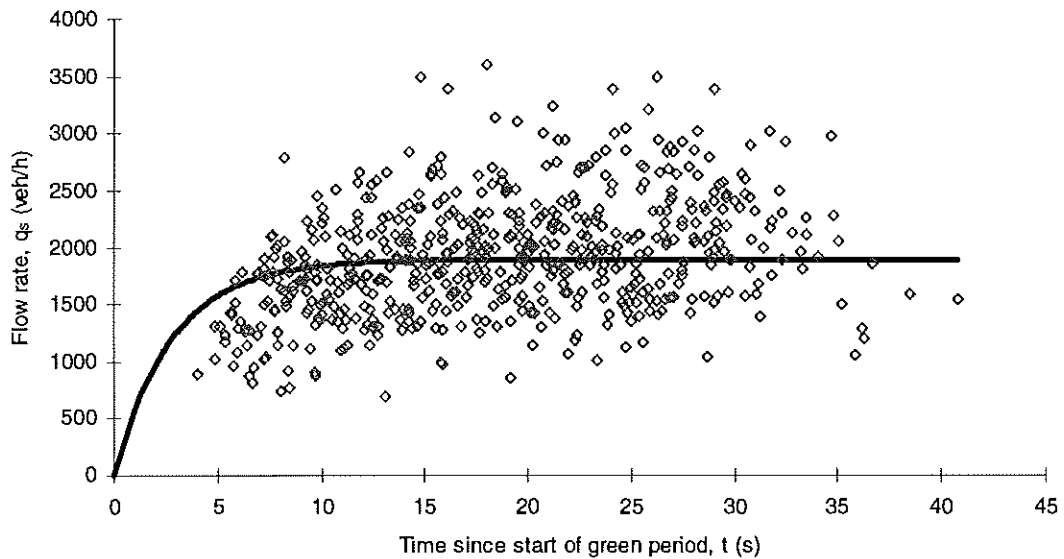


Figure B.8b – Measured and predicted queue discharge flow rates for Site 3196

**Site 3196: Middleborough Rd and Highbury Rd in East Burwood, Melbourne
(Through Isolated)**

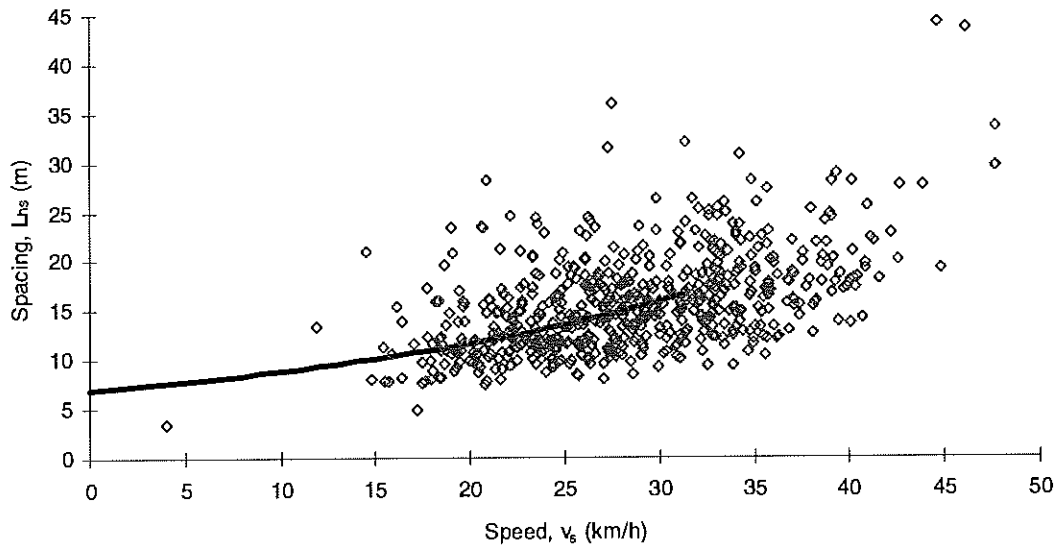


Figure B.8c – Vehicle spacing as a function of queue discharge speed for Site 3196

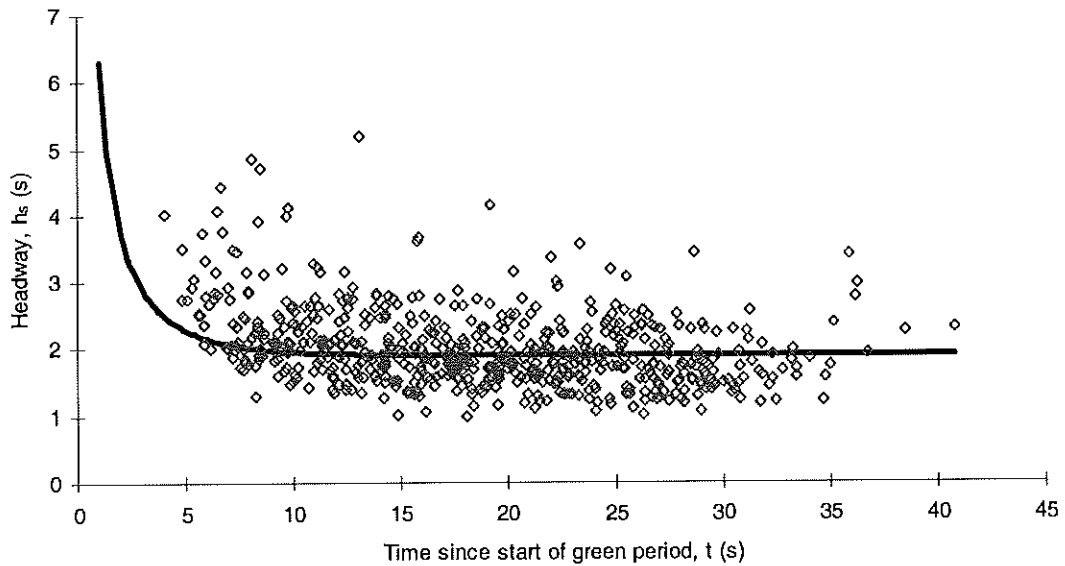


Figure B.8d – Measured and predicted queue discharge headways for Site 3196

**Site 4273: Toorak Rd and Tooronga Rd in Hawthorn East, Melbourne
(Through Isolated)**

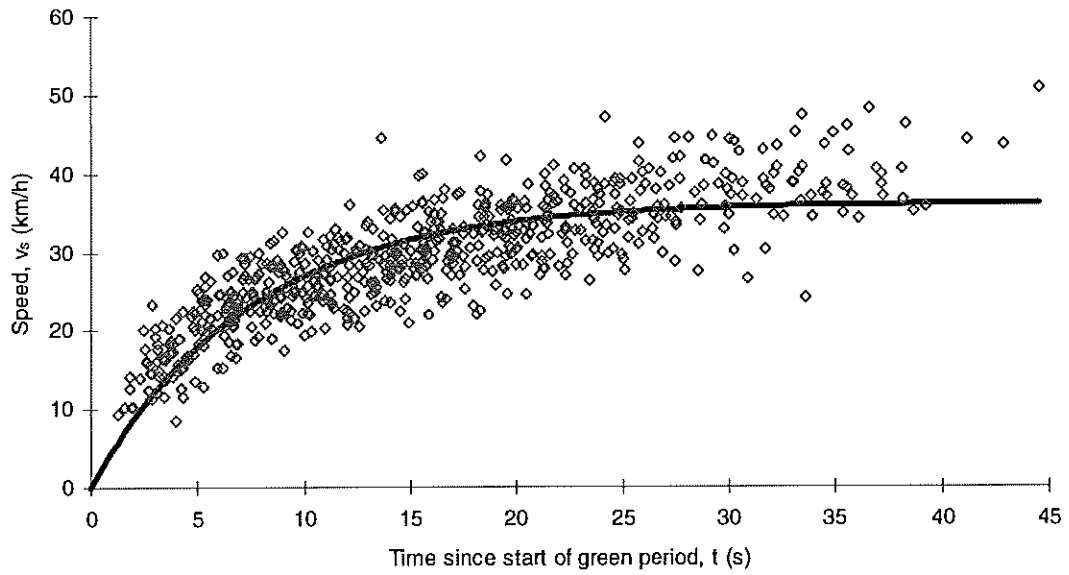


Figure B.9a – Measured and predicted queue discharge speeds for Site 4273

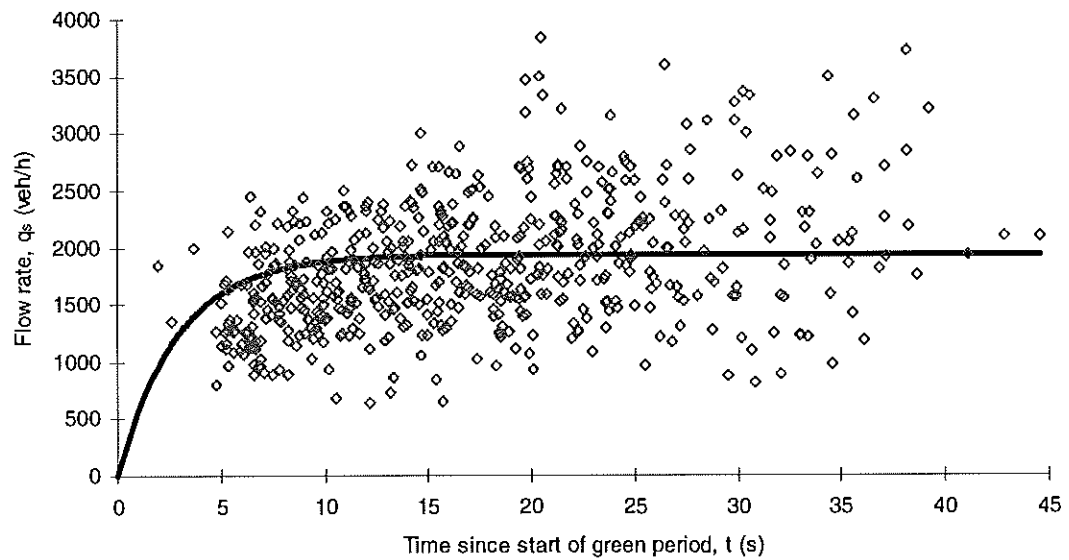


Figure B.9b – Measured and predicted queue discharge flow rates for Site 4273

**Site 4273: Toorak Rd and Tooronga Rd in Hawthorn East, Melbourne
(Through Isolated)**

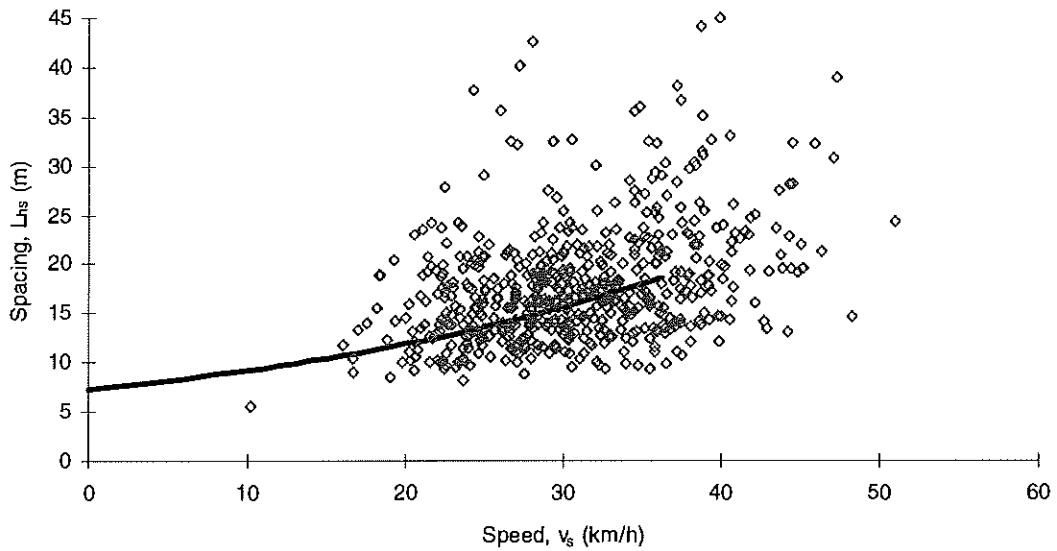


Figure B.9c – Vehicle spacing as a function of queue discharge speed for Site 4273

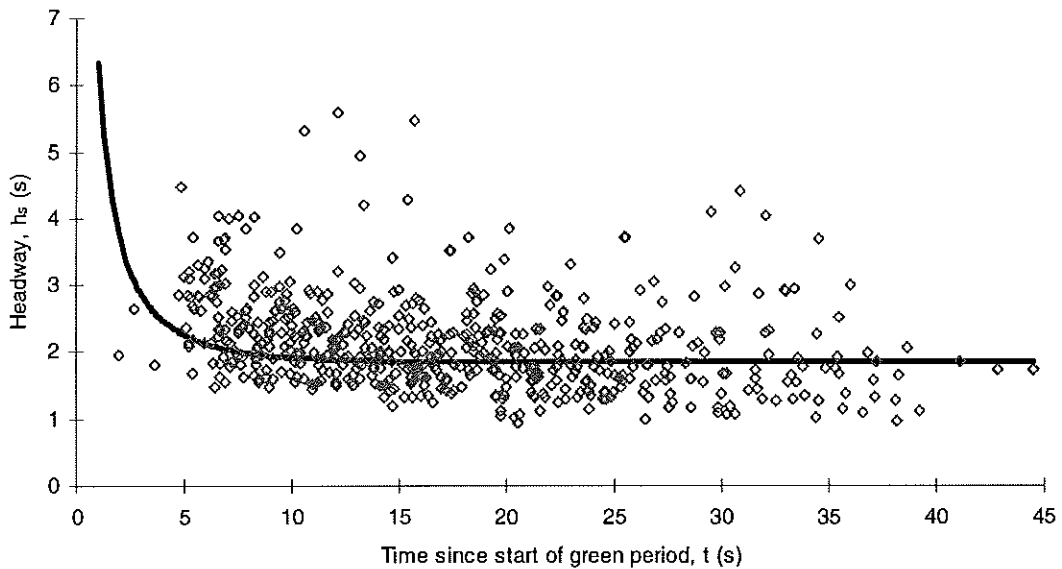


Figure B.9d – Measured and predicted queue discharge headways for Site 4273

**Site 849: Canterbury Rd and Mitcham Rd in Vermont, Melbourne
(Through Isolated)**

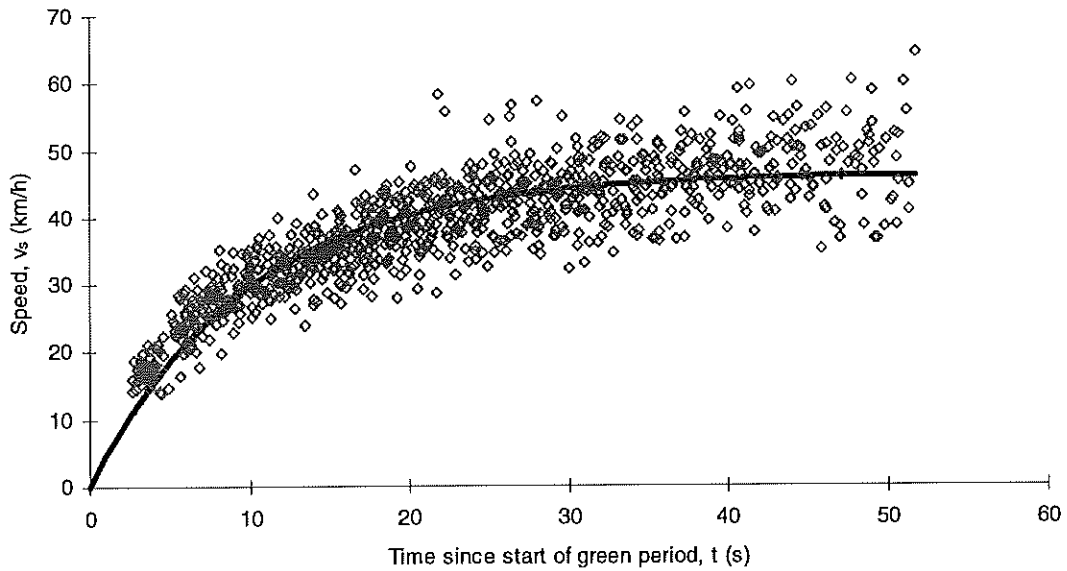


Figure B.10a – Measured and predicted queue discharge speeds for Site 849

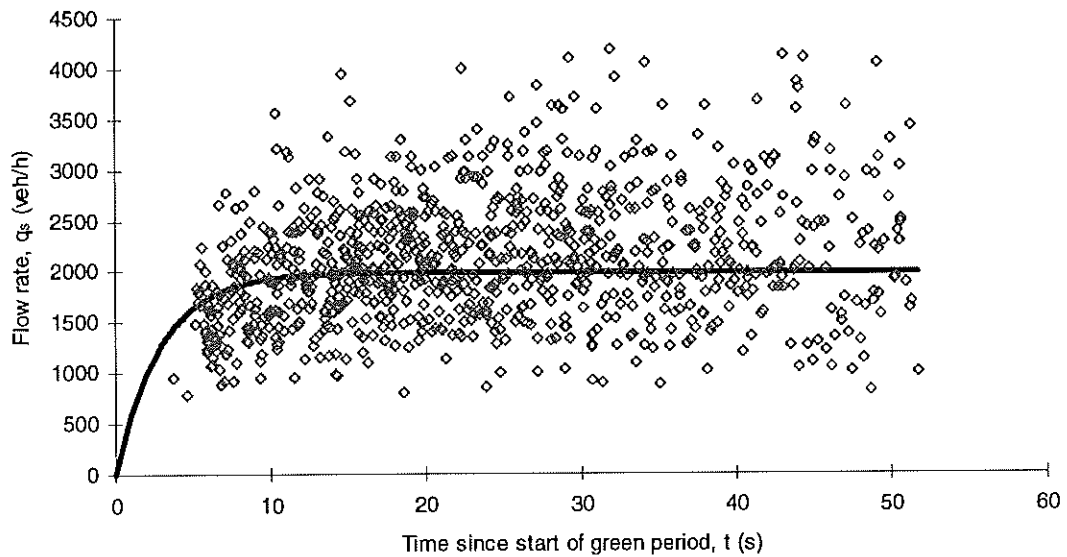


Figure B.10b – Measured and predicted queue discharge flow rates for Site 849

**Site 849: Canterbury Rd and Mitcham Rd in Vermont, Melbourne
(Through Isolated)**

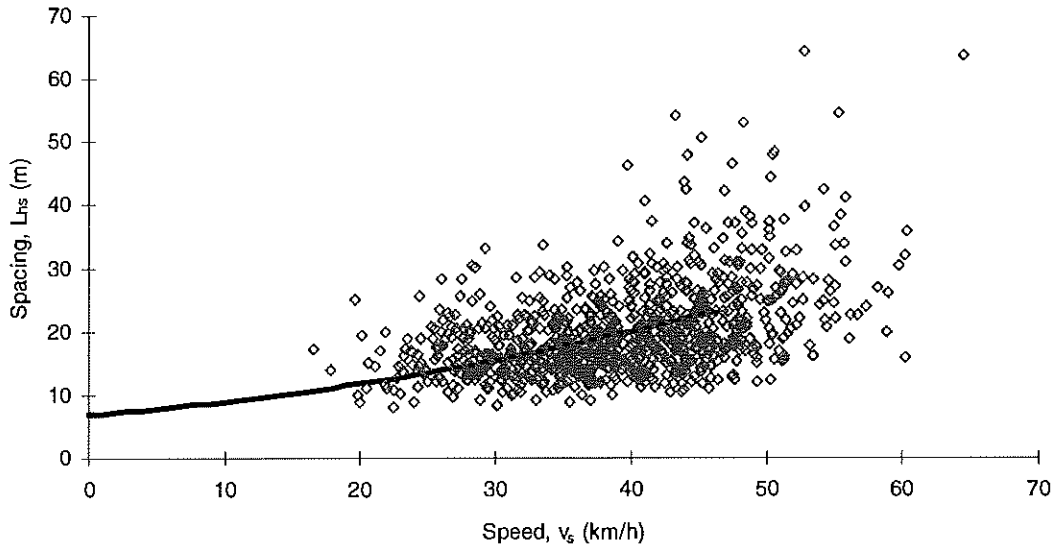


Figure B.10c – Vehicle spacing as a function of queue discharge speed for Site 849

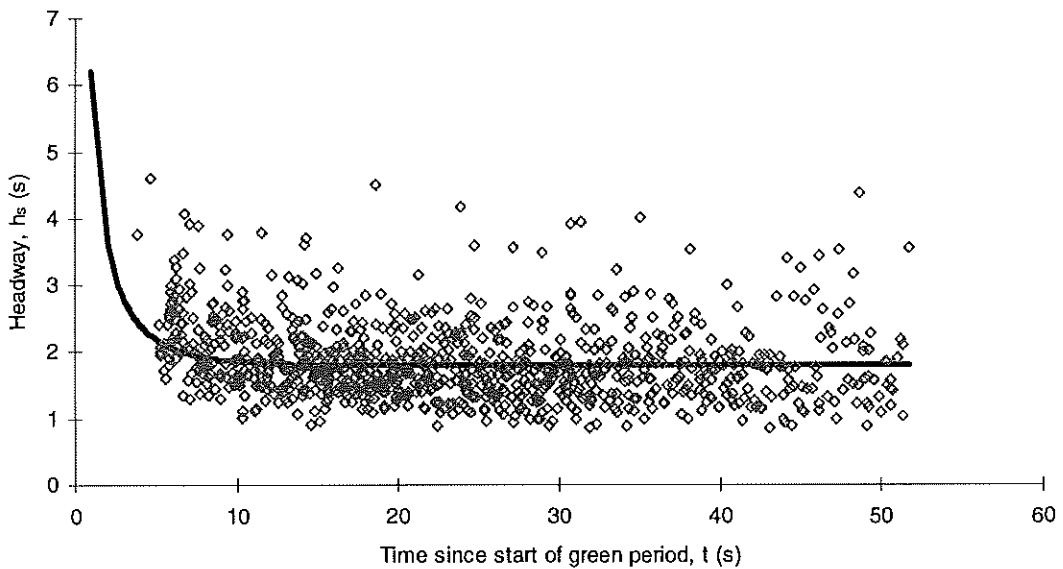


Figure B.10d – Measured and predicted queue discharge headways for Site 849

**Site 456: Ferntree Gully Rd and Stud Rd in Scoresby, Melbourne
(Through Isolated)**

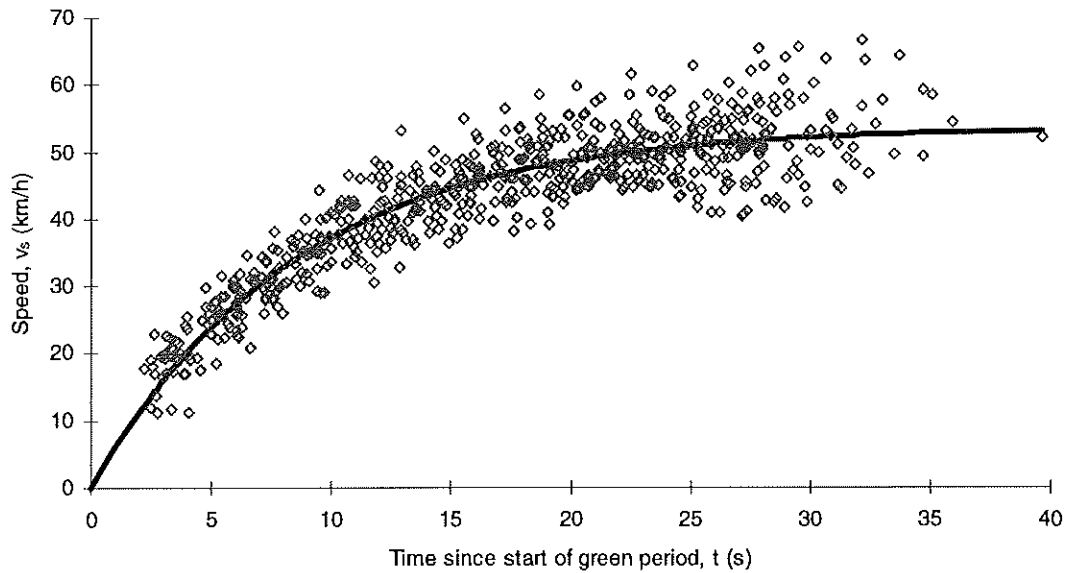


Figure B.11a – Measured and predicted queue discharge speeds for Site 456

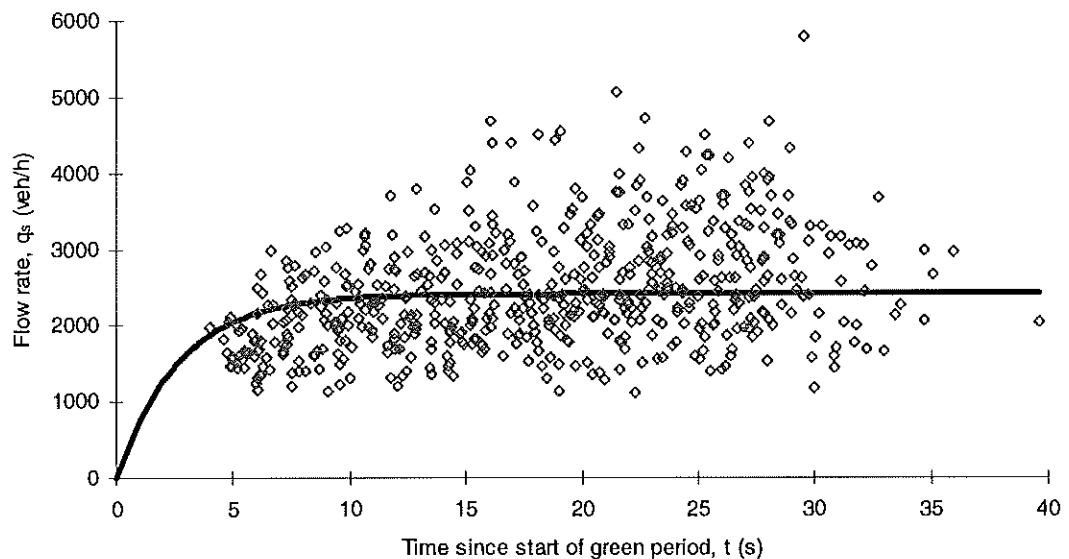


Figure B.11b – Measured and predicted queue discharge flow rates for Site 456

**Site 456: Ferntree Gully Rd and Stud Rd in Scoresby, Melbourne
(Through Isolated)**

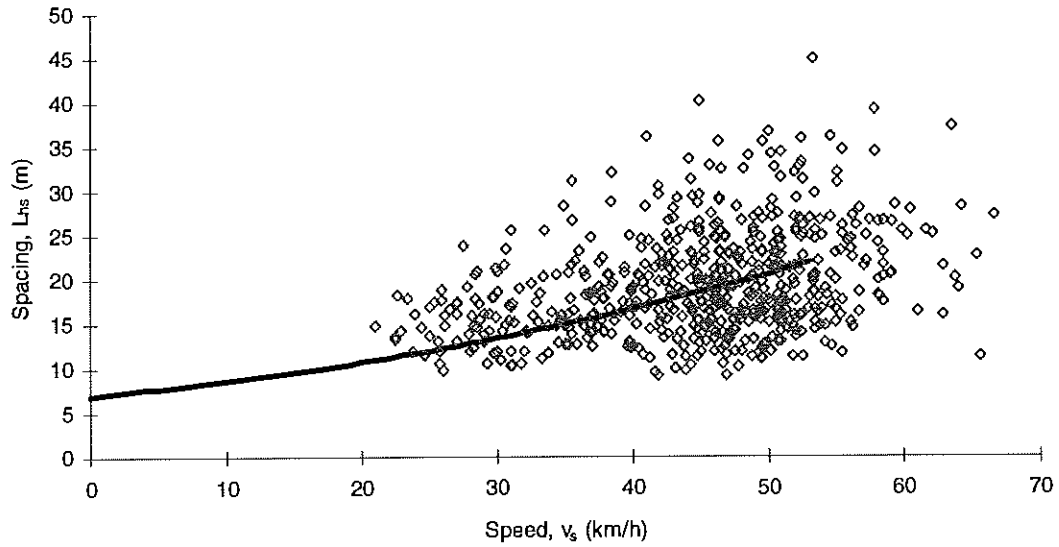


Figure B.11c – Vehicle spacing as a function of queue discharge speed for Site 456

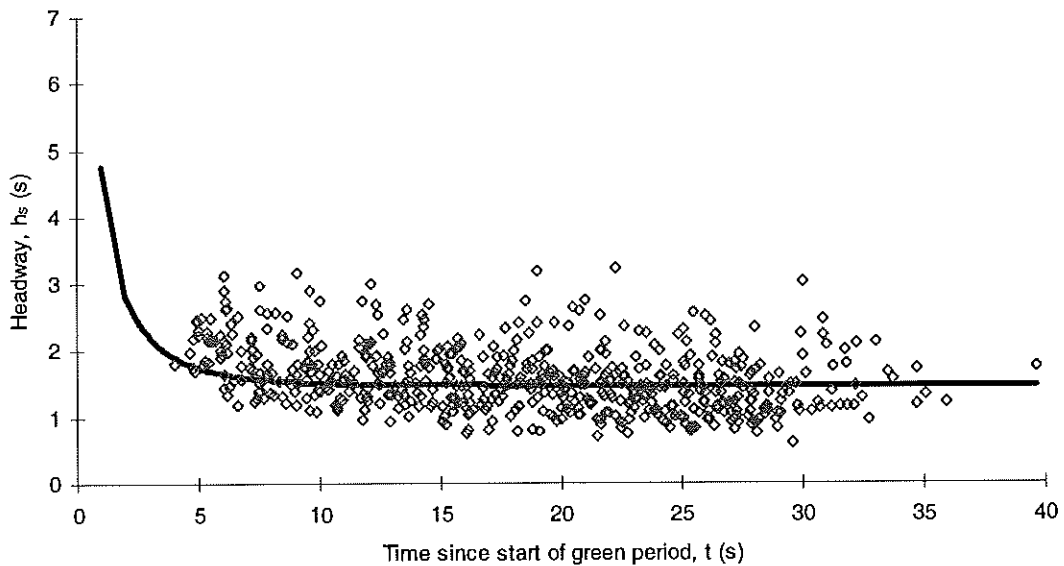
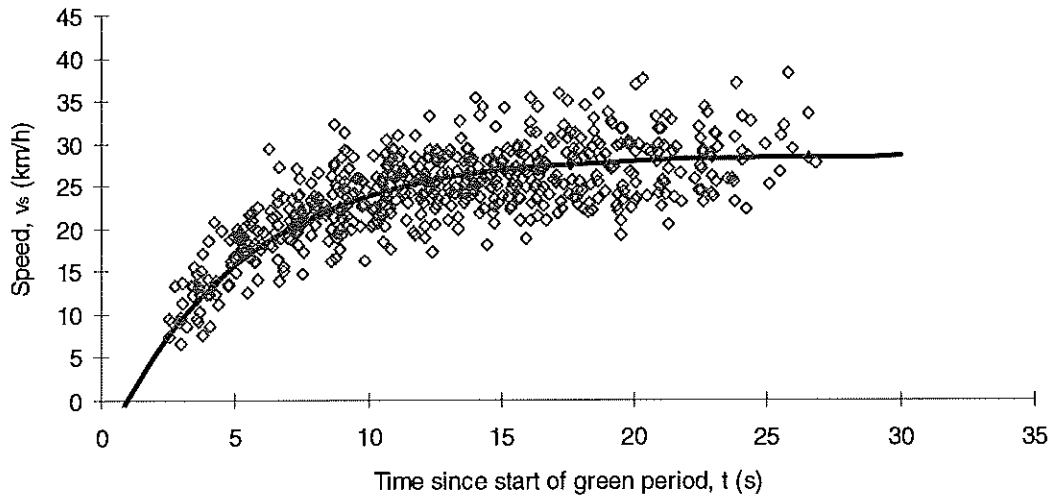
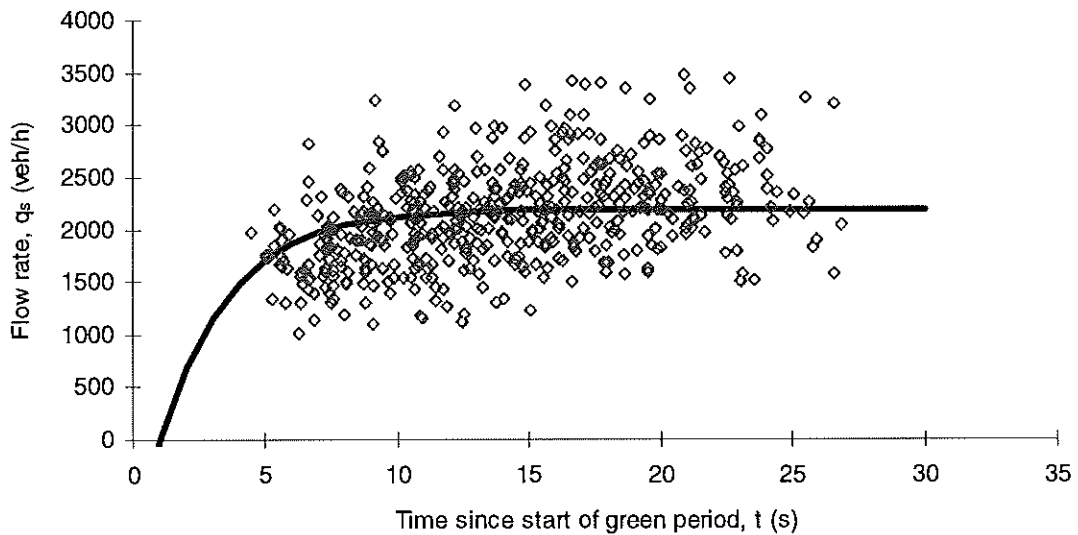


Figure B.11d – Measured and predicted queue discharge headways for Site 456

**Site 335: Doncaster Rd and Blackburn Rd, Melbourne
(Right-Turn Isolated)**



*Figure B.12a – Measured and predicted queue discharge speeds for Site 335:
Alternative Calibration Method 13: $v_L, h_{2L}, t_r = 1.0$*



*Figure B.12b – Measured and predicted queue discharge flow rates for Site 335:
Alternative Calibration Method 13: $v_L, h_{2L}, t_r = 1.0$*

**Site 335: Doncaster Rd and Blackburn Rd, Melbourne
(Right-Turn Isolated)**

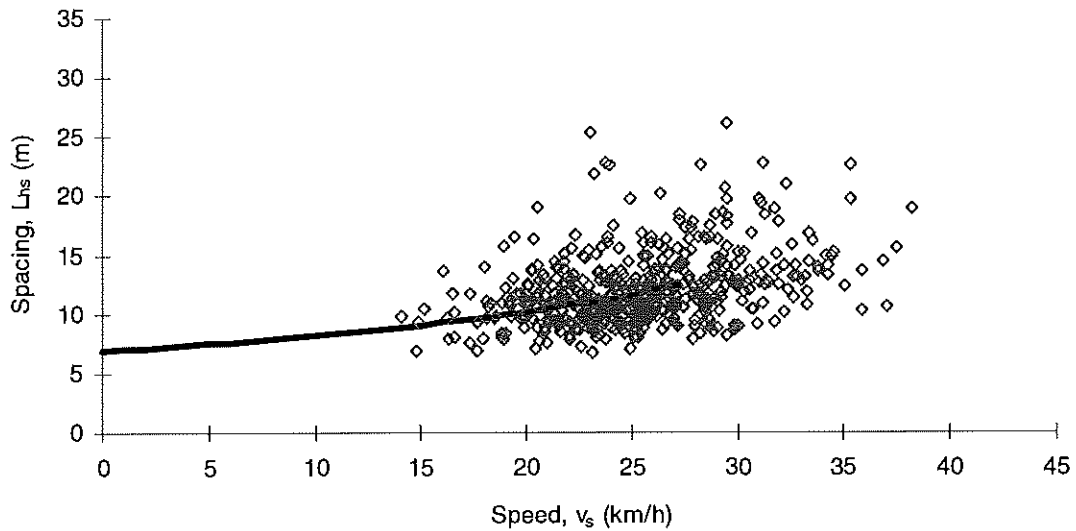


**Figure B.12c – Vehicle spacing as a function of queue discharge speed for Site 335:
Alternative Calibration Method 13: $v_L, h_{2L}, t_r = 1.0$**

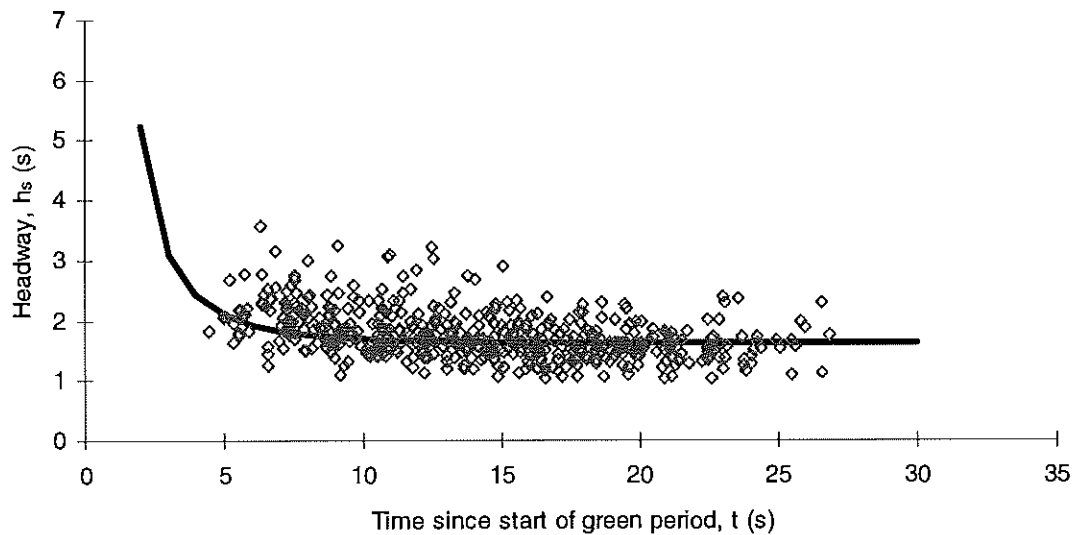


**Figure B.12d – Measured and predicted queue discharge headways for Site 335:
Alternative Calibration Method 13: $v_L, h_{2L}, t_r = 1.0$**

**Site 610: Military Rd and Murdoch St, Sydney
(Right-Turn Isolated)**

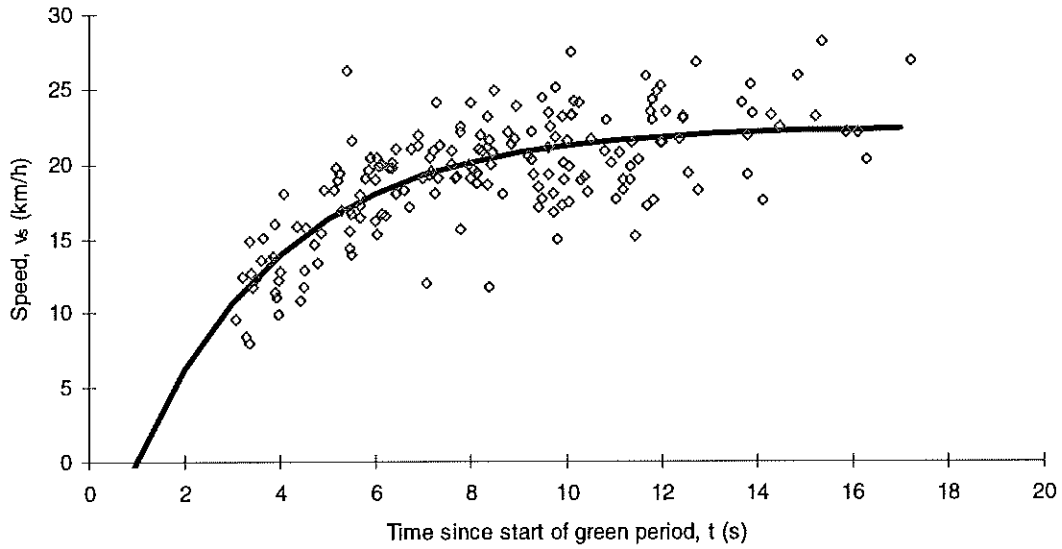


*Figure B.13a – Measured and predicted queue discharge speeds for Site 610:
Alternative Calibration Method 13: $v_L, h_{2L}, t_r = 1.0$*

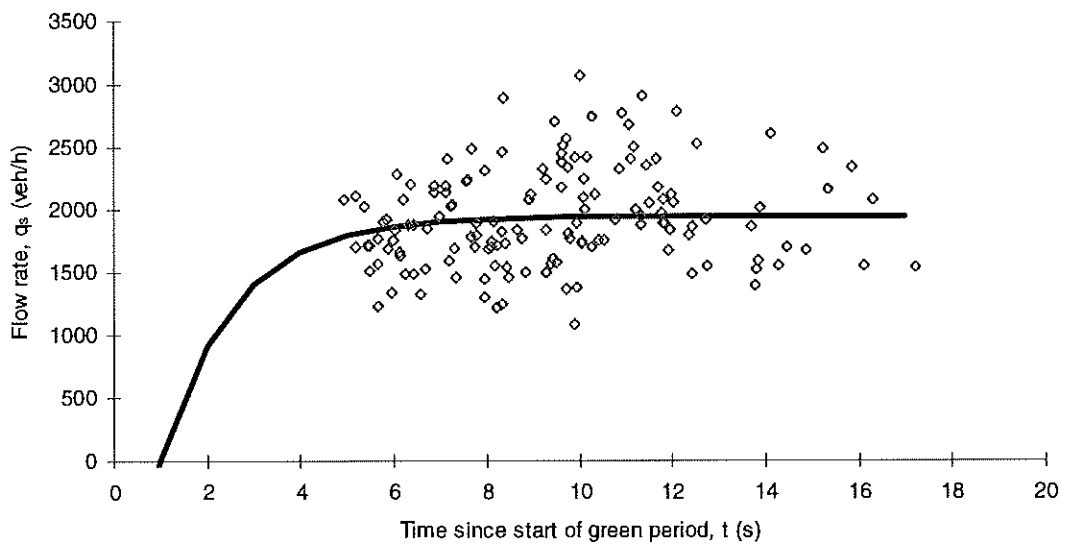


*Figure B.13b – Measured and predicted queue discharge flow rates for Site 610:
Alternative Calibration Method 13: $v_L, h_{2L}, t_r = 1.0$*

**Site 610: Military Rd and Murdoch St, Sydney
(Right-Turn Isolated)**

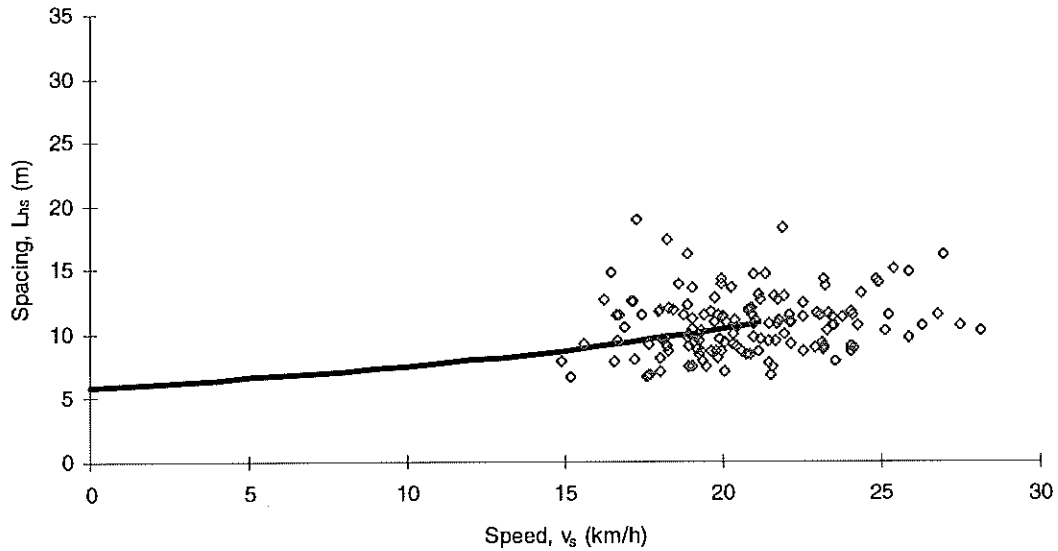


**Figure B.13c – Vehicle spacing as a function of queue discharge speed for Site 610:
Alternative Calibration Method 13: $v_L, h_{2L}, t_r = 1.0$**

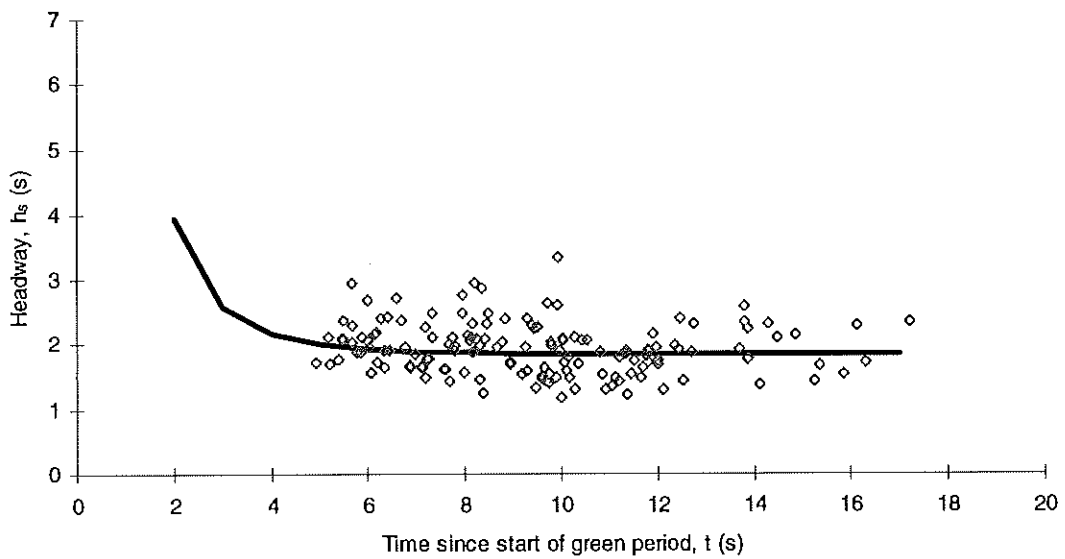


**Figure B.13d – Measured and predicted queue discharge headways for Site 610:
Alternative Calibration Method 13: $v_L, h_{2L}, t_r = 1.0$**

**Site 511: General Holmes Dve and Bestic St, Sydney
(Through Isolated)**

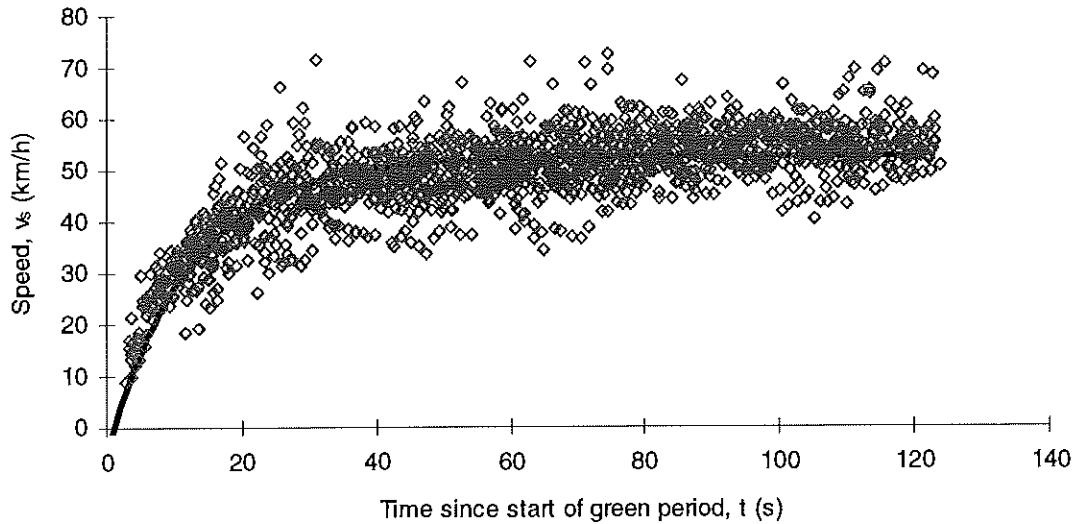


*Figure B.14a – Measured and predicted queue discharge speeds for Site 511:
Alternative Calibration Method 13: $v_L, h_{2L}, t_r = 1.0$*

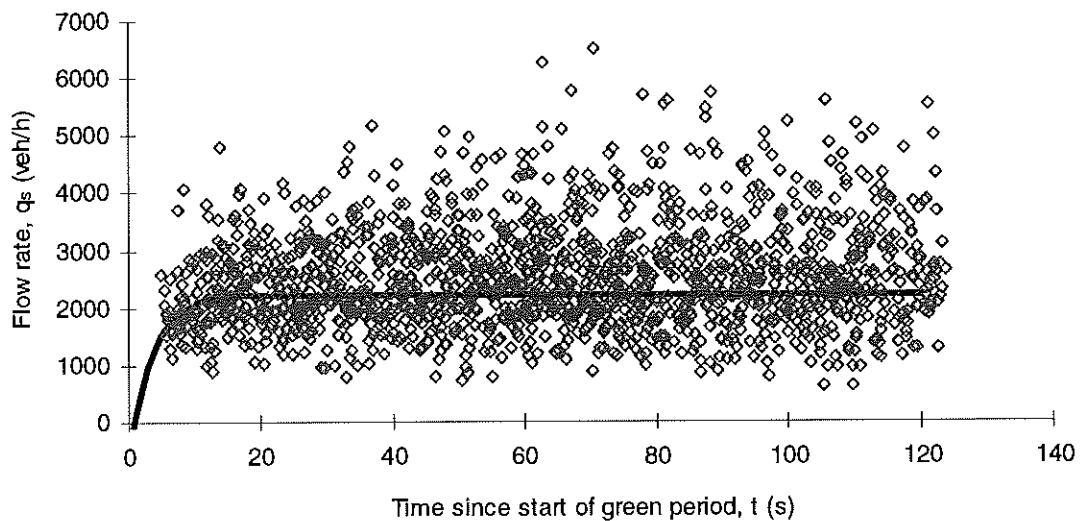


*Figure B.14b – Measured and predicted queue discharge flow rates for Site 511:
Alternative Calibration Method 13: $v_L, h_{2L}, t_r = 1.0$*

**Site 511: General Holmes Dve and Bestic St, Sydney
(Through Isolated)**

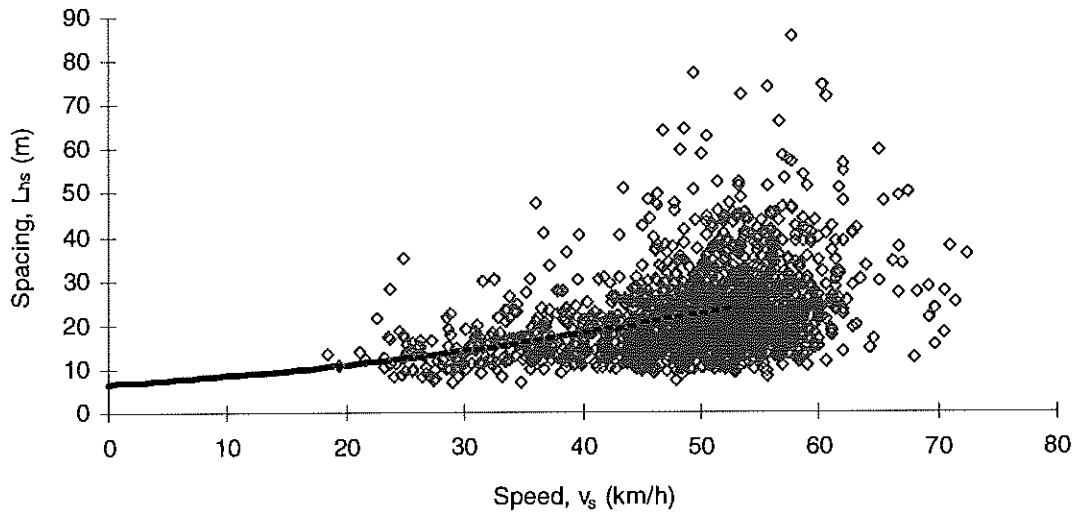


*Figure B.14c – Vehicle spacing as a function of queue discharge speed for Site 511:
Alternative Calibration Method 13: $v_L, h_{2L}, t_r = 1.0$*

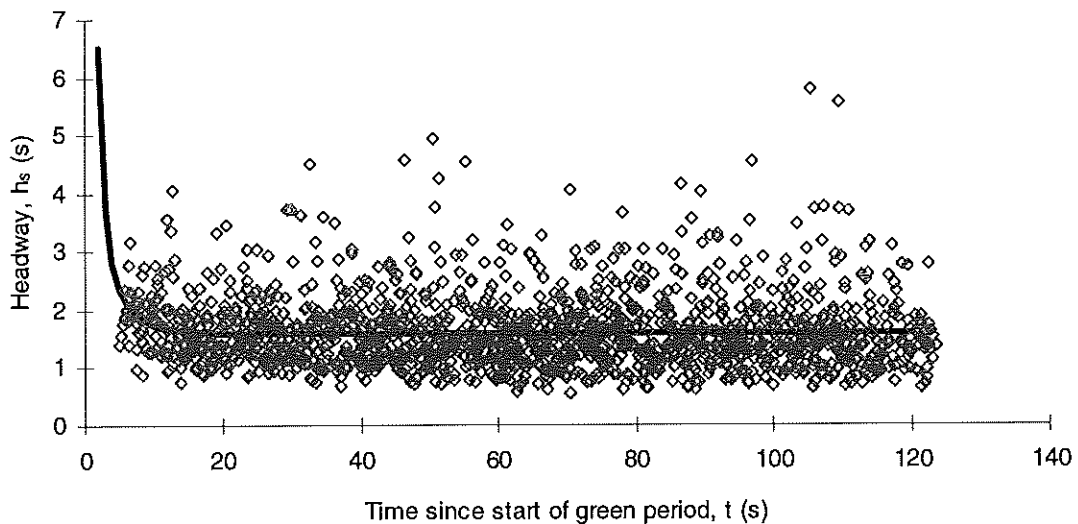


*Figure B.14d – Measured and predicted queue discharge headways for Site 511:
Alternative Calibration Method 13: $v_L, h_{2L}, t_r = 1.0$*

APPENDIX C

Diagrams Showing Space Time - Speed - Detection Zone Length Relationships for Sydney and Melbourne 1998 Survey Sites

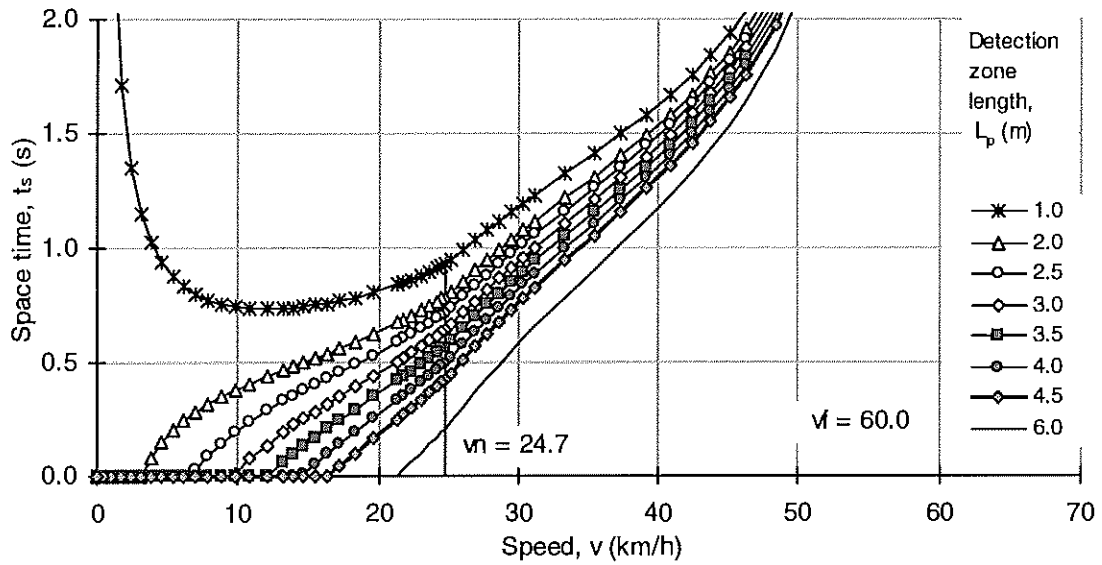


**Figure C.1 – Space time - speed - detection zone length relationships for Site 163:
Pacific Highway - Mowbray Rd (Chatswood, Sydney) -
right-turn lane (Lane 4) on Pacific Highway South approach**

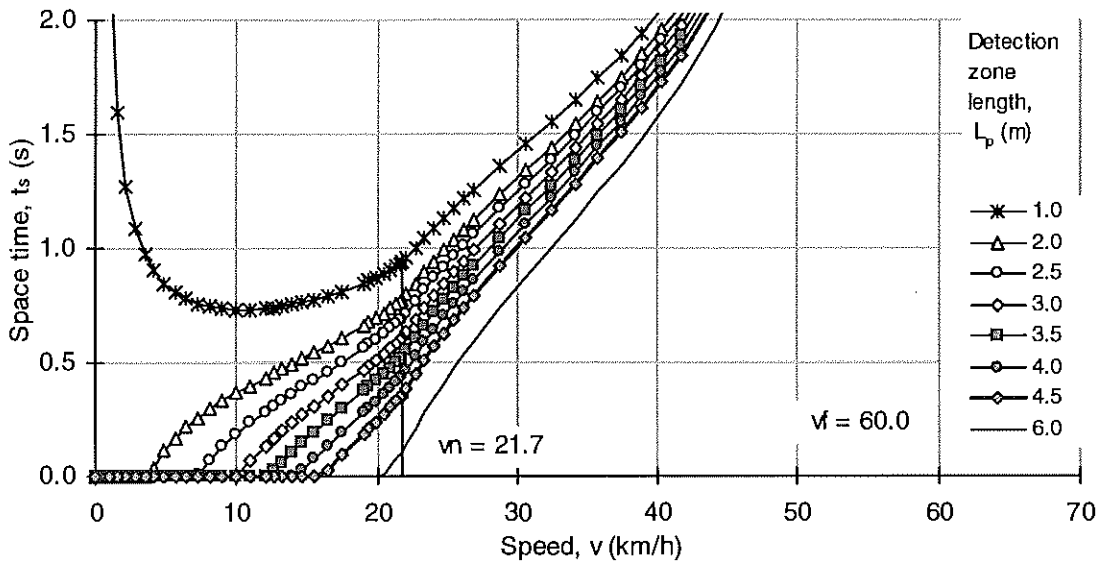


**Figure C.2 – Space time - speed - detection zone length relationships for Site 610:
Military Road - Murdoch Street (Cremorne, Sydney) -
right-turn lane (Lane 3) on Military Road West approach**

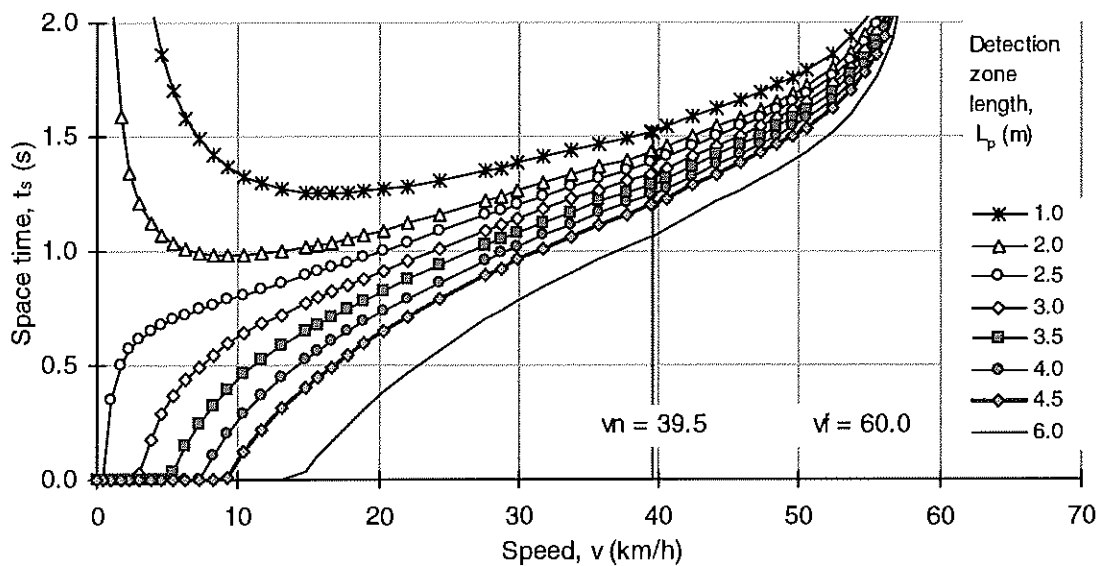


Figure C.3 – Space time - speed - detection zone length relationships for Site 1081: Lilyfield Road - Mary Street - James Street (Lilyfield, Sydney) - through lane (Lane 2) on Lilyfield Road Northwest approach

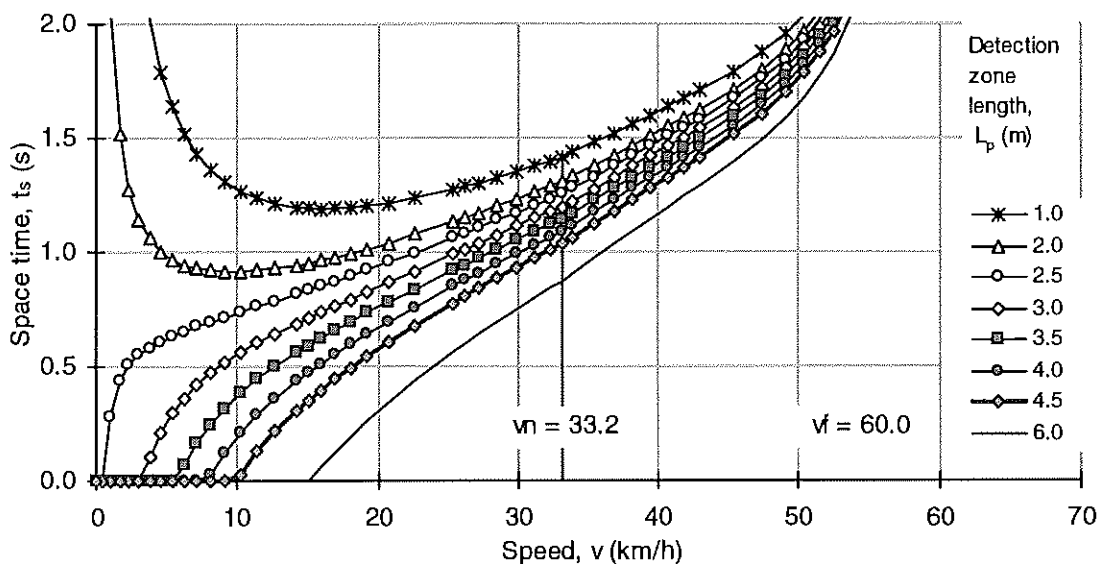


Figure C.4 – Space time - speed - detection zone length relationships for Site 413: Broadway - City Road (Ultimo, Sydney) - through lane (Lane 3) on Broadway East approach

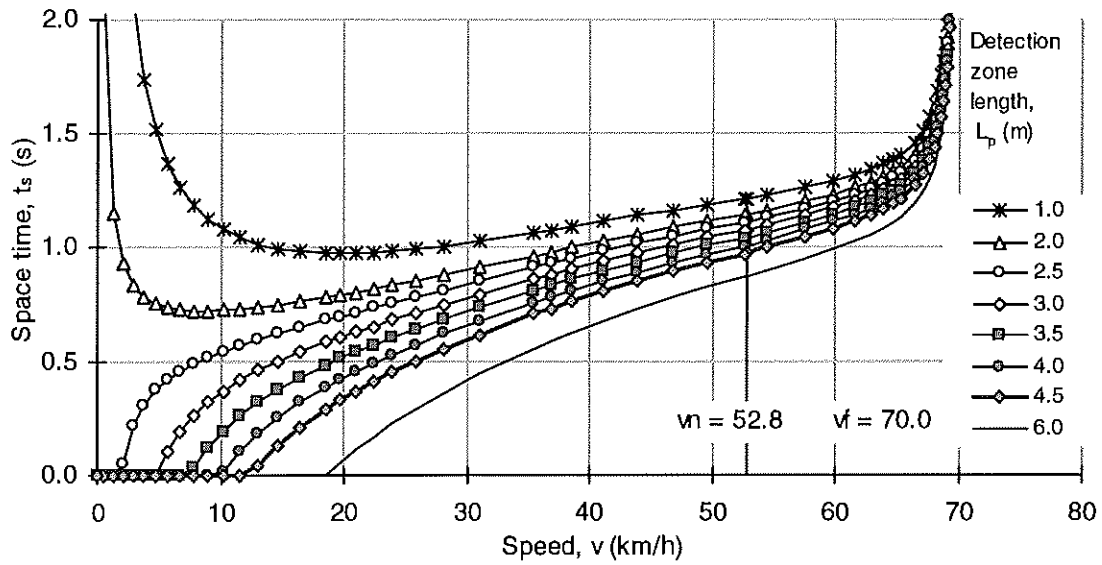


Figure C.5 – Space time - speed - detection zone length relationships for Site 511: General Holmes Drive - Bestic Street (Kyeemagh, Sydney) - through lane (Lane 2) on General Holmes Drive South approach

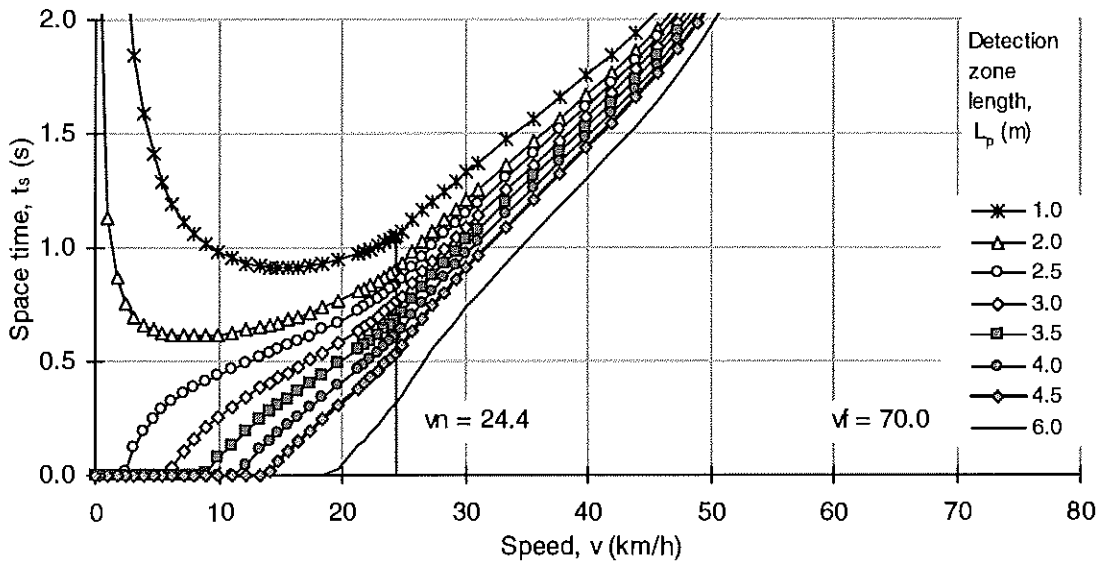


Figure C.6 – Space time - speed - detection zone length relationships for Site 121: Maroondah Highway - Mitcham Road (Mitcham, Melbourne) - right-turn lane (Lane 4) on Maroondah Highway East approach

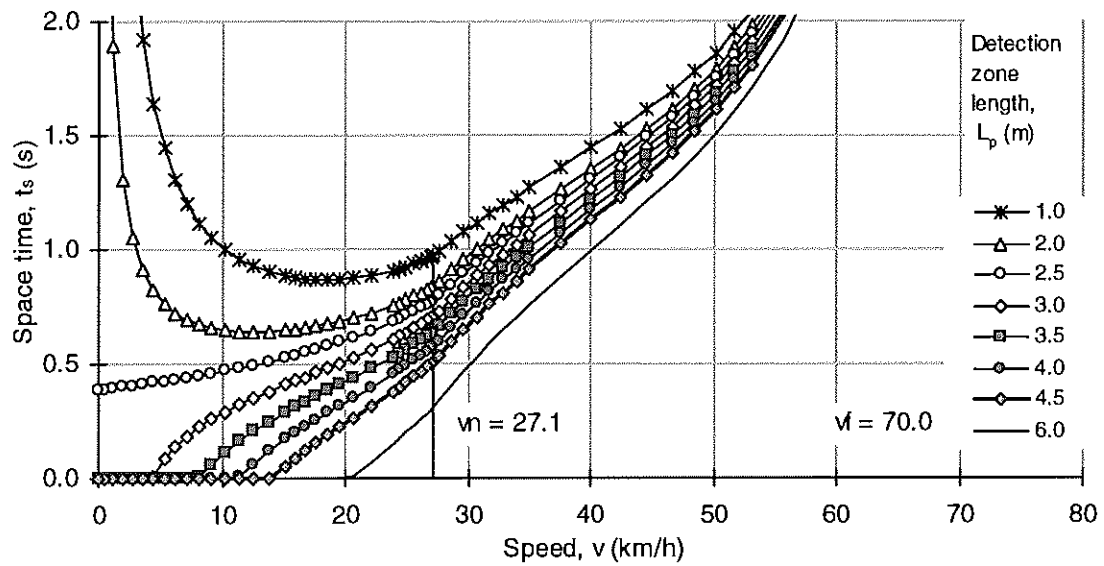


Figure C.7 – Space time - speed - detection zone length relationships for Site 335: Doncaster Road - Blackburn Road (East Doncaster, Melbourne) - right-turn lane (Lane 4) on Doncaster Road East approach

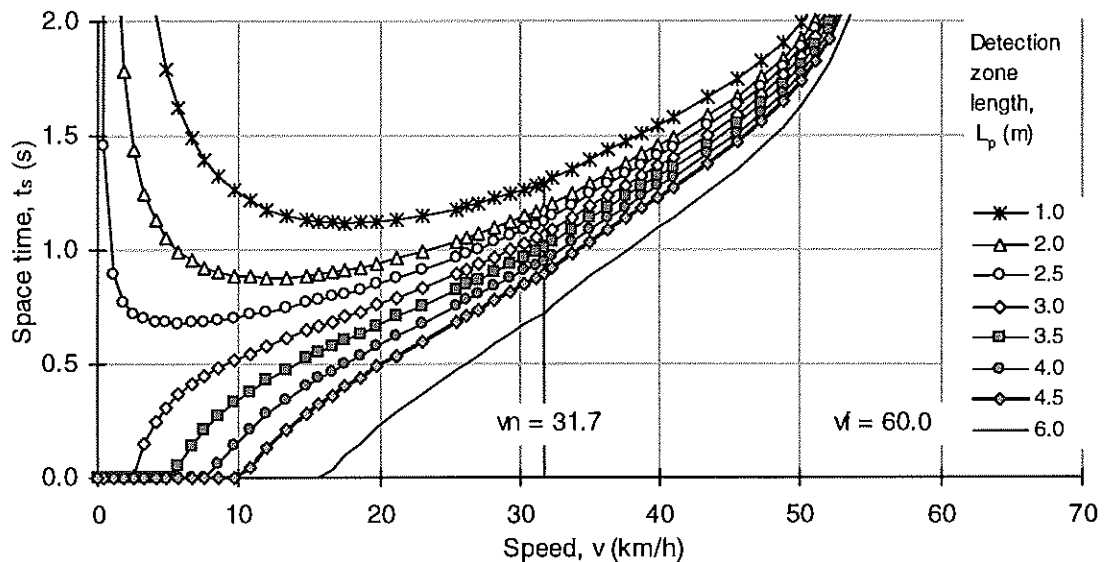
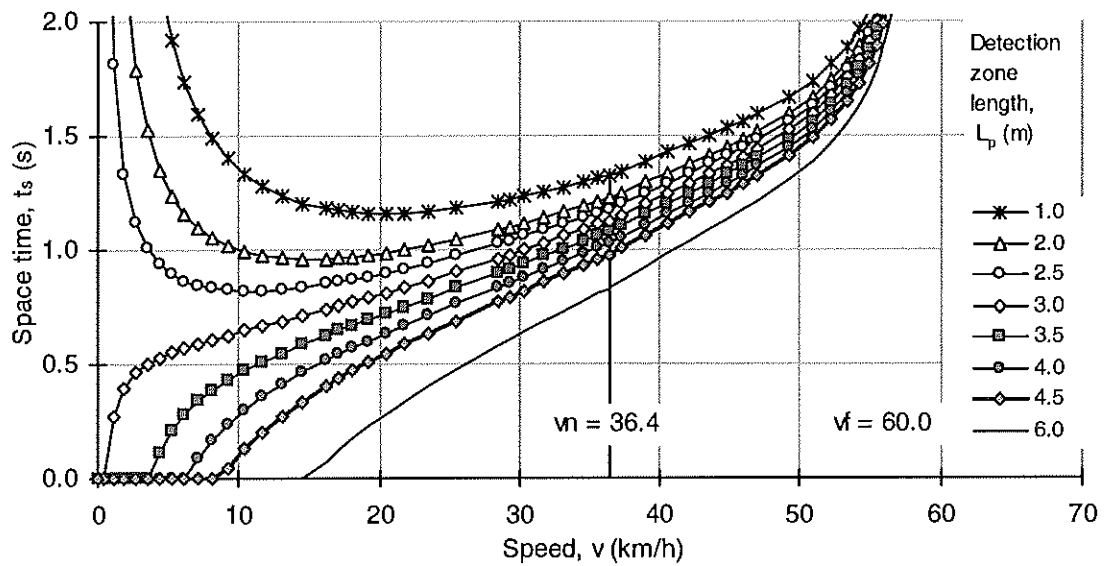
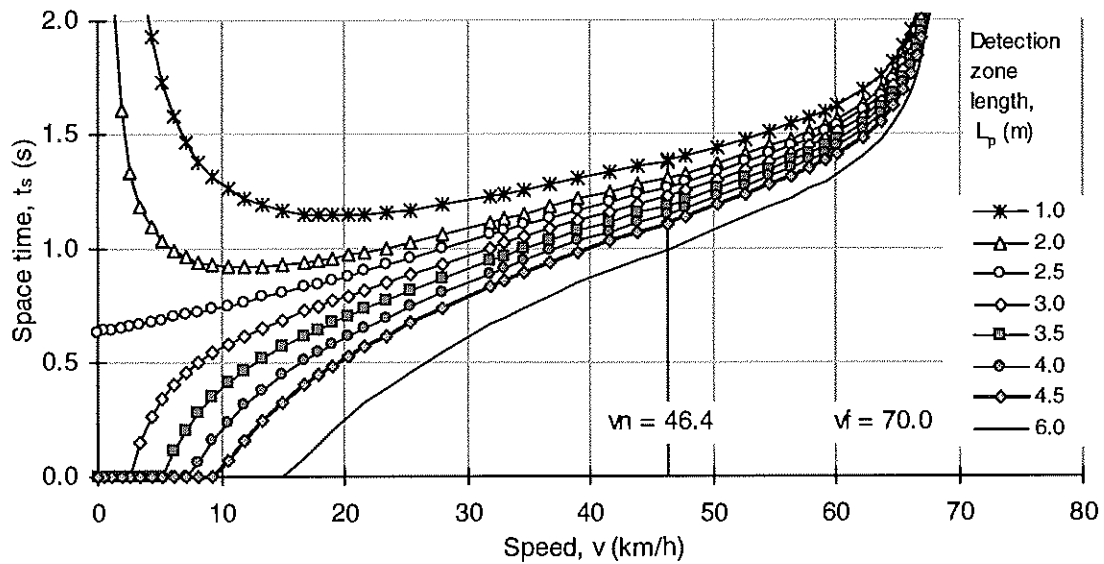


Figure C.8 – Space time - speed - detection zone length relationships for Site 3196: Middleborough Road - Highbury Road (East Burwood, Melbourne) - through and left-turn lane (Lane 1) on Middleborough Road North approach



**Figure C.9 – Space time - speed - detection zone length relationships for Site 4273:
Toorak Road - Tooronga Road (Hawthorn East, Melbourne) -
through lane (Lane 2) on Toorak Road West approach**



**Figure C.10 – Space time - speed - detection zone length relationships for Site 849:
Canterbury Road - Mitcham Road (Vermont, Melbourne) -
through lane (Lane 2) on Canterbury Road West approach**

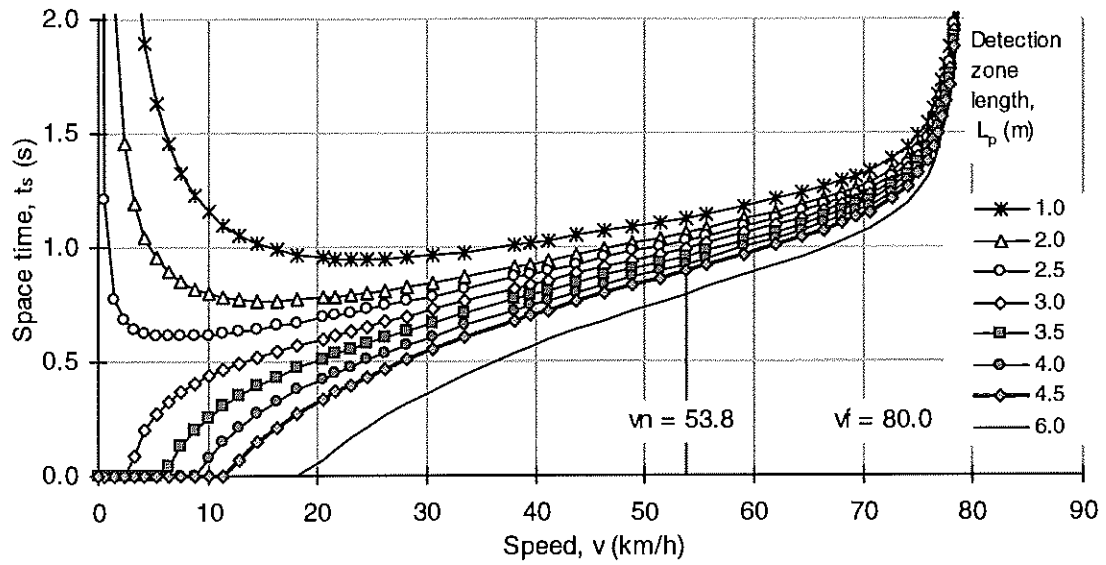


**Figure C.11 – Space time - speed - detection zone length relationships for Site 456:
 Ferntree Gully Road - Stud Road (Scoresby, Melbourne) -
 through lane (Lane 4) on Ferntree Gully Road West approach**

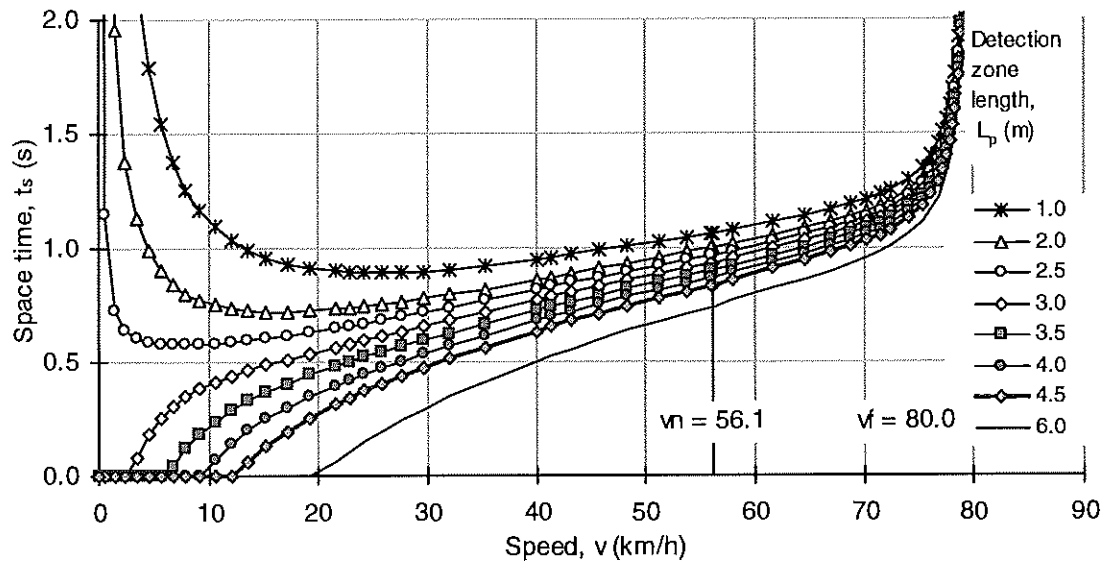


**Figure C.12 – Space time - speed - detection zone length relationships for Site Mell1:
 Ferntree Gully Road - Stud Road (Scoresby, Melbourne) -
 through lane (Lane 4) on Ferntree Gully Road West approach**

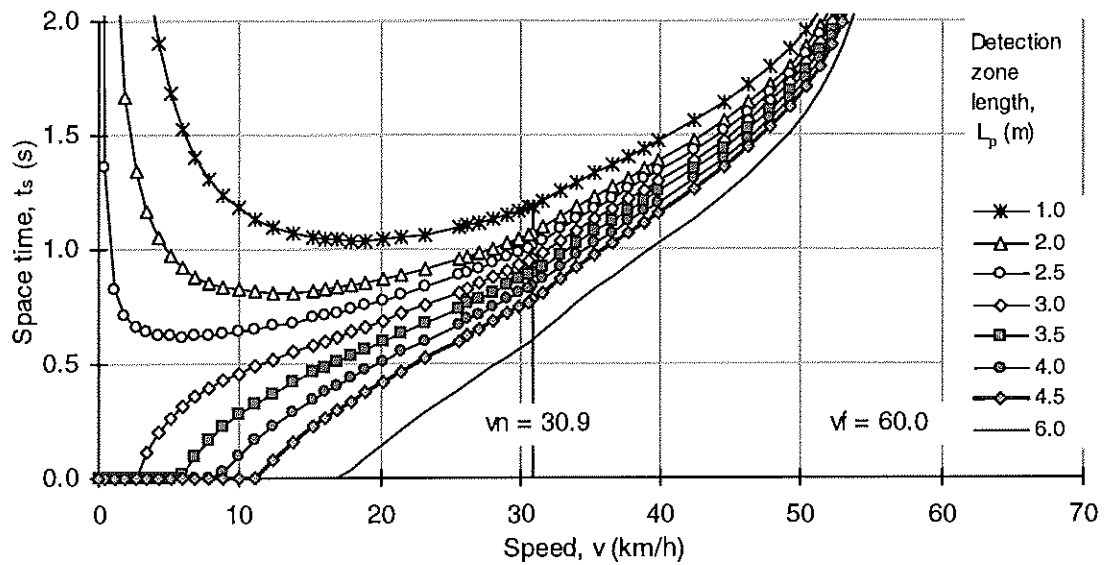


Figure C.13 – Space time - speed - detection zone length relationships for Site Mel2: Kooyong Road - Dandenong Road (Armadale, Melbourne) - through lane (Lane 1) on Kooyong Road North approach

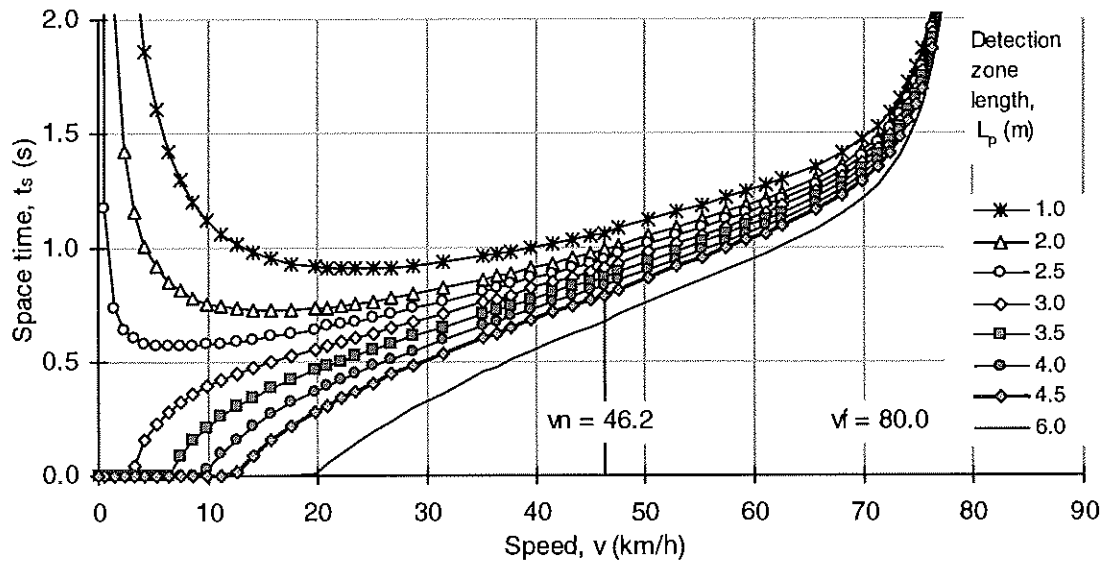


Figure C.14 – Space time - speed - detection zone length relationships for Site Mel3: South Eastern Arterial - Burke Road (Glen Iris, Melbourne) - through lane (Lane 3) on South Eastern Arterial West approach

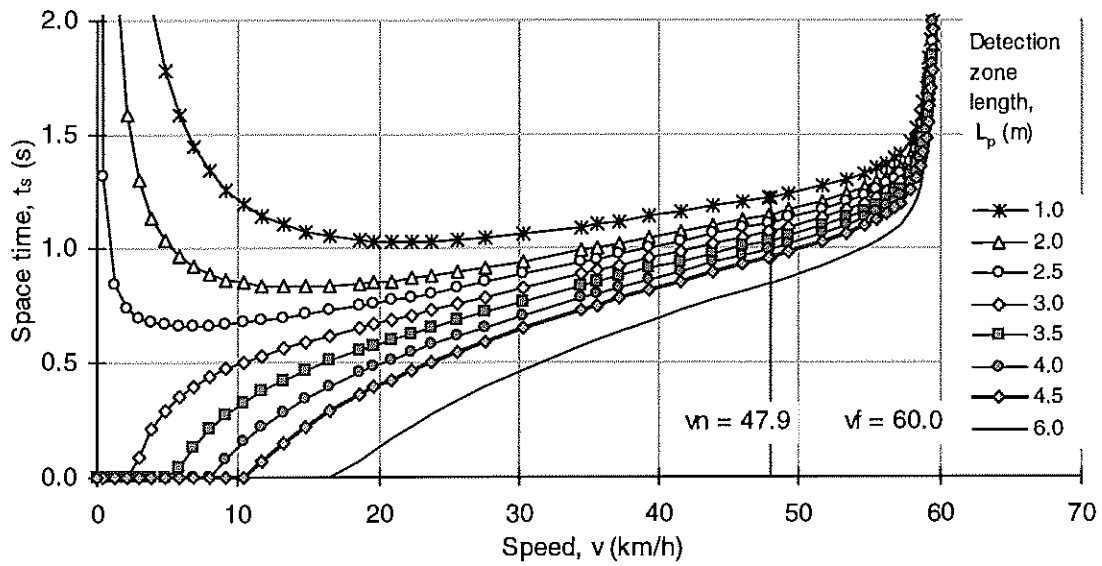


Figure C.15 – Space time - speed - detection zone length relationships for Site Mel4: Canterbury Road - Middleborough Road (Box Hill, Melbourne) - through lane (Lane 1) on Canterbury Road West approach

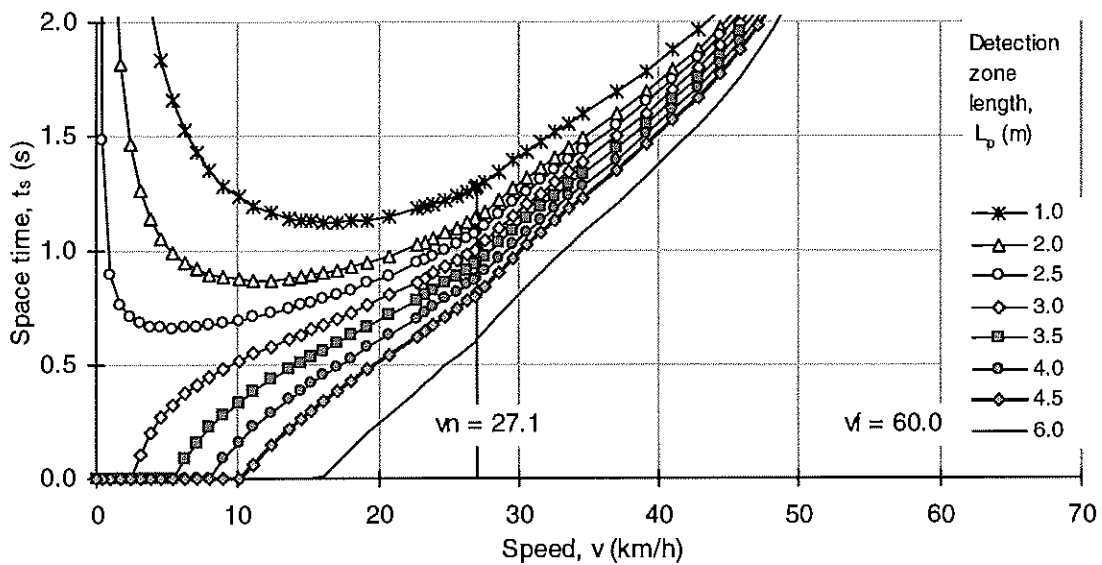


Figure C.16 – Space time - speed - detection zone length relationships for Site Mel5: Pedestrian Crossing on Canterbury Road (East Camberwell, Melbourne) - through lane (Lane 1) on Canterbury Road East approach

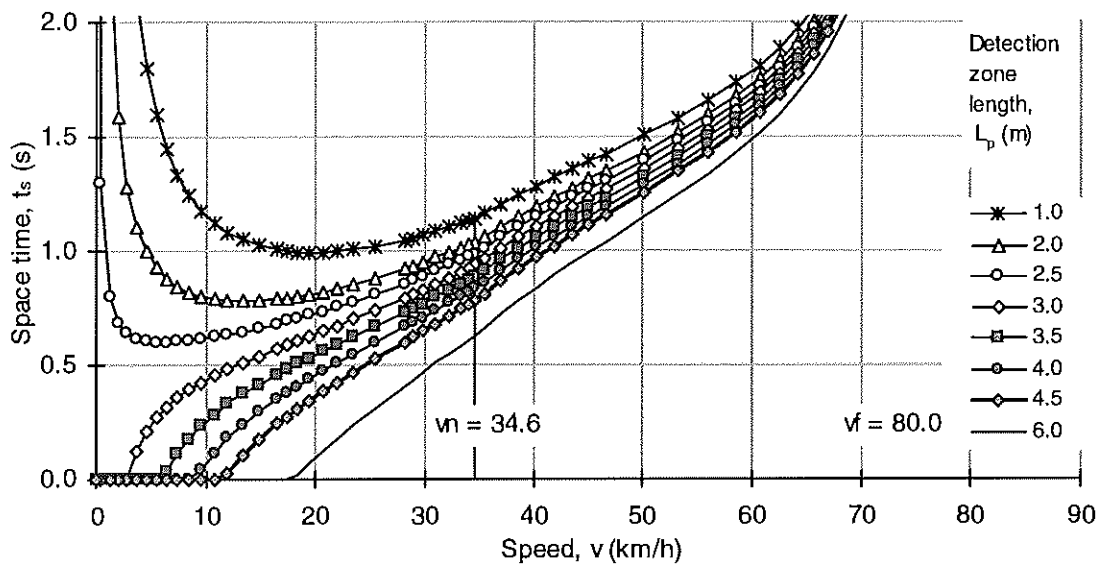


Figure C.17 – Space time - speed - detection zone length relationships for Site Mel6: Boronia Road - Wantirna Road (Wantirna, Melbourne) - through lane (Lane 2) on Boronia Road West approach

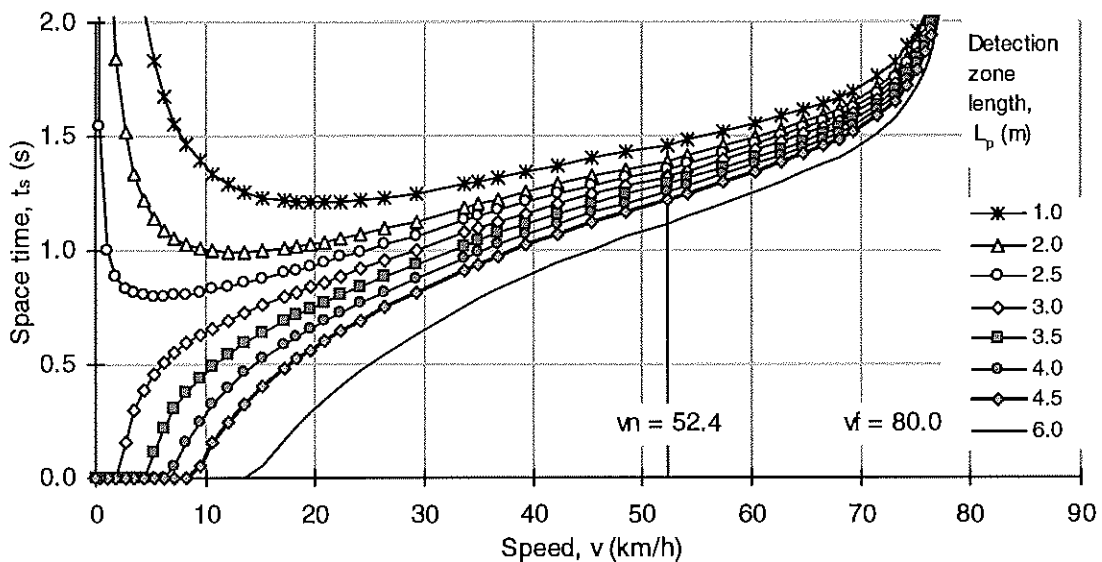


Figure C.18 – Space time - speed - detection zone length relationships for Site Mel7: Ferntree Gully Road - Scoresby Road (Knoxfield, Melbourne) - through lane (Lane 3) on Ferntree Gully Road West approach

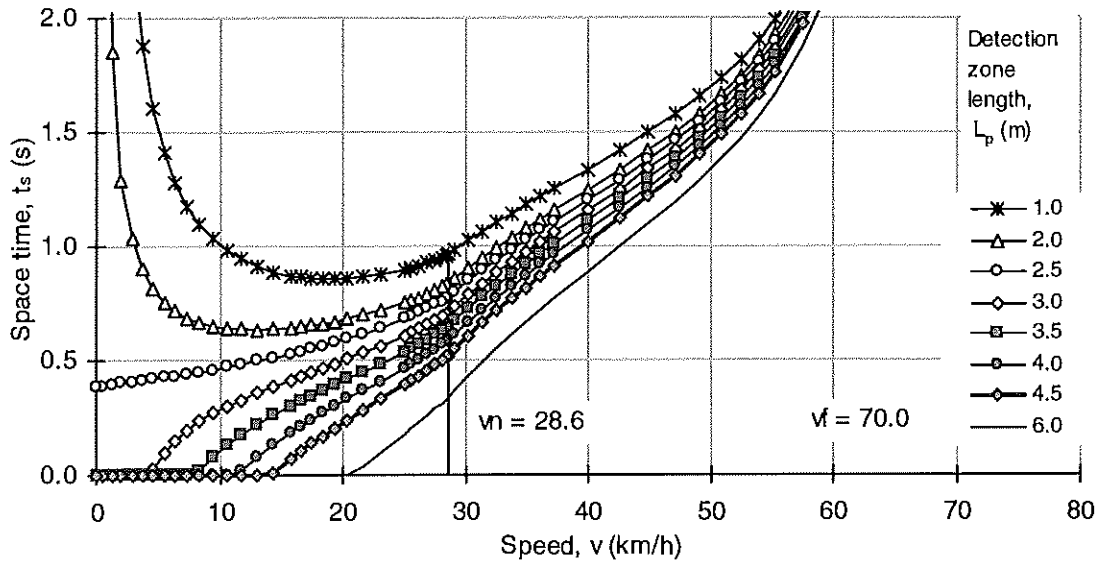


Figure C.19 – Space time - speed - detection zone length relationships for Site 335: Doncaster Road - Blackburn Road (East Doncaster, Melbourne) - right-turn lane (Lane 4) on Doncaster Road East approach Alternative Calibration Method 13: $v_L, h_{2L}, t_r = 1.0$

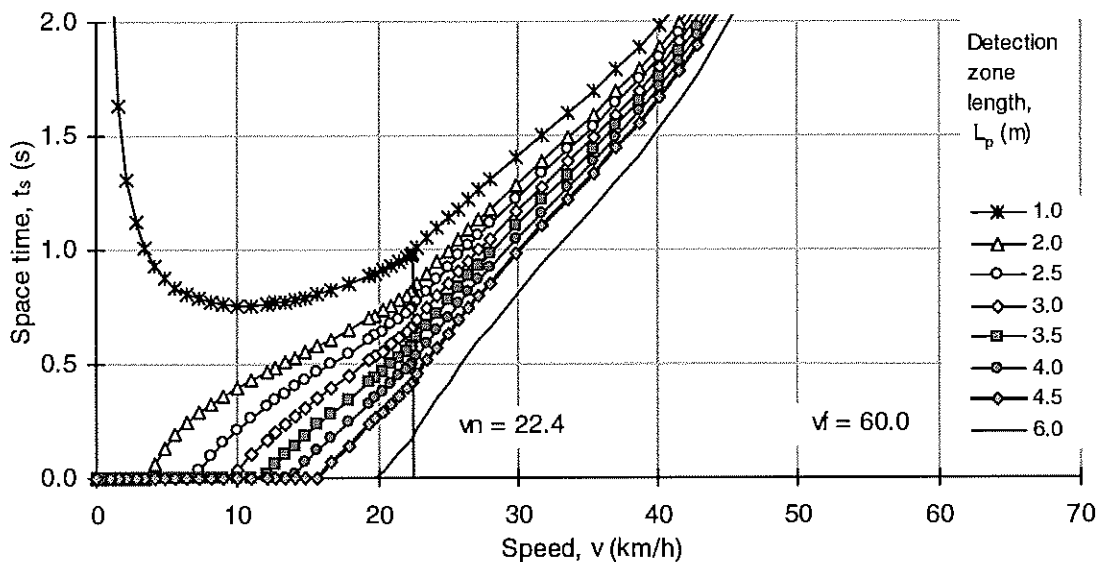
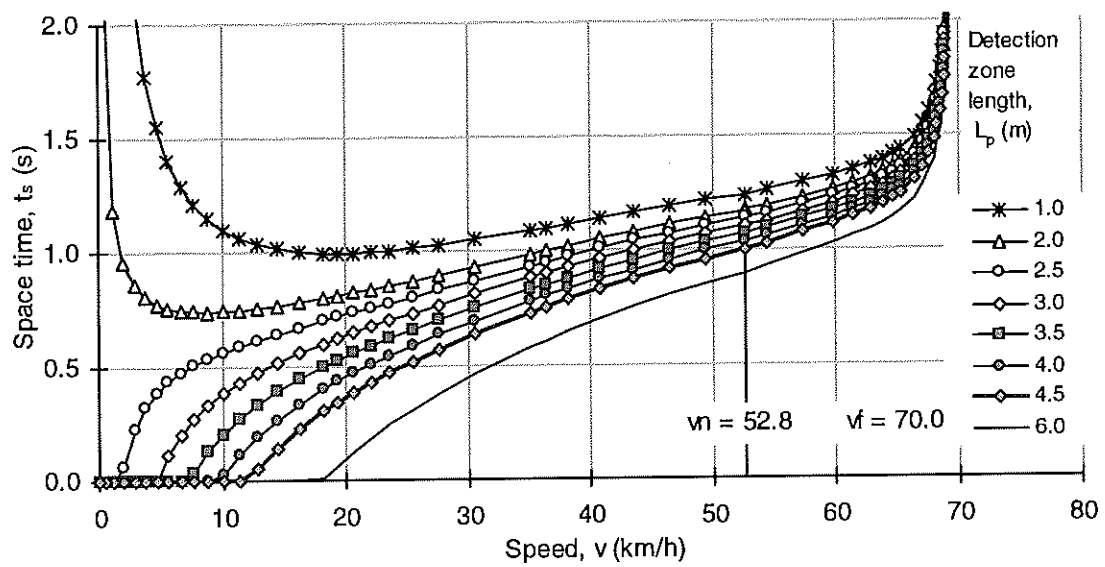


Figure C.20 – Space time - speed - detection zone length relationships for Site 610: Military Road - Murdoch Street (Cremorne, Sydney) - right-turn lane (Lane 3) on Military Road West approach Alternative Calibration Method 13: $v_L, h_{2L}, t_r = 1.0$



**Figure C.21 – Space time - speed - detection zone length relationships for Site 511:
 General Holmes Drive - Bestic Street (Kyeemagh, Sydney) -
 through lane (Lane 2) on General Holmes Drive South approach
 Alternative Calibration Method 13: $v_L, h_{2L}, t_r = 1.0$**